Mechanistic prediction of intestinal first-pass metabolism using *in vitro* data in preclinical species and in man

‘A thesis submitted to The University of Manchester for the degree of Doctor of Philosophy in the Faculty of Medical and Human Sciences’

2013

Oliver James Dimitriu Hatley

Manchester Pharmacy School

Contents

Word count: 71190

List of Figures

List of Tables

List of Appendix Figures

List of Appendix Tables

Abstract

The impact of the intestine in determining the oral bioavailability of drugs has been extensively studied. Its large surface area, metabolic content and positioning at the first site of exposure for orally ingested xenobiotics means its contribution can be significant for certain drugs. However, prediction of the exact metabolic component of the intestine is limited, in part due to limitations in validation of *in vitro* tools as well as *in vitro-in vivo* extrapolation scaling factors. Microsomes are a well established *in vitro* tool for extrapolating hepatic metabolism, however standardised methodologies for preparation in the intestine are limited, in light of complexities in preparation (e.g. presence of multiple non-metabolic cells, proteases and mucus). Therefore, the aims of this study were to establish an optimised method of intestinal microsome preparation via elution in the proximal rat intestine, and to determine microsomal scaling factors by correcting for protein losses during preparation. In addition, to assess species in another preclinical species (dog) and human as well as assessing and regional differences in scaling factors and metabolism.

Following optimisation of a reproducible intestinal microsome preparation method in the rat, the importance of heparin in limiting mucosal contamination was established. These microsomes were characterised for total cytochrome P450 (CYP) content, and CYP and uridine 5′-diphosphate glucuronosyltransferase (UGT) activities using maker probes of testosterone and 4-nitrophenol. Loss corrected microsomal scaling factors between two pools of n=9 rats was 9.6±3.5 (recovery 33%). A broad range of compounds (n=25) in terms of metabolic activity and physicochemical properties were screened in rat intestinal microsomes. The prediction accuracy relative to in house generated or literature *in vivo* estimates of the fraction escaping intestinal metabolism (F_G) through *in vitro-in vivo* extrapolation of observed metabolism and the derived scaling factors and either Caco-2 permeability of physicochemical permeability estimates utilising the Q_{gut} model. In the dog, regional differences in intestinal scaling factors and metabolic activities were explored, as well as relationships between the proximal intestine and liver in matched donors. Positive correlations in both hepatic activity and microsomal scalars were observed. Robust scaling factors were established using the 3 microsomal markers. A total of 24 compounds were screened for hepatic and intestinal metabolism in order to make *in vivo* estimates of F_G, the fraction escaping hepatic metabolism (F_H) and oral bioavailability (F). Estimates based on Caco-2 and physicochemical based scaling, as well as utilising a commercial PBPK software platform (ADAM model, Simcyp® v12) were broadly similar with generally reduced prediction accuracy in proximal physicochemical based Q_{gut} scaling, and improved predictions using Caco-2 Q_{gut} or PBPK approaches. Worse predictions were observed for compounds with high protein binding, transporter substrates and/or CYP3A inhibitors. Regional metabolism demonstrated peak metabolism in the proximal intestine, before declining distally. Human intestinal microsomes were prepared for jejunum and ileum tissue. Although samples were limited, regional differences in metabolic activities and scaling factors were also assessed, using correction markers and activity in 23 compounds. In all, 20 compounds overlapped between all three species. Comparison in $Fa.F_G$ between rat and human CYP3A substrates showed a modest relationship, however relationships between species and human were generally poor given the observed differing metabolic contributions of testosterone and 4-NP metabolite formation between species limited the observed relationships between species. However, within species, good estimates of oral bioavailability were observed. This is the largest know interspecies comparison of intestinal metabolism and scaling factors with microsomes prepared within the same lab.

Declaration

No portion of the work referred to in this thesis has been submitted in support of an application for another degree or qualification of this or any other university or other institute of learning.

Copyright Statement

i. The author of this thesis (including any appendices and/or schedules to this thesis) owns certain copyright or related rights in it (the "Copyright") and he has given The University of Manchester certain rights to use such Copyright, including for administrative purposes.

ii. Copies of this thesis, either in full or in extracts and whether in hard or electronic copy, may be made only in accordance with the Copyright, Designs and Patents Act 1988 (as amended) and regulations issued under it or, where appropriate, in accordance with licensing agreements which the University has from time to time. This page must form part of any such copies made.

iii. The ownership of certain Copyright, patents, designs, trade marks and other intellectual property (the "Intellectual Property") and any reproductions of copyright works in the thesis, for example graphs and tables ("Reproductions"), which may be described in this thesis, may not be owned by the author and may be owned by third parties. Such Intellectual Property and Reproductions cannot and must not be made available for use without the prior written permission of the owner(s) of the relevant Intellectual Property and/or Reproductions.

iv. Further information on the conditions under which disclosure, publication and commercialisation of this thesis, the Copyright and any Intellectual Property and/or Reproductions described in it may take place is available in the University IP Policy (see http://www.campus.manchester.ac.uk/medialibrary/policies/intellectual-property.pdf), in any relevant Thesis restriction declarations deposited in the University Library, The University Library's regulations (see http://www.manchester.ac.uk/library/aboutus/regulations) and in The University's policy on presentation of Theses.

List of Abbreviations

ADAM: advanced dissolution, absorption and metabolism
ACAT: Advanced Compartmental Absorption Transit
AUC: area under the curve

BCA: Bicinchoninic acid
BCRP: breast cancer resistance protein
BSA: bovine serum albumin

CL_{int}: intrinsic clearance
$CL_{int,u}$: unbound intrinsic clearance
$CL_{int,u,G}$: Intrinsic unbound clearance in the gut wall
$CL_{int,u,H}$: Intrinsic unbound clearance in the liver
$CL_{i.v}$: intravenous clearance
CL_{perm}: Clearance permeability
CL_R: renal clearance
CYP: cytochrome P450

DDT: dithiothreitol
DLM: dog liver microsomes
DMSO: Dimethyl sulfoxide

EDTA: ethylenediaminetetraacetic acid
E_G: Intestinal extraction ratio
E_H: Hepatic extraction ratio

F: oral bioavailability
F_a: fraction absorbed from the intestinal lumen
FDA: Food and Drug Administration
F_G: fraction escaping intestinal first pass metabolism
F_H: fraction escaping hepatic first pass metabolism
FM: Fraction metabolised
Fu_b: fraction of drug unbound from protein in the blood
$fu_{p:}$ fraction of drug unbound from protein in the plasma
$fu_{inc:}$ fraction of drug unbound from protein in the incubation

GIT: gastrointestinal tract
Gluc: glucuronide
GST:glutathione *S*-transferases
gmfe: geometric mean fold error

HBD: hydrogen bond donor(s)
7-HC: 7-hydroxycoumarin
HIIM:Human intestinal ileum microsomes
HIJM: Human intestinal jejunum microsomes
HIM: Human intestinal microsomes
HTD: high throughput dialysis
HW: Han Wistar rat

i.v.: intravenous
IVIVE: *in vitro-in vivo* extrapolation
IH: in house

KCl: potassium chloride
K_m: Michaelis-Menton constant (measure of binding affinity)

LC-MS/MS: liquid chromatography with tandem mass spectrometry
LLOQ: lower limit of quantification
LogP: the logarithm of the ratio of the concentration of unionized drug partitioned between octanol and water

MAD: maximal absorbable dose
MDR1a: multidrug resistance gene 1a
$MgCl_2$: magnesium chloride
MPPcm: microsomal protein per cm
MPPGI: microsomal protein per gram intestine
MPPGL: microsomal protein per gram liver
MPPGM: microsomal protein per gram intestinal mucosa
MRP: multidrug resistance protein

NCE: new chemical entitie
4-NP: 4-nitrophenol
NV: no value

OATP: organic anion-transporting polypeptide
OH TEST: hydroxy testosterone

Papp: apparent permeability
PBPK: physiologically-based pharmacokinetic
P_{eff}: effective permeability
PD: pharmacodynamics
PBS: phosphate buffered solution
PI: protease inhibitor
pKa: acid ionization constant
P-gp: p-glycoprotein
PhRMA: Pharmaceutical Research andManufacturers of America
p.o.: per oral
PSA: polar surface area

Q_{gut}: Hybrid parameter describing permeability and blood clearance in the intestine
Q_H: hepatic blood flow
Q_{villi}: Intestinal villus blood flow

r: radius
R^2: coefficient of determination
Rb: blood to plasma concentration ratio
RIM: rat intestinal microsomes
rmse: root-mean-square error
ROF: rate of formation

SAL: saccharic acid 1,4’ lactone
SD: Sprague Dawley rat
Stdev: Standard deviation of the mean
SULT: sulfotransferases

$t_{1/2}$: half-life
TEG: triethylene glycol
T_{SI}: Small intestinal transit time

UDPGA: uridine diphosphate glucuronic acid
UGT: uridine 5′-diphosphate glucuronosyltransferase
UPH2O:ultrapure H_2O

Vd_{ss}: volume of distribution at steady state
V_{max} : maximum rate of formation

Statement on 3 R's and animal usage in this PhD project

This work comes under the 3 R's commitments to reduce, replace and refine the use of animals within pharmaceutical drug research in line with Russel and Birch's (1959) original principles for humane experimatal techniques. All animals used in this study were sourced from ongoing project work, or animals which would otherwise have been euthanized as a result of retirement (due to age deeming them inappropriate for further study) or end of project research activities. The aim of this work from a 3 R's perspective is to provide greater understanding of intestinal metabolism in preclinical species and in humans, and increase confidence with applying *in vitro* methods for projection of *in vivo* intestinal metabolism. The hope is that the *in vitro* assay will provide a valid tool to pre-filter compounds for *in vivo* assessment, thereby reducing the number of animal studies required. Furthermore the data and understanding taken from this work will assist physiologically-based pharmacokinetic (PBPK) approaches by providing system parameters for making predictions of intestinal metabolism, again potentially reducing the number of *in vivo* studies required.

All *in vivo* work was conducted within AstraZeneca and was subject to internal ethical review and conducted in accordance with Home Office requirements under the Animals Scientific Procedures Act (1986).

Acknowledgments

I have been very lucky and I am extremely grateful for the opportunity to experience both academic and industrial perspective from my supervisors and all the people I worked with, and for their equally important help and contribution towards this work. I would like to thank my supervisors Chris, Alex, and Amin for their input and reflections and their trust in me. Chris has especially had a lot of headaches with regards to getting me established in the lab, work agreements between AZ and the university, as well as fantastic opportunities to go and work in Sweden, so I am especially grateful to him. Thanks also to Alex, who kindly agreed to supervise my project following my transfer from Sheffield, so I thank her for her significant contributions and comments to this work. Thanks also to Amin for providing an excellent opportunity to travel and apply my methodology in labs in America as part of research collaboration with both Bristol Myers-Squibb and Roche.

I would also like to make a special mention to colleagues in Astrazeneca who gave up their time to help and support my work, especially Michael Cocca who helped with sourcing lab supplies and equipment, Robin Smith who helped with showing me characterisation and depletion assays, Dave Temesi and Scott Martin who helped with the LC-MS/MS of the particularly difficult co-elution of all the testosterone metabolites. Furthermore, I am eternally grateful for the help of Anna-Lena Ungel, Constanze Hilgendorf and Åsa Sjöberg based at AstraZenca, Mölndal for there significant help with regard to the human work in Sweden as well as Costanze with regard to Caco-2 data. Also to Christine Pattison for help with sourcing commercial microsomes and help in validation of the coincubation methods, Neil Shearer for piecing back together all the equipment for the fu_{inc} assay, and Daniel Scotcher (CAPkR) for our combined work in preparation of dog hepatic microsomes. Also to Darren Jones and Peter Webborn for helping with sourcing of tissue and undertaking *in vivo* pharmacokinetic experiments. Also to Warren Keene, Paul Courtney, Richard Grant and John Swales for having the patience for my "just one thing" questions!

Thank you also to my wife Alma, and my and her parents and family for their love and support especially over the last few years. Also my loyal friends, especially Adam Darwich who is a good sounding board for my frustrations.

The Author

The author graduated from the University of Southampton with a BSc in Biomedical Sciences in July 2008. Following this, the author studied a MSc in Drug Discovery Skills at Kings Colledge London, which was a supported by the pharmaceutical industry, as part of which he spent 5 months placed in AstraZenca (Alderley Edge, UK). Following graduation with distinction, the author started this PhD at the University of Sheffield as part of a industrial CASE studentship programme with the Medical Research Council (MRC) and AstraZeneca, in 2009 under the guidance of Dr. Christopher Jones, Dr. Zoe Barter and Prof. Amin Rostami-Hodjegan and. After Prof. Rostami-Hodjegan's move to the University of Manchester in 2010, the author joined the Centre for applied Pharmacokinetic Research (CAPkR) under the supervision of Dr. Christopher Jones, Dr. Aleksandra Galetin, and Prof. Amin Rostami-Hodjegan.

Funding

This PhD was awarded under the industrial CASE student award scheme in collaboration with the Medical Research Council (MRC) and AstraZeneca.

List of contributed publications

Musther H, Olivares-Morales A, Hatley OJD, Liu B and Rostami-Hodjegan A (2013) Animal verses human oral drug bioavailability: Do they correleate? *European Journal of Pharmaceutical Sciences* in press.

Olivares-Morales A, Hatley OJD, Arrons L, Turner D, Galetin A and Rostami-Hodjegan A (2013) The Use of ROC Analysis for rhe Qualitative Prediction of Human Oral Bioavialblity from Animal Data. *Pharmacutical Research* in press.

Kostewicz ES, Arrons L, Bergstrand M, Bolger MB, Galetin A, Hatley O, Jamei M, Lloyd R, Pepin X, Rostami-Hodjegan A, Sjogren E, Tannergren C, Turner DB, Wagner C, Weitschies W and Dressman JB (2013) PBPK Models for the prediction of *in vivo* performance of oral dosage forms. *European Journal of Pharmaceutical Sciences* in press.

1. Introduction

1.1. Oral bioavailability

Principally for patient compliance and convenience of dosing, prescription of oral formulation is the preferred method of drug administration. Analysis of the top 200 prescribed pharmaceutical agents in 2011 reveals that, in the USA, 87% are administered orally (Bartholow, 2012; FDA Approved Drug Products, 2012). However, in order to reach the systemic circulation and provide adequate exposure at the target site, xenobiotics must overcome the sequential barriers of both absorption and first-pass metabolism (Wilkinson, 1987). These barriers ultimately determine the oral bioavailability (F) of a given drug (Lin et al., 1999) (**Equation 1-1**, **Figure 1-1**).

Equation 1-1 $F = Fa \cdot F_G \cdot F_H$

where Fa is the fraction of oral dose absorbed from the intestinal lumen, F_G is the fraction of the drug entering the enterocytes that escapes first-pass gut wall metabolism and F_H is the fraction of drug that escapes first-pass hepatic metabolism and biliary secretion.

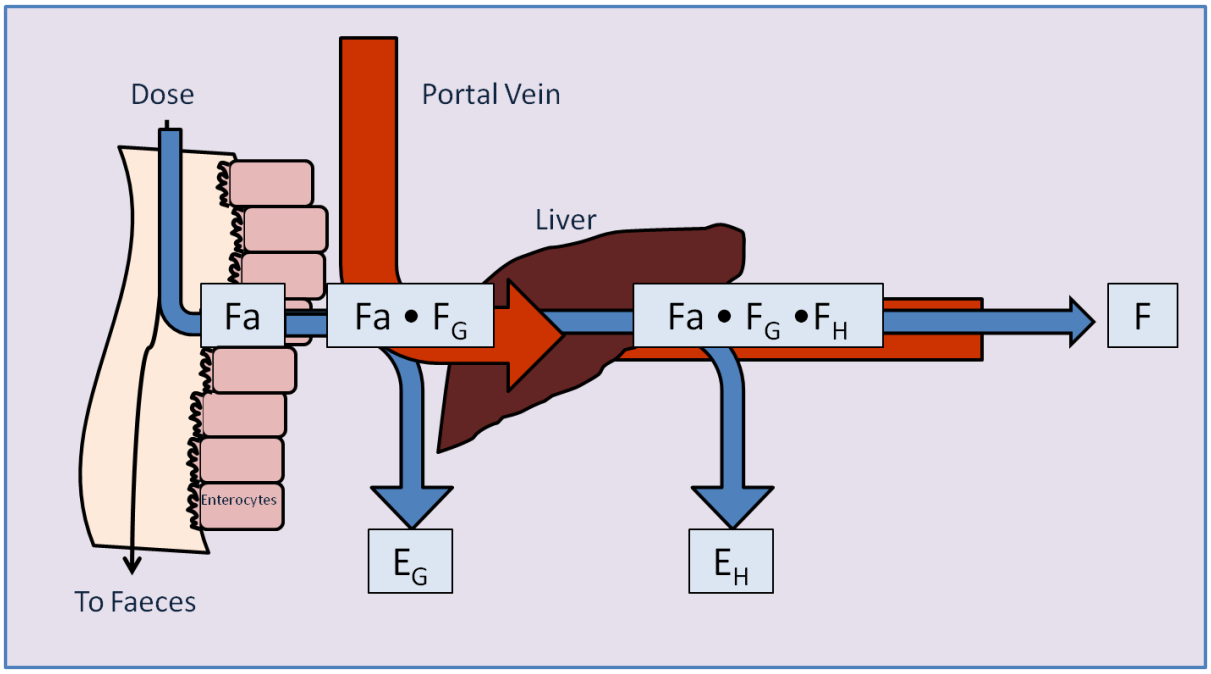

Figure 1-1 Bioavailability (F) of oral drugs is dependent on the fraction absorbed from the gut (Fa) and extraction via respective hepatic and intestinal first-pass metabolism.

F_G : Fraction escaping intestinal metabolism, F_H: fraction escaping hepatic metabolism, E_G: Intestinal extraction ratio, E_H: Hepatic extraction ratio. Figure adapted from Roland and Tozer, (2010).

In some cases, these barriers to the systemic circulation are very high resulting in drugs with low bioavailability. Low bioavailability is undesirable for financial reasons in terms of increasing the amount of drug required, although increasing the dose and/or dose frequency within reasonable patient compliance limits is still feasible. However, more critically, as a consequence of low bioavailability (F <30%) a greater incidence of interindividual variation is expected (Hellriegel et al., 1996). These variables include patient's age, weight, degree of obesity, type and degree of disease severity, and patient's genetic makeup (Rowland and Tozer, 2010). In addition, environmental factors (e.g. diet) and metabolic drug-drug interactions may further contribute (Rowland and Tozer, 2010). These inter-individual variations can be exaggerated in drugs with a narrow therapeutic window (concentrations between those which are significant enough to elicit a desired therapeutic effect and those that prove toxic), e.g. the immunosuppressant's cyclosporine A and tacrolimus, for which organ-graft rejection or patient toxicity can be observed over a narrow change in exposure (Paine et al., 2002). Consequently, understanding the extent of metabolism for new chemical entities (NCE's) during drug research and development (R & D) programs is an important step to the design and optimisation of compounds to have acceptable pharmacokinetic (PK) properties to engage the specific target site of action for the required duration, in order to elicit a desired pharmacodynamic (PD) effect.

A key element in determining the probability of success of a given drug series for driving investment decisions (i.e. first in man studies) is the predictions of efficacious human dose, maximal absorbable dose (MAD) and therapeutic safety margin. These assessments are driven by both *in vitro* and preclinical *in vivo* data predictions of human intravenous (i.v.) and *per oral* (p.o.) drug clearance profiles. The fundamental pharmacokinetic parameters which drive these predictions are estimates of Fa, clearance (CL), volume of distribution at steady state (Vd_{ss}), half-life ($t_{1/2}$) and F (van de Waterbeemd and Gifford, 2003). A determining factor in the probability of success is therefore dependant on how well these estimates are made.

1.2. Hepatic first pass metabolism

The liver is the major site of first-pass metabolism, because of its size and high content of drug metabolising enzymes (e.g. cytochrome P450s (CYPs) and uridine 5′-diphosphate glucuronosyltransferase (UGTs)) (Lin et al., 1999). The prediction of human i.v. CL is particularly important in R & D as it provides insight into the rate and route(s) of metabolism and elimination of the drug from the body. Therefore, CL is a central

parameter in selecting the size of the dose to achieve target concentration, and along with the Vd_{ss}, determines $t_{1/2}$, and therefore the frequency of dosing required. I.v. clearance provides an estimate of hepatic clearance, by subtraction of the renal elimination component (CL_R), assuming that metabolism from other extrahepatic tissues is negligible.

However, by considering only hepatic metabolism, a general trend of under-prediction of human drug clearance is observed (Iwatsubo et al., 1997; Fisher and Labissiere, 2007; Galetin, 2007). For example, recently in a PhRMA collaborative study, it has been reported that whilst estimates of F_H may have relative predictive success for estimating i.v. clearance (with a 69% high prediction accuracy), oral clearance estimates are poor (23% high prediction accuracy) (Poulin et al., 2011). Scaling of hepatic clearance demonstrated relative success as a result of detailed understandings of the physiological parameters (e.g. hepatic blood flow and hepatic scaling factors (Barter et al., 2007) involved in both *in vitro-in vivo* extrapolation (IVIVE) (Obach, 2001; Ito and Houston, 2005; Houston and Galetin, 2008), and by using (modified) allometric relationships to estimate human *in vivo* data from preclinical species (Obach et al., 1997; Ward et al., 2005). As is the case for this PhRMA study however, frequently the intestinal component is ignored since estimates of the contribution of the intestine to oral clearance are limited by a lack of established *in vitro* tools, scaling factors and understanding of intestinal species differences (Galetin et al., 2008; Cubitt et al., 2009; Kostewicz et al., 2013). The impact of the intestinal component however, cannot be ignored.

1.3. Intestinal first pass metabolism

Extrahepatic metabolism has been demonstrated in lung (De Kanter et al., 2004; de Graaf et al., 2006), kidney (De Kanter et al., 2004; de Graaf et al., 2006; Gill et al., 2012) and intestinal tissues (De Kanter et al., 2004; van de Kerkhof et al., 2005; de Graaf et al., 2006; van de Kerkhof et al., 2008; Cubitt et al., 2009; Gertz et al., 2010; Cubitt et al., 2011; Gertz et al., 2011; Groothuis and de Graaf, 2013). Lin and Lu (2001) surmised that the intestinal mucosa is the most important extrahepatic site of drug biotransformation, supported by the ability to metabolize drugs by numerous pathways involving phase I and phase II reactions (Pacifici et al., 1988; de Waziers et al., 1990; Prueksaritanont et al., 1996). In fact, several *in vivo* studies have demonstrated that the small intestine contributes substantially to the overall first-pass metabolism of cyclosporine A (Kolars et al., 1991), nifedipine (Holtbecker et al., 1996), midazolam (Paine et al., 1996) and verapamil (Fromm et al., 1996). Therefore, the small intestine is an important organ for elimination of drugs. The

potential exists for substantial presystemic metabolism due to its large surface area, its significant metabolic content and low blood outflow meaning the substrate is cleared slowly (Lin et al., 1999; Kaminsky and Zhang, 2003; Paine et al., 2006; Galetin et al., 2010).

1.4. Intestinal absorption

The small intestine is the major site of absorption of nutrients and water as well as xenobiotics in the gastrointestinal tract (GIT), whereas the stomach and colon play only minor roles (DeSesso and Jacobson, 2001; DeSesso et al., 2008). The small intestine is split into three non-anatomically distinct regions; duodenum, jejunum, and ileum, of which comprise the jejunum and ileum comprise almost equal proportions in humans (**Table 1-1**) (DeSesso and Jacobson, 2001; DeSesso et al., 2008). Each of the regions can be defined by differences in both their absorptive and secretory capacities, and a general narrowing of the lumen from the proximal to distal ends. In humans, the duodenum is both the shortest and widest. The duodenum subsequently merges with the next proximal two-fifths of the small intestine classified as jejunum, which is both thicker and wider than the ileum, comprising the longer remaining distal end (Tortora and Derrickson, 2006). The defined proportions are however distinct across species (DeSesso and Jacobson, 2001; Balimane and Chong, 2005; DeSesso et al., 2008). For example, the GIT tract of the dog is relatively short (due to a small colon) and simple compared to human due to minimal folding of the intestinal wall (Kararli, 1995). Furthermore, as in the rat, there is little visible differentiation between the segments, however it is apparent that unlike the human, the proportion of jejunum makes up around 90% of the small intestine (DeSesso et al., 2008).

The macro- and micro-scopic features of the human intestine serve to vastly increase the surface area available for absorption. The circular folds (valves of Kerckring), villi, and microvilli (present at the luminal side of enterocytes) increase the area available for absorption in man 30-fold and 600-fold, respectively (Balimane and Chong, 2005; Thelen and Dressman, 2009). For humans, the area available for absorption is much larger. Despite being only 5 times longer than the rat intestine, the surface area is approximately 200 times greater (**Table 1-1**). This an observation attributed to the lack of the valves of Kerckring in the rat (DeSesso and Jacobson, 2001). It should be noted however that body weight is approximately 300 fold larger in the rat (250g *vs* 75kg) therefore normalisation of intestinal surface area for body weight provides the rat with a much greater potential for both drug absorption, and hence metabolism.

Table 1-1 Approximate lengths and surface areas of human, dog and rat small intestine.
Data derived from DeSesso et al., (2001; 2008), Karali,(1995), Pappenheimer (1998), Brown et al., (1997).

	Human			Dog			Rat		
Region of GI Tract	**Segment length (cm)**	**% total**	**Absolute Surface Area (m^2)**	**Segment length (cm)**	**% total**	**Absolute Surface Area (m^2)**	**Segment length (cm)**	**% total**	**Absolute Surface Area (m^2)**
Duodenum	25	4%		25	6%		10	7%	
Jejunum	260	43%		360	90%		125	89%	
Illeum	315	53%		15	4%		5	4%	
Total	600		200	400		30	140		1.6

Table 1-2 Transit times and Q_{villi} for rat dog and human.

Species	Transit time (h)	Q_{villi} (l/h)
Rat	2.6-3.3[a]	0.34[1] (0.08-0.67)[e]
Dog	1.85[b]	5.61[2] (2.15-8.46)[f]
Human	3.32 (1.8-8)[a,c]	18[3 g]

a DeSesso et al., (2008).
b, Dressman et al.,(1986).
c Yu and Amidon, (1999).
e: Malik et al,(1976), Delp et al., (1991; 1998), Bjorkman et al., (1993), Klemm and Moody, (1998), Granger et al.,(1980).
f:Eade et al., (1977), Chou and Grassmick, (1978), Granger et al.,(1980).
g: Yang et al., (2007)
1: Based on assumptions of intestinal blood flow representing 15.5% cardiac output, and mucosal 70% of intestinal, and villus 60% of mucosal(Malik et al., 1976; Granger et al., 1980; Lin et al., 1999; Valentin, 2002).By contrast liver Q_H is around 1 l/h (Brown et al., 1997)
2: Based on assumptions of intestinal blood flow representing 10% cardiac output, and mucosal 80% of intestinal, and villus 60% of mucosal (Granger et al., 1980; Lin et al., 1999; Valentin, 2002). By contrast liver Q_H is around 43 l/h (McEntee et al., 1996; Taylor et al., 2007).
3: Based on assumptions of intestinal blood flow representing 10% cardiac output, and mucosal 80% of intestinal, and villus 60% of mucosal (Granger et al., 1980; Valentin, 2002; Yang et al., 2007). By contrast liver Q_H is around 89 l/h (Kato et al 2003).

The histology of the entire small intestine wall consists of four layers, mucosa, submucosa, muscle layers (muscularis) and the serosa (Tortora and Derrickson, 2006) (**Figure 1-2**). The mucosa composes the outermost layer and is split into three components; a superficial lining of epithelium, the lamina propria, and the muscularis mucosa (Lin et al., 1999). The lamina propria provides structural support for the epithelial cells, and contains blood capillaries, lymph vessels and nerve fibres (Thelen and Dressman, 2009). The epithelium composes the inner most layer of mucosa facing the lumen of the bowel, and consists predominantly of a single layer of enterocytes which line both the villi and the crypts of Lieberkühn (referred to from now on as crypts), from which epithelial cells originate and differentiate. The epithelium is heterogeneous, consisting also of mucus-secreting goblet cells, endocrine cells, Paneth cells and M cells (Thelen and Dressman, 2009). However, it is the enterocytes which are responsible for the majority of the digestion and absorption of drugs and nutrients in the human small intestine, and contain transporters (e.g. P-glycoprotein (P-gp), breast cancer resistance protein (BCRP)), and the metabolic enzymes responsible for xenobiotic biotransformation.

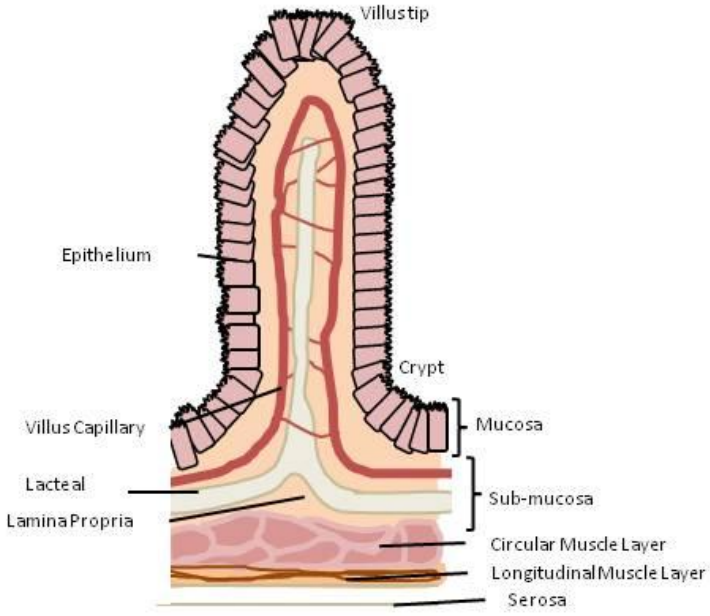

Figure 1-2 Cross section of intestinal villus along the crypt to villus tip axis.

1.4.1. Intestinal transporters

Drug absorption is governed by the surface area of the intestine, intestinal transit, the drug concentration gradient and the thickness of the unstirred water layer. Furthermore, the effective permeability (P_{eff}) across the intestinal mucosa drug absorption is also largely dependent on the physiochemical properties of the drug, namely the dose/dissolution ratio, the extent of chemical degradation or metabolism in the lumen, lipophoilicity, luminal complex binding, and particle size (Lennernas, 2007b). Multiple pathways for absorption are available. The process of passive drug absorption occurs most commonly via the transcellular route (through the cellular membrane) or less frequently in the case of smaller hydrophilic molecules via the paracellular route (via the tight junctions between the enterocytes).

The intestine contains several transporters present in the apical membrane that can actively up take or efflux xenobiotics from the villous tips of the apical membrane of the enterocytes (Pang, 2003). P-gp is product of the multidrug resistance gene 1a (MDR1a) and in humans is localized in the bile canalicular surface of hepatocytes, apical surface of proximal tubules in kidneys, columnar epithelial cells of the intestine, and capillary cells of the brain and testis. The role of P-gp as a multidrug transporter is coupled with its extremely broad substrate specificity, which overlaps with CYP3A (Lin et al., 1999). The observation of the low bioavailability of dual P-gp and CYP3A substrates (e.g. cyclosporine and tacrolimus) strengthens their proposed interplay in recirculation of xenobiotics (Mouly and Paine, 2003). Indeed, the introduction of oral P-gp inhibitors reduces rather than increases intestinal first-pass extraction (Benet and Cummins, 2001; Christians et al., 2005). It can therefore be reasonably assumed that following efflux, a fraction of the extruded xenobiotics can be reabsorbed, thus increasing intracellular residence time and hence exposure of drugs to metabolising enzymes (Watkins, 1997; Benet and Cummins, 2001; Christians et al., 2005). Moreover, P-gp may preferentially remove primary drug metabolites from the enterocyte to limit product inhibition (Watkins, 1997). In this fashion it appears that the barrier to xenobiotics is maintained as the metabolising potential of the intestine decreases, however their correlation is still debated (Lown et al., 1997). However, whether these luminally excreted metabolites are re-absorbed by the intestine further down the tract later remains as speculation..

Additional efflux transporters are also present in the intestine at the apical (e.g. multidrug resistince protein 2 (MRP2)) and basolateral (e.g. MRP1) membranes with differing

regional distributions. Data from mRNA expression in human has shown MRP1 to have ubiquitous expression in non-same subjects (Nakamura et al., 2002) and studies incorporating intra-individual variability (Zimmermann et al., 2005). MRP2 expression along the tract in both humans and rat has been reported to decrease distally (Pang, 2003; Zimmermann et al., 2005). BCRP is also of significant interest in determining oral bioavailability due to its overlapping substrate specificity with P-gp (Bruyere et al., 2010) . BCRP shows a general ubiquitous trend of distribution in the small intestine (Bruyere et al., 2010).

Recently mRNA expression has implicated a number of apical uptake transporters including members of the organic anion-transporting polypeptide (OATP) transporter families OATP1A2, OATP2B1 (Glaeser et al., 2007). OATP1B1 and OATP1B3, which were previously thought to be liver-specific have also been reported (Glaeser et al., 2007), however, their role in intestinal uptake is likely to be minimal (Galetin et al., 2010).

1.4.2. Species differences in absorption

Excellent relationships have been reported for Fa between several preclinical species (e.g. rat and monkey, but not dog) and human, through both carrier-mediated absorption or passive diffusion mechanisms (Chiou and Barve, 1998; Chiou et al., 2000; Chiou and Buehler, 2002; Cao et al., 2006). In general dog is regarded as a poor model of human absorption by demonstrating higher absorption than in man. This has been suggested to be related to several characteristics of the dog intestine, including the longer length of villi, increased protein binding, and the impact of a reduced gastrointestinal pH on weak base absorption (Chiou et al., 2000). The pH in the dog intestine is approximately one unit above human in the fasted state (Dressman, 1986; Chiou et al., 2000) and therefore may affect compounds for which solubility is highly dependent on pH. Furthermore, given that many water-soluble neutral compounds show greater absorption in dogs (Chiou and Buehler, 2002), it is possible that the size and frequency of the tight junction for paracellular transport may be greater in dogs than primates, making the intestinal membrane more leaky (He et al., 1998; Chiou et al., 2000).

Furthermore, the dog demonstrates both a higher bile salt secretion rate and concentration than that observed in human (Kararli, 1995). As a result, this could potentially modify the intestinal membrane structure and therefore make increase the permeability for drug transport, or alternatively facilitate the absorption of poorly water-soluble drugs by

increasing their solubility (Chiou et al., 2000). These factors may work in a concerted fashion to promote absorption, since contrary to the facilitation of good absorption, the intestinal transit time of the dog is the shortest compared to both rat and human (**Table 1-2**).

Limited information on transporter expression has been shown in the dog. However, based on mRNA data, P-pg expression is reported to peak in the ileum, whilst BCRP expression declines distally (Haller et al., 2012). Expression of P-gp, and MRP2 mRNA and protein in rat intestine are reported to show similar expression to humans, with decreased expression reported distally (Cao et al., 2006; Takano et al., 2006).

1.5. Relevance of Intestinal metabolism

Although the small intestine is regarded primarily as an absorptive organ in the uptake of orally administered drugs, once the victim drug has reached the intracellular site in the enterocytes it may be venerable to metabolism within the enterocytes. Whist intestine CYP3A (major intestinal isoform) expression only accounts for approximately 1% of hepatic CYP3A (Yang et al., 2004; Paine et al., 2006; Galetin et al., 2010), and CYP activity generally appears to be lower in the intestine on a mg per microsomal protein basis, correction for organ respective mean population CYP abundance demonstrated comparable metabolism potential as the liver in the intestine (Galetin and Houston, 2006).

Furthermore, the blood flow (Q) in the intestinal villus capillary (Q_{villi}) is low *vs.* liver (hepatic blood flow, Q_H) (**Table 1-2**). Therefore, with increased residence time, the opportunity for organ extraction ratio (E) is increased (Lin et al., 1999) (**Equation 1-2**). In reality, blood flow in the intestine is dynamic since linked to the metabolic demands of the intestine. Blood flow is increased following ingestion of a meal, however following exercise, blood flow is significantly reduced, and therefore affects both absorption and intestinal first pass metabolism (Lin et al., 1999).

Equation 1-2 $CL_{ORGAN} = Q \cdot E$

In vivo, the enterocytes make up around 90% of the cells in the epithelium (Kararli, 1995), and contain both phase I e.g. CYPs (de Waziers et al., 1990; Zhang et al., 1999; Paine et al., 2006), and phase II enzymes e.g. UGTs, sulfotransferases (SULTs), glutathione *S*-transferases (GSTs) (Strassburg et al., 2000; Tukey and Strassburg, 2001; Lennernas, 2007a; Lennernas, 2007b; Ritter, 2007).

Differential enzyme expression occurs as enterocytic stem cells migrate from the crypt, and mature on reaching the villus tip (Weiser, 1973; Pinkus and Windmueller, 1977; Murray et al., 1988; Traber et al., 1992; Fasco et al., 1993), a process spanning around 4 days in humans and 3 days in rodents (Kaminsky and Zhang, 2003). Following maturation, the cells are sloughed off into the mucus and excreted in the faeces.

The distribution of intestinal enzymes have been mapped according to mRNA levels (Zhang et al., 1999; Bock et al., 2002; Cao et al., 2006; Shin et al., 2009b), protein levels (Bonkovsky et al., 1985; Murray et al., 1988; de Waziers et al., 1990; Kolars et al., 1994; Tukey and Strassburg, 2001; Paine et al., 2006; Mitschke et al., 2008) spectrophotometric properties (Watkins et al., 1987; Paine et al., 1997; Zhang et al., 1999) and through activity (Fasco et al., 1993; Paine et al., 1997; Bock et al., 2002; Shiratani et al., 2008; Bruyere et al., 2009), with particular focus on phase I CYP enzymes.

1.5.1. Intestinal CYP expression

Intestinal CYP expression has been shown to be regulated independently of hepatic expression, and the complement of enzymes expressed is reduced (Lown et al., 1994; von Richter et al., 2004) (**Figure 1-3**). Intestinal enzyme also shows a large intra- as well as inter-individual variability (Thummel et al., 1996; Paine et al., 1997; Obach, 2001). Substantial regional variation is observed in both enzyme expression and activities. For example, in human, the highest protein levels of CYP3A4, CYP2C9 and CYP2C19 protein are detected in the proximal region of the intestine, and decline distally (Paine et al., 1997; Lapple et al., 2003; Galetin et al., 2008). In the case of other enzymes however, CYP2S1 and CYP2J2 enzymes are expressed ubiquitously along the GIT (Paine et al., 2006).

A

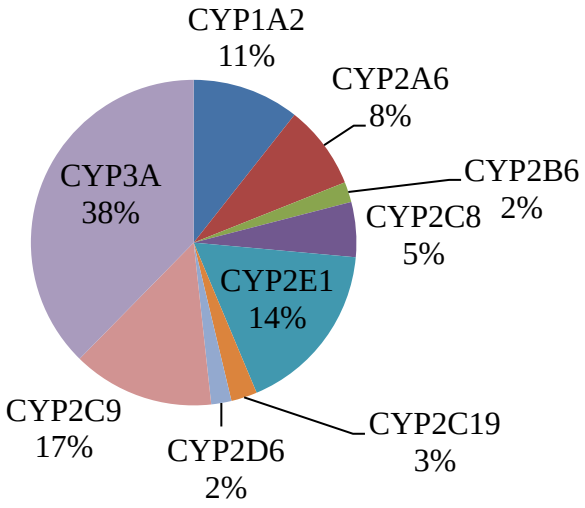

B

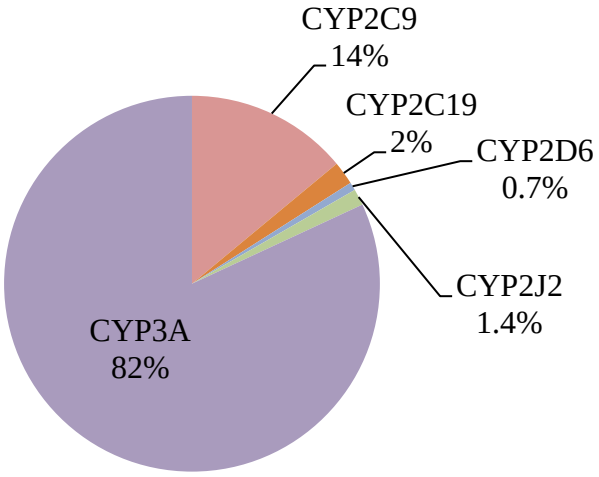

Figure 1-3 Human CYP liver (A) and intestinal (B) abundance. Human Liver (n=42 to 241), Human Intestine (Duodenum/proximal Jejunum) (n=31).

Estimates of CYP abundance in the human liver (**Figure 1-3A**) is based on the meta analysis of 42 to 241 liver samples (Rostami-Hodjegan and Tucker, 2007) . Proximal human intestine CYP abundance (**Figure 1-3B**) shows mean data for 31 donors (Paine et al., 2006). The major CYP enzyme expressed in the human intestine is CYP3A, which represents around 80% of all intestinal CYPs (Paine et al., 2006; Galetin et al., 2010). The total amount of CYP3A expressed in the human small intestine (65.7–70.5 nmol) represents approximately 1% of the estimated hepatic levels. Reported mean levels of intestinal CYP3A protein is 50 pmol/mg microsomal protein from 31 donors. In contrast, mean values for the liver is 155 pmol/mg microsomal protein based on date derived from

219 donors (Rowland Yeo et al., 2003; Paine et al., 2006; Rostami-Hodjegan and Tucker, 2007). The highest CYP3A catalytic activity (e.g. midazolam 1'OH formation) is also situated in the proximal region, rising slightly from duodenum to jejunum, and declining sharply toward the distal ileum (Paine et al., 1997; Zhang et al., 1999; Ding and Kaminsky, 2003).

The change in total CYP and UGT enzyme expression shows comparable distribution patterns in both expression and activity along the human intestine (Zhang et al., 1999; Strassburg et al., 2000; Tukey and Strassburg, 2001). Similar distribution patterns have been observed in the monkey, rat and dog (Zhang et al., 1996; Nakanishi et al., 2010; Heikkinen et al., 2012).

In all species, it appears that CYP3A and UGT metabolism are dominant routes of elimination in the intestine. However, between species, as is illustrated in **Table 1-3**, expression varies both in the intestinal enzymes present and enzyme family orthologues. Whilst the CYP families are conserved between species, when making comparisons to human, it is important to recognize that both orthologues and expression patterns in the intestine can differ quite dramatically between species For example, CYP2B expression is reported rival that of CYP3A in the Wistar rat (Mitschke et al., 2008). The monkey is similar to human since it demonstrates high proximal CYP3A expression (Nishimura et al., 2007).

The distribution of CYP3A12 and CYP2B11 along the dog intestine have recently been described using mass spectrometry based protein determination, and the specific enzyme substrate activity markers of temazepam (CYP2B11) and nordiazepam (CYP3A12) (Heikkinen et al., 2012). In this reported study, peak abundance (11.7 pmol/mg and 6.1 pmol/mg for CYP3A12 and CYP2B11, respectively) and activity was observed in the third segment. Lowest abundances and activity were observed in the distal segments (Heikkinen et al., 2012)(**Figure 1-4**). It should be noted that the patterns of activity is not parallel to expression. Despite a relatively specific CYP3A probe, it nordiazepam is a specific for human CYP3A and therefore may not be specific for dog CYP3A. Therefore, this may reflect the role of other ezymes which may addtinally contribute to substrate metabolism. In cases where activity is low relative to expression, this may represent the detection of non functional enzyme, for example enzyme undergoing intracellular protein translation and vesicle transport, or alternatively degradation.

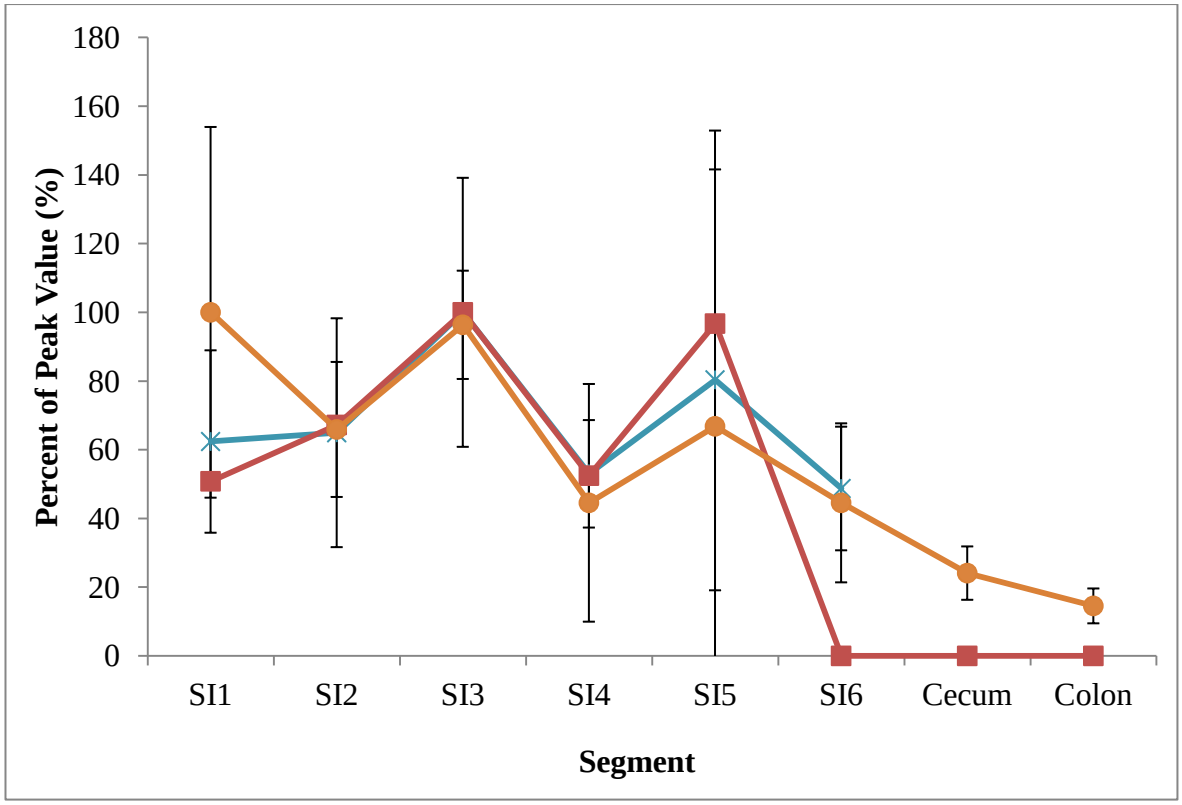

Figure 1-4 Regional distributions of CYP3A12 content (✳), CYP2B11 content (■), and temazepam CYP3A substrate activity (●) along the course of the dog intestine.

N=4. Segments 1-6, small intestine, segment 7: cecum, segment 8: colon. (Heikkinen et al., 2012).

Table 1-3 Reported mRNA, protein and activity of CYP enzymes detected within the intestine of human, rat, dog, monkey and mouse.

CYP Subfamily	Human[a,b]			Rat [a,b,c,d]			Dog[e,f,g]			Monkey[h,i]			Mouse[j,k,l]		
	CYP	mRNA	Pr/Act	CYP	mRNA	Pr/Act	CYP	mRNA	Pr/Act	CYP	mRNA	Pr/Act	CYP	mRNA	Pr/Act
CYP1A	1A1	+	+	1A1	+/-	+				1A1	+/-	+	1A1	+	+†
	1A2	+/-	+ /-										1A2	-	
CYP2A				2A6	-	-				2A23	+	+			
CYP1B	1B1	+	-										1B1	+	+†
CYP2B	2B6	+/-	+	2B1	+	+				2B6	+/-		2B9	-	+Δ
													2B10	+	
													2B19	+	
													2B20	+	
CYP2C	2C8	+	+	2C6	+	-				2C20	+		2C29	+	+Δ
	2C9	+	+	2C11	-	-/+*							2C37	-	
	2C18	+	-		+								2C38	+	
	2C19	+	+		-								2C40	+	
CYP2D	2D6	+	+	2D1	+/-	+	2D15	+	+	2D17	+/-	+			
CYP2E	2E1	+ /-		2E1	-					2E1	+/-		2E1	+	+
CYP2J	2J2	+	+	2J3	+	+				2J2	+				
		-		2J4		+									
CYP3A	3A4	+	+	3A1	+/-	+	3A12	+	+	3A64	+		3A11	+	+Δ
	3A5	+		3A2	+/-	+	3A26	+/-		3A4#	+		3A13	+	
				3A9	+	+				3A5	+		3A16	+	
				3A18	+	+							3A25	+	
				3A62	+								3A44	+	

Pr: protein expression, Act: activity + positive signal, +/- weak signal, - no signal *Strain difference †weak ΔGeneral antibody # Previously referred to as CYP3A8. a)(Komura and Iwaki, 2011) b: (van de Kerkhof et al., 2007b), c: (Mitschke et al., 2008), d:(Zeldin et al., 1997), e: (Haller et al., 2012), f: (Heikkinen et al., 2012), g:(Kyokawa et al., 2001), h: (Nakanishi et al., 2010), i: (Nakanishi et al., 2011), j:(Prueksaritanont et al., 1996), k:(Zhang et al., 2003), l:(Emoto et al., 2000).

1.5.2. Intestinal phase II expression

In addition to the liver and kidney, UGTs are highly expressed in the gastrointestinal tract (Fisher et al., 2001; Ritter, 2007). Indeed, it is noted that in some cases the capacity of UGT1A1 appears to rival that of the liver (Fisher et al., 2001; Kaminsky and Zhang, 2003). The distribution of UGTs is reportedly analogous to that of CYP, decreasing distally from the pylorus (Tukey and Strassburg, 2001; Galetin et al., 2010). Reported UGT family and orthalogue expression can be compared between species in **Table 1-4**. The ability of measure absolute protein abundances of UGT enzymes using antibodies is limited in light of their sequence similarities, and location within the endoplasmic reticulum. The main UGT enzymes expressed at levels higher than the liver in the human intestine are UGT1A5, UGT1A7, UGT1A8 UGT1A10 and UGT2B17 (Ohno and Nakajin, 2009). UGT1A8 and UGT1A10 are selectively expressed in the human intestine and not in the liver (Ohno and Nakajin, 2009).

The probe compound raloxifene and its glucuronidation between species demonstrates how differences in UGT expression between species can have a dramatic impact on intestinal metabolism. In the human, raloxifene is extensively glucuronidated to raloxifene 4-β glucuronide by UGT1A10, a UGT isoform exclusively expressed in the human intestine (Jeong et al., 2005). A comparatively minor pathway is the glucuronidation to raloxifene 6β-glucuronide metabolised by UGT1A8. Since UGT1A10 is not expressed in the rat intestine, metabolism can only occur through the minor pathway, and as such is reflected in the significant differences in intestinal extraction between rats and human (Jeong et al., 2005).Given its high intrinsic clearance of raloxifene relative to UGT1A8 this explains a low observed F (2%) in human verses the rat (39%) (Jeong et al., 2005). Raloxifene is a clear example where caution should be used when interpreting preclinical information of UGT1A10 substrates.

Similarly, intestinal sulphation can differ dramatically between species. For low dose drugs such as ethinylestradiol and salbutamol which are SULT enzyme substrates, SULT1A3 metabolism may limit their F (Mizuma et al., 2005; Cubitt et al., 2011). Of note, SULT1A3 is specific to the human intestine (Riches et al., 2009), and is not reported to be expressed in animal models (Shin et al., 2009a).

Table 1-4 Reported mRNA, protein and activity of UGT enzymes detected within the intestine of human, rat, dog, monkey and mouse.

UGT family	Human [a,b,c]			Rat [b,d,e,f]			Dog [g]			Monkey [a]			Mouse [h]		
	UGT	mRNA	Pr/Act	UGT	mRNA	Pr/Act	UGT	mRNA	Pr/Act	UGT	mRNA	Pr/Act	UGT	mRNA	Pr/Act
UGT1A	1A1	+	+	1A1	+	+	1A6	+		1A1	+		1A1	+	
	1A3	+/-		1A2	+	+				1A2	+		1A6	+	
	1A4	+/-	-	1A3	+					1A6	+		1A7	+	
	1A5	+	-	1A5	+/-					1A8	+		1A8	+/-	
	1A6	+/-	+/-	1A6	+					1A9	+				
	1A7	+/-		1A7	+										
	1A8	+	+	1A8	+/-	+									
	1A9	+/-													
	1A10	+	+												
UGT2A	2A2	+		2A1	+										
UGT2B	2B4	+/-	-	2B1	-	+				2B9	+		2B34	+	
	2B7	+	+/-	2B2	-	+				2B18	+/-		2B35	+	
	2B10	+/-	-	2B3	+					2B20	+		2B36	+/-	
	2B15	+		2B6	+/-					2B30	+/-				
	2B17	+/-		2B8	+										
	2B28	+		2B12	+	+									

Pr: protein, Act: activity. + positive signal, +/- weak signal, - no signal. a:(Komura and Iwaki, 2011), b: (van de Kerkhof et al., 2007b), c: (Ritter, 2007), d: (Shelby et al., 2003), e: (Grams et al., 2000), f: (Jeong et al., 2005), g:(Bock et al., 2002), h: (Buckley and Klaassen, 2007).

The presence of these diverse classes of enzymes at the site of absorption demonstrates the potential of the intestine as an extrahepatic organ to contribute significantly to the first-pass metabolism of xenobiotics. In terms of defining the E_G of orally ingested drugs, several *in vivo*, *in situ* and *in vitro* methods exist. However in light of their potential limitations, which will be addressed, a certain element of caution should be exercised when interpreting their functional utility to assess and aid F_G prediction strategies.

1.6. Estimating intestinal metabolism *in vivo*

The argument for a low contribution of the intestinal to overall first-pass metabolism is partly based on the low levels of metabolising enzymes present compared to the liver. Furthermore, since the intestine is the first site of exposure to xenobiotics, as such, higher drug enterocyte cell concentrations are observed than in hepatocytes. Therefore, it is reasonable to assume that the lower density of enzyme in the gut wall compared to the liver would increase the likelihood of enzyme saturation and, hence, less extraction (Lin et al., 1999). However, a recent analysis of the relative contributions of the fraction absorbed (Fa), the fraction escaping first pass metabolism (F_G), and the fraction escaping hepatic elimination (F_H) on bioavailability on 309 drugs studied in humans have indicated that for 30% of the compounds, F_G was less than 0.8, highlighting the importance of incorporating intestinal metabolism in both bioavailability and dose predictions in drug discovery and development (Varma et al., 2010).

However, in the absence of data derived from administration of compound in the anhepatic stage of liver transplant surgery (Kolars et al., 1991; Paine et al., 1996) or intestinal perfusions (von Richter et al., 2001) using portal vein cannulations which both have limited application in the human due to ethical limitations, the estimation of F_G *in vivo* is difficult. Multiple sites of sampling have been applied in rat models, however this is labour intensive and low throughput, and as such is not routinely applied (Mistry and Houston, 1985; Murakami et al., 2003; Quinney et al., 2008; Kuze et al., 2009; Matsuda et al., 2012). Particular confounding factors therefore in the estimation of F_G are in part driven through the difficulties in defining the exact contribution of the intestine indirectly from more conventional i.v. and p.o. dosing strategies.

The estimation of F_G from i.v. and p.o. data is based on the assumption of negligible metabolism in enterocytes after i.v. administration and that systemic clearance of a drug after i.v. dose (corrected for renal excretion) reflects only hepatic elimination (E_H).

However, the integrity of this assumption may not be entirely valid, as illustrated in the case of midazolam where an average 8% extraction ratio after i.v. administration of midazolam has been reported in anhepatic patients (and up to 26% in one patient) (Paine et al., 1996; Galetin et al., 2010). The F_G can also be estimated by comparing oral area under the curve (AUC) following administration the presence of grapefruit juice which inhibits CYP3A4 (Gertz et al., 2008a), however this is limited to CYP3A substrates only, and it assumes that all CYP3A4 metabolism is inhibited in the intestine, and there is no effect on transporters or on the liver . In addition, as is the case for i.v. and p.o. indirect measures of F_G, because of the inherent difficulties of separating out both Fa and F_G components of oral bioavailability, to limit the effect of (Fa) it is important that the dose administered is in solution. In fact, in the absence of experimental data, the general assumption in these cases is the Fa is 1 (i.e. absorption is complete) (Galetin et al., 2008; Gertz et al., 2010), which can result in an under-estimation of F_G. In reflection of this limitation, in some studies the Fa and F_G components are represented by the dual parameter, FaF_G (Kato et al., 2003; Akabane et al., 2010).

It should also be noted that the sensitivity of hepatic blood clearance ($CL_{H,b}$) to the value of hepatic blood flow (Q_H) (common range from 17.1 to 25mL/min/kg) ultimately limits the confidence in the value F_G obtained (Galetin et al., 2010; Kadono et al., 2010). This is especially important for compounds with potential to alter Q_H and/or demonstrate high E_H, which are most sensitive to the values of Q_H employed e.g. felodipine and verapamil (Galetin et al., 2010).

Table 1-5 Comparison of methods for estimating F_G *in vivo*/in situ.

Model	Advantages	Assumptions/Limitations
Portal vein sampling	Direct sampling before hepatic metabolism	Surgical methods required, recovery time after surgery Unethical in human
Anhepatic models (e.g. hepatic shunt)	Diversion of liver ensures intestinal contribution to be studied directly	Requires surgical techniques, low throughput Frequently disease model patients in human – poor relation to healthy population.
In situ (e.g. gut loop, Loc-i-gut)	Ability to look at different intestinal regions	Surgical techniques required, expensive in human Limited viability in rodents, use of anaesthetics can influence outcome Extraction assumed as perfusion rate limited – not valid for permeability limited compounds
Inhibition of intestinal enzymes (e.g. ABT-rodent, grapefruit juice human)	Simple, potential to inhibit either liver or intestinal enzymes (especially in rat) for separate elucidation	Intestinal enzymes are inhibited - assume other enzyme pathways do not compensate Difficult to separate Fa and F_G components If liver is not inhibited, assume iv is purely hepatic component
iv po dosing	Simple, high throughput	Indirect measure of F_G Difficult to separate Fa and F_G components Oral dose not administered at site of absorption Assume iv is purely hepatic component (minus renal if available) Assumption of liver blood flow

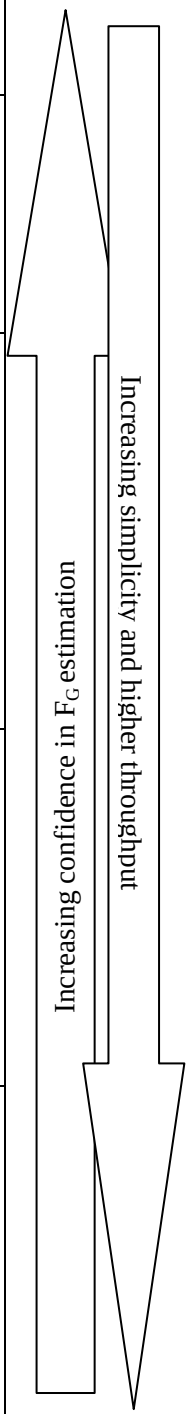

The disadvantage of *in vivo*/ *in situ* models is therefore that it is impossible to separate the variables involved in the process of absorption, i.e. it is not possible to identify individual rate-limiting factors (Le Ferrec et al., 2001; van de Kerkhof et al., 2007b). In addition, the given the difficulties in isolating the separate contributions of the liver and intestine (Galetin et al., 2008), and identifying the respective Fa and F_G components, the ability to quantifiably investigate intestinal drug metabolism *in vivo* is limited. A more mechanistic approach, therefore, is to utilise an *in vitro* approach to assess organ specific roles in metabolism, which can be applied to the screening/problem-solving of NCEs during drug discovery.

1.7. Estimating intestinal metabolism *in vitro*

Various *in vitro* methods can be utilised to study intestinal metabolism, for example Ussing chamber preparations (van de Kerkhof et al., 2006), everted gut sacs (Barr and Riegelman, 1970), precision cut tissue slices (De Kanter et al., 2004; van de Kerkhof et al., 2005; de Graaf et al., 2006; Martignoni et al., 2006), enterocyte preparations (Klippert et al., 1982; Koster and Noordhoek, 1983; von Richter et al., 2004) and, intestinal microsomes (Weiser, 1973; Dawson and Bridges, 1981; Bonkovsky et al., 1985; Fasco et al., 1993; Paine et al., 1996; Paine et al., 1997; Cotreau et al., 2000; Galetin and Houston, 2006; van de Kerkhof et al., 2007b; Bruyere et al., 2009; Cubitt et al., 2009). However, unlike the liver where both whole cell hepatocytes as well as subcellular fractions (e.g. microsomes) are routinely used in predicting E_H (Houston, 1994; Houston and Carlile, 1997; Obach et al., 1997; Obach, 2001; Ito and Houston, 2004), no consensus has been categorically reached as to the best *in vitro* models to quantitatively characterise and extrapolate intestinal metabolism data since *in vitro* methods are varied, and each can be chosen for evaluating various aspects of metabolism (and in some cases permeability), with both advantages and disadvantages associated with each technique (**Table 1-6**). Most work recently has focused on both the utility of intestinal slices (De Kanter et al., 2004; van de Kerkhof et al., 2005; de Graaf et al., 2006; Martignoni et al., 2006; van de Kerkhof et al., 2006; van de Kerkhof et al., 2007a; van de Kerkhof et al., 2008; Groothuis and de Graaf, 2013) and intestinal microsomes (Galetin and Houston, 2006; Cubitt et al., 2009; Gertz et al., 2010; Cubitt et al., 2011).

The application of precision-cut tissue slices has been extensively characterised, and offer a medium throughput approach and very efficient use of intestinal samples, since slices can be very thin (250-400 μM), and remain metabolically active and viable, and contain the

full complement of enzymes transporters and cofactors. Furthermore, this approach allows for comparative metabolism between both organs and between species as it is readily applied to other tissues (e.g. kidney, liver) (De Kanter et al., 2004; de Graaf et al., 2006). Relative contributions of organs can therefore be assessed. However, there are a few limitations, the difficulties in distributing substrates evenly (Houston and Carlile, 1997), and the lag time in phase II metabolism (van de Kerkhof et al., 2006). In the case of microsomes, addition of the pore forming alamethacin is routinely applied and this allows access for the endoplasmic reticulum where UGT resides (Fisher et al., 2000). Furthermore, whilst scaling up to whole intestine and *in vivo* is simple based on slice weight and organ weight with no issues with recovery losses in preparation, comparison prediction accuracy has not been fully defined (Groothuis and de Graaf, 2013). Finally, they are not amenable to long term storage and high throughput screening.

The advantages of using microsomes include their capacity for long-term storage, amenability for high throughput application, and ample characterization of optimal incubation conditions (Ekins et al., 1999). However, their disadvantages are well understood, in that some enzymes may be more labile following preparation, and also require the addition of expensive cofactors for optimal activity to replace those lost in preparation. Limited information is available on physiological concentrations of these cofactors, and therefore optimised slight excess concentrations are frequently utilised in order to ensure no limitation of enzyme activity (Kilford et al., 2009; Obach, 2011). For example UDP-glucuronic acid concentration of approximately 400 nmol/g hepatic tissue (Goon and Klaassen, 1992). Therefore microsomal concentrations of 5mM UDPGA (Kilford et al., 2009) is likely to be in excess. Overestimation of *in vivo* clearance is possible in this case, however it is more common that clearance is underpredicted to a greater extent from microsomal incubations than from cellular models e.g hepatocytes (Houston and Carlile, 1997; Obach, 2001).

Coupled to the removal of cytosolic enzymes, microsomes also therefore absent of the full complement of enzymes available for metabolism, and as such can display a bias in xenobiotic metabolism. For example, product accumulation due to loss of sequential metabolism pathways may result in a possible feedback inhibition effect (Hewitt et al., 2007). In addition, the removal of the outer plasma membrane results in the loss of any transporter protein systems which may be important for either the uptake or efflux of the drug and/or metabolites (Hewitt et al., 2007). Furthermore, the loss of structural integrity

Table 1-6 Comparison of methods for investigating intestinal contribution *in vitro*.

Model	Advantages	Assumptions/Limitations
Isolated tissue perfusions	Controlled Vascular and luminal perfusion	Applicable to animal tissues Limited tissue viability (2-3hrs) limits application to DDI or slowly metabolised compounds High dilution complicates analysis
Everted sac	Fast and inexpensive Regional comparisons metabolism and absorption	Applicable to animal tissues Limited tissue viability (2-3hrs) limits application to DDI or slowly metabolised compounds Generally applied to absorption studie Presence of smooth muscle and seros adds to barriers for absorption
Ussing chamber	Application to Human and other species Removal of serosa and smooth muscle wall removes barriers to absorption Bidirectional movement of compounds can be observed Combined effects of transporters and metabolism	Limited tissue viability (2-4hrs) limits application to DDI or slowly metabolised compounds Generally applied to absorption studies Scaling up to whole intestine undefined
Precision-cut slices	Efficient use of tissue through thin slices Metabolism Combined effects of transporters and metabolism	Bidirectional transport or metabolites or parent compound cannot be applied Lag in metabolism of Phase II compounds
Enterocyte preparations	Whole cell models without need to cofactors	Harvests likely to be contaminated with various other intestinal cell types and display low activities making analysis difficult Bidirectional transport or metabolites or parent compound cannot be applied Limited information of scaling factors
S9/Microsomes	Amenable for long term storage (-80^{o}C) High throughput Metabolism studies Scaling and correction approaches well established	Requirement for expensive cofactors Phase II studies require pore forming additives Scaling factors available but not yet fully defined Bidirectional transport or metabolites or parent compound cannot be applied Yield and activities affected by preparation methodology
Cell lines e.g. Caco-2	Useful for high throughput absorption studies	Poor reproducibility between labs Low expression of metabolic enzymes

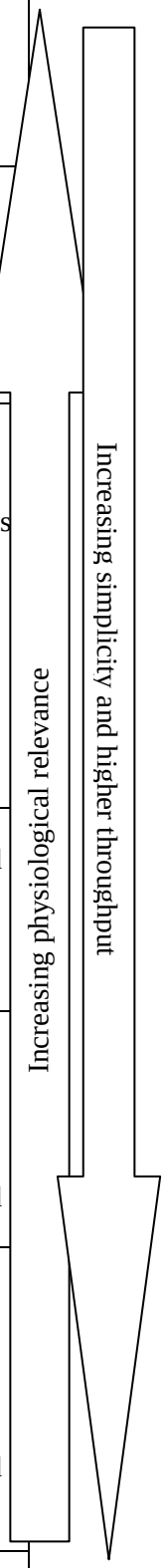

results in an *in vitro* incubation matrix where there is a greater potential for nonspecific binding than in comparison to the intact cell. However, well established methods for scaling of metabolism, and correcting for microsomal binding are routinely available and applied (Houston, 1994).

Measures of intestinal *in vitro* metabolism data may be obtained using intestinal microsomes for CYP and UGT metabolism using corresponding cofactors (Cubitt et al., 2009; Gertz et al., 2010) or cytosol (Cubitt et al., 2011) to account for alternative pathways e.g. sulfation. However, caution should be applied when utilising microsomal data from samples obtained from microsomal scraping due to reduced activity and protein yield in comparison to enterocyte elution (Mohri and Uesawa, 2001; Galetin and Houston, 2006). Alternative strategies employ hepatic microsomes for the initial assessment of intestinal CL_{int} following the normalisation for the isoform enzyme abundance data e.g. CYP3A (von Richter et al., 2004; Galetin and Houston, 2006; Gertz et al., 2010). However, this should only be utilised with caution unless confident of the main enzymatic route of elimination in and between species.

Despite these limitations, of all the *in vitro* tools, intestinal microsomes have been most widely utilised, a reflection of both their ease of use, commercial availability, as well as their most thoroughly characterised enzymology and kinetics. However, more serious limitations with *in vitro* literature data for either of these methods corresponding to sufficient validation for making estimates of intestinal metabolism *in vivo.*

1.8. Intestinal microsome preparation

In the liver, the isolation of subcellular fractions is well established from direct tissue homogenisation (Wilson et al., 2003; Barter et al., 2007). However, this is not optimal in the intestine, and care in enterocyte preparation is important. Application of scraping of the intestinal mucosa using glass slides or metal spatulas provides preparations contaminated with lymphocytes, plasma cells, granulocytes, macrophages, red blood cells, connective tissue cells, and mucus (Hulsmann et al., 1974b; Lin et al., 1999). Intestinal mucus represents a particular problem to microsomal preparation since this tends to aggregate cellular and subcellular material and as such influences the homogeneity of the preparations (Hulsmann et al., 1974b; Kaminsky and Fasco, 1991)..

Scraping is a highly mechanical procedure and therefore the damage of CYP is a characteristic feature of scraping techniques (Kaminsky and Fasco, 1991). This is since

some of the enterocytes become lysed and the CYP enzymes may be denatured following exposure to the digestive enzymes present in the intestine (Lin et al., 1999; Galetin and Houston, 2006). In contrast, chemically based elution protocols provides a more gentle isolation technique, is less likely to damage the cells, and results in higher enzyme activity and CYP yield (Bonkovsky et al., 1985; Kaminsky and Fasco, 1991; Lin et al., 1999; Mohri and Uesawa, 2001; Galetin and Houston, 2006).

The buffers utilised in intestinal microsome preparation play a significant role in the preservation of enzyme activity. As such isotonic sucrose, dithiothreitol (DTT) (a thiol to prevent degradation of CYP (a heme thiol) by proteases), Ethylenediaminetetraacetic acid (EDTA) (metal chelating agent for deactivation of metal-dependant enzymes) are routinely utilised, in additional to histidine (an antioxidant) and anticoagulants, e.g. heparin (Fasco et al., 1993; Emoto et al., 2000; Mohri and Uesawa, 2001). However, the preparation of intestinal microsomes, even when taking these protective measures is considered to be difficult compared with hepatic microsomes, because intestinal microsomes are exposed to abundant intestinal proteases (e.g. various serine and cysteine proteases) during their isolation (Emoto et al., 2000; Ganapathy et al., 2006; Komura and Iwaki, 2008). Trypsin, a potent serine protease, is synthesised as the inactive pro-enzyme trypsinogen and packaged into vesicles is a product of the pancreas secreted into the intestine (Ganapathy et al., 2006). Presence of these proteases is associated with decreased CYP yields and activity, and both single and combined cocktails of protease inhibitors have been utilised and reported to be beneficial (Mohri and Uesawa, 2001; Komura et al., 2002; Komura and Iwaki, 2008; Bruyere et al., 2009). Comparisons however between studies are limited since preparation methods are highly varied in the literature (**Figure 1-5**), and best practices for microsomal preparation are not fully established, and the effect of preparation on activities and protein yields has not been characterised.

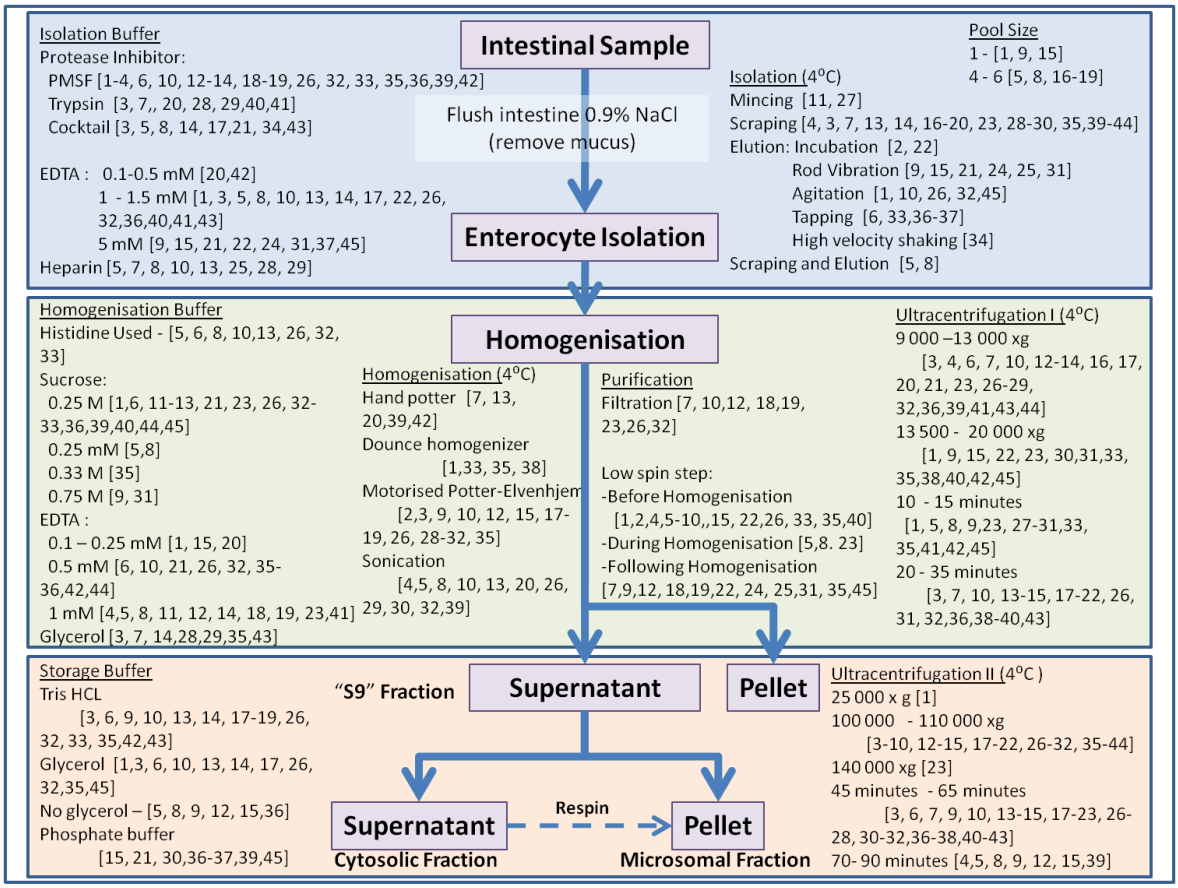

Figure 1-5 Schematic for of literature reported methods for intestinal microsome preparation.

References in **Appendix 7.1.**

1.9. Extrapolation of *in vivo* intestinal metabolism

A fundamental measure obtained from *in vitro* metabolism is intrinsic clearance (CL_{int}), which provides a raw measure of organ metabolic capacity activity independent of blood flow and blood binding, which can be scaled to the whole organ by means of a physiologically based scaling factor (Houston and Galetin, 2008). However, it is important for IVIVE that measures of protein yields reflect that the process of microsome preparation is an inefficient process, and therefore requires correction for protein lost in preparation by measurement of a microsomal specific marker (e.g. CYP content) in both the starting homogenate and final microsome preparation (Wilson et al., 2003).

1.9.1. Intestinal scaling factors

In the case of the intestine, very few scalars have been published from separate studies. Literature values for rat, dog and human can be found in **Table 1-7**. The lack of validation, limited reports and full characterisation of scaling strategies preclude confidence in extrapolation to *in vivo* using microsomal scaling factors.

As a result other strategies have been utilised in order to estimate intestinal intrinsic clearance for example, based on CYP3A abundance (Gertz et al., 2010). However, CYP isoform expression and microsomal scaling factors in the human intestine based on limited datasets (n=20) in contrast to liver (meta-analysis of n=241 for CYP abundance, and 108 for microsomal scalar) (Barter et al., 2007; Rostami-Hodjegan and Tucker, 2007), and from samples prepared by mucosal scraping, which can bias the estimate for reasons stated above (Paine et al., 2006; Cubitt et al., 2009; Cubitt et al., 2011). It must be also noted that this scaling strategies relies on CYP3A abundance from a limited dataset of characterised abundance data. Furthermore, as illustrated in the case of tacrolimus, F_G showed a general overprediction trend. The underestimation of the clearance of this drug may be a reflection of the alternative elimination pathways of this compound via UGT-mediated metabolism. Since no absolute UGT abundance data is available, incorporation of UGT metabolism into these reported F_G prediction's was not possible (Gertz et al., 2010).

Regional differences have been reported for the intestinal microsomal scalars (14.5-23.5 mg protein/g mucosa for duodenum and ileum, respectively, (Paine et al., 1997; Cubitt et al., 2009). In contrast, a single value for the whole intestine has been reported for scaling of intestinal cytosolic metabolic data (Cubitt et al., 2011), which may affect the assessment of the contribution of intestinal relative to hepatic sulphation. Regional scalars incorporating correction for losses have been reported in dog, but values are limited in terms of donors (n=4) (Heikkinen et al., 2012). No know corrected scalars have been reported in the rat.

Table 1-7 Reported literature values of microsomal scalars for proximal intestinal in rat, dog and human.

Scalar	Rat	Dog	Human	References
Microsomal protein (mg) per intestine (MPPI)	27.2±2.5 ϕ∏ 19.93ϕΔ 9.39±0.10∏			(Dawson and Bridges, 1981), (Bruyere et al.) (Yoon et al., 2011)
		170.04Δ		(Powell, 2006)
			452∏	(Zhang et al., 1999)
			2977ΔΨ	(Paine et al., 1997)
			1012.5	(de Waziers et al., 1990)
Microsomal Protein (mg) Per Gram (g) Mucosa (MPPGM)	10-15Δ		20.56Δ	(Hoensch et al., 1985)
			1.54 ±0.55Δ¥ Ψ	(Cubitt et al., 2009)
			15.2Δ¥	(Bruyere et al., 2010)
			8.4 Δ+	(Hoensch et al., 1979)
		54ϕ ∏ Ψ		(Heikkinen et al., 2012)
			3.9 ±0.2	(Pacifici et al., 1988)
Microsomal Protein (mg) Per Gram (g) Intestine organ (MPPGI)	2.0-3.0∏			(Borm et al., 1983a)
	2.1 ±0.2†			(Martignoni et al., 2006)
	2.39 ±0.11			(Koster and Noordhoek, 1983)
		12ϕ ∏ Ψ		(Heikkinen et al., 2012)
			0.37 ± 0.07*	(Bruyere et al., 2010)
			3.11 Δ ¥ Ψ	(Paine et al., 1997)

Key: ϕ proximal 60 cm of intestine, † microsomes obtained from direct tissue homogenisation, Δ microsomes obtained by Scraping, ∏ microsomes obtained by elution, ¥ duodenal surgical specimen, + ileum Sample, * microsomes obtained by scraping and elution, Ψ correction for losses made

1.9.2. The Q_{gut} model and PBPK approaches

Reasonable attempts have been made to extrapolating the exact relative contributions of the human, dog and rat intestine within physiology based pharmacokinetic (PBPK) models with varying degrees of mechanistic complexity (Cong et al., 2000; Agoram et al., 2001; Gertz et al., 2011; Heikkinen et al., 2013). For example, Advanced Compartmental Absorption Transit (ACAT) or the advanced dissolution, absorption and metabolism ADAM model which are multi-compartmental models which incorporate various physiological and compound specific parameters. For example, The ADAM model divides the GI-tract into nine segments that are heterogeneous in terms of size, abundance of enzymes and transporters, transit time, pH and bile salt concentration (Jamei et al., 2009;

Darwich et al., 2010). However, these models are limited by the lack of extensively defined drug specific parameters. In order to obtain true confidence in PBPK modelling of intestinal metabolism requires data with absolute transporter/enzyme abundances and/or adequate scaling factors, incorporating regional differences in these estimates and inter-individual variability data from large cohort of individuals with appropriate covariate analysis either in preclinical species or in man. Furthermore, many drug specific parameters are frequently not available, especially in early stages of drug development, and as such screening approaches are more relevant.

A simplified Q_{gut} model (**Equation 1-3**) represents a more simple one compartmental approach. Whilst this dramatically simplifies the regional differences in metabolism and transport expression and activities, relying heavily on the impact of Q_{gut}, a hybrid parameter consisting of both Q_{villi} (villus blood flow) and cellular permeability (CL_{perm}) (**Equation 1-4**) to drive prediction of F_G. Utilisation of this strategy provided modest predictions for low to medium intestinal extraction drugs. However, the highest prediction inaccuracy was seen for drugs with moderate to high intestinal extractions (F_G <0.5) (Gertz et al., 2010). This simple model provides an accessible approach for investigating intestinal metabolism, and has not knowingly been validated using microsomal based scaling approaches incorporating both CYP and UGT metabolism, and furthermore utilised as a tool to assess differences in intestinal metabolism between species.

Equation 1-3 $$F_G = \frac{Q_{GUT}}{Q_{GUT} + fu_G \times CLu_{int,G}}$$

Equation 1-4 $$Q_{GUT} = \frac{Q_{villi} \times CL_{perm}}{Q_{villi} + CL_{perm}}$$

1.10. Aims

The primary aim of this thesis is to determine intestinal microsomal scaling factors in preclinical species (rat and dog) as well as in human. In order to achieve this, it is first necessary to establish the best practice and develop a reproducible method for intestinal subcellular preparation, focusing predominantly on the use of enterocyte elution method. Since the sensitivities of the method of enterocyte preparation, homogenisation, and the impact of buffers have not previously been systematically assessed in one lab, the sensitivities of the method will be critically assessed. The reproducibility of the method will also be determined.

Correction for any potential losses during microsomal preparation will be made using multiple markers, namely CYP content, CYP and UGT activity probes (testosterone 6β-hydroxylation and 4-nitrophenol glucuronide formation, respectively. Activity probes will also be utilised in order to make cross-species comparisons and characterisation utilising the same preparation method. In addition, intestinal microsomes from individual species will be used to assess metabolic activity for a range of selected compounds using substrate depletion approach at low substrate concentration. Since intestinal yields are small, a validation of a combined CYP and UGT cofactor approach (Kilford et al., 2009) will be investigated in alamethacin activated intestinal microsomes in order to maximise efficiency of incubations.

Selection of compounds in this study will focus on drugs with available literature *in vivo* data and which undergo varying degrees of reported intestinal metabolism. A broad range physicochemical and pharmaceutically diverse marketed drugs, predominantly CYP3A and UGT substrates, will be investigated in intestinal microsomes from each species. Where data were not available, additional *in vivo* studies will be performed in rat and dog.

Regional variations of intestinal microsomal scaling factors and activities will also be examined in the dog and human in order to determine the contributions of different intestinal segments towards first-pass metabolism. Furthermore, comparison between dog proximal intestinal and hepatic microsomal scalars and metabolic activity data obtained in the same animal will be made.

Derived microsomal scaling scalars will be used to generate measures of unbound intestinal metabolic intrinsic clearance for both preclinical species and human. Metabolic data for selected drugs will be combined with generated permeability data in Caco-2 in

order to assess prediction accuracies of F_G estimates compared to *in vivo* measures of F_G using the Q_{gut} model. Since cross species comparisons in the literature are limited by different studies and microsomal preparations, and the low incidence of reported overlap of substrates, species differences in E_G will be assessed for the selected drug set in the current study.

Finally, prediction of intestinal absorption (estimated by compound physiochemical properties or Caco-2 based permeability data) and intestinal metabolism in each species will be used to assess the ability to predict oral drug bioavailability in individual species and to perform cross-species comparison.

1.11. Compound selection for studying intestinal metabolism

The compounds selected for this study were primarily selected on the basis of intestinal metabolism potential and previous literature studies e.g. Gertz et al., (Yang et al., 2007; 2010), and therefore the majority of compounds were substrates of either CYP3A4 or UGT. Rat, dog and human *in vivo* estimates of intestinal F_G through comparison of literature i.v. and p.o. data were compiled. The compounds studied in each species and the major route of metabolism is indicated in **Appendix Table 7-1**. Estimates of *in vivo* F_G for each species can be found in the respective chapters. A total of 29 compounds were studied, with 20 undergoing complete cross-species comparison across rat, dog and human.

2. Rat intestinal microsome preparation optimisation

2.1. Introduction

The estimation of the extent of intestinal metabolism from *in vitro* experiments depends both on the use of a validated and viable *in vitro* matrix, and the ability to extrapolate to *in vivo*. In case of intestinal microsomes, there is poor confidence in the scaling factors employed and as such is the primary aim of this PhD investigation. However, in order to facilitate reliable estimates of intestinal metabolism *in vivo* requires metabolically competent microsomes to be able to mimic the *in vivo* situation as best as possible.

Given the low availability of human tissue, the rat was selected as model for optimisation of the microsomal preparation procedure. In addition, a range of literature data available in this species (**Table 2-1**, **Table 2-2**), and its relevance to preclinical development of NCE's rationalised its choice further.

Intestinal microsomes have often been prepared by the scraping of the intestinal mucosa using a glass slide or spatula (Stohs et al., 1976; Lindeskog et al., 1986; Takemoto et al., 2003). However, scraping increases potential for mucosal contamination by other intestinal cell types, connective tissues and mucus (Hulsmann et al., 1974a; Lin et al., 1999). Alternatively, elution of enterocytes can be used. This method is advantageous as it has been reported to increase cell viability (87% *vs.* 61%, elution *vs.* scraping) (Borm et al., 1983c) and activity of microsomes (Mohri and Uesawa, 2001; Galetin and Houston, 2006) relative to mucosal scraping (**Table 2-1**).

Various sources are available in the literature which have utilised elution for preparation of intestinal microsomes, and the most comprehensive is described by Fasco et al., (1993). However, the cumulative effects of differing procedures are difficult to systematically assess as intestinal length, enterocyte preparation method, homogenisation, protease inhibitors used, as well as buffer constituents vary among the studies, as summarised in (**Figure 1-5**,**Table 2-2**). Most recently, use of a cocktail of protease inhibitors has resulted in the best protection of intestinal CYP enzymes (Bruyere et al., 2009). However, even studies using the same elution agent (e.g. Ethylenediaminetetraacetic acid (EDTA)), differed in the enterocytes preparation method where vibration using metal rods (Dawson and Bridges, 1981), gentle agitation (Fasco et al., 1993), tapping, or vigorously shaking (von Richter et al., 2004) were applied. Furthermore, studies vary with elution times and EDTA concentrations, and no systematic evaluation has taken place.

Table 2-1 Comparison of CYP and UGT activities in rat intestinal microsomes prepared through elution or scraping

Study	Protease inhibitor	Enterocyte Isolation Method	testosterone 6β-OH hydroxylation rate pmol/min/mg	4-NP glucuronidation nmol/min/mg
Takemoto et al.,(2003)	Cocktail	Scraping	42 ±2	3.8 ±1.6
Mohri et al., (2001)	PMSF	Scraping	<LOQ	2.1 ±0.33
Mohri et al., (2001)	PMSF	Elution	268.7 ±0	7 ±0.81

Cocktail: 1 µM APMSF, 1mgml-1 trypsin inhibitor, 10µM leupeptin, 0.04 Uml^{-1} aprotinin, 1 µM bestatin

Table 2-2 Comparison of rat mucosal, microsomal and cytochrome contents from studies utilising different isolation, homogenisation intestinal length and protease inhibitor conditions.

Study	n	Protease inhibitor	Enterocyte Isolation Method	Enterocyte Homogenisation Conditions	Wet wt of mucosa (g)	Microsomal Protein (mg) /cm (MPPcm)[a]	Specific CYP content (nmol/ mg protein)
†Damre et al., (2009)	4	PMSF	Mincing	Sonication		0.68	0.085
†Damre et al., (2009)	4	PMSF	Sc	Sonication		2.74	0.196
ϕBorm et al., (1983a; 1983b)	4	None	E (V - 40 min) 5mM EDTA	Potter-Elvehjem		0.15	0.065
ϕShirkey et al., (1979)	6	None	E (V- 35 min) 5mM EDTA	Potter-Elvehjem	~2		0.031
ϕDawson and Bridges, (1981)	6	None	E (V - 30 min) 5mM EDTA	Motor driven potter	1.94±0.07	0.45	0.16
ϕBruyere et al., (2009)	6	Cocktail	Sc & E (S- 20 min) 1.5mM EDTA	Motor driven potter / Sonication		0.33 ϕ^{Δ}	0.23
ϕBruyere et al.,(2009)	6	None	Sc & E (Sh- 20 min) 1.5mM EDTA	Motor driven potter / Sonication			0.13

E: Elution, V:vibration, Sc: Scraping, Sh:shaking a: no correction for losses, †from intestinal segment 20-25 cm proximal from the cecum, ϕ from 60 cm proximal intestine, Δ Correspondence data for male wistar rats, PMSF: phenylmethanesulphonyl fluoride, Cocktail: Antipan, Aprotinin, Bestatin, E64

In light of the 'toughness' of the enterocytes, sonication is generally used in addition to rotor driven homogenisation using a Potter-Elvejhem, based on the findings of Lindeskog et al., (1986). Since the process of microsome isolation is an inefficient process, release of maximal microsomal protein is important both in terms of yields and determining accurate measure of intestinal scaling factors. However, although CYP enzymes are sensitive to the sonication process (Hoensch et al., 1985), the impact of intensity has not been explored.

In addition, conflicting reports exist for the addition of glycerol which is routinely utilised in liver microsome preparation (Wilson et al., 2003). Glycerol is reported to infer up to 30% protection to CYP during homogenisation (Stohs et al., 1976); however, conversely no beneficial effect has also been reported (Bruyere et al., 2009). Furthermore, whilst heparin has been shown to increase the yield of microsomal protein by up to 30% through preventing agglutination and protein aggregation, this is at the expense of a reduced CYP concentration. However, the benefits of the inclusion of this anticoagulant may not be fully realised due to the impact of mucus contamination on microsomal recovery (Shirkey et al., 1979).

The overall potential impact of factors discussed above on total CYP contents and the resultant intestinal scalars have not been assessed systematically so far. As demonstrated in **Table 2-2**, specific CYP content can vary 8 fold between methods. Furthermore, given that the techniques employed for enterocyte and microsomal preparation have the potential to influence the microsomal protein yield (**Table 2-2**), the choice of a method may also affect the resulting scaling factors (Galetin et al., 2010).

2.2. Aims

Important parameters for both assessing sensitivity and reproducibility are good enzyme contents (implying but not necessarily meaning good activities) and yields of microsomal protein. Using the rat as a model for method optimisation, and primary markers of microsomal protein yields and CYP content, key parameters which may critically influence intestinal microsome preparation: elution time and EDTA concentrations; intensity of homogenisation; and the presence of heparin and glycerol, will be investigated. The direct systematic comparisons of intestinal microsome optimisation and impact of microsomal scaling factors will be discussed.

2.3. Materials and Methods

2.3.1. Reagents

All laboratory chemicals were purchased from either Sigma (Dorset, UK) unless detailed in the text. Product codes at time of writing are provided in parenthesis.

2.3.2. Source of animal tissue

The strain of rat investigated was the male albino Han-Wistar (Harlan, UK), 289 ±21 g, ranging from 9-10 weeks. Rats were subject to a 12/12 light cycle, and housed on solid bottom cages with Fibretron 6 (or 6 mesh) wood products for bedding and supplied with paper flake, rat tunnel and wooden chew block as environmental. The rats were fed on rat and mouse No.1 maintenance (RM1, SDS, Essex, UK), and water supplied by an automatic water system, both *ad lib*.

2.3.3. Optimisation of intestinal microsome preparation

Rat intestinal microsomes were prepared in-house at AstraZeneca, Alderley Park, UK. Since intestinal microsome yields are low, intestinal microsomes were pooled each day from of 3 rats as this was seen to provide increased yields without compromising preparation time, and therefore microsome quality. Animals were euthanised by rising CO_2 at approximately the same time each day (8.30-9.30am). Animals were either surplus to ongoing project study requirements or utilised from other ongoing in-house studies, and as such not solely sacrificed for removal of the intestine. Animals were bled prior to organ procurement in order to remove proteases present in the blood and thus reduce damage to intestinal CYPs, since the intestine (like the liver) is highly perfused (Bruyere et al., 2009). Death was confirmed by cervical dislocation, and the first 60 cm of intestine proximal to the pylorus was removed. The intestinal length of 60 cm (approximately 50% of the total rat intestinal length (Kararli, 1995) was selected as the most routinely utilised length in the literature (Shirkey et al., 1979; Dawson and Bridges, 1981; Fasco et al., 1993; Bruyere et al., 2009), and would therefore serve as a good comparator for assessment of primary parameters deemed important in prepared microsomes; i.e., microsomal yield and CYP content. Furthermore, the highest CYP content is reported in the proximal end of the intestine (duodenum and jejunum) (Zhang et al., 1996), and therefore this procedure should provide the greatest accuracy in measurements of CYP content.

Following extraction, the intestine was flushed to remove partially digested food material and excess mucus, using a wash buffer solution (pH 7.4) of 0.9% w/v NaCl (Fischer

Scientific, UK) and 0.5 mM dithiothreitol (DTT) (#D5652), a thiol, to prevent degradation of CYP. Furthermore, a protease inhibitor (PI) cocktail (#P8340) was added to prevent protease damage to CYP. Whilst this cocktail is known to have inhibitory potential to rat CYP2D [1] (Bruyere et al., 2009), this enzyme is reported to have more significant importance in the lower parts of the intestine (Mitschke et al., 2008). All solutions were prepared the day prior to isolation (with the exception of DTT which was added extemporaneously) and stored at 4°C. Excess fat was then removed from the tissue, and the segment blotted dry and weighed. Rat ages, body weights and 60cm intestinal weights from each preparation can be found in **Appendix Table 7-2.**

On transfer to the lab, intestines were flushed with 30ml of Solution A, pH7.4, consisting of phosphate buffered solution (PBS) buffer without Ca^{2+} and Mg^{2+} (#D5652) (used in all subsequent preparation buffers), 27 mM Sodium Citrate monobasic (#71497), 0.5 mM DTT, and PI (0.1% v/v, used at the same concentration in all subsequent solutions). Sodium citrate promotes cell to cell contact breakdown since it is an anti-coagulant, and acts to prepare cell dissociation prior to elution (Weiser, 1973). Intestines were then filled with solution A and reclamped, and incubated on ice in a trough of Solution A for 30 minutes. The entire preparation was performed at 4°C to limit warm ischemia and proteolysis.

The method for intestinal microsome preparation via elution was based on the method of Fasco et al., (1993), however 3 key steps based on differing reports in the literature were chosen for optimisation: elution conditions; homogenisation conditions; and two buffer constituents glycerol and heparin. A summary of the variables tested for intestinal microsome preparation is shown in **Figure 2-1**.

[1] Reported in publication as inhibition towards CYP2B, however reported in thesis and personal communication as towards CYP2D2 up to 50% inhibition, and CYP2D1 up to 30% inhibition (Bruyere A (2011) Personal Communication.)

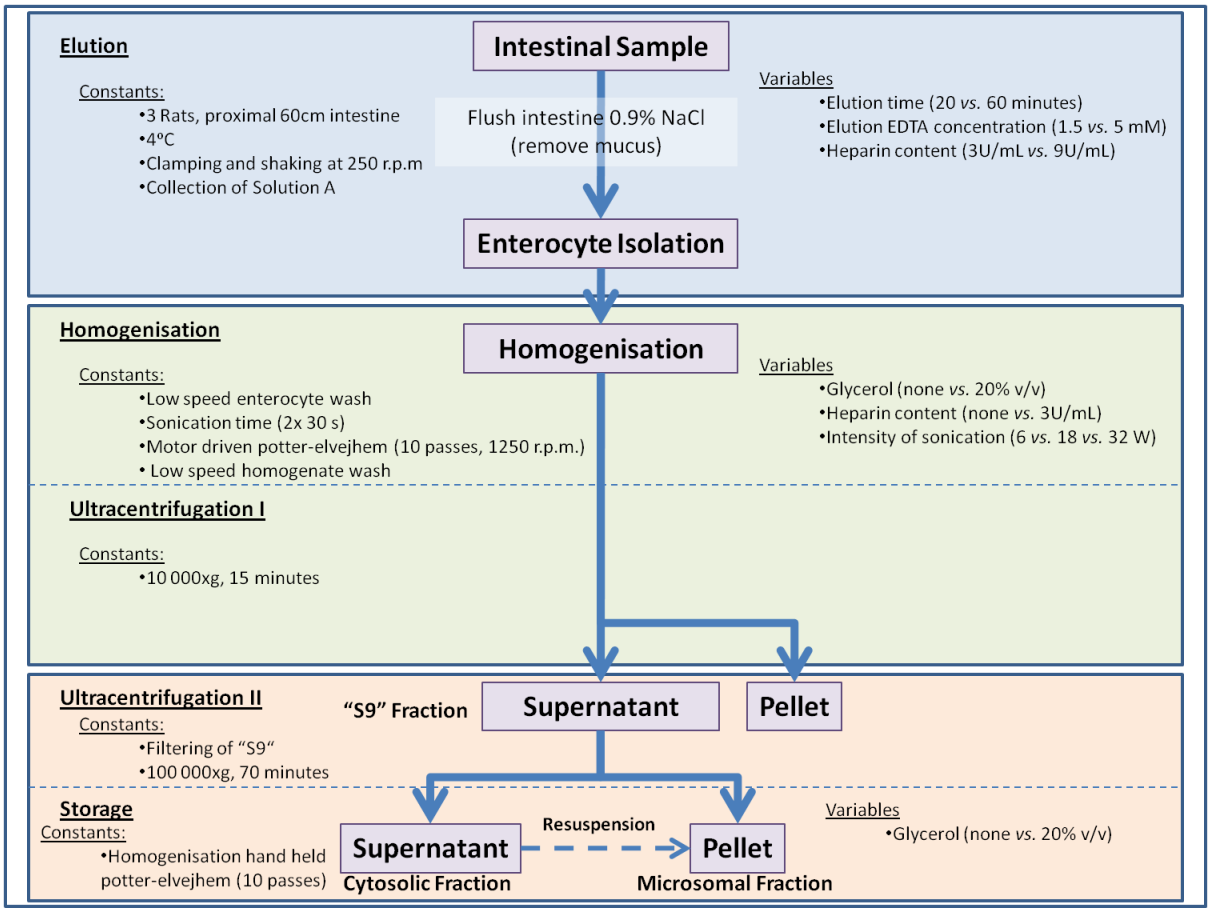

Figure 2-1 Schematic of general microsomal preparation and variables tested for optimisation

2.3.3.1. Enterocyte elution conditions

Intestinal microsomes were prepared by EDTA based calcium elution. EDTA binding to calcium disrupts the joining of cadherins responsible for cell adhesion, and allows cell detachment (Panorchan et al., 2006). Solution B (pH 7.4) contained PBS, EDTA (#EDS), 0.5 mM DTT and PI with 3 UI/ml heparin (#H3393). Heparin was used to reduce protein trapping by mucus and therefore improve pellet formation. When incubation conditions were varied, EDTA concentrations of 1.5 mM were compared to 5 mM.

Following incubation in solution A, intestines were subsequently flushed with solution B in order to collect the solution A elutant. Intestines were then filled until distended with solution B, clamped shut, and placed in a conical flask containing an incubation buffer solution (pH 7.2) of PBS and 20% v/v glycerol (#G2025) and then agitated on ice at 250 rpm (Orbital Shaker SSL1, Stuart) for 20 minutes. Solution B was drained into a conical flask and intestines flushed with 10ml of solution B, refilled with the same solution,

clamped and reagitated for a further 20 minutes two more times. When using a shorted incubation time of 20 minutes, the intestine was flushed with solution B following a 5 minute and two 10 minute incubations.

2.3.3.2. Homogenisation conditions

In order to minimise mucus contamination, the collected raw intestinal mucosa (containing enterocytes) was centrifuged at 2,000xg (Sorvall legend RT centrifuge, Thermo Fisher Scientific) for 10 minutes in pre-weighed centrifuge tubes published previously (Fasco et al., 1993). This procedure was repeated 2 further times to wash the pellet. Following the final centrifugation, the pellet was weighed (mucosal weight) and taken up by 3 ml of homogenisation buffer per g of cells. This buffer (pH 7.4) contained PBS, 0.25 M Sucrose (#S9378), 0.5 mM EDTA, 5 mM histidine (#H7750) and PI. Disruption of cells was achieved using a Potter-Elvejhem rotating homogeniser (10 passes, 1250 rpm) (IKA KS130 Basic). Homogenate was treated with an ultrasonic probe (VCX130PB, vibracell, Sonics, Newtown, USA) for 2 x 10 seconds burst (30 seconds between each burst), using a 10 -25 ml tip to disrupt the cell membranes. When comparing the effect of homogenisation conditions the amplitude of the sonication was varied to 20% (6W), 60% (18W) and 100% (30W). The obtained homogenate was re-homogenised using the Potter-Elvejhem. A 4 ml sample of homogenate was then collected and utilised for protein and CYP measurements for correction for losses. Homogenate was spun at 1,000xg for 4 minutes three times, washing the pellet in homogenate buffer and collecting the supernatant.

Homogenate was ultracentrifuged at 10,000xg (Optima LE-80K, Beckman Coulter, 50.2Ti rotor) for 15 minutes to pellet the mitochondria, peroxisomes, intact cells, lysosomes and nuclei. The ‘S9’ supernatant was filtered through NYTAL filter mesh (pore size: 150 µm) (Lockertex, Warrington, UK) and then ultracentrifuged for 70 minutes at 100 000xg. The final pellet was re-homogenised with 10 passes on ice in a 5ml Potter-Elvehjem homogeniser in Tris hydrochloric acid (HCl) (#T5941) buffer (pH 7.4) containing PI with or without 20% v/v glycerol (#G6279). Microsomal samples were stored on ice (for immediate protein and CYP content analysis) and remaining yield stored at -80°C.

2.3.3.3. Assessment of the heparin and glycerol effect

The effect of addition of glycerol (20% v/v) to the homogenisation buffer (Solution C) and the storage buffer (Solution D) was investigated. Glycerol is routinely used with liver microsome preparation (Wilson et al., 2003) and other extrahepatic microsomes e.g. lung

(Burke and Orrenius, 1979) since it is reported to protect CYP during homogenisation (Stohs et al., 1976). Furthermore the addition of heparin (3Ul/ml) to the homogenisation and centrifugation buffer (solution C) was tested to attempt to increase microsomal yield since it prevents aggregation caused by mucus contamination (Stohs et al., 1976). Finally, the impact of using 9U/ml heparin in the incubation buffer (solution B) was investigated, using no glycerol or heparin in solution C. All experiments investigating the effects of glycerol and heparin were undertaken following homogenisation at 100% amplitude (30W) sonication and 5 mM EDTA.

2.3.4. Determination of protein content

The total protein content of both homogenate and microsome samples was assessed using the Bicinchoninic acid (BCA) Assay (#23227, Pierce Biotechnology, IL, USA,) based on the method of Smith et al., (1985). Unknown diluted sample concentrations (1:20 and 1:10 for microsomes and 1:20 and 1:50 for homogenate diluted in 0.1M potassium phosphate buffer, pH 7.4) were plated in triplicate on black 96 well clear flat bottomed plates (#3631, Costar, NY, USA,), diluted in 1:8 (sample: working reagent), incubated at 37^{o}C for 30 minutes, and absorbance read at 562nm using a Tecan safire 2 spectrafluor (Tecan Group Ltd, Switzerland). Protein concentrations where quantified by extrapolation to a bovine serum albumin (BSA) standard curve (range 2 to 0.025 mg/ml) using the regression data analysis tool pack in Microsoft Excel 2007 (Microsoft, WA, USA).

2.3.5. Determination of Cytochrome P450 content

A Shimadza UV-24001 Double Beam spectrophotometer was used to measure CYP content of intestinal homogenate and microsomal samples. Measurement of CYP was achieved using the method of dithionate-difference spectroscopy (Matsubara et al., 1976) where the difference between the CO-complex of ferrous CYP and the oxidized pigment are measured. The method of reduced minus oxidised difference spectrum method (Omura and Sato, 1964) was not used to prevent interference by any haemoglobin which might have contaminated the samples (Wilson et al., 2003). Homogenate and microsomal preparations were diluted to 3 mg/ml with 0.025 M potassium phosphate buffer, containing 1.15% w/v potassium chloride (KCl) (#P9541) and 30% v/v glycerol as per Wilson et al., (2003), except that this solution was at pH 7.4 rather than pH 7.25. Samples where bubbled for 1 minute (1-2 bubbles/sec) with carbon monoxide (CO), transferred to 1ml semi-micro cuvettes (#634-2501, VWR, Pennsylvania, USA) and a baseline reference measured

between 400 and 600 nm. A fresh solution of 200 mg/ml sodium dithionite (#157953) was prepared in assay solution, and 10 µl added extemporaneously to sample cuvettes. Samples were inverted 4 times, and left to stand for 4 minutes before reading. The absorbance of samples between 390 and 600 nm was recorded and the difference in absorbance between 450 (absorbance maxima) and 490 nm (isobestic point) measured. The concentration of CYP in the sample was determined using **Equation 2-1.** All samples were analysed in triplicate.

Equation 2-1 $$nmolCYP.mg^{-1} = \frac{\Delta\, Absorbance_{\,450-490\,nm}}{\varepsilon_{450-490} mM^{-1} cm^{-1}.[\text{Protein (mg.ml}^{-1})]}$$

Where $\varepsilon_{450\text{-}490}$ = 104 mM/cm (Matsubara et al., 1976).

2.3.6. Recovery and correction for losses

The microsomal specific marker of measured CYP content was utilised to act as a of a measure of loss (recovery factor) of microsomal protein (Wilson et al., 2003; Barter et al., 2007; Smith et al., 2008). Recovery was calculated in a similar fashion to these studies; except that total protein content in homogenate was also corrected for the sample of homogenate removed prior to ultracentrifugation to increase recovery precision (**Equation 2-2**). Corrected measures of microsomal protein normalised for intestinal weight, mucosal yield or per cm (MPPcm) of intestine length were determined using **Equation 2-3**, **Equation 2-4**, and **Equation 2-5**, respectively.

Equation 2-2

$$Recovery\ Factor = \frac{nmoles\ CYP_{mic} \times mg\ Protien_{mic}{}^{-1} \times total\ mg\ Protein_{mic}}{nmolesCYP_{hom} \times mg\ Protein_{hom}{}^{-1} \times (total\ mg\ Protein_{hom} - mg\ protein\ removed_{\,\text{hom}})}$$

Equation 2-3 $$Corrected\ MPPGI = \frac{mg\ Protein_{mic} \times gram\ of\ intestine^{-1}}{Recovery\ Factor}$$

Equation 2-4 $$Corrected\ MPPGM = \frac{mg\ Protein_{mic} \times gram\ of\ mucosa^{-1}}{Recovery\ Factor}$$

Equation 2-5 $$Corrected\ MPPcm = \frac{mg\ Protein_{mic} \times cm\ length\ of\ intestine^{-1}}{Recovery\ Factor}$$

Where hom= homogenate and mic = microsomes.

2.3.7. Data analysis

Tests comparing means using Student's t-test to test for statistical significance at a level of 5%of individual mucoasl yields, microsomal CYP content, recovery, and values of corrected and uncorrected of MPPGI, MPPGM, and MPPcm for each preparation method was calculated using SPSS Statistics version 20 (IBM, Chicago, Illinois, USA).

2.4. Results

Optimisation of rat intestinal microsome preparation comprises two main investigations, the impact of the initial enterocyte elution conditions, and effect of changes to the intensity of homogenisation. Investigations were assessed in isolation, and also with the presence of buffer constituent's glycerol and/or heparin, as detailed below.

2.4.1. Investigating the impact of enterocyte elution conditions

Use of different EDTA concentration (1.5 and 5mM) and 60 minutes incubation resulted in no significant differences in mucosal (i.e. enterocyte) yield, CYP content, or uncorrected microsomal protein yield (**Figure 2-3**). Mean mucoasl yield and microsomal yield was however marginally higher in the presence of increased EDTA concentration. Comparison of 20 and 60 minute elution procedures undertaken at 5mM EDTA indicated that incubation times of 20 minutes produced a significantly lower mean mucosal yield (0.25 *vs.* 0.47 g/g intestine, $p<0.05$) (**Table 2-3**); however, a statistically higher CYP content (138.6 nmol/mg *vs.* 45.6 nmol/mg, $p<0.05$) was observed. No statistical difference was observed in values of uncorrected microsomal yields, although the mean value was lower.

Recovery and therefore correction for losses was not possible for 60 minute incubations as the CYP spectrum was below the limit of quantification for the homogenate samples under these conditions (**Figure 2-2A**). Incubations of 20 minutes did however yield homogenate with enough CYP content to calculate microsomal recoveries and correct for losses during microsomal preparation (**Figure 2-2B**); however, CYP content was still low.

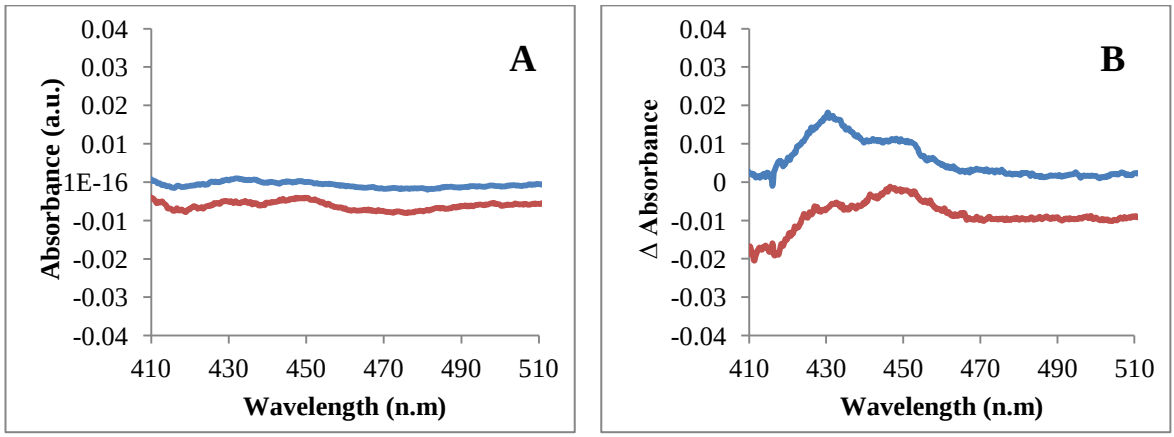

Figure 2-2 Representative plot of homogenate and microsomal CYP spectra at 3mg/ml using 5mM EDTA and 60 minute incubation (A) or 5mM EDTA and20 minute incubation (B).

Blue: homogenate, Red: microsomes.

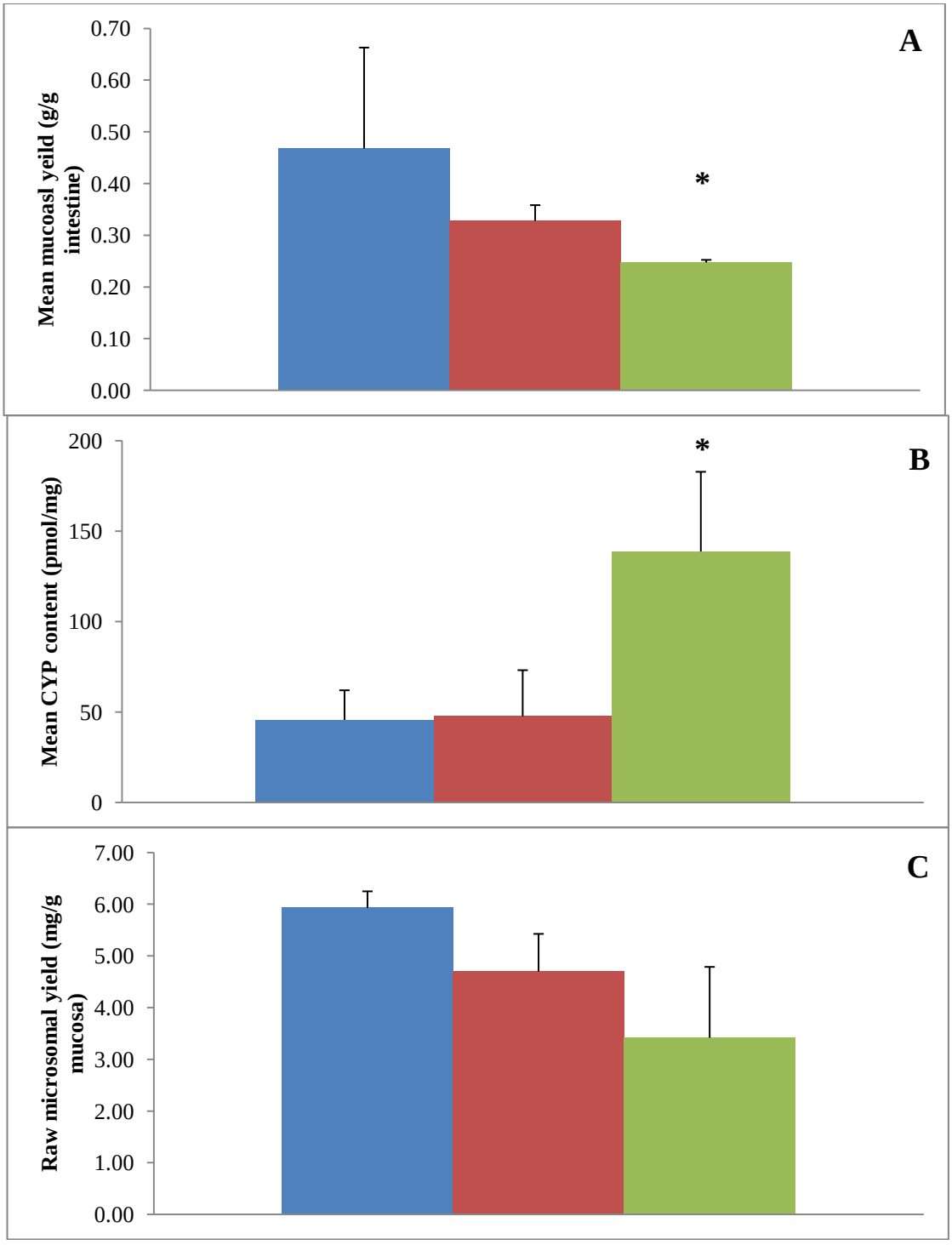

Figure 2-3 Comparison of mean enterocyte yields (A) specific microsomal CYP contents (B) and uncorrected protein yields per gram intestine (C) under varied incubation times and concentrations.

Blue: 5mM EDTA, 60 minutes; Red: 1.5mM EDTA 60 minutes; Green: 5mM EDTA, 20 minutes. Homogenisation sonication intensity was set at 20% (6W) and N=3 for all incubation conditions. *: $p<0.05$.

2.4.2. Investigating the impact of homogenisation conditions

A range of homogenisation conditions were investigated and their impact on either CYP content or microsomal yield was assessed. No significant change in specific CYP content was observed following homogenisation at sonication intensities of 6, 18 or 30W (138.6, 112.1 and 127.0 nmol/mg, respectively) (**Figure 2-4A**,**Table 2-3**).Elution conditions were kept unchanged throughout at 5mM for 20 minutes, and no differences were observed in mean mucoasl yields. However, the yield of raw microsomal protein was statistically higher (3.42 *vs.*7.77 mg, $p<0.05$) following treatment at the highest intensity (30W) (**Figure 2-4B**). This resulted in a 2.7 fold higher total CYP content of 8.8 *vs.* 24.4 nmol, $p<0.05$, for 6W and 30W, respectively.

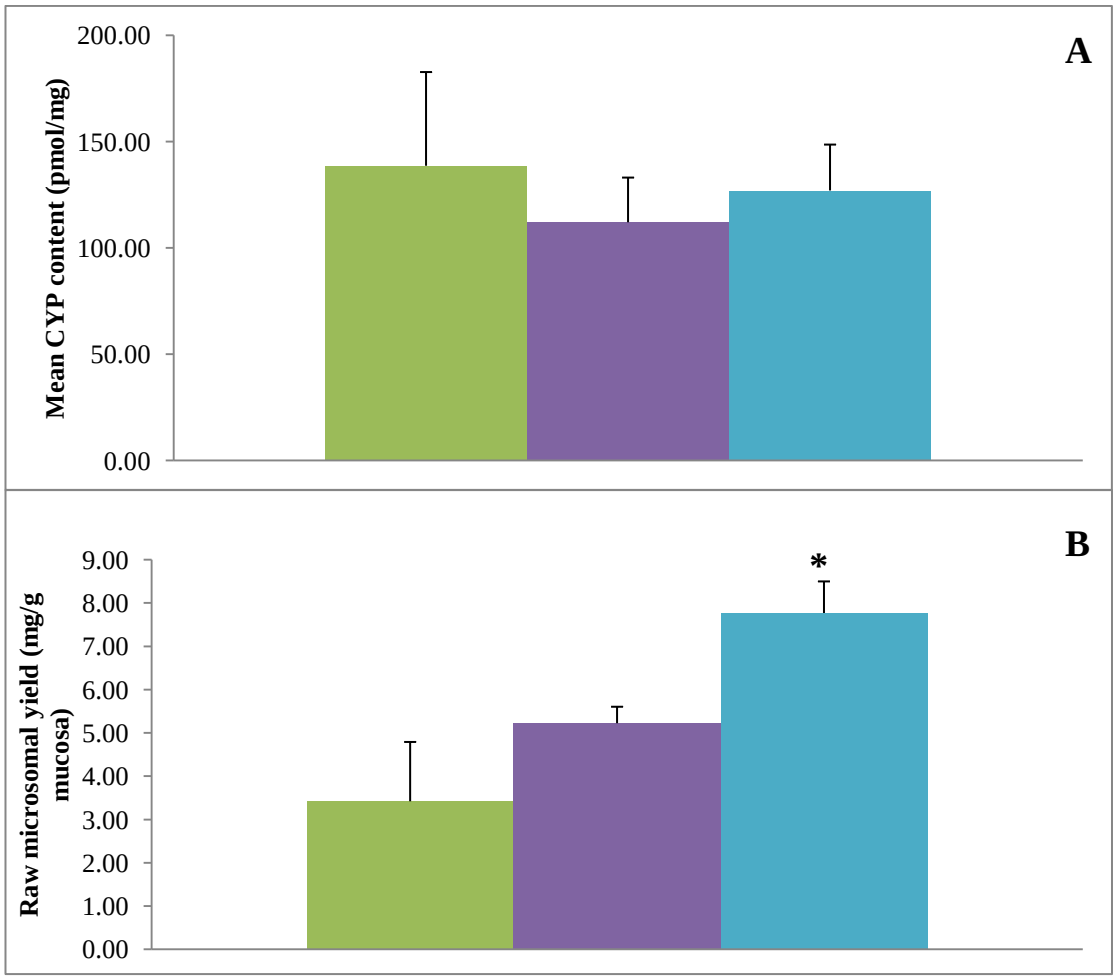

Figure 2-4 Comparison of specific microsomal CYP contents (A) and uncorrected protein yields per gram intestine (B) under varied homogenisation sonication intensities.

Green: 20% (6W), Purple: 60% (18W), Turquoise: 100% (30W). Incubation conditions were 5mM EDTA, 20 minutes and N=3 for all homogenisation intensities. *: $p<0.05$ relative to 20% (6W).

2.4.3. Investigating the impact of heparin and glycerol

The effect of addition of 20% v/v glycerol both to the homogenisation (solution C) and storage buffers (solution D) resulted in a high mean CYP content (203.1 nmol/mg) (**Figure 2-5**, **Table 2-3**). However, the CV was high (75%), and mean uncorrected MPPGM compared to the 100% (30W) sonication control was reduced (from 1.68 to 1.38 mg/g mucosa). The addition of 3U/ml heparin to both solutions B and C (in combination to the glycerol in solutions C and D) resulted in a 1.8-fold increase in a mean mucosal yield (0.39 *vs.*0.22 g/g intestine), and an increased mean uncorrected MPPGM yield (2.77 mg/g mucosa). However, mean CYP content, was reduced compared to no heparin control (127.0 nmol/mg *vs.* 95.9 nmol/mg). The removal of heparin from solution C, increase in heparin content from 3U/ml to 9U/ml in solution B, and removal of glycerol from solutions C and D resulted in the highest mean CYP specific content, (243.6 ±107.7 pmol/mg , $p<0.05$, CV 44%). Mean uncorrected microsomal yields were however significantly reduced under these conditions (5.77 *vs.* 7.77 MPPGM, $p<0.05$). The highest mean CYP total content was also observed under these conditions (28.3, 13.3, 16.7 and 24.4 nmol for heparin and glycerol, glycerol and 30W sonication control, respectively). Furthermore, similar to the observations seen previously with the addition of heparin, mean mucosal yields were 2.2-fold higher ($p<0.05$) in comparison with no glycerol controls.

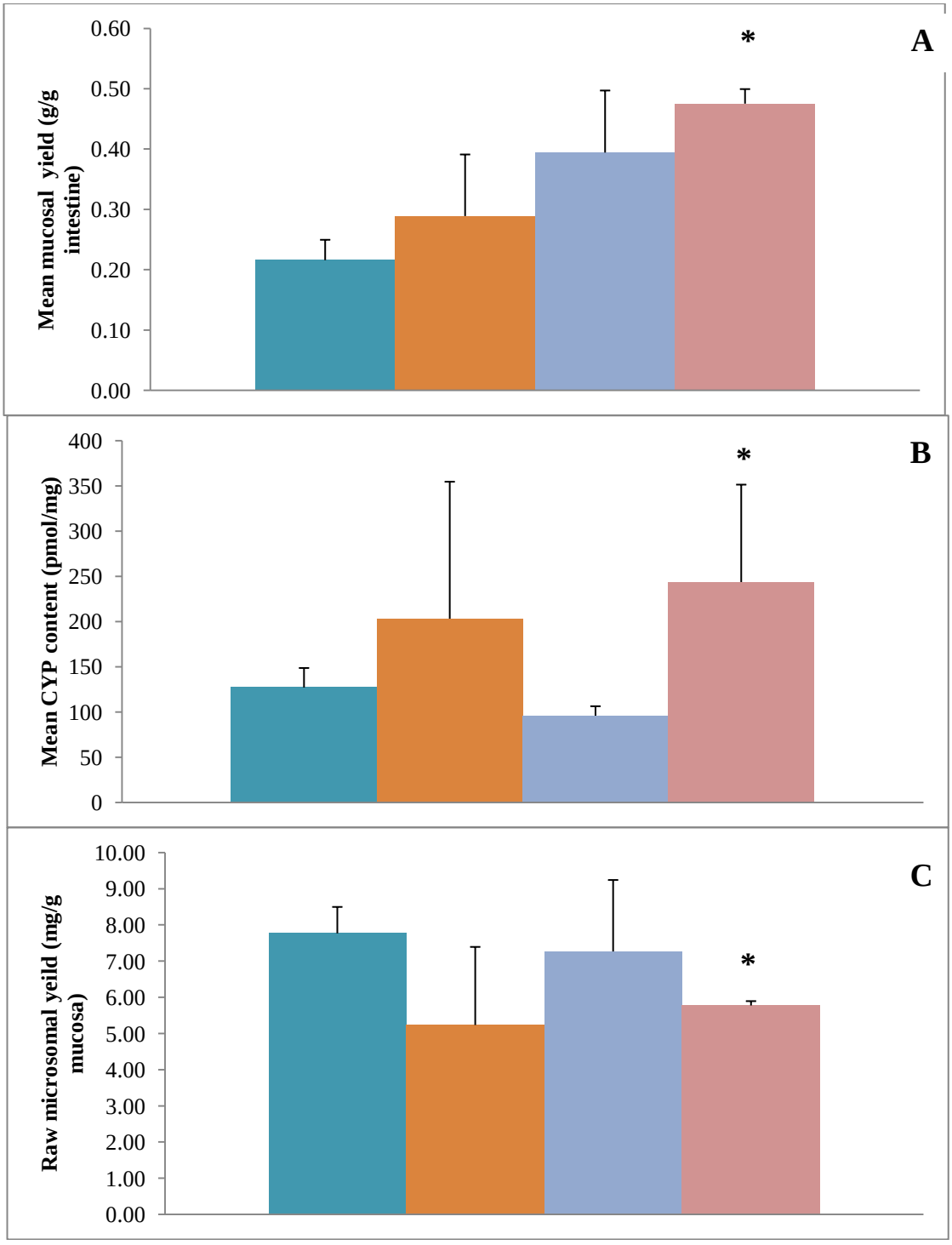

Figure 2-5 Comparison of mean mucosal yields (A) specific microsomal CYP contents (B) and uncorrected protein yields per gram intestine (C) under varied homogenisation sonication intensities.

Turquoise: No heparin or glycerol, Orange: glycerol added to all, Blue: glycerol and heparin added to all, Pink: heparin 9U/ml in solution B, no glycerol. Incubation conditions set at 5mM EDTA, 20 minutes, homogenisation intensity at 100% (30W) and N=3 for all buffer conditions. *: $p<0.05$ relative to No heparin or glycerol.

2.4.4. Recovery and correction for losses

The effect of the preparation methods on recoveries and intestinal scalars is summarised in **Figure 2-7** and **Table 2-3**. Mean mucoasl yields were greatest at 5 mM EDTA and longer incubation (60 minute (condition 1) and also when heparin content was increased in solution B (condition 8) using 20 minute incubation (0.47 and 0.48 g/g intestine, respectively). Mean specific CYP content was however 5.3-fold lower in condition 1 relative to condition 8 (**Table 2-3**). Recoveries of microsomal protein were the highest with the inclusion of glycerol and/or heparin; however, the inclusion of glycerol alone resulted in the highest variability (CV 64%). In comparison to the 100% (30W) sonication control (condition 5) the CV was 50%. In the presence of heparin alone (condition 8), the microsomal recovery was 2.6-fold higher than condition 5 with a CV of 12.9%.

Table 2-3 Summary of mucosal yields, CYP content and recoveries, and respective scalars resulting from differing preparation methodologies.

Condition	#	Mean mucosal yield (g/g intestine)	Mean CYP content (pmol/mg)	Recovery (%)	MPPGI (mg/g)	MPPGM (mg/g)	MPPcm (mg/cm)	Total CYP content (nmol)
EDTA_A_Son_A	1	0.47 ±0.20	45.6 ±16.4	H<LOQ	H<LOQ	H<LOQ	H<LOQ	11.5 ±4.5
EDTA_B_Son_A[a]	2	0.33 ±0.03	47.6 ±25.5	H<LOQ	H<LOQ	H<LOQ	H<LOQ	8.2 ±7.1
EDTA_C_Son_A	3	0.25 ±0.01	138.6 ±44.1	19.8 ±8.1	4.6 ±1.6	18.7 ±6.8	0.38 ±0.12	8.8 ±0.7
EDTA_C_Son_B	4	0.27 ±0.02	112.1 ±21.0	12.7 ±7.4	14.2 ±8.4	51.5 ±27.4	1.07 ±0.58	20.1 ±7.9
EDTA_C_Son_C	5	0.22 ±0.03	127.0 ±21.6	15.1 ±7.5	13.5 ±8.2	59.6 ±27.8	1.13 ±0.71	24.4 ±13.0
Glycerol[b]	6	0.29 ±0.10	203.1 ±151.4	28.5 ±18.2	7.9 ±7.7	27.9 ±22.5	0.72 ±0.72	16.7 ±8.4
Glycerol_Hep_A[b]	7	0.39 ±0.10	95.9 ±10.5	31.9 ±14.7	9.5 ±3.3	24.0 ±4.1	0.76 ±0.23	13.3 ±5.3
Hep_B[b]	8	0.48 ±0.02	243.6 ±107.7	38.7 ±5.0	7.2 ±1.3	15.1 ±2.1	0.65 ±0.15	28.3 ±14.1

Data represent mean +/- sd of n=3. EDTA_A: 5mM EDTA, 60 minutes, EDTA_B: 1.5mM EDTA, 60 minutes. EDTA_C: 5mM EDTA, 20 minutes, Son_A: 20% (6W) sonication, Son_B: 60% (18W) sonication, Son_C: 100% (30W) sonication, Hep_A: 3U/ml in solution C, Hep_B: 9U/ml in solution B, H<LOQ: Homogenate CYP below limit of quantification, a: data derived from n=3 tissues, n=2 CYP measurements, b: Incubation conditions: 5mM EDTA, 20 minutes; homogenisation conditions: 100% (30W) sonication, Heparin was present at 3U/ml in solution B in all preparations except preparation 8.

The highest microsomal protein yields were observed in the longer incubations (preparations 1 and 2) for all the normalised corrected scalars. No significant differences in corrected scalars expressed per gram intestine (MPPGI) or per cm (MPPcm) were observed for all the 100% (30W) sonication preparations (condition 5-8). However, a significantly lower (3.9-fold) scalar was obtained for preparation 8 *vs.* preparation 5 when expressed on a gram mucosa. Fold differences in MMPGI and MPPcm were 1.7 fold. A 2.2- fold difference in mucosal yields was observed. An example wavelength scans of microsomal and homogenate samples from preparation 8 are shown in **Figure 2-6**. Peaks are observed at 557, 450 and 428 nm.

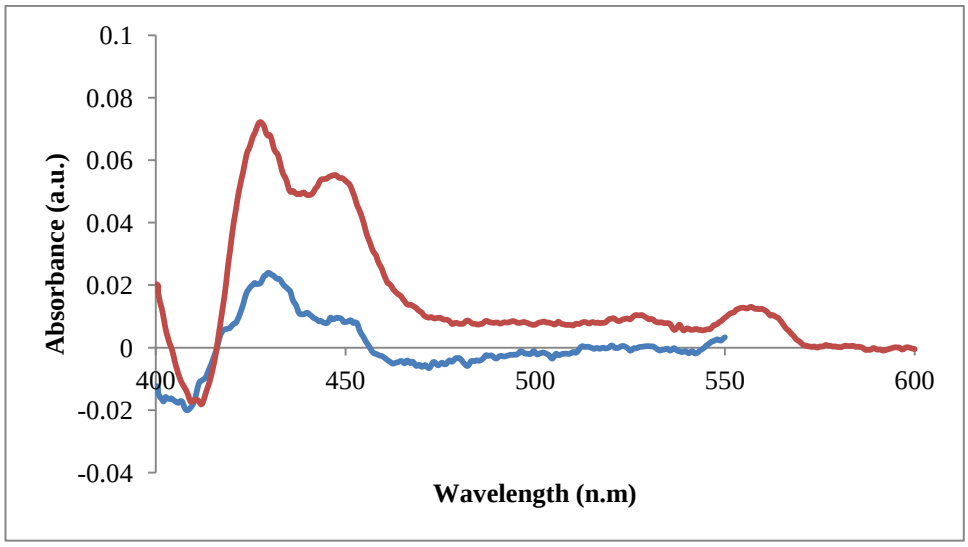

Figure 2-6 Representative plot of homogenate and microsomes CYP spectra at 3mg/ml for preparation 8.

Blue: homogenate, Red: microsomes.

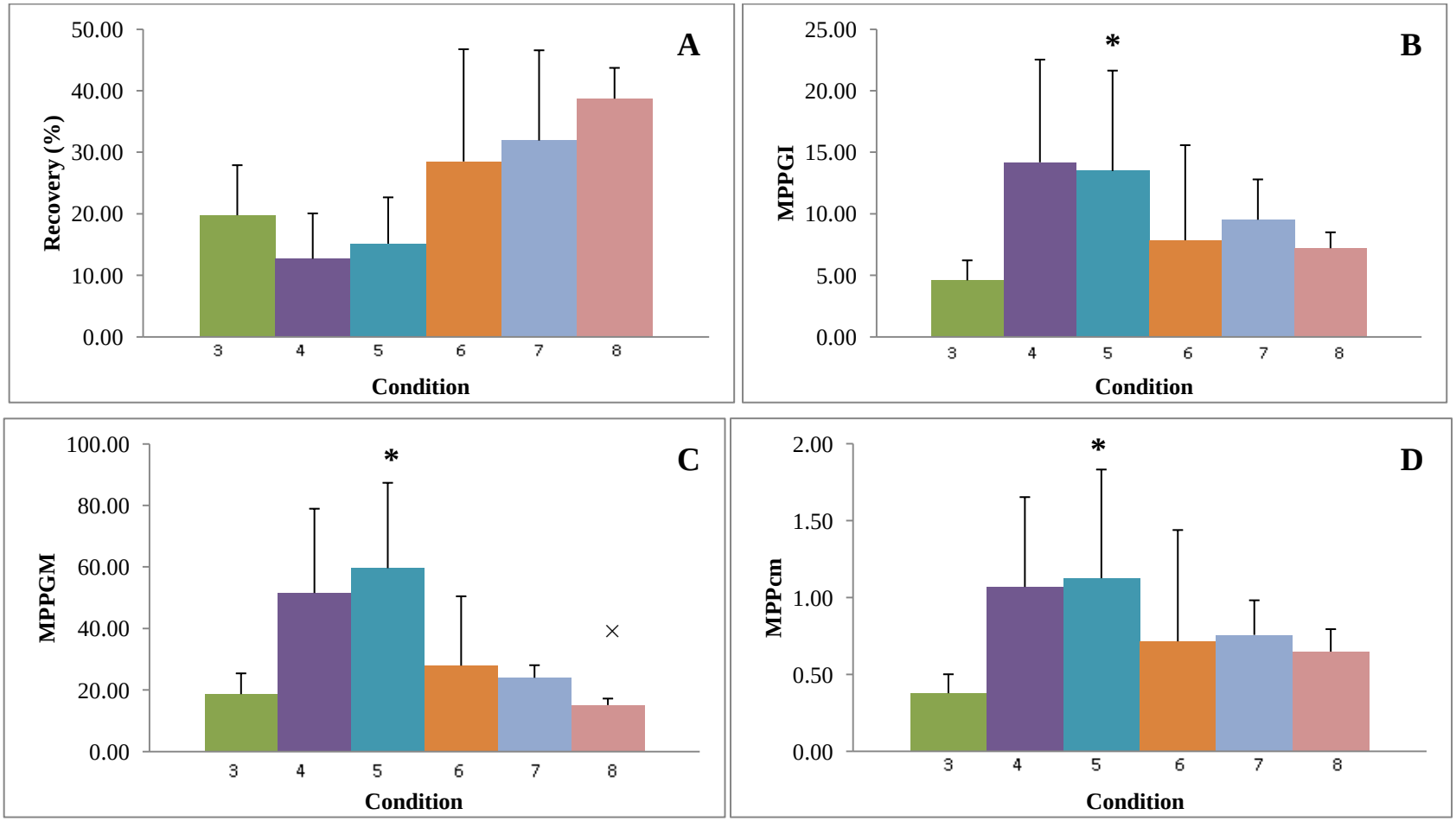

Figure 2-7 Comparison of microsomal recoveries (A), and scalars expressed as MPPGI (B), MPPGM (C) and MPPcm (D).

*: significantly different to condition 3 ($p<0.05$), ×: significantly different to condition 5 ($p<0.05$). Condition numbers correspond to those in **Table 2-3**.

2.5. Discussion

Given the reported superiority of activities of intestinal microsomes prepared by elution vs. scraping (Mohri and Uesawa, 2001; Galetin and Houston, 2006), this technique was selected as best practice. However, the varied preparation techniques employed in the literature meant the requirement for method optimisation and validation. Markers of CYP content and intestinal yield were selected as markers since more viable microsomes would be expected to be more metabolically active, and furthermore provide more sensitive measure of intrinsic clearance. Furthermore, a balance of increased yield is required for the ability for multiple repeated marker measures to assess reproducibility and increase confidence in measures of metabolism potential of screened compounds. Key steps were chosen with which to optimise the method included, firstly factors effecting enterocyte elution; incubation time and EDTA concentration. Secondly, factors affecting microsomal protein and CYP yields were assessed; homogenisation sonication intensity, and buffer constituents: glycerol and heparin. It was observed that subtle changes to the method impacted both CYP enzyme contents as well as microsomal yields.

2.5.1. Impact of preparation conditions on microsomal CYP content yield

EDTA binding to calcium disrupts the joining of cadherins responsible for cell adhesion, and allows cell detachment (Panorchan et al., 2006). Two commonly applied EDTA concentrations of 1.5mM and 5mM were chosen for comparison (Dawson and Bridges, 1981; Fasco et al., 1993). When compared using a 60 minute incubation time, CYP content was below the limits of detection in intestinal homogenate meaning no reliable estimate of recoveries could be made, and therefore microsomal scaling factors could not be calculated. Due to the heterogeneous expression of various cell types other than enterocytes in the intestinal mucosa (consisting also of e.g. mucus-secreting goblet cells, endocrine cells, Paneth cells), the enterocytes only account for around 25% of the total wet weight (Burke and Orrenius, 1979; van de Kerkhof et al., 2006; Thelen and Dressman, 2009). Therefore, a shorter incubation time (20 minutes) was selected in order to ensure minimal contamination of other non-enterocytic cell types and provide increased measure of CYP contents for making more reliable recovery estimates. As a result, a statistically lower mucosal (i.e. enterocyte) wet weight yield (1.9-fold), and higher microsomal CYP content (138.6 nmol/mg *vs.* 45.6 nmol/mg, $p<0.05$) was observed, suggesting a reduced contamination. Furthermore, it is likely that a reduced preparation time may impact on an increased CYP yield through reduced damage (Burke and Orrenius, 1979). However, it

was not possible to suggest if this was a result of a decreased P420 denaturation characteristic of P450 inactivation (Stohs et al., 1976) due to the low content of CYP in the 1hr incubation samples (**Figure 2-2**.)

The application of sonication to promote increased release of microsomal protein has been demonstrated to be necessary to ensure complete disruption of enterocytic cells (Lindeskog et al., 1986). This may not be surprising taking into account their location as a barrier for the body to the external environment. However, CYP enzymes are sensitive to the intensity of homogenisation, as demonstrated in preparation of liver microsomes, where 7-ethoxycoumarin O-deethylase activity, decreases following treatment at 30W for over 20 seconds (Hoensch et al., 1985). Given these sensitivities, it was therefore important to ensure that increasing homogenisation intensities would not impact intestinal microsome preparation.

Using increasing homogenisation intensities (6, 18, 30W, all 2 sets of 10 seconds) no significant change in CYP content was observed. However, microsomal yields were statistically higher (approximately 2-fold) and in agreement with a 1.5-fold increase in yield of total CYP, suggesting that there was a minimal induced damage to P450, whilst increasing the overall microsomal yields since recovery was almost unchanged (19.5 *vs.* 21.6% for conditions 3 and 5, respectively). Therefore, 20 minute incubation with 5mM EDTA was selected as optimal preparation conditions for enterocytes.

Glycerol is routinely added to homogenisation buffers during the preparation of hepatic microsomes. Its addition has been reported to protect CYP during homogenisation procedure and has been applied with success to other extrahepatic microsomes e.g. lung (Burke and Orrenius, 1979). Mean specific CYP content in the absence of glycerol was 36% lower than when it was present in the homogenisation buffer (solution C). This was in line with previously reported data which suggested a 25-35% reduction when glycerol is excluded (Stohs et al., 1976). However, the inclusion of glycerol was poorly reproducible since the CV increased from 44% to 75% compared to the no glycerol control, and there was no significant difference in the total CYP protein (8.8 ±0.7 nmol *vs.*16.7 ±8.4 nmol for conditions 5 and 6 respectively). Therefore, inclusion of glycerol was not seen to be beneficial for intestinal microsomal preparation considering its poor reproducibility, in agreement with recent reports (Bruyere et al., 2009). Alternative strategies, including heparin was therefore trialed to attempt to improve microsome preparation further.

Intestinal mucus represents a particular problem to microsomal preparation since it tends to aggregate cellular and subcellular material and as such influences the homogeneity of the preparations (Hulsmann et al., 1974b; Kaminsky and Fasco, 1991). Strategies for limiting mucus contamination are predominantly focused around flushing of the intestine prior to enterocyte isolation. Preparation of enterocytes via elution partially limits, mucus contamination than scraping techniques by the more selective isolation of the epithelial layer from the underlying lamina propria (Shirkey et al., 1979), however prevention of mucus contamination not complete. The addition of heparin prevents agglutination and protein aggregation, and has been reported to increase the protein yield up to 30%, but at the expense of decreasing the CYP concentration (Stohs et al., 1976; Burke and Orrenius, 1979).

Similar to the literature, the addition of heparin to solution C had a dramatic effect on both microsomal protein yields and specific CYP contents. When heparin and glycerol were both present and compared to the no addition control (preparation 5) there was a 31% reduction in specific CYP content and a 3.3-fold increase in raw microsomal protein yield. No literature values are available for the effect of heparin alone at 9U/ml in solution B. However, the inclusion of heparin resulted in a 1.8-fold increase in CYP specific content to values similar to 0.23 ±0.04 nmol/mg reported in the literature (Bruyere et al., 2009). Furthermore, microsomal protein was also increased, resulting in a 1.7-fold increase in total CYP content, the highest for all conditions investigated.

2.5.2. Impact of preparation conditions on recovery and correction for losses

So far, corrected scaling factors for the rat intestine have not been reported in the literature. However, estimates of microsomal recovery in rat intestine measured through aryl-esterase activity have been reported to be between 45 and 60% (Stohs et al., 1976; Shirkey et al., 1979). Mean recovery in this investigation in the absence of heparin and/or glycerol was between 12.7 and 19.8 %. Inclusion of glycerol increased recovery to 28.5-31.9%. The highest recovery (38.7%) was however observed in condition 8, when 9U/ml heparin was present in solution B during elution with a low CV (13%). This also corresponded to a 2.2-fold increase in mucosal yield, suggesting that heparin provides a greater wet weight of enterocytes, most likely through preventing aggregation of protein by mucus. Total mean mucosal yields expressed per intestine using this method were 2.56 ±0.24g (0.48 g/g intestine), similar to those reported previously (0.33 g/intestine) (Shirkey et al., 1979; Dawson and Bridges, 1981; Borm et al., 1983c) (**Table 2-2**). The largest yields of raw

microsomal protein were also observed under these conditions, suggesting that increased heparin content in the in the initial elution also was beneficial for higher microsomal yields, most probably due to a decreased mucus contamination. Corrected MPPcm (0.65 ±0.15 g/cm) from the final optimised method was higher, compared to uncorrected estimated values of 0.45 (Dawson and Bridges, 1981) and 0.33 g/cm (Bruyere et al., 2009) (**Table 2-2**).

The impact of homogenisation intensity had the greatest effect on microsomal scalars. Comparing the 20% (6W) and 100% (30W) homogenisation, there was a significant 2-fold increase for all normalised scalars. However, when comparing all the homogenisations at 30W, only when expressed per gram mucosa was there any significant difference between conditions 5 and 8. In this case, a significantly lower (3.9-fold) scalar was obtained for condition 8 *vs.* condition 5 when expressed on a gram mucosa. By comparison, fold differences in MPPGI and MPPcm were 1.7-fold. Interestingly, the fold difference between MPPGM and either MPPGI and MPPcm for preparation 8 was however 2.2-fold, reflecting the observed fold difference in mucosal yields between both preparations. These findings highlight the sensitivity of this scalar therefore to the increased wet weight of mucosal cells yielded with addition of 9U/ml heparin in solution B. Therefore, when comparing between labs, a normalisation based on intestinal weight or length may be more comparative, whereas measures based on a per gram mucosa basis may lead to increased discrepancies, unless mucosal yields are also provided.

The current study represents the first systematic report on the assessment of the impact of different preparation conditions of intestinal microsomes on corresponding corrected microsomal scalars within the same lab. An optimised method for microsome preparation was made (**Figure 2-8**). As demonstrated, the technique employed for enterocyte preparation and intestinal microsomal preparation influences both the specific and total enzyme content, as well as the microsomal protein yield. Unlike MMPGM expressed scalars, no significant differences in corrected scalars of MPPGI or MPPcm were observed for all the 100% (30W) sonication preparations (conditions 5-8). This indicates that this scalar was very sensitive to the wet weight of mucosa, and suggests the impact of preparation methods on the value of intestine scaling factor and highlights the difficulties in making direct comparisons between labs.

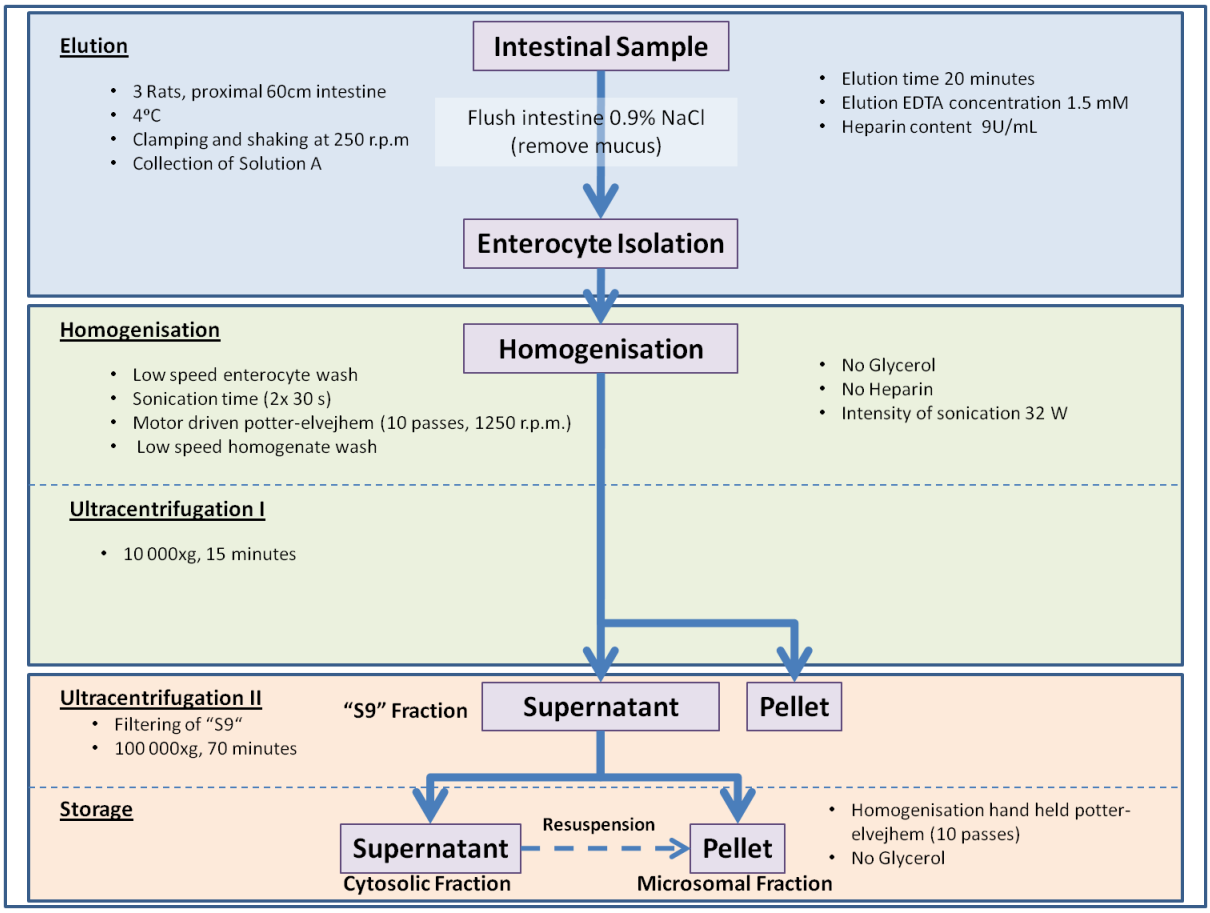

Figure 2-8 Summary of optimised intestinal microsome preparation method

Comparisons between labs are also dependant on the resulting microsomal active enzyme present following preparation. When observing the microsomal spectra in the rat intestinal microsomes and homogenate, a peak around 420-430nm was also observed. Originally it was assumed that this was a product of denaturisation of CYP to P420, either by mechanical damage (e.g. sonication), or this process is natural/spontaneous. Spontaneous denaturation of CYP to P420 is characteristic of rat intestinal microsome preparations (but not in rabbits, guinea-pigs or hamsters) (Burke and Orrenius, 1979). However, this has been reportedly limited in the presence of protease inhibitors (Stohs et al., 1976) which were present in all preparations. Therefore, whilst P420 may be making up a part of this peak area, on closer inspection this peak was at around 428nm, and therefore it is more likely that this represents the presence of other heme containing proteins, either methaglobin (436nm) or cytochrome b_5 (γ band 424 nm). Both methaglobin and cytochrome b_5 show an additional peak at 552nm and 557 nm respectively, which is also observed. Looking at the total spectrum however (**Figure 2-1**), this observation suggests that the peak around 420-430nm is most likely cytochrome b5, since this also displays and

α-band at 557 nm, and β-band at 525 which are both present in these intestinal microsomes (Klingenberg, 2003), and its content similar to levels of CYP (0.18 nmol/mg) has also been reported in the rat (Dawson and Bridges, 1981), measured using the Omura and Sato, (1964) reduced minus oxidised difference spectrum method. Since the method employed in this work was the Matsubara et al., (1976) method, it was not possible to measure the absolute abundance of this protein in these samples.

2.6. Conclusions

The impact of subtle variations of intestinal microsome preparation to elution conditions, homogenisation intensities and the effect of heparin and glycerol were examined. A shorter incubation time using 5mM EDTA and 9U/ml heparin, and 30W sonication, were preferential to an increased CYP specific and total content in the proximal 60cm of male rat intestine. This optimised methodology will be applied to characterise rat, dog and human intestinal metabolism.

3. Characterisation of rat intestinal microsomes

3.1. Introduction

In order to best understand the main metabolic routes of elimination between species it is important to consider respective differences in enzyme expression and activity. In the proximal Han Wistar (HW) rat intestine, whilst CYP3A is a major isoform, CYP2B1 is also a dominant enzyme expressed (Fasco et al., 1993; Zhang et al., 1996; Mitschke et al., 2008). There is limited information regarding the characterization of activity of the full comlimetent intestinal enzymes in HW rat, in contrast to data reported for Sprague-Dawley (SD) rat (Sohlenius-Sternbeck and Orzechowski, 2004). Therefore, since HW was the strain being utilised in this study it was necessary to characterise the intestinal microsomes prepared from the optimal methodology described in **Chapter 2**.

In terms of CYP metabolism, testosterone has been utilised previously to characterise CYP enzymes in a matrix simultaneously, since the various metabolites formed are markers for multiple enzymes (Sonderfan et al., 1989; Sohlenius-Sternbeck and Orzechowski, 2004; Chovan et al., 2007; Bruyere et al., 2009) (**Table 3-1**, **Figure 3-1**). Furthermore, hydroxy testosterone (OH TEST) metabolites, especially 6β-OH TEST, are a frequently reported marker (Mohri and Uesawa, 2001; Takemoto et al., 2003; Bruyere et al., 2009) (**Table 2-1**), and therefore can be a good comparator to the literature data. UGT metabolism in the intestine has been characterised previously using UDP-glucuronosyltransferase (UGT) substrate 4-nitrophenol glucuronidation (4-NP gluc) (Mohri and Uesawa, 2001; Takemoto et al., 2003).

Previous analysis (Dawson and Bridges, 1981) and in house results (**Chapter 2**) has shown that yields of intestinal microsomes are however low, and as such there is a requirement to utilise them as efficiently as possible. Combined CYP and UGT cofactors have been utilised previously in liver microsomes, and enabled the combined screening of CYP and UGT metabolism (Kilford et al., 2009). However, any potential limitations of using these in combination in intestinal microsomes have not been characterised. The ability to screen simultaneously for CYP and UGT metabolism provides the advantage of observing sequential and or combined substrate metabolism, especially useful since compounds are invariably not sole substrates for only one metabolic pathway. The caveat, however, is it is not possible to distinguish by which metabolic pathway investigational compounds are eliminated.

Table 3-1 Testosterone metabolites and respective rat CYP isoform

Metabolite	CYP Isoform
2α-OH TEST	2C11, (3A2)
2β-OH TEST	3A1, 3A2, (1A1)
6α-OH TEST	2A1*
6β-OH TEST	85% specific to 3A1, 3A2, 2A2*, 1A1, 2C13*, (1A2, 2C11)
7α-OH TEST	2A1*, 2A2*
15α-OH TEST	2A2, (2C12*, 2C13*)
15β-OH TEST	3A1, (2A2)
16α-OH TEST	2C11, 2B1, (2B2*, 2C7*, 2C13*)
16β-OH TEST	2B1, (2B2*, 3A1, 3A2)
Androstenedione	2C11, 2B2*, 2B1, (2A2*, 3A1, 3A2)

Minor metabolies enzyme pathways are shown in parenthesis. * not reported to be expressed in rat intestine (**Table 1-3**). Adapted from Arlotto et al., (1991) and Sohlenius-Sternbeck et al., (2004).

The complete set of compounds investigated between species and basic molecular properties is described in **Appendix Table 7-1**. These compounds were selected on the implication of intestinal metabolism being involved in their metabolism, and the ability to look at cross species comparison based on the combination of literature and in house data. These compounds range in major elimination pathways, although the majority of compounds are metabolised by CYP3A (e.g. midazolam, buspirone, furosemide), considering its relevance in the human intestine. In addition, a limited number of compounds which undergo predominantly UGT mediated elimination where also selected e.g. raloxifene and 7-hydroxycoumarin (7-HC).

3.2. Aims

The current study aims to characterise rat intestinal microsomes in terms of CYP content, and CYP and UGT metabolism, and assess the differences between two separate pools of microsomes prepared by the same method. Furthermore, to compare metabolic activities and the effects of combined *vs.* individual cofactors using commercially available rat intestinal microsomes. Finally, to look at prediction of F_G using the in house prepared intestinal microsome pools and compare these to *in vivo* estimates of rat F_G.

3.3. Materials and Methods

3.3.1. Reagents

All laboratory chemicals were purchased from either Sigma (Dorset, UK) unless detailed in the text. Product codes at time of writing are provided in parenthesis.

3.3.1. Intestinal microsome pools

Rat intestinal microsomes (RIM) were prepared by the optimised elution method outlined in **Chapter** 2, and summarised in (**Figure 2-8**). Microsomes on three separate occasions were prepared fresh and characterised for both microsomal and homogenate CYP content in order to determine microsomal recovery (**Equation 2-2, Equation 2-3**). Activity of RIM towards testosterone hydroxylation and 4-NP gluc was also investigated (see below). Microsomes prepared previously via the optimised method (preparation 8, **Chapter 2**) were pooled to form Pool 1 (n=9 rats). A second set of 3 preparations were pooled to form Pool 2 (n=9 rats). Intestinal microsomes were also prepared from frozen rat intestinal tissue (n=3 occasions of n=3 samples). Finally for comparison, on one occasion, microsomes were prepared from scraped intestinal tissues by cutting along the length of intestine and gentle scraping with a glass microscope slide (n=1 occasions of n=3 samples).

Commercially available pool microsomes were also used as a comparator to those produced in house. HW (R6000.I, lot #0810335, 90 male donor pool), and SD (R1000.I, lot #1010043, 135 male donor pool) were obtained from Xenotech (Tebu-Bio Ltd., Peterborough, Cambridgeshire, UK). Microsomes were stored at -80^{o}C prior to experiments.

3.3.2. Assessment of CYP activity in RIM

CYP enzyme activities of in house prepared and commercial RIM were determined using the probe substrate testosterone. Formation of all testosterone metabolites was monitored following incubations of RIM at 1mg/ml 0.1 M phosphate buffer (pH7.4) and 100µM Testosterone (internal AZ compound inventory stock) concentration (2-fold human K_m) (Obach et al., 2001; Takemoto et al., 2003). RIM were incubated in triplicate with 1mM NADPH (#481973, Calbiochem, San Diego, USA) for 5 minutes at 37^{o}C shaken at 900 rpm using a CAT SH10 Heater shaker (Hamiliton robotics, Reno, Nevada, USA). Reaction was initiated by addition of Testosterone. Final organic solvent (methanol) content was <1% v/v. Samples at 2.5, 5, 15, 30 and 60 minutes were quenched 1:1 with ice cold methanol containing internal standard (1µM 11-β OH TEST) and stored overnight at -

20°C. The following day, samples were diluted with 200µl ultra pure (UP) H_2O, and spun at 3000 rpm for 15 minutes, and 200 µl of supernatant taken for analysis. Samples were quantified using a standard curve of all the metabolites using a LTQ Orbitrap with Accela pump (Thermo Scientific, Waltham, MA, USA), using an electrospray interface in positive mode. Samples (10µl) were injected onto a ZORBAX RRHD Eclipse Plus C18 2.1 x 50 mm, 1.8µm column (Aligent, Santa Clara, CA, USA) heated to 55°C. Cone voltage and gas flow and capillary temperature and voltage were 2.8V, 30l/h, 350°C and 30V. Flow rates and gradients and sample traces are provided in **Appendix Table 7-3** and **Appendix Figure 7-1.**

Following optimisation of the method to increase reproducibility and sensitivity of the method based on increasing efficiency of protein precipitation (1981), samples were quenched 1:2 (sample : quench) in ice cold acetonitrile containing internal standard (1µM 11-β OH TEST)and stored overnight at -20°C. The following day, plates were spun at 3000 rpm for 15 minutes, and 50 µl supernatant diluted in 200 µl UPH_2O. Samples were quantified using a Waters Acquity UPLC system with a PDA coupled to a G2 Q-ToF MS (Waters, Milford, MA, USA), and a Acquity UPLC BEH C18 column, 130Å, 1.7 µm, 2.1 mm X 100 mm and Acquity UPLC column with an in-Line Filter Kit made up of the same phase (Waters). Sample (25µl) was detected using an electrospray interface in positive mode, and source and desolvation temperatures, and desolvation and cone gas flows of 120°C and 400°C, and 800l/h and 20l/h, respectively. Cone voltage was 30V. Flow rates gradients are shown in **Appendix Table 7-3**.

3.3.3. Assessment of glucuronidation in RIM

UGT activity of 4-NP gluc was determined for in house, microsomes and commercial RIM. Metabolite formation was monitored following incubations of 1mg/ml in 0.1 M phosphate buffer (pH7.4) and 100µM 4-NP concentration (>2-fold human K_m) (Takemoto et al., 2003). Microsomes were activated by incubation with alamethicin (#A4665) (50 µg/mg protein) on ice for 15 min as reported previously (Fisher et al., 2000; Cubitt et al., 2009; Kilford et al., 2009; Gill et al., 2012).

RIM were incubated in triplicate with 3.4mM $MgCl_2$ (#M8266), 115µM D-Saccharic acid 1,4 lactone monohydrate (SAL) (#S0375), 1.15mM EDTA (#EDS) and 5mM Uridine 5′-diphosphoglucuronic acid trisodium salt (UDPGA) (#U6751) for 5 minutes at 37°C shaken at 900 rpm using a CAT SH10 Heater shaker. EDTA is a chelating agent added to prevent

Cu^{2+} ions within the incubation causing inhibition of the UGT enzymes (Letelier et al., 2007). Inclusion of SAL inhibits the β-glucuronidase mediated conversion of glucuronide metabolites back to parent compounds during the incubation and $MgCl_2$ is a requisite for the UGT reaction (Boase and Miners, 2002; Walsky et al., 2012).

Reaction was initiated by addition of 4-NP and final organic solvent (methanol) content was 1% v/v. Samples at 2.5, 5, 10, and 20 minutes were quenched with 1:1 with ice cold acetonitrile containing internal standard AZ1 and stored overnight at -20^{o}C. The following day, samples were diluted with 200µl H_2O, and spun at 3000 rpm for 15 minutes, and 200 µl of supernatant taken for analysis. Samples were quantified using a standard curve of 4-Nitrophenyl β-D-glucuronide (#73677) using a LTQ Orbitrap with Accela pump (Thermo Scientific, Waltham, MA, USA) and Synergi MAX-RP 80 Å, 4 µm, 50x2.0mm (Phenomenex, Torrance, CA, USA) with guard filter of the same phase. Flow rates and gradients are provided in **Appendix Table 7-3**.

3.3.4. Intrinsic clearance

3.3.4.1. Source of compounds

Compounds in **Appendix Table 7-1**with high purity were selected from AZ internal compound stocks (solid or in 10mM DMSO) except for 7-Isopropoxy-3-phenyl-4H-1-benzopyran-4-one (ipriflavone) (#381551), raloxifene hydrochloride (#R1402), losartan (#61188), bisoprolol fumerate (#B2185) , atorvastatin (Molekula, Gillingham, UK, #17630611), irbesartan (Saquoia Research Products Ltd, Pangbourne, UK, #SRP01502i) saquinavir mesylate (Saquoia, #SRP01070s), and midazolam hydrochloride (Saquoia, #SRP065525m).

3.3.4.2. Rat intestinal depletion incubations

Depletion experiments for determination of intrinsic clearance (CL_{int}) for RIM in house pools at were carried out at 1mg/ml in 0.1M phosphate buffer (pH 7.4). Microsomes were activated by incubation on ice with alamethacin (50 µg/mg) for 15 min. Coincubation with 50 µg/mg alamethacin has been shown previously to not effect CYP3A kinetics (Fisher et al., 2000). Microsomes were co-incubated in duplicate at 37^{o}C with both CYP and UGT cofactors (1mM NADPH, 3.4mM $MgCl_2$, 115µM SAL, 1.15mM EDTA (#EDS), and 5mM UDPGA as per Kilford et al., (2009) for 5 minutes and agitated at 900 rpm using a CAT SH10 heater shaker. Incubations were started by spiking of 1µM of compound. Final organic solvent (DMSO) was 1%. Samples where quenched using ice cold acetonitrile (3:1

quench to sample) containing the internal standard AZ1.The total incubation time was 40 minutes. Quenched samples were stored overnight at -20^{o}C. The following day, samples were diluted with 200µl UPH_2O, and spun at 3000 rpm (Sorvall legend RT centrifuge) for 15 minutes, and 200 µl of supernatant taken for analysis.

3.3.4.3. Use of combined *vs.* individual cofactors in commercial intestinal rat microsomes

In order to investigate the impact of using combined *vs.* individual CYP and UGT incubations, 8 compounds were chosen. The compounds selected were raloxifene, midazolam, amitriptyline, ipriflavone, irbesartan, losartan, nicardipine and 7-hydroxycoumarin (7-HC) selected on the basis of their reasonable F_G prediction (except in the case of 7-HC which was selected as a quality control (QC) marker for UGT metabolism), in order to further assess the impact on estimates of F_G. Combined CYP and UGT incubations were the same as those utilised for the determination of CL_{int} by depletion in the in house prepared pools (**3.3.4.2**), and individual cofactor incubation conditions were identical to those utilised for testosterone (CYP) (**3.3.2**) and 4-nitrophenol (UGT) (**3.3.3**) rate of formation (ROF) experiments.

3.3.4.4. LC-MS/MS

All samples except furosemide were analysed using an Agilent 1100 HPLC system coupled to a Micromass Quattro Ultima triple quadruple mass spectrometer using an electrospray interface in positive mode. Samples (25µl) were eluted at 20^{o}C using a hypersil GOLD 175 Å, 5µm, 30x2.1mm column (Thermo Scientific) using a flow rate of 0.4 ml/min and 0.1% formic acid in organic (methanol) and inorganic (UPH_2O) solvents. Source temperature was 120^{o}C, desolvation temperature was 350^{o}C, desolvation gas flow rate was 700 l/h and cone gas flow rate was 24 l/h. Furosemide (10µl sample) was analysed using a Quattro Premier Mass Spectrometer coupled to a Waters Acquity UPLC system using a Kinetic C18 100 Å, 2.6µm, 50 x 4.6 mm column (Phenomenex) and a flow rate of 0.725ml/min. The 2 minute gradients are shown in **Appendix Table 7-5**. Source and desolvation temperatures were identical, however the cone gas flow rate was 70 l/h. Individual compound mass transitions and column voltages are shown in **Appendix Table 7-4**. Data was integrated using Quanlynx v4.1 (Waters).

3.3.4.5. Intrinsic clearance determination in RIM

The linear rate of change of compound over the time course for each compound in duplicate was analysed in Excel to determine halflife ($t_{1/2}$) and the elimination rate constant (k). The rate constant was used to calculate the intrinsic clearance (CL_{int}) (**Equation 3-1**). The CL_{int} values were corrected for fu_{inc} to generate unbound measures of intrinsic clearance ($CL_{int,u}$). The mean and stdev of unscaled $CL_{int,u}$ (µL/min/mg protein) have been presented for each drug. Representative depletion profiles are shown in **Appendix Figure 7-2** and **Appendix Figure 7-3** for each compound.

Equation 3-1 $CL_{int} = \frac{k \cdot V}{Protein_{total}}$

where k, V and $Protein_{total}$ represent elimination rate constant, volume of incubation and amount of microsomal protein in assay, respectively.

3.3.4.6. Correction for nonspecific binding

A high throughput equilibrium dialysis method was used to determine fu_{inc} in RIM at 1 mg/ml, using a 96-well Micro-Equilibrium Dialysis Device HTD (HTDialysis, LLC, Gales Ferry, CT, USA) and dialysis membrane strips (12-14kDa molecular mass cut off) (#1103, HTDialysis). Microsomes were made up in 0.1M phosphate buffer (pH 7.4), and compounds were spiked in at 1µM concentrations. Compound spiked microsomes were aliquot into the donor wells in triplicate, with buffer placed in acceptor wells. The plate was incubated at 37^{o}C and left to equibrilate on a plate shake (450 rpm) for 4 hours. Following incubation samples from both the acceptor and donor sides of the membrane were transferred to 96 well plates and quenched in acetonitrile containing internal standard AZ1. Sample preparation and LC-MS/MS methods were the same as those for microsomal incubations. Fu_{inc} was calculated as the ratio of acceptor to donor both normalised for internal standard using **Equation 3-2** (Gertz et al., 2008b). CL_{int} was corrected for microsomal binding using **Equation 3-3** to calculate $CL_{int,u}$.

Equation 3-2 $$fu_{inc} = \frac{peak\ area\ acceptor\ /\ \ peak\ area\ internal\ standard}{peak\ area\ donor\ /\ \ peak\ area\ internal\ standard}$$

Equation 3-3 $$CL_{int,u} = \frac{CL_{int}}{fu_{inc}}$$

3.3.5. Investigation of rat *in vivo* intestinal metabolism

In order to provide measures of prediction success, estimates of *in vivo* F_G were made using the same in house HW strain. These were made by the indirect measure of comparing i.v. and p.o. administration of the rat compound set at low doses in order to prevent saturation of intestinal metabolic enzymes. Doses and formulations are shown in **Table 3-2**. The i.v. doses were administered in n=2 rats through bolus administration in the tail vein. P.o. administration (n=2) was by oral gavage into the stomach. P.o. doses were administered as solutions in propylene glycol (#W29004), and tested at 1:1 and 1:10 dilutions of 1M HCl for observations of precipitation at low pH. Blood samples were collected at t=5, 20, 40 minutes, 1.5, 3, 6, 12 and 24 hours for i.v. dosing. P.o. blood samples were taken at t=15, 30 minutes, 1, 2, 3, 6, 12 and 24 hours. Blood samples (0.3ml collected in lithium heparin tubes) were stored at 4^{o}C until they were prepared for storage. Blood samples of 60µl were taken and diluted 1:1 in water for frozen storage (-20 ºC). The remaining samples were spun at 1000rpm for 2 minutes to separate out the plasma (~120-150ul) which was frozen (-20ºC). For analysis, blood and plasma samples were thawed, and from these smaller samples were quenched in a 3:1 ratio (acetonitrile plus internal standard AZ1: blood/plasma sample). Remaining sample was refrozen in case of reanalysis. A standard curve prepared from a 2mM stock and spiked into blood and plasma matrix for determination of sample time course concentrations and limit of quantification were quenched in the same way. Samples were placed in the freezer for at least 1 hour before final preparation and LC-MS/MS analysis as described previously for microsomal depletion. Individual compound mass transitions and column voltages are shown and 2 minute gradients were the same as applied for RIM depletion sample analysis.

I.v. and p.o. time *vs.* concentration data were input into Pheonix Winnonlin v6.2 (using Connect 1.2 and i.v.i.v.C Toolkit 2.0) (Pharsight, California, USA) in order to determine the kinetic parameters of half life ($t_{1/2}$) and respective area under the curves (AUC). Estimates of *in vivo* blood to plasma ratio (R_b) for each compound were determined by comparing blood and plasma concentrations (**Equation 3-4**). Parameters of i.v. systemic clearance ($CL_{i.v}$) and oral bioavailability (F) were determined using **Equation 3-5** and **Equation 3-6**. Estimates of hepatic extraction were made using $CL_{i.v.}$ and subtracting any literature reported renal clearance data ($CL_{R\ plasma}$ corrected for in house determined R_b) of the drug to derived hepatic clearance (CL_H) (**Equation 3-7**) and normalising for hepatic blood flow (Q_H) (**Equation 3-8**). It was assumed CL_R represent excretion clearance and no

renal metabolism is occurring. Reported literature rat liver blood flow ranges from 55 to 161 ml/min/kg (Casado et al., 1987; Davies and Morris, 1993; Brown et al., 1997), varying in both experimental technique used, and strain and sex of rat. Based on an internal assessment of relationship between cardiac output and body weight, a hepatic blood flow in the rat was selected as 72 ml/min/kg being the most appropriate to describe the in house strain (Brown et al., 1997). In order to determine the extent of the intestinal component (i.e. extent of absorption (Fa) and F_G), F was divided by 1-E_H (F_H) (**Equation 3-9**).

Equation 3-4 $R_b = \frac{C_{blood}}{C_{plasma}}$

Equation 3-5 $CL_{i.v.} = \frac{Dose_{i.v.}}{AUC_{i.v.}}$

Equation 3-6 $F = \frac{AUC_{p.o.}}{AUC_{i.v.}} \cdot \frac{DOSE_{i.v.}}{DOSE_{p.o.}}$

Equation 3-7 $CL_H = CL_{i.v.blood} - \left(\frac{CL_{R\,(plasma)}}{Rb}\right)$

Equation 3-8 $E_H = \frac{CL_H}{Q_H}$

Equation 3-9 $Fa \cdot F_G = \frac{F}{(1-E_H)}$

3.3.6. Determination of *in vitro* effective permeability from Caco-2 data

The apparent Caco-2 apical to basolateral (A to B) permeability (P_{app}) for the test set of compounds was determined in a generic assay on a separate AZ site. Cells were incubated in Hank's buffered salt solution (HBSS, Gibco, Life Technologies, CA, USA) at pH 7.4 and the assay was initiated by addition of 10 µM of test compound. Calculation of P_{app} was achieved using **Equation 3-10**. P_{app} to P_{eff} scaling was based on an in house AZ derived Caco-2 P_{app} to P_{eff} relationship **Equation 3-11**.

Equation 3-10 $P_{app}[cm/s] = \frac{(\Delta Q/\Delta t)}{(A \cdot C_D)}$

where ($\Delta Q/\Delta t$) [cm/s] is the cumulative amount of test compound transported over time to the basolateral (receiver) side, A is the surface area of the monolayer membrane (cm^2) and C_D is the average drug concentration in the donor chamber over the period which ($\Delta Q/\Delta t$) was determined.

Equation 3-11 $LOGP_{eff} = LOGP_{app} \cdot 0.7233 - 0.0854$

Table 3-2 Dose formulations and amounts for 22 drugs administered i.v. and p.o. to Han Wistar rats

					i.v. Dose			p.o.		
Compound	**i.v. Formulation**	**p.o. Formulation**	**MW**	**Salt MW**	**mg/kg**	**µmol/kg**	**Volume ml/kg**	**mg/kg**	**µmol/kg**	**Volume ml/kg**
Amitriptyline	Saline	Propylene Glycol	277.41	313.87	2.00	6.37	2.00	5.00	15.93	5.00
Atorvastatin	20% DMA: 80% UPH_2O	Propylene Glycol	558.65	558.65	4.00	7.16	2.00	5.97	10.68	5.00
Bisprolol	Saline	Propylene Glycol	325.45	325.45	1.30	4.00	2.00	3.25	10.00	5.00
Bumetanide	20% DMA: 80% UPH_2O	Propylene Glycol	364.42	364.42	2.00	5.49	2.00	5.00	13.72	5.00
Buspirone	Saline	Propylene Glycol	385.51	421.97	1.85	4.38	2.00	4.62	10.95	5.00
Cyclosporine	Saline	Propylene Glycol	1202.62	1202.62	2.00	1.66	2.00	6.01	5.00	5.00
Diclofenac	Saline	Propylene Glycol	296.15	318.13	1.37	4.30	2.00	3.42	10.74	5.00
Diltiazem	Saline	Propylene Glycol	414.52	450.98	2.00	4.43	2.00	5.00	11.09	5.00
Furosemide	20% DMA: 80% UPH_20 [b]	Propylene Glycol	330.75	330.75	1.32	4.00	2.00	3.31	10.00	5.00
Indomethacin	30% DMA:30% TEG:40% Citrate	Propylene Glycol	357.79	357.79	1.00	2.79	2.00	5.00	13.97	5.00
Ipriflavone	Saline	Propylene Glycol	280.32	280.32	2.00	7.13	2.00	5.00	17.84	5.00
Irbesartan	Saline/20% DMA: 80% UPH_2O [b]	Propylene Glycol	428.54	428.54	1.71	4.00	2.00	4.29	10.00	5.00
Losartan	Saline	Propylene Glycol	422.92	461.00	2.00	4.34	2.00	5.00	10.85	5.00
Midazolam	Saline	Propylene Glycol	325.77	362.23	1.00	2.76	2.00	4.42	12.20	5.00
Nicardipine	20% DMA: 80% Saline	Propylene Glycol	479.53	515.99	2.00	3.88	2.00	5.00	9.69	5.00
Pirenzepine	Saline	Propylene Glycol	351.41	376.72	2.00	5.31	2.00	5.00	13.27	5.00
Raloxifene	20% DMA: 80% UPH_2O	Propylene Glycol	473.59	510.04	2.00	3.92	2.00	5.00	9.80	5.00
Saquinavir	30% DMA:30% TEG:40% Citrate	Propylene Glycol	670.85	766.96	2.00	2.61	2.00	5.00	6.52	5.00
Sildenafil	Saline	Propylene Glycol	474.58	666.71	2.00	3.00	2.00	5.00	7.50	5.00
Simvastatin	20% DMA: 80% UPH_2O[b]	Propylene Glycol	418.57	418.57	4.00	9.56	2.00	5.00	11.95	5.00
Tacrolimus	20% DMA: 80% UPH_2O[b]	Propylene Glycol	804.02	803.00	4.00	4.98	2.00	5.00	6.23	5.00
Terfenadine	20% DMA: 80% UPH_2O [a]	Propylene Glycol	471.68	471.68	2.00	4.24	2.00	5.00	10.60	5.00
Verapamil	Saline	Propylene Glycol	454.61	555.45	2.71	4.89	2.00	6.79	12.22	5.00

a: HCL added drop wise until completely dissolved, b: NaOH added drop wise until completely dissolved, TEG: triethylene glycol, DMA: Dimethylacetamide, UPH_2O: ultra pure H_20

3.3.7. Prediction of P_{eff} from physicochemical data

Physicochemical parameters of hydrogen bond donors and polar surface area were collated for all compounds investigated. Predicted P_{eff} was estimated using **Equation 3-12** as described previously (Winiwarter et al., 1998). The application of P_{eff} values using this approach towards the prediction of F_G was assessed in comparison to F_G based on Caco-2 permeability data and applied towards measuers of $CL_{int,u}$ derived from both in house and commercial RIM.

Equation 3-12 $$LOGP_{eff} = -2.546 - 0.011 \cdot PSA - 0.278 \cdot HBD$$

where PSA is the polar surface area and HBD are the number hydrogen bond donors. PSA and HBD for the test compounds were estimated using the Selma PSA method (Bruneau, 2001), and can be found in **Table 3-7**.

3.3.8. Prediction of F_G from *in vitro* data

$CL_{int,u}$ values were scaled to give $CL_{int,u}$ per gram of tissue by correcting the values for the corresponding pool microsomal recovery (**Equation 3-13**). Commercial microsomes were scaled using mean scalars obtained from both pools 1 and 2. CL_{perm} was calculated using P_{eff} and the calculated cylindrical surface area of the 60cm segments with radius of 2.2mm (DeSesso and Jacobson, 2001) (**Equation 3-14**). Q_{gut} was calculated using CL_{perm} and rat Q_{villi} of 0.33 l/h (**Table 1-2**) (**Equation 3-15**). F_G was predicted using the Q_{gut} model as per Yang et al., (2007) (**Equation 3-16**). The fraction unbound in the gut (fu_G) was assumed to be 1, since this has been shown to provide the greatest accuracy of prediction when using the Q_{gut} model (Yang et al., 2007). Estimates of $Fa.F_G$ were made using the established relationship between Caco-2 permeability and rat *in vivo* absorption as defined by Amidon *et al.*, (1988) (**Equation 3-17**).

Equation 3-13 $$CL_{int,u,G} = CLu_{int} \cdot MPPGI \cdot Intestine\ Segment\ Weight$$

Equation 3-14 $$CL_{perm} = P_{eff} \cdot cylindrical\ surface\ area$$

Equation 3-15 $$Q_{gut} = \frac{Q_{villi} \cdot CL_{perm}}{Q_{villi} + CL_{perm}}$$

Equation 3-16 $$F_G = \frac{Q_{GUT}}{Q_{GUT} + fu_G \cdot CLu_{int,G}}$$

Equation 3-17 $$Fa = 1 - e^{-2 \cdot Peff}$$

3.3.9. Data analysis

Tests for bias and precision of estimated F_G from *in vitro* data were calculated as geometric fold error (gmfe), (**Equation 3-16**) and rooted mean squared error (rmse) (**Equation 3-19**) (Sheiner and Beal, 1981; Fahmi et al., 2008). The gmfe does not allow over- and under-predictions to cancel each other out and therefore indicates an absolute deviation from the line of unity (Gertz et al., 2010).

Equation 3-18 $$gmfe = 10^{\frac{1}{n}\sum\left|log\left(\frac{predicted}{observed}\right)\right|}$$

Equation 3-19 $$rmse = \sqrt{\frac{1}{n}\sum(predicted - observed)^2}$$

Scatter plots of CL_{int} and F_G were compiled in Microsoft Excel (2007) and Matlab v7.14.0 (2012a, Mathworks, Natick, MA, USA). Tests comparing means using Student's t-test to test for statistical significance at a level of 5% was applied using SPSS Statistics version 20 (IBM).

Qualitative zoning of predicted low F_G values was performed by classification into categories of true positive (TP), false positive (FP), true negative (TN) and false negative (FN) (**Figure 3-1**). High F_G was defined as >0.5, and low F_G <0.5.

A stricter classification approach based on prediction success of low F_G compounds with a F_G less than 0.3 ($F_{G,<0.3}$), medium F_G within the range of 0.3 and 0.7 ($F_{G,0.3\text{-}0.7}$), and finally a high F_G of greater than 0.7 ($F_{G,>0.7}$) (**Figure 3-2**).

Finally, prediction success was analysed using log(observed/predicted) *vs.* observed, using a prediction accuracy cutof ±0.3 log units (representing 50% underprediction (0.5 fold) and 100% overprediction (2 fold)).

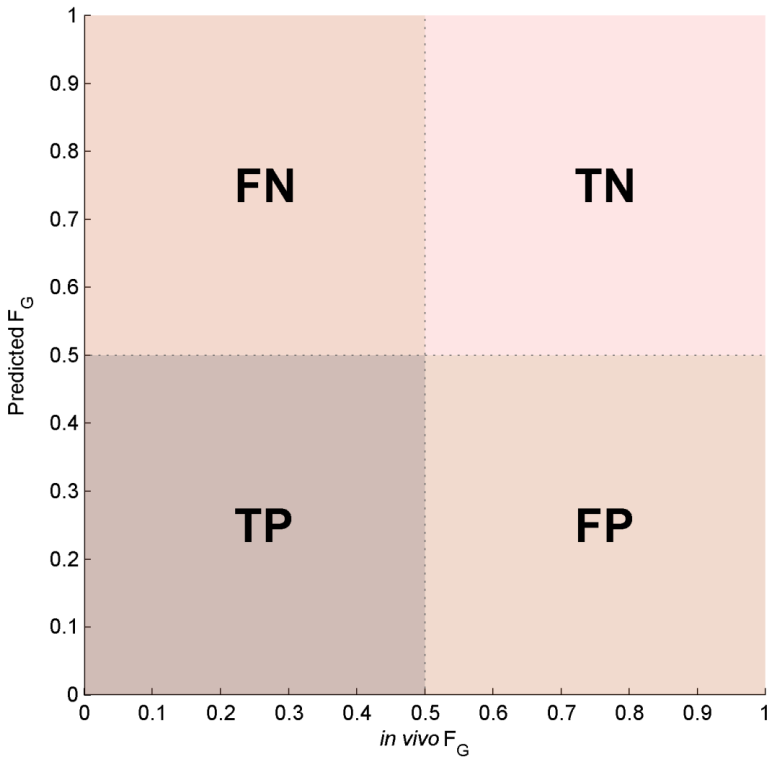

Figure 3-1 Representation of prediction success classifications of low F_G for test compounds.

True positive: (TP), false positive: (FP), true negative: (TN) and false negative: (FN)

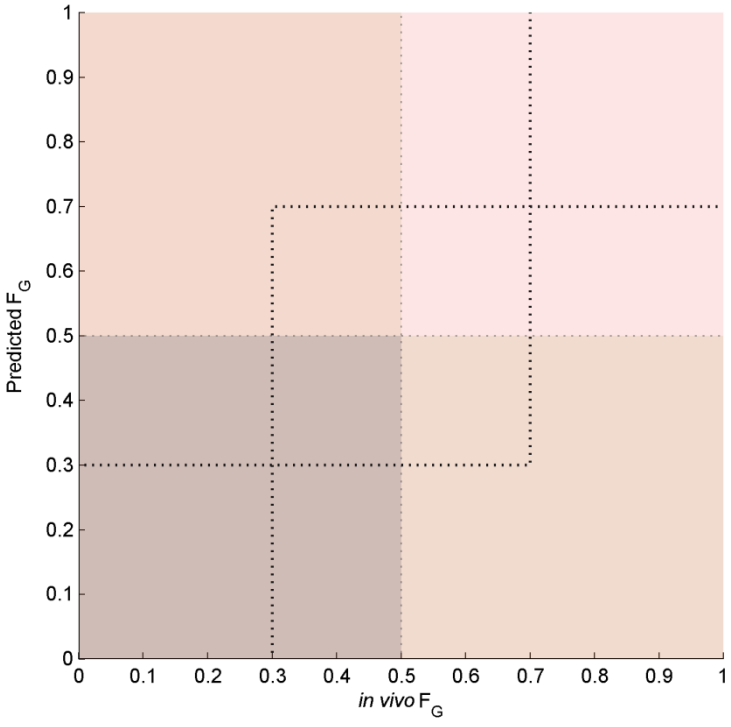

Figure 3-2 Representation of prediction success classifications using 0.3 and 0,7 cutoffs for high and low F_G extraction respectively.

3.4. Results

3.4.1. Microsomal recovery in pools

Mean specific CYP content fell 39% in freeze thawed (FT) Pool 1 (**Table 3-3**). CYP content was not however further reduced over two additional FT cycles. Similar CYP levels to pool 1 after FT were observed in microsomes prepared from frozen intestinal tissue and measured fresh. No further reduction in CYP was observed following FT. Specific content was 51% lower in Pool 2 *vs.* Pool 1. Similar levels were observed in microsomes prepared by gentle scraping.

Table 3-3 Specific CYP content measured fresh and over 3 FT cycles

Pool	Fresh[a]	FT1[a]	FT2[a]	FT3[a]
Pool 1	243.6 ±107.7	148.7 ±28.3.2	148.5 ±13.5	136.4 ±11.3
Pool 2	119.4 ±75.1	ND	ND	ND
Frozen	127.7 ±12.9	154.3±17.2	166.5±25.0	166.3±43.8
Scraping	115.3	ND	ND	ND

a: pmol/mg microsomal protein, ND: not determined

The microsomal recovery based on measuring CYP content in both homogenate and microsomes for each of the pools is shown in **Table 3-4**. The highest recovery was seen in the freshly prepared pools using elution (Pools 1 and 2). Although the recovery in pool 1 was the highest, it was not significantly different to pool 2. Recoveries in all preparations ranged from 20.8 to 38.7% (CV 13 to 18%). The lowest mean recoveries were observed for microsomes prepared by scraping and from frozen tissue. Differences in microsomal scalars were also not significant ($p>0.2$). Corrected yields based on per gram intestine ranged from 7.2 to 16.4 mg/g intestine. Mean MPPGI for pools 1 and 2 which were freshly prepared by elution was 9.7 ±3.6 mg/g intestine.

3.4.2. Testosterone metabolite rate of formation in RIM

The rate of formation of 4 major testosterone metabolites, 6β-, 16α-, 16β-OH TEST and androstenedione in each of the pools is shown in **Table 3-5**. The activity in pools 1 and 2 following one freeze thaw cycle showed mean increase of 16β-OH TEST and Androstenedione formation within 2-fold (1.4- and 1.7-fold, respectively). Mean 6β- and 16α-OH TEST formation was however 2.2- and 2.5-fold higher in pool 2, respectively. Mean 6β-OH TEST formation was lowest in scrapped microsomes (66.1 pmol/min/mg

Table 3-4 Microsomal recoveries and scalars in intestinal microsomal pools

Pool	Intestine weight (g)	Mucosal yield (g/g tissue)	Recovery (%)[a]	MPPGI (mg/g tissue) [a]	MPPGM (mg/g mucosa) [a]	MPPcm (mg/cm intestine length) [a]
Pool 1 [b]	5.4 ±0.3	0.48 ±0.02	38.7 ±5.0	7.2 ±1.3	15.1 ±2.1	0.65 ±0.15
Pool 2 [b]	5.3 ±0.2	0.47 ±0.06	27.5 ±5.1	12.1 ±3.9	25.9 ±7.4	1.06 ±0.33
Frozen [b]	5.5 ±0.5	0.66 ±0.02	22.4 ±7.3	13.8 ±2.7	20.9 ±4.5	1.26 ±0.18
Scraping [c]	5.0 ±0.3	0.49	20.80	11.40	23.00	0.95

a: based on CYP content in microsomes and homogenates from 60cm segments from 9 week old male rats, b: mean of 3 rats on 3 occasions. c: mean of 3 rats on 1 occasion

Table 3-5 Maximal rate of formation of testosterone hydroxylation and 4-nitrophenol glucuronide metabolites in intestinal microsome pools

Pool	6β-OH TEST (pmol/min/mg)	16α-OH TEST (pmol/min/mg)	16β-OH TEST (pmol/min/mg)	Androstenedione (pmol/min/mg)	4-NP Gluc (nmol/min/mg)
Pool 1 (Fresh)[a]	ND	ND	ND	ND	ND
Pool 1 (FT)[b]	85.3 ±32.5	77.5 ±5.2	42.6 ±3.8	560.7 ±6.6	70.4 ±8.9
Pool 2 (Fresh)[a]	113.3±30.9	55.1 ±13.1	61.2 ±4.3	429.9 ±30.9	84.8 ±28.6
Pool 2 (FT)[b]	187.5 ±77.8	87.3±31.7	74.1 ±39.4	548.7±188.7	71.4 ±5.9
Frozen (FT)[b]	ND	ND	ND	ND	13.0 ±5.3
Scraping (FT)[b]	66.1±4.8	86.4 ±9.2	73.9 ±5.4	457.0 ±60.4	46.1 ±1.68
Commercial HW[b]	190 ±53.5	86.9 ±4.1	121.7 ±11.8	314.5 ±55.3	56.1 ±4.1
Commercial SD[b]	167.2 ±43.7	155.9 ±10.2	132.8 ±4.74	371.6 ±7.2	55.6 ±4.7

a: mean of 3 preparations in triplicate, b: 1 occasion in triplicate, Fresh: microsomes analysed on day of preparation before freezing
FT: microsomes analysed following 1 FT cycle, ND: not determined. pmol/min/mg refers to pmol/min/mg of microsomal protein

microsomal protein). No differences were observed for the other testosterone metabolites. Mean 6β-OH TEST formation was similar to in house pools in commercial HW and SD microsomes. Mean 6β-OH TEST formation in fresh and FT microsomes (pool 2) where 113.3 and 187.5 pmol/min/mg microsomal protein. Androstenedione formation was 1.7 fold higher for in house pools *vs.* commercial SD microsomes. 16α-OH TEST formation was 1.8 fold lower in commercial HW microsomes compared to commercial SD microsomes.

3.4.2. 4-NP glucuronidation in RIM

Mean 4-NP gluc formation was the same in both pool 1 and pool 2 following one FT cycle (70.4 and 71.4 nmol/min/min, respectively) (**Table 3-5**). Mean activity in fresh microsomes showed the highest formation rates, however this was not significant compared to the FT microsomes. Activity in microsomes prepared via scraping was 1.5-fold lower than pools 1 and 2. The lowest activity was observed in microsomes prepared through use of frozen intestinal tissue (13.0 nmol/min/mg microsomal protein). Activity in commercial microsomes was similar for both strains, with activities lower than the in house elution pools from fresh tissue, and higher than those prepared via scraping.

3.4.3. Rat intestinal incubations

3.4.3.1. Rat intestinal microsomal binding

The fu_{inc} in rat intestinal microsomes for the compounds investigated is shown in **Table 3-6**. Microsomal binding ranged from 0% for 7-hydroxycoumarin, pirenzepine, and furosemide to 98% for terfenadine.

3.4.3.2. Pool 1 *vs.* pool 2 unbound intrinsic clearance comparison

Measures of unbound clearance corrected for protein binding showed a range of microsomal clearance (**Table 3-6**). In pool 1 microsomal clearance ranged from 2.6 to 31928 µl/min/mg, and in pools 2 from 0.1 to 39704 µl/min/mg, for diclofenac and terfenadine respectively. Mean $CL_{int,u}$ of midazolam was similar in both pools (22.0 and 19.9 µl/min/mg for pool 1 and 2, respectively). The correlation between $CL_{int,u}$ values obtained in the two pools of RIM is shown in **Figure 3-3**. The correlation between the pools was strong (R^2=0.998, $p<0.001$), with 61% of compounds within 2-fold. Mean fold difference between the pools was 4-fold. The greatest fold difference was observed for compounds with $CL_{int,u}$ below 10 µl/min/mg (diclofenac and furosemide, 23 and 27- fold respectively). Excluding these compounds, mean fold difference was 2-fold.

Table 3-6 Mean fu_{inc} and $CL_{int,u}$ determined in rat intestinal pools and commercial HW microsomes using combined and individual CYP and UGT cofactors

			$CL_{int,u}$ (µl/min/mg microsomal proetein)[a]				
			In house Combined Cofactors		Commercial HW pool		
Study #	Compound	fu_{inc}[a]	Pool 1	Pool 2	Combined Cofactors	CYP Cofactors	UGT Cofactors
1	7-Hydroxycoumarin	1.00	196.5	264.2	271.7	0.9	327.3
2	Amitriptyline	0.20	24.3	19.9	23.8	5.3	3.0
3	Atorvastatin	0.57	5.3				
4	Bisporolol	0.89	5.4	0.9			
5	Bumetanide	0.92	2.8	7.3			
6	Buspirone	0.91	3.2	1.4			
8	Cyclosporine A	0.82	21.0	30.8	13.7		
9	Diclofenac	0.98	2.6	0.1	5.0		
10	Diltiazem	0.85	21.8	26.7			
13	Furosemide	1.00	2.9	0.1			
14	Indomethacin	0.88	48.9	62.4			
15	Ipriflavone	0.28	495.0	550.3	72.0	59.1	7.3
16	Irbesartan	0.79	31.9	35.9	15.2	1.5	9.4
17	Losartan	0.87	34.8	14.8	10.0	0.1	9.0
18	Midazolam	0.72	22.0	19.9	12.3	18.2	2.8
19	Nicardipine	0.09	1780.2	3106.2	865.7	1048.0	1.2
21	Omeprazole	0.90	7.6				
22	Pirenzepine	1.00	3.9	2.7			
23	Raloxifene	0.06	1135.3	1654.3	1042.1	9.8	927.0
24	Saquinavir	0.11	3948.8	6414.7			
25	Sildenafil	0.73	23.8	18.4			
26	Simvastatin	0.93	13.6	41.5			
27	Tacrolimus	0.32	705.7	627.3			
28	Terfenadine	0.02	31928.2	39704.4			
29	Verapamil	0.65		29.1	6.9		

a: incubations at 1 mg microsomal protein/ml at compound concentration of 1µM.

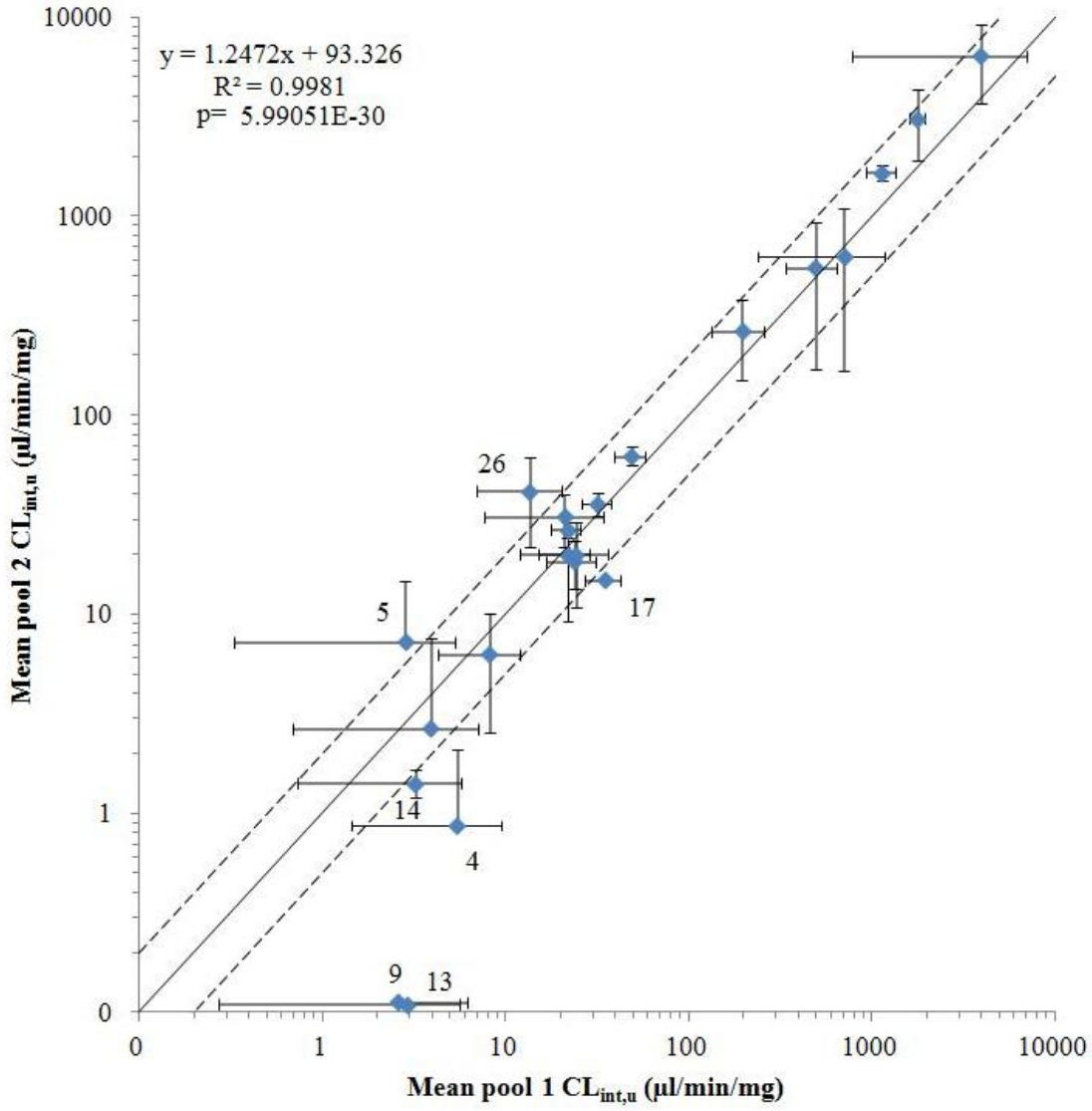

Figure 3-3 Correlation between $CL_{int,u}$ in pool 1 and pool 2 rat intestinal microsomes.

Solid line represents line of unity, dashed lines 2-fold. 9:diclofenac, 13:furosemide, 4:biosoprolol, 14:indomethacin, 5:bumetemide, 17:losartan, 26:simvastatin. n=22. Data represent mean ±stdev of n=3 of duplicate incubations. µl/min/mg represents µl/min/mg microsomal protein.

3.4.3.3. Comparison of commercial and in house intestinal microsomal pools

The mean $CL_{int,u}$ for a number of selected compounds (n=11) overlapping with those studied previously in house microsomes were screened in commercial microsomes using combined CYP and UGT cofactors is shown in **Table 3-6**. Mean $CL_{int,u}$ ranged from 5 to 1042 µl/min/mg from diclofenac and raloxifene respectively. There was a

positive correlation between both commercial and in house rat intestinal microsomes (R^2=0.77, p<0.001) (**Figure 3-4**). However, 54% of compounds studied showed a greater than 2-fold difference. Mean fold difference was 2.5-fold. Good correlation was observed for midazolam, amitryptiline, 7-HC and raloxifene.

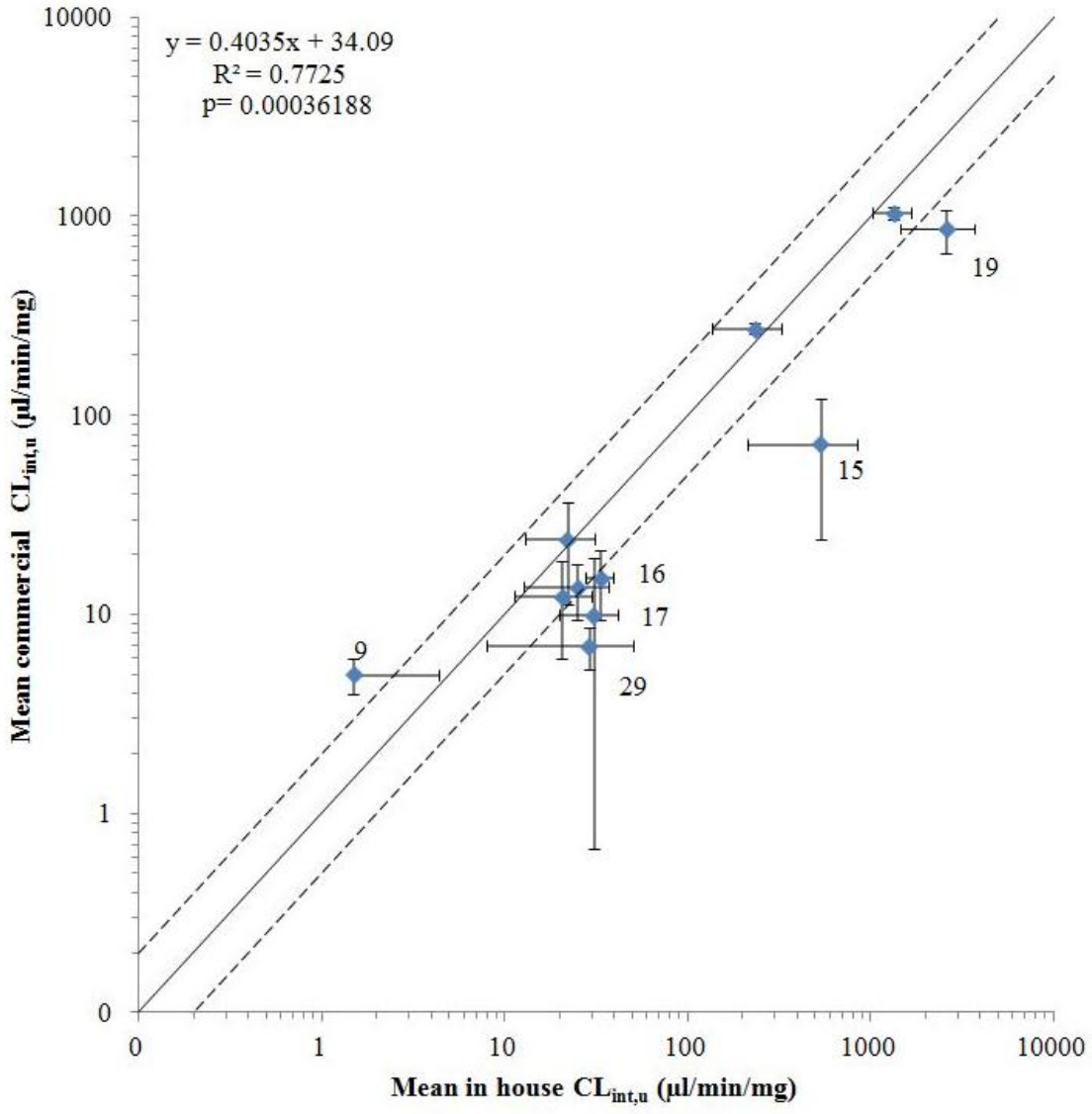

Figure 3-4 Correlation between $CL_{int,u}$ for in house and commercial rat intestinal microsomes using combined CYP and UGT cofactors (n=11).

Solid line represents line of unity, dashed lines 2-fold. 9: diclofenac, 29: verapamil, 3: losartan, 4: ibesartan, 5: ipriflavone, 19: nicardipine. Data represent mean ±stdev of n=3 of duplicate incubations. µl/min/mg represents µl/min/mg microsomal protein.

3.4.3.4. Comparison of combined *vs.* individual CYP and UGT cofactors

Mean $CL_{int,u}$ for CYP incubations in commercial microsomes ranged from 0.1 to 1048 µl/min/mg for losartan and nicardipine, respectively. Mean $CL_{int,u}$ for UGT incubations ranged from 1.2 and 927 µl/min/mg microsomal protein for nicardipine and raloxifene, respectively. The main route of elimination for midazolam, nicardipine and ipriflavone was via CYPs, whereas glucuronidation was the major clearance pathway for 7-HC, raloxifene, irbesartan and losartan. In the case of amitryptiline, significant reduction in $CL_{int,u}$ was observed using individual *vs.* combined cofactors (8.3 vs. 23.8 µl/min/mg microsomal protein) .

When comparing mean $CL_{int,u}$ obtained in the presence of combined cofactors and additive $CL_{int,u}$ for individual cofactors, a strong positive correlation was observed (R^2=0.966, $p<0.001$) (**Figure 3-5**). Observed $CL_{int,u}$ were within 2-fold for all compounds, with the exception of amitryptiline. Observed mean CV was lowest for individual cofactors (39% *vs.* 58% for individual and combined cofactors, respectively). Mean fold difference was 1.4-fold.

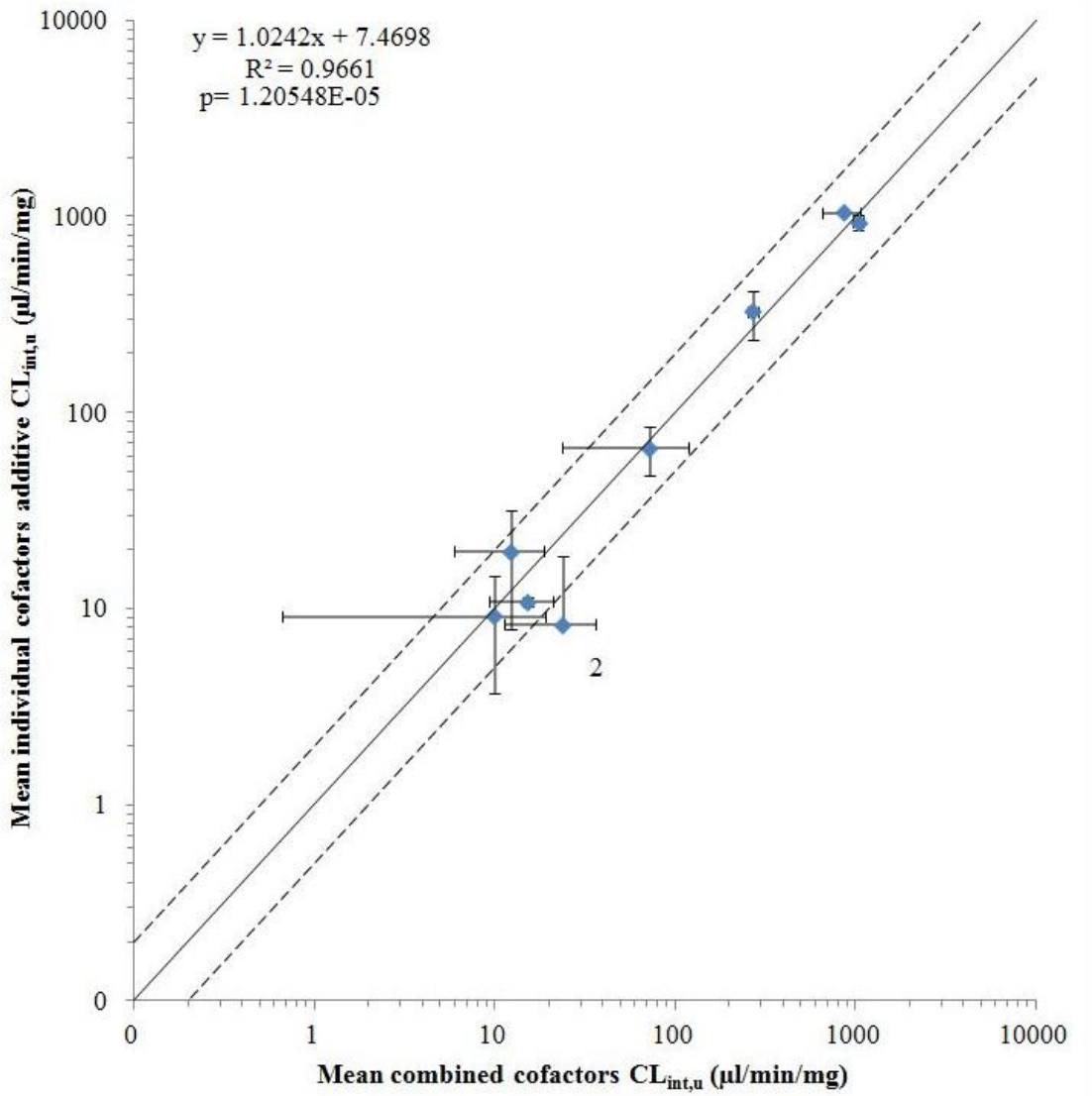

Figure 3-5 Correlation between $CL_{int,u}$ for commercial HW rat intestinal microsomes using combined and individual CYP and UGT cofactor incubations.
Solid line represents line of unity, dashed lines 2-fold. 2: amitriptyline. Data represent mean ±stdev of n=3 of duplicate incubations. µl/min/mg represents µl/min/mg microsomal protein.

3.4.4. Scaling of intestinal metabolism

3.4.4.1. Rat Q_{gut} and Fa prediction

Of all the compounds screened, Caco-2 P_{app} ranged from 0.13 (furosemide) to 121 $x10^{-6}$ cm/s) (indomethacin), and 29% of compounds displayed low Caco-2 permeability ($\leq 10x10^{-6}$ cm/s). Estimates of rat intestinal Q_{gut} based on physiochemical properties of individual compounds and Caco-2 permeability data is shown in **Table 3-7**. For 5 compounds P_{app} and subsequently Q_{gut} could not be determined (i.e. Q_{gut} <0.01 l/h) based on physicochemical properties, namely cyclosporine, bumetamide, furosemide, saquinavir, and tacrolimus. Maximal Q_{gut} based on physiochemical properties was 0.27 l/h

(amitriptyline). The range of Q_{gut} was estimated between 0.01 l/h (pirenzepine and furosemide) and 0.23 l/h (indomethacin) for Caco-2 based estimates. P_{eff} values for cyclosporine could not be predicted using in house Caco-2 data, and therefore an *in vivo* P_{eff} value was taken from the literature (Zakeri-Milani et al., 2008).

Estimates of Fa based on physicochemical data ranged from <0.01 (cyclosporine) and 1.00 (midazolam, 7-HC, buspirone, pirenzepine, diltizem, amitriptylone, ipriflovone and verapamil). Based on Caco-2 data, estimated Fa ranged from 0.21 (pirenzepine) to 1.00 (midazolam, 7-HC, indomethacin, atorvastatin, cyclosporine, nicardipine, ipriflavone and diclofenac). The largest discrepancies in estimated Fa between physicochemical and Caco-2 based estimates were observed for pirenzepine (5-fold), atorvastatin (5-fold), tacrolimus (14-fold), saquinavir (70-fold), and cyclosporine (100-fold).

Table 3-7 Q_{gut} estimates based on physicochemical data and Caco-2 permeability data

	Physicochemical				Caco-2			
Compound	**PSA**	**HBD**	**Q_{gut} (l/h)**	**Fa[b]**	**P_{app} A-B (10^{-6}cm/s)**	**P_{eff} (10^{-4} cm/s)**	**Q_{gut} (l/h)**	**Fa[b]**
7-Hydroxycoumarin	51	1	0.14	1.00	61.68	7.41	0.19	1.00
Amitriptyline	1	0	0.28	1.00	13.70	2.49	0.10	0.99
Atorvastatin	119	4	0.01	0.19	18.49	3.10	0.12	1.00
Bisporolol	64	2	0.07	0.96	6.85	1.51	0.07	0.95
Bumetanide	130	4	<0.01	0.15	1.73	0.56	0.03	0.67
Buspirone	60	0	0.18	1.00	11.02	2.13	0.09	0.99
Cyclosporine A	290	5	<0.01	<0.01	NV	3.34[a]	0.12	1.00
Diclofenac	55	2	0.09	0.98	111.60	11.37	0.23	1.00
Diltiazem	56	0	0.19	1.00	9.61	1.93	0.09	0.98
Furosemide	130	4	<0.01	0.15	0.13	0.09	0.01	0.16
Indomethacin	69	1	0.11	0.99	121.00	12.06	0.23	1.00
Ipriflavone	37	0	0.22	1.00	57.37	7.03	0.19	1.00
Irbesartan	82	1	0.08	0.98	13.31	2.44	0.10	0.99
Losartan	87	2	0.04	0.83	2.72	0.78	0.04	0.79
Midazolam	20	0	0.25	1.00	36.24	5.04	0.16	1.00
Nicardipine	114	1	0.04	0.81	26.51	4.02	0.14	1.00
Omeprazole	71	1	0.10	0.99	NV	NV	NV	NV
Pirenzepine	64	1	0.12	1.00	0.20	0.12	0.01	0.21
Raloxifene	74	2	0.06	0.91	6.23	1.41	0.07	0.94
Saquinavir	179	6	<0.01	0.01	1.96	0.61	0.03	0.71
Sildenafil	105	1	0.05	0.88	40.27	5.44	0.17	1.00
Simvastatin	77	1	0.09	0.99	NV	NV	NV	0.95
Tacrolimus	186	3	<0.01	0.07	73.60	8.42	0.20	1.00
Terfenadine	46	2	0.10	0.99	5.76	1.33	0.06	0.93
Verapamil	56	0	0.19	1.00	12.70	2.36	0.10	0.99

a: Zakeri-Milani et al.,(2008) , b: based on **Equation 3-17**. NV: no value available due to poor MS signal.

3.4.4.2. *In vivo* F_G determination

Literature and in house generated values of F_G in the rat are summarised in **Table 3-8**. For the dataset investigated, F_G ranged from 0% (buspirone, furosemide, sildenafil, nicardipine and amitriptyline) to 98% (diclofenac). Pharmacokinetics could not be described for tacrolimus or simvastatin at the doses and route of i.v. administration used. $Fa.F_G$ values ranged from 0.00 (nicardipine, terfenadine) to 1.00 (midazolam, buspirone, bisoprolol, sildenafil, diltiazem, diclofenac, amitriptyline and verapamil). No literature data were available for pirenzepine, terfenidine or simvastatin. In cases where it had not been possible to determine the extent of metabolism at the dose used, and the ethical limitations of repeating dosing and using increased doses (e.g. midazolam central nervous system effects), literature values were selected for the assessment of F_G prediction success and are indicated in **Table 3-8**. Intestinal metabolism determined by portal vein cannulation if available in the literature and was selected as the most accurate measure of F_G. Out of the 23 compounds with *in vivo* $Fa.F_G$ estimates, 11 compounds indicated high intestinal extraction ($Fa.F_G<0.5$).

3.4.4.3. Prediction of F_G using metabolic data from in house pools

Summaries of predicted rat F_G using $CL_{int,u}$ data obtained using in house intestinal microsomes are shown in **Table 3-9**. Estimates of F_G based on compound physicochemical properties ranged from 0.00 (cyclosporine, terfenidine, saquinavir, nicardipine and tacrolimus) to 0.95 for diclofenac. F_G values predicted using Caco-2 data ranged from 0.00 (terfenadine and saquinavir) to 0.98 (diclofenac). Mean CV between the two in house pools for all compounds for Caco-2 based scaling was 32%. Estimates of E_G for compounds with a fu_{inc} <0.3 *vs.* >0.3 demonstrated a mean CV of 46% *vs.* 25%.

Correlations of *in vivo* $Fa.F_G$ and predicted F_G using either physicochemical or Caco-2 based permeability estimate is shown in **Figure 3-6**. R^2 values were similar between both scaling strategies (0.29 and 0.30, respectively). Predictions of F_G were within 2-fold for 65% and 59% of compounds for physicochemical and Caco-2 based estimates respectively **Table 3-13**. Prediction accuracy was the same between Caco-2 based *vs.* physicochemical

Table 3-8 Rat in house and literature *in vivo* pharmacokinetics

	In House				Literature	
Compound	**R_b**	**F**	**F_H[d]**	**Fa.F_G**	**Fa.F_G**	**References**
Amitriptyline	0.94	0.00	0.00	1.00	1.00	(Bae et al., 2009)
Atorvastatin	1.26	0.04	0.55	0.07	0.10	(Lau et al., 2006)
Bisporolol[a]	9.99	0.33	0.23	1.00	0.17	(Buhring et al., 1986; Tahara et al., 2006)
Bumetanide	0.35	0.10	0.23	0.43	0.61	(Han et al., 1993; Lee et al., 1994; Kim et al., 2000b)
Buspirone	0.67	0.00	0.00	1.00	1.00	(Caccia et al., 1983; Caccia et al., 1986; Wong et al., 2007)
Cyclosporine A	1.73	0.68	0.97	0.70	0.25	(Sangalli et al., 1988; Luke et al., 1990; Kawai et al., 1998; Molpeceres et al., 1998; Lee et al., 2000; Tanaka et al., 2000; Hirunpanich et al., 2006)
Diclofenac[c]	0.48	0.98	0.66	1.00	1.00	(Peris-Ribera et al., 1991; Grace et al., 2000; Kim et al., 2006; Reyes-Gordillo et al., 2007; Deguchi et al., 2011)
Diltiazem	0.99	0.02	0.00	1.00	0.15	(Choi et al., 2006; Bertera et al., 2007)
Furosemide	0.90	0.11	0.99	0.11	0.39	(Hammarlund and Paalzow, 1982; Kim et al., 1993; Kim et al., 2000a; Deguchi et al., 2011)
Indomethacin	0.38	0.88	0.99	0.89	0.86	(Matsuda et al., 2012)
Ipriflavone	1.03	0.05	0.36	0.14	0.22	(Kim and Lee, 2002; Chung et al., 2009; Lee et al., 2009)
Irbesartan[c]	0.50	0.08	1.00	0.08	0.23	(Davi et al., 2000)
Losartan	0.64	0.33	0.74	0.44	0.87	(Moon et al., 1998)
Midazolam[a]	0.40	0.00	0.00	1.00	0.72	(Kuze et al., 2009; Matsuda et al., 2012)
Nicardipine	0.53	0.00	0.64	0.00	1.00	(Higuchi and Shiobara, 1980; Piao and Choi, 2008; Chung et al., 2010)
Omeprazole[a]					0.22	(Watanabe et al., 1994; Katashima et al., 1995; Lee et al., 2007)
Pirenzepine[b]	1.19	0.08	0.75	0.11		
Raloxifene	1.08	0.06	0.70	0.09	0.15	(Kosaka et al., 2011; Matsuda et al., 2012)
Saquinavir[b]	0.52	0.05	0.35	0.14	0.14	(Shibata et al., 2002)
Sildenafil	0.56	0.00	0.00	1.00	1.00	(Walker et al., 1999; Shin et al., 2006)
Tacrolimus[a]					0.63	(Takada et al., 1991; Hashimoto et al., 1998)
Terfenadine	1.98	0.02	0.00	0.00[e]		
Verapamil	0.65	0.01	0.00	1.00	1.00	(Chen et al., 2008; Choi et al., 2008; Hu et al., 2011)

a: literature value used for assessing prediction accuracies, b not corrected for renal clearance, c: enterohepatic circulation, d: Q_H=72 ml/min/kg, e: reclassified Fa.F_G as 0.00 due to high intestinal CL_{int}

estimates (rmse=0.34). Prediction accuracy for compounds with *in vivo* estimates of F_G<0.5 was decreased in both cases (rmse= 0.39 and 0.37) with 46% and 42% within 2-fold for physicochemical and Caco-2 based scaling, respectively. The highest incidence of TN and lowest of FP was observed for Caco-2 based scaling (45% and 5%). However, the lowest incidence of FN and highest TP was observed using physicochemical based scaling (3% and 43%).

Improved correlations (R^2=0.40 and 0.43 for physicochemical and Caco-2 based scaling) were observed correcting estimates of F_G for estimates of Fa (**Figure 3-7**). Estimates of *in vitro* Fa.F_G were within 2-fold for 65% and 73% of compounds for physicochemical and Caco-2 based estimates respectively **Table 3-13**. Observed CV in Fa.F_G estimates using combined data from in house pools using was 32% and 31% for physicochemical and Caco-2 based estimates, respectively.

Overprediction of Fa.F_G for Caco-2 based scaling was observed for atorvastatin and irbesartan. Underprediction was observed for raloxifene, saquinavir, and tacrolimus. Predictions within 2-fold for compounds with *in vivo* Fa.F_G<0.5 were 42% and 45% for physicochemical and Caco-2 based scaling. Rmse was 0.43 and 0.38 for physicochemical and Caco-2 respectively.

Incorporation of Fa to estimates of F_G improved furosemide and pirenzepine prediction and changed classification from a FN to TP. No improvement was observed for irbesartan. In both correlations, atorvastatin was better predicted using permeability/Q_{gut} based on physicochemical properties. Predictions based on compounds physicochemical properties resulted in poor success for cyclosporine, sildenafil, tacrolimus and pirenzepine. Improved prediction success was observed when Caco-2 data was incorporated for these compounds, however tacrolimus was poorly predicted using both scaling methods. Buspirone prediction was poor using Caco-2 based scaling.

Overall TN classification was higher using Caco-2 *vs.* physicochemical based scaling (41% *vs.* 35%). However, incidence of TP for Caco-2 based scaling was 41% *vs.* 48% for physiochemical based scaling (**Table 3-10**). Overall TN and TP classification was high, with 82% prediction success and 83% in Caco-2 and physiochemical scaling methods, respectively.

Table 3-9 Summary of mean F_G values determined in house and commercial rat intestinal microsomes using Q_{gut} based on either physiochemical and Caco-2 based permeability estimates

Compound		Physicochemical F_G		Caco-2 F_G	
Study #	Name	In house[a]	Commercial[b]	In house[a]	Commercial[b]
1	7-Hydroxycoumarin	0.20 ±0.10	0.15 ±0.01	0.25 ±0.11	0.19 ±0.01
2	Amitriptyline	0.81±0.07	0.80 ±0.08	0.62 ±0.10	0.60 ±0.13
3	Atorvastatin	0.34 ±0.04		0.91 ±0.01	
4	Bisporolol	0.90 ±0.09		0.90 ±0.09	
5	Bumetanide	0.41 ±0.29		0.73 ±0.23	
6	Buspirone	0.42 ±0.10		0.60 ±0.10	
8	Cyclosporine A	0.00 ±0.00	0.00 ±0.00	0.65 ±0.15	0.87 ±0.15
9	Diclofenac	0.97 ±0.06	0.85 ±0.03	0.99 ±0.03	0.94 ±0.01
10	Diltiazem	0.72 ±0.08		0.55 ±0.10	
13	Furosemide	0.69 ±0.29		0.70 ±0.29	
14	Indomethacin	0.96 ±0.02		0.93 ±0.04	
15	Ipriflavone	0.15 ±0.09	0.55 ±0.16	0.13 ±0.08	0.50 ±017
16	Irbesartan	0.47 ±0.09	0.65 ±0.08	0.52 ±0.09	0.69 ±0.08
17	Losartan	0.42 ±0.02	0.65 ±0.21	0.39 ±0.02	0.63 ±0.22
18	Midazolam	0.80 ±0.08	0.87 ±0.06	0.72 ±0.10	0.81 ±0.08
19	Nicardipine	0.01 ±0.01	0.02 ±0.00	0.02 ±0.01	0.05 ±0.01
21	Omeprazole	0.43 ±0.05		NV	
22	Pirenzepine	0.93 ±0.08		0.63 ±0.30	
23	Raloxifene	0.02 ±0.01	0.02 ±0.00	0.02 ±0.01	0.02 ±0.00
24	Saquinavir	0.00 ±0.00		0.00 ±0.00	
25	Sildenafil	0.47 ±0.07		0.73 ±0.06	
26	Simvastatin	0.61 ±0.21		0.56 ±0.21	
27	Tacrolimus	0.00 ±0.00		0.13 ±0.07	
28	Terfenadine	0.00 ±0.00		0.00 ±0.00	
29	Verapamil	0.66 ±0.13	0.90 ±0.02	0.51 ±0.13	0.82 ±0.04

a: Mean and Stdev of 2 pools, n=3 in duplicate, b: Mean and Std n=3 in duplicate, NV: no value

Incidence of correct and incorrect $Fa.F_G$ estimation based on stricter prediction critera plotted on **Figure 3-7** are shown in **Table 3-11**. For phyiscochemical based scaling, correct catergorisation of $Fa.F_{G,<0.3}$ was 30%, $Fa.F_{G,\ 0.3\text{-}0.7}$ was 4% and $Fa.F_{G,<0.7}$ was 26% (Total correct 61%). Incorrect catergorisation was 13% in each case. For Caco-2 based scaling, total correct catergorisation was 68%, with 32,14 and 23% for $Fa.F_{G,<0.3}$, $Fa.F_{G,\ 0.3\text{-}0.7}$ and $Fa.F_{G,<0.7}$, respectively.

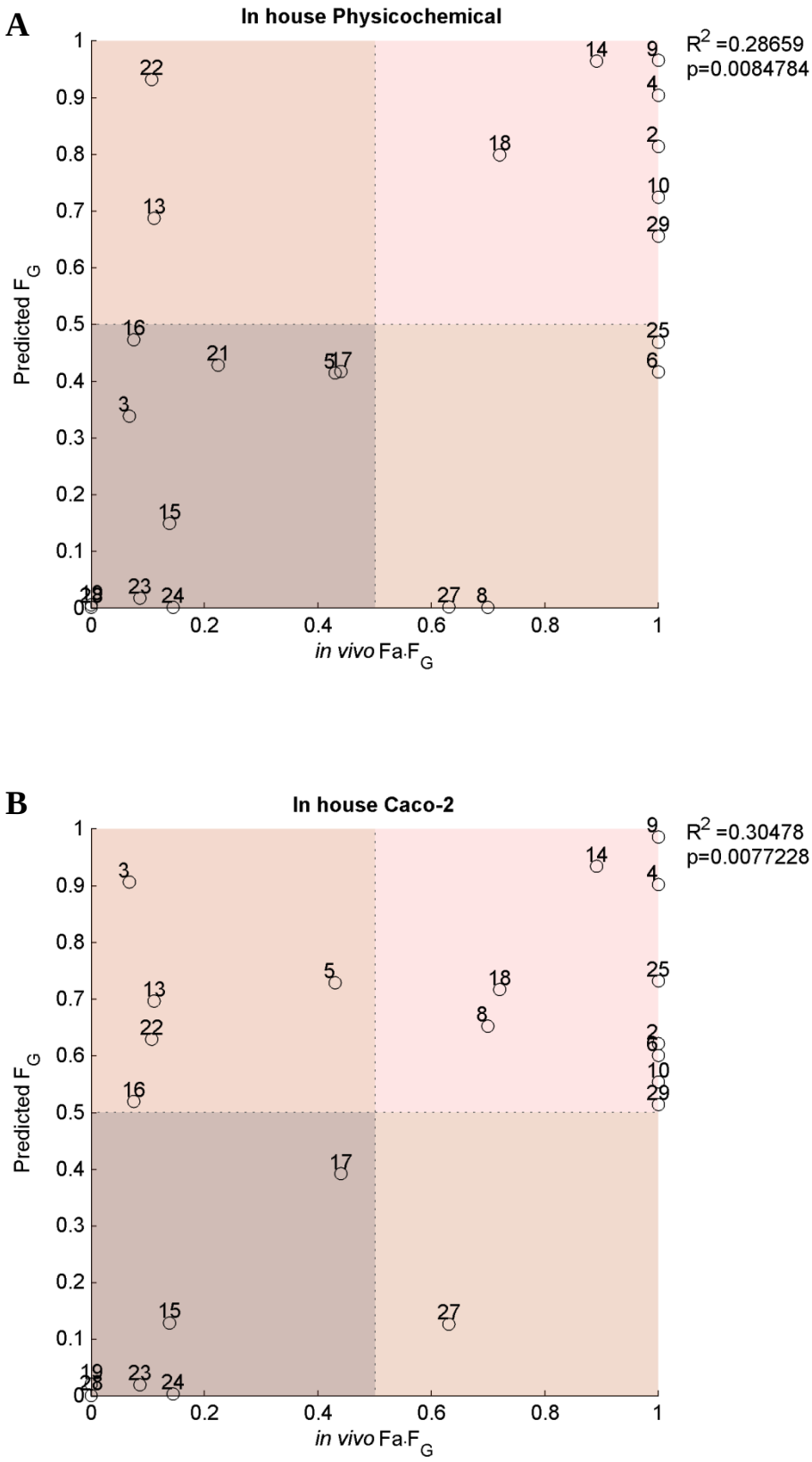

Figure 3-6 Comparison of *in vivo* Fa.F_G *vs.* predicted F_G from *in vitro* $CL_{int,u}$ from in house rat intestinal microsomes and permeability data based on either physicochemical (A) Caco-2 (B) data.

Compound numbers relate to **Table 3-9**. Data represents mean of two in house pools.

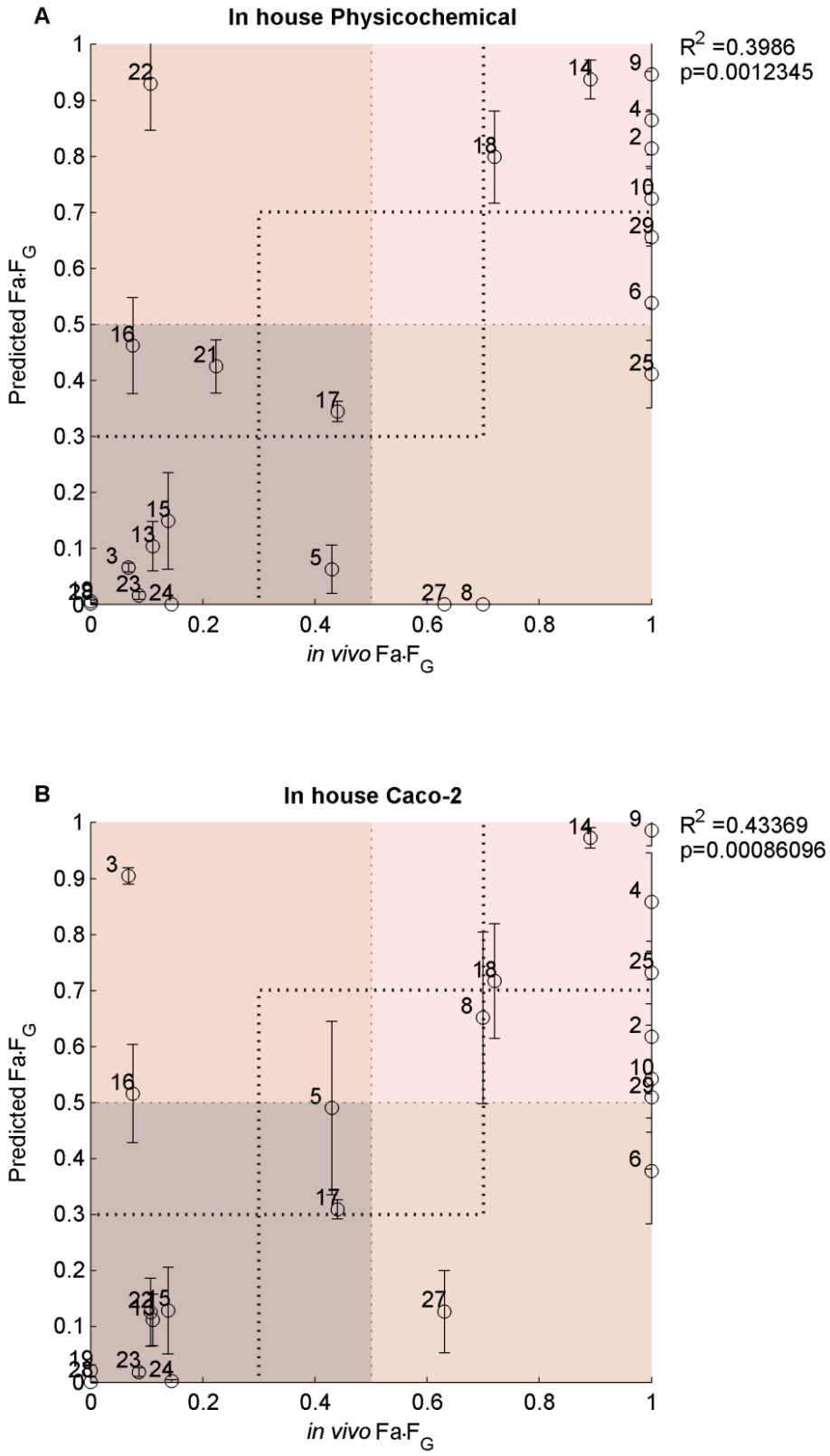

Figure 3-7 Comparison of *in vivo* $Fa.F_G$ *vs.* predicted $Fa.F_G$ from *in vitro* $CL_{int,u}$ from in house rat intestinal microsomes and permeability data based on either physicochemical (A) Caco-2 (B) data.

Compound numbers relate to **Table 3-9**. Data represents mean and Stdev of two in house pools.

Table 3-10 Incidence of low F_G categorisation using either predicted F_G or predicted $Fa.F_G$ *vs.* observed Fa.FG using metabolism data and either physicochemical or Caco-2 based scaling methodologies.

F_G						$Fa.F_G$					
Physicochemical			**Caco-2**			**Physicochemical**			**Caco-2**		
Class	**N**	**%**	**Class**	**N**	**%**	**Class**	**N**	**%**	**Class**	**N**	**%**
TP	10	43%	TP	6	27%	TP	11	48%	TP	9	41%
TN	7	30%	TN	10	45%	TN	8	35%	TN	9	41%
FP	4	17%	FP	1	5%	FP	3	13%	FP	2	9%
FN	2	9%	FN	5	23%	FN	1	4%	FN	2	9%

In all the cases $CL_{int,u}$ was obtained using in house rat intestinal microsomes, as listed in **Table 3-6**.Values of Q_{gut} and Fa used are as listed in **Table 3-7**.

Table 3-11 Incidence of $Fa.F_{G,<0.3}$, $Fa.F_{G,0.3-0.7}$ and $Fa.F_{G,>0.7}$ correct and incorrect categorisation for predicted and observed $Fa.F_G$ using metabolism data and either physicochemical or Caco-2 based scaling methodologies.

	$Fa.F_G$									
	Physicochemical					**Caco-2**				
		Correct		**Incorrect**			**Correct**		**Incorrect**	
	$Fa.F_{G,<0.3}$	7	30%	3	13%	$Fa.F_{G,<0.3}$	7	32%	2	9%
	$Fa.F_{G,0.3-0.7}$	1	4%	3	13%	$Fa.F_{G,0.3-0.7}$	3	14%	1	5%
	$Fa.F_{G,>0.7}$	6	26%	3	13%	$Fa.F_{G,>0.7}$	5	23%	4	18%
∑	23	14	61%	9	41%	22	15	68%	7	32%

Prediction accuracy based on the ratio of observed/predicted clearance for $Fa.F_G$ estimated demonstrated 73% of compounds within 2 fold for Caco-2 based estimates, and 57% for physicochemical estimates (**Figure 3-8**). Improved predictions using Caco-2 approaces were seen for pirenzepine, buspirone, cyclosporine, bumetamide and sildenafil, and worse for atorvastatin.Worst estimates in both stratergies were seen for raloxifene, saquinavir, nicardipine and tacrolimus.

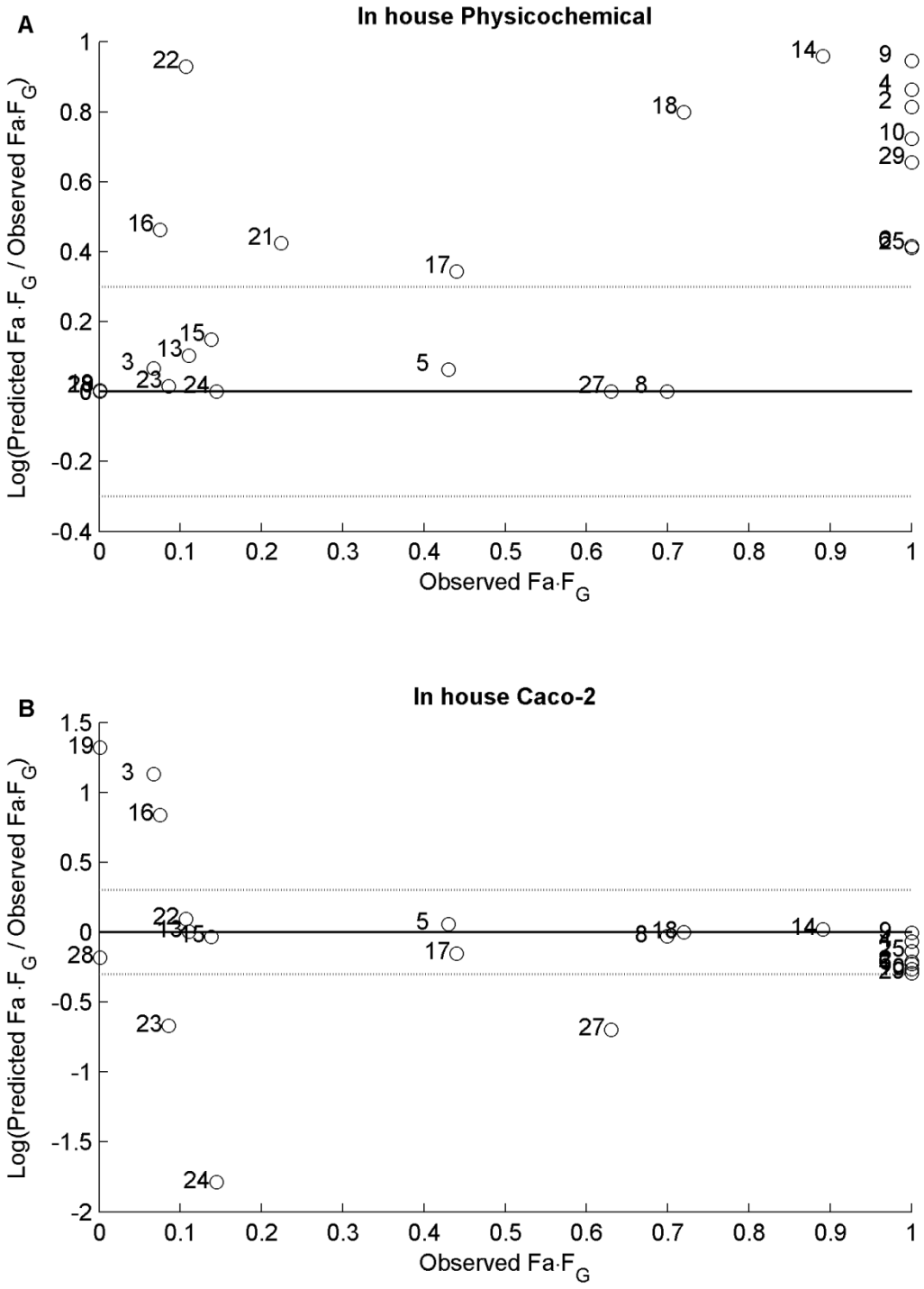

Figure 3-8 Precision of predictions of $Fa.F_G$ using physicochemical (A) and Caco-2 (B) based scaling of *in vitro* rat intestinal metabolic data.

The dotted lines at ±0.3 log units represents 50% underprediction and 100% overprediction precision limits.

3.4.4.4. Estimates of F_G for in house *vs.* commercial pools

Estimates of F_G for in house and commercial microsomes based on Caco-2 and physicochemical Q_{gut} predictions are shown in **Table 3-9**. Estimates ranged from 0.02 for raloxifene in both Caco-2 and physicochemical based estimates, and 0.86 (verapamil) and 0.92 (diclofenac) in Caco-2 based scaling strategies. Comparative plots of *in vivo* and predicted $Fa.F_G$ to display prediction success in both intestinal microsome pools are shown in **Figure 3-9**. Poor prediction was observed for both sets of microsomes for irbesartan, however a worse prediction for ipriflavone was observed in commercial microsomes. TP and TN classed compounds were well predicted in both sets of microsomes.

Characterisation of prediction success on the basis of low F_G is shown in **Table 3-12**. Improved incidence of TP was observed in physicochemical based permeability approaches using in house microsomes (56% *vs.* 22%). Incidence of TN and TP was improved for commercial microsomes using Caco-2 based permeabilities.

Prediction of bias for $Fa.F_G$ is displayed in **Table 3-14**. Estimates for compounds with high intestinal extraction ($Fa.F_G<0.5$) was high for in house microsomes compared to commercial microsomes. Using commercial microsomes, the greatest prediction accuracy slightly improved using physicochemical *vs.* Caco-2 based scaling strategies (rmse 0.30 *vs.* 0.33, gmfe 2.31 *vs.* 3.57). For both set of microsomes, however, increased correlation was observed using Caco-2 based permeability estimates.

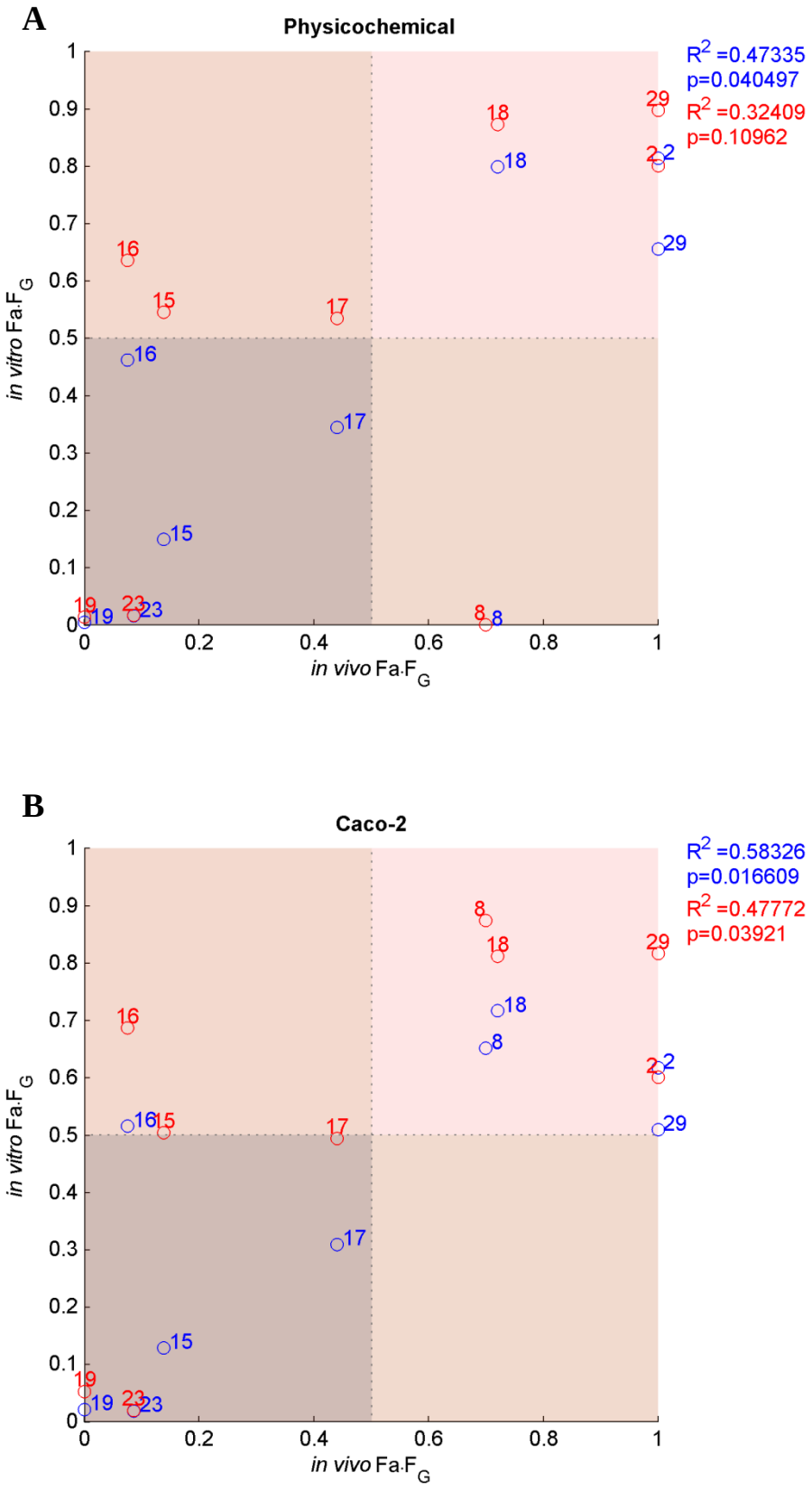

Figure 3-9 Comparison of *in vivo* $Fa.F_G$ *vs.* predicted $Fa.F_G$ from *in vitro* $CL_{int,u}$ from commercial rat intestinal microsomes and permeability data based on either physicochemical (A) Caco-2 (B) data.

Compound numbers relate to **Table 3-9**.

Table 3-12 Incidence of low F_G categorisation using predicted Fa.F_G *vs. in vivo* Fa.F_G for in house and commercial rat intestinal microsomes

Physiochemical						Caco-2					
In house			Commercial			In house			Commercial		
Class	N	%	Class	N	%	Class	N	%	Class	N	%
TP	5	56%	TP	2	22%	TP	4	44%	TP	3	33%
TN	3	33%	TN	3	33%	TN	4	44%	TN	4	44%
FP	1	11%	FP	1	11%	FP	0	0%	FP	0	0%
FN	0	0%	FN	3	33%	FN	1	11%	FN	2	22%

Table 3-13 Description of bias (gmfe), rmse and percentage within 2-fold of unity for predictions of $Fa.F_G$ and F_G for either total set of drugs or for a subset of drugs for which *in vivo* F_G<0.5 for both Caco-2 and physicochemical based scaling strategies.

F_G						$Fa.F_G$					
Physicochemical			**Caco-2**			**Physicochemical**			**Caco-2**		
	n	23		n	22		n	23		n	22
	>2-fold (%)	35		>2-fold (%)	41		>2-fold (%)	35		>2-fold (%)	27
	<2-fold (%)	65		<2-fold (%)	59		<2-fold (%)	65		<2-fold (%)	73
	gmfe	0.78		gmfe	1.04		gmfe	0.25		gmfe	0.94
	rmse	0.34		rmse	0.34		rmse	0.35		rmse	0.30
F_G<0.5	n	13	$Fa.F_G$<0.5	n	12	$Fa.F_G$<0.5	n	12	$Fa.F_G$<0.5	n	11
	>2-fold (%)	54		>2-fold (%)	58		>2-fold (%)	58		>2-fold (%)	55
	<2-fold (%)	46		<2-fold (%)	42		<2-fold (%)	42		<2-fold (%)	45
	gmfe	1.11		gmfe	1.93		gmfe	0.22		gmfe	0.89
	rmse	0.39		rmse	0.37		rmse	0.43		rmse	0.38

gmfe: geometric fold error, rmse: root mean squared error

Table 3-14 Description of bias (gmfe), rmse and percentage within 2-fold of unity for predictions of the $Fa.F_G$ compounds screened in both commercial and in house intestinal microsome for both Caco-2 and physicochemical based scaling strategies.

Physiochemical						Caco-2					
In house			**Commercial**			**In house**			**Commercial**		
	n	10		n	10		n	10		n	10
	>2-fold (%)	30		>2-fold (%)	60		>2-fold (%)	30		>2-fold (%)	40
	<2-fold (%)	70		<2-fold (%)	40		<2-fold (%)	70		<2-fold (%)	60
	gmfe	0.29		gmfe	0.85		gmfe	1.19		gmfe	1.82
	rmse	0.29		rmse	0.34		rmse	0.25		rmse	0.28
$Fa.F_G$<0.5	n	6	$Fa.F_G$<0.5	n	6	$Fa.F_G$<0.5	n	5	$Fa.F_G$<0.5	n	5
	>2-fold (%)	33		>2-fold (%)	83		>2-fold (%)	60		>2-fold (%)	80
	<2-fold (%)	67		<2-fold (%)	17		<2-fold (%)	40		<2-fold (%)	20
	gmfe	1.18		gmfe	2.33		gmfe	1.82		gmfe	3.59
	rmse	0.22		rmse	0.30		rmse	0.21		rmse	0.33

3.5. Discussion

3.5.3. Microsomal pool characterisation

Microsomes were prepared to create 2 pools in order to determine reproducibility of the elution method, and furthermore make estimates of rat intestinal metabolism. Comparing Pool 2 prepared using identical techniques to Pool 1, a lower recovery but higher scalar were observed, but these results were not statistically significant. A similar mucosal yield could be achieved through scraping intestinal tissue gently using a glass microscope slide. However the use of frozen rat intestinal tissue resulted in a larger mucosal yield. When flushed, unlike fresh tissue, the intestine was easily striped of its mucosa. This may in part be down to the simple tube like structure of the intestine which, unlike human tissue, is not folded (Kararli, 1995; DeSesso and Jacobson, 2001).

Mean CYP content was 2-fold lower in pool 2 *vs.* pool 1 when measured fresh. Pool 1 however showed a 39% reduction on CYP content following one FT cycle. Subsequent FT cycles showed no further decrease suggesting that the CYP was stable following the initial freezing. Interestingly, in frozen tissue, when microsomes were measured on the day of preparation the CYP levels were similar across the FT samples, suggesting that any reduction of CYP occurs following the first freezing of either tissue or microsomes.

A fall in specific CYP content following freezing was not matched by any significant reductions in testosterone metabolite formations in pool 2. The main metabolites observed were 6β-, 16α-, 16β-OH TEST and androstenedione. These represented the activities of CYP3A1, and CYP2B. No peaks were observed for 2α- or 6α-OH TEST suggesting that little/no 2C11 or 2A1 content was present. This was different to previous results observed in Sprague Dawley rats where 6α-OH TEST formation was high (Sohlenius-Sternbeck and Orzechowski, 2004). Interestingly in commercial SD microsomes, 2α-OH TEST or 6α-OH TEST formation was not observed, however the highest 16α-OH TEST was seen possibly indicating a role of CYP2C11. Intestinal CYP2A1 is not detected at an mRNA level in Wistar rats (Zhang et al., 1996), and CYP2C11 is not reported to have any protein expression (Mitschke et al., 2008). However, CYP2B is a major enzyme expressed in Wistar rat intestines, accounting for the majority of CYP expression (Fasco et al., 1993; Zhang et al., 1996; Mitschke et al., 2008). Androsteinedione was also the major metabolite observed in all microsomes studied; suggesting CYP3A was is not the dominant route of metabolism in the rat intestine. 6β-OH TEST formation in HW rat intestinal microsomes

prepared by elution microsomes was slightly below previous reports (268.7 ±0), however this is likely due to the shorter length of intestine used (30cm) and the reported decreasing CYP3A content in the rat small intestine (Zhang et al., 1996; Mitschke et al., 2008). In line with previous reports using microsomes prepared through scraping of the intestinal tissue, the lowest activity in CYP3A (6β-OH TEST formation) was observed (Mohri and Uesawa, 2001; Galetin and Houston, 2006).

The rate of 4-NP glucuronidation was also low in microsomes prepared through scraping compared to elution's from fresh tissue. No reduction in activity was observed in glucuronidation activities using fresh or FT microsomes. Glucuronidation was however 10 fold higher than previously reported (7.00 ±0.81nmol/min/mg) (Mohri and Uesawa, 2001). Glucuronidation was lowest in microsomes prepared from frozen tissue, and therefore may be a result of the increased mucosal tissue in the initial enterocyte elution procedure, similar to observations in scraped microsomes.

3.5.4. Rat intestinal pool clearance

Compounds selected for screening represented a diverse range of metabolism pathways and expected intestinal metabolism. The impact of 2% albumin has been reported to improve extrapolation of UGT metabolism by reducing enzyme specific competitive inhibition of glucuronidation clearance by free fatty acids (FFA), which are released from microsomal membranes during incubation (Rowland et al., 2008). However in the one occasion this was trialed in rat intestinal microsomes, no metabolism was observed, suggesting that protein binding was potentially limiting metabolism, and was not included for subsequent deleption experiments. When comparing rat intestinal pools, similar measures of unbound intrinsic clearance were observed for matched compounds, and a strong correlation was observed between the pools (R^2= 0.998, $p<0.001$), with 61% of compounds within 2-fold. The poorest correlation was observed for compounds with a $CL_{int,u}$ <10µl/min/mg. This however most likely represents the reduced sensitivity of depletion for compounds with a low rate of metabolism (requirement for at least 20% of substrate metabolism) (Jones and Houston, 2004).

A positive but weaker correlation (R^2= 0.773, $p<0.001$) was observed between mean $CL_{int,u}$ and $CL_{int,u}$ determined from commercial microsomes. Of the smaller subset of 11 compounds, 6 showed increased metabolism for in house microsomes. Of these compounds, 50% undergo CYP1A2 metabolism to some extent (pirenzepine, ipriflavone and nicardipine). It was not possible

to determine if this was CYP1A2 related as no testosterone metabolite is selective for this enzyme. Good correlation was observed for midazolam, amitriptyline, 7-HC and raloxifene.

Microsomal yields were low from intestinal tissue, and as a way of maximising their potential for screening of compounds, a combination of CYP and UGT cofactors were utilised. As a way of validation of the use of combined cofactors, these were compared to the individual CYP and UGT cofactors as per Kilford et al (2009), in the absence of 2% bovine serum albumin. Eight compounds were screened in commercial microsomes using both incubation techniques. The additive $CL_{int,u}$ were strongly correlated (R^2=0.966, $p<0.001$), with only amitriptyline outside 2-fold suggesting no limitations to the use of combined cofactors in intestinal microsomes as observed previously (Kilford et al., 2009). Indeed, the advantage of combination of cofactors was highlighted in the case of amitryptiline, where a significant reduction in $CL_{int,u}$ was observed using individual *vs.* combined cofactors (8.3 vs. 23.8 µl/min/mg microsomal protein), suggestive of sequential phase I and phase II metabolism .

3.5.5. *In vitro* F_G determination

Estimates of F_G using microsomal metabolism data and either Caco-2 or physicochemical based scaling strategies were similar. The worst estimates in physicochemical based scaling was observed for compounds which had a PSA >100Å (e.g. cyclosporine, tacrolimus, sildenafil and pirenzepine.) This is likely to be related to the lack of compounds with PSA >100Å in the original study dataset from which the relationship to *in vivo* P_{eff} was made (Winiwarter et al., 1998; Gertz et al., 2010). As a result, the prediction for these compounds was improved when Caco-2 data was used to make estimates of CL_{perm}. Estimates were however made worse for atorvastatin.

As expected, when comparing estimates of intestinal metabolism to measured $Fa.F_G$ values, the highest prediction accuracy was seen when F_G was corrected for predicted intestinal absorption ($Fa.F_G$), with an increase in incidence of TP from 27% to 41% for Caco-2 based scaling. Correlations were also stronger for both Caco-2 and physicochemical based methods. For Caco-2 and physicochemical based scaling, 73% and 65% of compounds were within 2-fold of *in vivo* values for the whole data set, however this was reduced when considering high extraction compounds (*in vivo* $Fa.F_G<0.5$), where compounds under 2-fold were 45% and 42% respectively. Description of bias (gmfe) was 0.89 and 0.22 for Caco-2 and physicochemical based scaling for compounds with an *in*

vivo $Fa.F_G$<0.5. Rmse was 0.38 and 0.43 respectively. Overall TN and TP classification was high, with 82% prediction success and 83% in Caco-2 and physiochemical scaling methods, respectively.

When assess using more constrained $Fa.F_G$ boundaries, the overall success of Caco-2 based scaling was highlighted with an increased correct catergorisation (68% *vs.*61%). Furthermore, low and middle range $Fa.F_G$ compounds showed the most improved predictions (32% and 13% *vs.* 30% and 4%). Prediction accuracy was also assessed by comparing the ratio of obereved/predicted *vs.*observed clearance. Again, improved accuracy was observed for Caco-2 scaling (73% *vs.*55% within 2 fold).

Overprediction of $Fa.F_G$ for Caco-2 based scaling was observed for atorvastatin, nicardipine and irbesartan. Underprediction was observed for raloxifene, saquinavir, and tacrolimus. However, given that raloxifene and saquinavir are highly protein bound compounds, a small error in measured fu_{inc} can subsequently affect the determined $CL_{int,u}$ (Gertz et al., 2010). The mean CV of F_G was 32% between the two pools. However, interestingly, the CV for compounds with a fu_{inc} <0.3 was 46%. For compounds with a fu_{inc} >0.3, the CV was lower (25%). Furthermore, raloxifene and saquinavir display low solubility (<10µM, **Appendix Table 7-7**) and may drive the higher F_G observed *in vivo*.

Classification of compounds based on low F_G prediction indicated a higher incidence of TP using physicochemical based permeability estimates, and a higher success of TN for Caco-2 based scaling. The reason for this observation may be 2-fold. FP in physicochemical permeability estimates may in part be related to the previously described limitations of estimating permeabilities for compounds with a PSA >100Å using the described formula. Secondly, the lower incidence of Caco-2 TP success may be in part down to the species differences in P_{eff} between rat and human, in light of the relationship being derived based on observed human P_{eff}. Although, rat absorption has been described as a good predictor of human absorption (Zhao et al., 2003; Cao et al., 2006), it is likely that species differences may contribute to differences in the actual observed rat P_{eff}. However, utilisation of a reported relationship between human P_{eff} and rat P_{eff} significantly reduced prediction accuracies in this investigation (Zakeri-Milani et al., 2007).

Best practice for P_{eff} estimation from Caco-2 data would be to incorporate P_{app} data derived in the presence of transport inhibitors in order to obtain an intrinsic permeability. This would therefore remove any transporter mediated transport effects and provide a "best

case" scenario in terms of Fa and CL_{perm}, and allow improved P_{eff} extrapolations since this would negate differences between transport expression (e.g. P-pg) in cell lines between laboratories, and furthermore between species. Data was produced in house for some compounds studied, especially for the P-pg substrates saquinavir, raloxifene and furosemide, where up to 4 fold differences in P_{app} were observed (**Appendix Table 7-7**). However, incorporation of this data did not improve estimates of $Fa.F_G$ for these compounds since these estimates were already well predicted and *in vivo* $Fa.F_G$ was very low (<0.25). Conversely, for compounds with a higher F_G (e.g. terfenadine and indinavir in human) (Gertz et al., 2011) improved predictions using a PBPK approach have been observed for these class of compounds P-pg transported compounds, suggesting that a more dynamic PBPK model is better suited rather than the static Q_{gut} model to incorporate transporter effects. Tacrolimus is a P-pg substrate and was very poorly predicted using all scaling attempts (FN). It is likely that improved prediction in the rat may be observed using a PBPK approach since the *in vivo* F_G was high (0.63).

For terfenadine, given the substantial metabolism which was observed in intestinal microsomes, this compound *in vivo* $Fa.F_G$ estimate was reclassified to 0.00, as it is likely that this was instead a miscalculation of the *in vivo* intestinal component based on the high hepatic clearance of this compound. This reflected the limitations in using the *in vivo* indirect method employed in this study to estimate the metabolic intestinal component.

Estimates of the *in vivo* contribution of the intestine to oral bioavailability were made using indirect measures of i.v. clearance and oral bioavailability. Low doses were selected in order to minimise saturation of intestinal enzymes (Lin et al., 1999). Measures of F_G are often described by indirect measures of intestinal metabolism by comparing i.v. clearance and p.o. F. However, there are several assumptions, for example negligible metabolism occurring in enterocytes after i.v. administration and that systemic clearance of a drug after i.v. dose (corrected for renal excretion) reflects only hepatic elimination (E_H). The validity of this assessment has been proved to be invalid for certain compounds where enterocytic contribution has been observed following i.v. administration, e.g. midazolam (Galetin et al., 2010). Furthermore, using this indirect method, estimates of intestinal metabolism are sensitive to the value hepatic blood flow used (Kadono et al., 2010).

In this study, for a number of compounds, e.g. terfenidine (as discussed above), bisoprolol, sildenafil and midazolam, the exact intestinal contribution was masked by the estimated

hepatic component. In some cases where the intestinal component was not determined, an alternative literature references were selected. For example, in the case of midazolam, the F_G based on portal vein cannulation was utilised (Murakami et al., 2003; Kuze et al., 2009). The use of the more labour intensive cannulation of portal vein can more accurately account for intestinal metabolism by sampling at the site following absorption and passage through enterocytes, before reaching the liver (Murakami et al., 2003; Kuze et al., 2009; Matsuda et al., 2012). However, the requirements for this specialised procedure, and ethical limitations around these techniques precluded the use of these methods in this study.

In agreement with other estimates of midazolam F_G using indirect methods available in the literature, the apparent midazolam contribution is calculated as F_G=1. However, utilisation of cannulation techniques reveal the intestinal contribution to be F_G=0.72 (Kuze et al., 2009; Matsuda et al., 2012). As well as for midazolam, successful applications of this method have been demonstrated in the literature for other compounds, e.g. indomethacin and raloxifene (Kuze et al., 2009; Matsuda et al., 2012). Interestingly, estimates of indomethacin and raloxifene were similar to those derived from cannulation based methods, most likely due to the low hepatic contributions which prevent the masking of the intestinal component. As with the indirect measures, no mass balance was available to determine Fa, and as such the *in vivo* intestinal component is represented in this report by the dual parameter $Fa.F_G$.

Atorvastatin was poorly predicted using Caco-2 based scaling strategies. Whilst the hepatic component for this compound was significant, it was not a limitation to the estimation of the hepatic component in this case. The solubility of atorvastatin compound is high (Lennernas, 2003) (confirmed using in house solubility studies, **Appendix Table 7-7**), and given the administration of the oral formulation in solution, and the precipitation test at lower pH therefore limit the possibility for reduced *in vivo* absorption as a result of precipitation. However, the *in vitro* estimate of Caco-2 P_{eff} (3.1×10^{-4} cm/s) was 8 fold higher than what has been reported previously in the rat (0.4×10^{-4} cm/s) (Mandal et al., 2010). Using this estimate, F_G was 0.64 and $Fa.F_G$ 0.35, which was improved but still outside 2-fold. It was difficult to determine *in vivo* $Fa.F_G$ for irbesartan since this drug showed enterohepatic recycling in the rat in line with previous reports (Davi et al., 2000).

Using a smaller data set of compounds, the prediction accuracy was increased; however this is biased as these compounds were selected for comparison to commercial on the basis of their relative prediction success. However, when comparing estimates, gmfe for low *in vivo* $Fa.F_G$ (<0.5) commercial microsomes was increased to 3.57 and 2.31 in Caco-2 and physicochemical based scaling for compounds respectively. A reduction in TP and increase in FN classifications were observed using commercial microsomes using physicochemical based permeability estimation *vs.* in house microsomes. Although no change using the Caco-2 based approach was observed, there was an increase in borderline cases (e.g. ipriflavone and losartan). As a result, care should be taken when using scaling factors which have not been characterised to the microsomal pool under investigation. Furthermore, this may reflect differences in metabolic enzymes present between commercial and in house prepared intestinal microsomes. This may be due to differences in preparation in which the protection of enzymes is different. For example, in human, scrapping has been reported to result in a more detrimental effect on CYP2C19 activity and a modest effect on CYP3A4, whilst CYP2C9 and CYP2D6 substrates show comparible activites to elution prepared microsomes (Galetin and Houston, 2006). Reductions in UGT activites have also been shown using different preparation methods (Mohri and Uesawa, 2001). In this study, as discussed previously, whilst CYP3A 6β-OH TEST activity was similar to in house activity, there was a reduced androsteinedione (CYP2C and CYP2B) and 4-NP gluc (UGT) activities in commercial microsomes. Alternatively this may be influenced by environmental factors, e.g. diet, since this can influence enzyme expression in the intestine through induction or inhibition (Hoensch et al., 1976). In the case of the Xenotech commercial microsomes, UGT activites were similar for both strains.

The worst prediction was seen for ipriflavone and irbesartan, and this corresponded to lower $CL_{int,u}$ activity when compared to in house pools. Therefore, this may indicate metabolic differences in active enzymes between the microsomes rather than issues with scalars. Both undergo CYP and UGT metabolism. Ipriflavone undergoes CYP3A and CYP2C mediated metabolism (Moon et al., 2007), Irbesartan also undergoes CYP2C metabolism, however, the major clearance pathway for the rat as was observed in commercial microsomes is UGT metabolism (Perrier et al., 1994; Moon et al., 1998). Furthermore formation of the CYP2C metabolite 16α-OH TEST was not significantly different between in house and commercial Wistar microsomes. UGT clearance was however was lower in commercial microsomes by 86% for ipriflavone and 55% for

irbesartan. The rate of 4-NP glucuronidation was 79% (21% reduced) to in house microsomes, however since this is a major substrate for UGT1A6 (Hanioka et al., 2001a) this does not represent the full complement of UGT enzymes. Irbesartan is glucuronidated predominantly by UGT1A3 (Perrier et al., 1994). The UGT enzymes involved in the ipriflavone glucuronidation pathway have not been reported.

3.6. Conclusions

Two pools of rat intestinal microsomes were prepared using the optimised methodology and showed good reproducibility in terms of enzyme activities for both CYP and UGT metabolism. Testosterone hydroxylation highlighted major enzyme pathways of CYP2B and CYP3A in the rat. Glucuronidation is also a major elimination pathway. Activities from scraping or frozen tissues were lowest. Frozen tissue in the rat may have limited use due to the simple structure of the tissue meaning it does not remain stable. Coincubation was shown to provide equal results to individual phase I and phase II cofactor incubations, and was beneficial in cases of sequential metabolism (e.g. amitriptyline). Scaling approaches of in house $CL_{int,u}$ using Caco-2 Q_{gut} approaches provided improved estimates of rat intestinal contribution over physicochemical approaches. Prediction accuracy based on the ratio of observed/predicted clearance for $Fa.F_G$ estimated demonstrated 73% of compounds within 2 fold for Caco-2 based estimates, and 57% for physicochemical estimates. Prediction accuracy based on correct allocation $Fa.F_G$<0.3, 0.31-0.7 and >0.7 showed 61% and 68% accuracy for physicochemical and Caco-2 based estimates. Scaling of commercial microsomal using in house scalars data was generally worse than in house metabolism scaling. However this may be due to differences in metabolic enzymes present. For example, this may be due to differences in preparation, or due to environmental factors, e.g. diet. Each pool should therefore be characterised using its own set of markers (both phase I and phase II).

4. Scaling factors for intestinal metabolism in dogs: Examining interindividual and regional variability, and correlations to hepatic scaling factors

4.1. Introduction

The beagle dog is a regulatory and industrially established preclinical species routinely used in both toxicity studies through chronic dosing, but also as a tool for making assessments of pharmacokinetic performance of drugs within drug research and development programs. *In vitro* screening may be performed on a large array of drugs using hepatic microsomes or hepatocytes to drive pre-clinical drug development (Smith et al., 2008). Microsomal protein per gram liver (MPPGL) scalars for dog hepatic metabolism have previously been reported where correction for losses have been applied (Baarnhielm et al., 1986; Smith et al., 2008), with values of 43 and 55 (48-62) mg/g liver respectively. Most recently values of 43.5 and 67.5mg/g liver have been reported from frozen livers (Heikkinen et al., 2012).

At the onset of this project, no known scalars for dog intestine were available. However, recently, corrected regional scalars have also been published (Heikkinen et al., 2012). Regional expression of microsomal protein appears to peak in the middle of the intestine, and shows a general decline distally **Figure 4-1**. Similar distributions are observed for CYP3A12 and CYP2B11 protein expression and activities. However, knowledge of the dog intestine is limited to one study using 4 dogs.

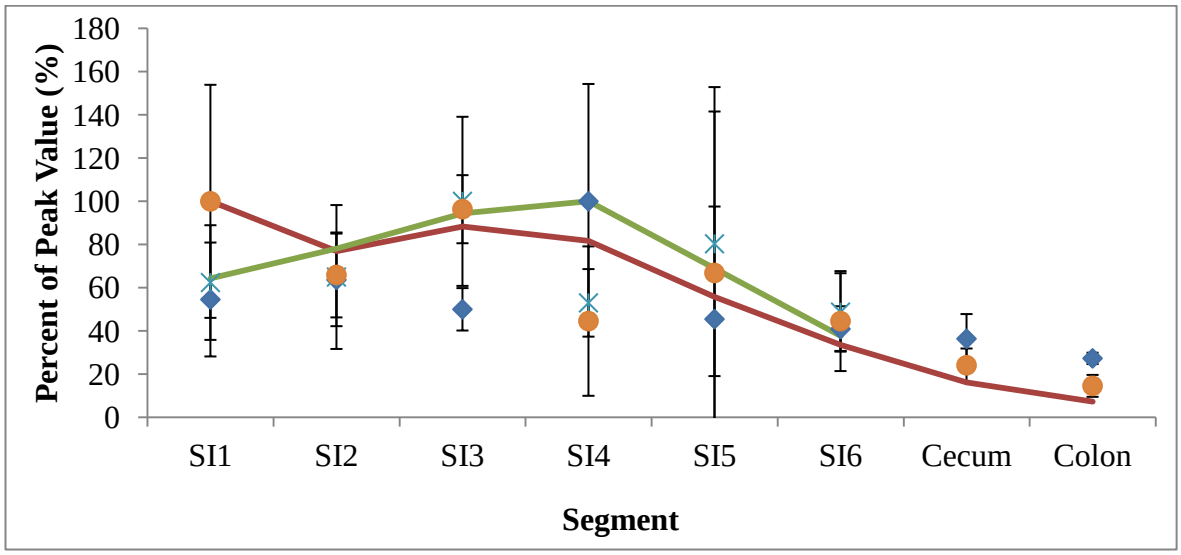

Figure 4-1 Reported regional distributions (% of peak) for MPPGI (◆), CYP3A12 content expressed per mg of microsomal protein(✳), CYP3A12 abundance per gram of tissue (-), activity towards the probe substrate temazepam per mg of microsomal protein (●) and per gram of tissue (-). Data from (Heikkinen et al., 2012). n=4.

The dog intestine is relatively short and simple with minimal visible differentiation between segments (Kararli, 1995). In the dog small intestine, the duodenum is reported to comprise the proximal 25 cm and ileum the final 15cm, with the remainder described as jejunum (Kararli, 1995). However, given the length of the beagle intestine relative to rat, and its similarities to that of the human gastrointestinal tract in terms of folded structure (Kararli, 1995), the dog presents an opportunity for observation of regional trends in both intestinal scalars and activity.

4.2. Aims

The primary aims of this chapter are to derive scalars for intestinal and hepatic tissue for both male and female dogs, and based on donor availability to utilise the female dog to characterise regional differences in scalars. The secondary aims are to assess differences in metabolic activity between liver and intestine and also within intestinal regions using specific probes. Rate of formation probes (CYP – 6β-OH TEST; UGT – 4-NP gluc), as well as screening a broad range of compounds using combined CYP and UGT cofactors and a substrate depletion approach. *In vitro-in vivo* extrapolation of generated $CL_{int,u}$ data will be performed using defined scalars to predict E_G and E_H. Comparison to *in vivo* measures of E_H and E_G will also be discussed.

4.3. Materials and Methods

4.3.1. Dog microsomal preparation

Male (47 ±2 months, 13.9 ±2.8 kg) and female (104 ±20 months, 12.6 ±2.6 kg) beagle dogs deemed surplus to further project use were euthanised by overdose of i.v. phenobarbital. Death was confirmed by exsanguination and draining of the jugular arteries. Dog small intestine was collected whole, and split into six equal segments *circa* 60cm in length and flushed. Segment chosen for isolation was placed in 750ml polypropylene bottle (Sovril, #75006443) for microsome isolation. Dog intestinal microsomes where prepared from fresh tissue following the method described for rat intestinal microsomes (**Chapter 2**). The only exception was that elution's were carried out over 30 minutes instead of 20 minutes to account for the increased trapping of enterocytes in the folded intestinal structure. At the same time, both livers and kidneys were harvested from the donors. The liver was weighed, and weighted tissue samples taken (three from the largest left lateral lobe, and on occasion two from the smallest quadrate lobe) and frozen. Liver microsomes were only prepared from the large left lateral lobe. Kidneys were processed and are subject to a separate PhD investigation (Daniel Scotcher, CAPkR).

Dog liver microsomes were only prepared from the dog donors from which intestinal segment 1 was used (3 male and 3 female dogs). Tissue samples from the same donor were prepared on two separate occasions using different operators in order to assess the impact of inter-day and inter-operator variability. Weighted liver samples were finely chopped with scissors and homogenised using a hand held bladed tissue homogeniser (Omni, GA, USA). Homogenates were further homogenised using a motorised potter, 30W sonication and subject to ultracentrifugation as previously described for rat intestinal microsome preparation (**Chapter 2**).

4.3.2. Determination of dog microsomal liver and intestinal scalars

MPPGL and MPPGI were determined using measures of CYP content, and 6β-OH TEST and 4-NP gluc formation activity markers for correction for losses expoeriments in freshly prepared dog intestinal homogenate and microsomes. Asseays were performed as described previously using RIM (**Section 3.3.2** and **Section 3.3.3**), except that homogenate was also screened for activity. Concentrations of 2 mg/ml were used for analysis of homogenate and microsomal CYP content. For CYP and UGT ROF experiments, intestinal homogenates and microsomes were incubated at 1mg/ml. Liver homogenates and

microsome incubations were undertaken at protein concentrations of 0.5mg/ml. The cofactors and starting concentrations of testosterone and 4-NP were the same as described in rat microsomes. However, in both cases samples were taken at 2.5, 5, 10, and 20 minutes. Linearity was observed up to 10 minutes. The calculation of recovery for ROF experiments was based on the maximal observed rate of formation in the homogenate or microsome matrix (**Equation 4-1**). Calculation of the recovery factor was similar to calculation based on CYP concentrations (**Equation 4-2**). Calculation of MPPGI, MPPGM and MPPcm were made using the derived recovery factors as applied previously (**Equation 2-3 to Equation 2-5**).

Equation 4-1 $$ROF_{max,matrix} = \frac{\Delta Concentration}{Time}$$

Where matrix is either homogenate or microsomal protein and ΔConcentration is under zero order conditions.

Equation 4-2

$$Recovery\ Factor = \frac{ROF_{max,mic} \times mg\ Protein_{mic}^{-1} \times total\ mg\ Protein_{mic}}{ROF_{max,hom} \times mg\ Protein_{hom}^{-1} \times total\ mg\ Protein_{hom}}$$

4.3.3. Dog microsome intrinsic clearance and microsomal binding

Individual CL_{int} experiments were carried out in DIM and DLM for matched segment 1 and liver donors on 3 occasions in duplicate. Segments 2, 3 and segment 6 prepared microsomes were respectively pooled and screened in duplicate on 2 occasions in order to assess regional metabolism contribution. Cofactor and substrate concentrations were the same as in RIM (**Section 3.2.4.2**). Incubation times were 30 minutes. The compounds used, and their MS transitions are shown in **Appendix Table 7-5**. Representative depletion profiles for each compound in DIM and DLM are shown in **Appendix Figure 7-2** and **Appendix Figure 7-3.** Control CL_{int} incubations were also performed for each drug in DLM with no cofactor present to account for any potential cofactor independent loss of the drug over the incubation time. Representative depletion profiles for each compound no cofactor controls in DLM are also shown in **Appendix Figure 7-2** and **Appendix Figure 7-3**.

Incubations were undertaken at protein concentrations of 1mg/ml and at compound concentrations of 1µM. The fu_{inc} was determined at 1mg/ml for the complete set of

compounds screened in the dog (**Appendix Table 7-1**) in DLM as described previously for RIM (**Section 3.3.4.6**). Only selected compounds which had shown high binding in the rat were tested for the extent of nonspecific binding in segment 1 DIM.

In order to assess relationships between liver and the intestinal activity, values of hepatic and segment 1 $CL_{int,u}$ for CYP3A substrate compounds normalised for literature reported CYP3A12 content (Heikkinen et al., 2012). Reported values for microsomal CYP3A12 content in male and female hepatic microsomes where 70.5, 128 pmol/mg, and intestinal microsomes, 5.9 and 9.75 pmol/mg (n=2 per sex). Values of hepatic and segment 1 $CL_{int,u}$ for CYP3A substrate compounds were also normalised for mean testosterone 6β-OH TEST formation rates for male and female liver and intestinal microsomes.

4.3.4. Dog intestinal permeability and Fa

P_{app} to P_{eff} scaling from AZ in house Caco-2 data was made using an AZ in house derived P_{app} to P_{eff} relationship as defined previously (**Equation 3-11**). Where Caco-2 data was unavailable, values were derived from literature or alternatively from physicochemical relationships (**Equation 3-12**). Physiological parameters used were the average length of intestine from this study (**Table 4-2**) and an intestinal radius of 0.53cm (Pappenheimer, 1998) for scaling to values of CL_{perm} (**Equation 3-14**). Q_{gut} estimation was made using **Equation 3-15**. The value of Q_{villi} was 5.61 l/h (**Table 1-2**).

Estimates of dog Fa were made using the relationship between small intestinal transit time (T_{SI}), radius, and P_{eff} (Yu and Amidon, 1999) (**Equation 4-3**). Small intestinal transit time in the dog is estimated to be 1.85 hours (Dressman, 1986).

Equation 4-3 $$Fa = 1 - \left(1 + \frac{2 \cdot P_{eff} \cdot T_{SI}}{7 \cdot R}\right)$$

4.3.5. Scaling of dog intestinal and hepatic extraction

Scaling of dog intestinal clearance was achieved the derived scaling factors (**Equation 3-13**). Predictions of F_G were made using the Q_{gut} model (**Equation 3-16**). Values of CL_H were estimated using the 'well-stirred' liver model (**Equation 4-4**) using measured hepatic unbound intrinsic clearance ($CL_{int,u,H}$) observed in DLM , measures of fraction unbound in the blood (fu_b) and a value of liver blood flow (Q_H) of 42.5 l/h (55 ml/min/kg) (McEntee et al., 1996; Taylor et al., 2007). Measures of fu_b were made using measured of unbound in the plasma (fu_p) (**Section 4.3.6**) and correcting for in house or literature *in vivo* R_b values (**Equation 4-5**). E_H was calculated by normalising CL_H by Q_H (**Equation 4-6**).

Equation 4-4 $$CL_H = \frac{Q_H \cdot fu_b \cdot CL_{int,u,H}}{Q_H + fu_b \cdot CL_{int,u,H}}$$

Equation 4-5 $$fu_b = \frac{fu_p}{R_b}$$

Equation 4-6 $$E_H = \frac{CL_H}{Q_H}$$

4.3.6. Fraction unbound in dog plasma

Measures of fu_p were determined in 10% dog plasma by equilibrium dialysis. Plasma was diluted in an isotonic solution of isotonic solution of 0.013M Potassium phosphate monobasic (Sigma, #P0662), 0.075M NaCl, 0.054M Sodium phosphate dibasic (Sigma, #255793), pH 7.4 and placed in donor wells 96-well Micro-Equilibrium Dialysis Device HTD and dialysis membrane strips (12-14kDa molecular mass cut off). Acceptor wells were loaded with isotonic solution. Compounds were incubated at 20µM compound shaken for 18 hours at 37ºC. Following incubation samples from both the acceptor and donor sides of the membrane were transferred to 96 well plates and quenched in acetonitrile containing internal standard AZ1. Sample preparation and LC-MS/MS methods were the same as those for microsomal incubations. Calculation of fu_p was the same as calculation of fu_{inc} using the ratio of acceptor and donor peaks, each respectively normalised for internal standard (**Equation 3-2**).Measures of fu_p were also made in rat plasma.

4.3.7. Investigation of dog *in vivo* intestinal metabolism

Literature values of *in vivo* intestinal metabolism were limited for the compounds used in this study, therefore estimates of *in vivo* F_G were made for a small number of compounds using in house Beagle dogs. The difference in measures of fu_p in the rat and dog were used in order to generate estimates of plasma levels in the dog based on in house rat pharmacokinetic data (**Chapter 3**) The i.v. doses were administered in n=2 dogs through bolus administration. P.o. administration (n=2) was by oral gavage into the stomach. P.o. doses were administered as solutions, and tested at 1:1 and 1:10 dilutions of 1M HCl for observations of precipitation at low pH. Doses and formulations are shown in **Table 4-1**. Blood samples were collected at t=5, 20, 40 minutes, 1.2, 3, 4, 6, 12 and 24 hours for i.v. dosing. p.o. blood samples were taken at t=5, 10, 20, 40 minutes, 1, 2, 4, 6, 12 and 24 hours. Blood and plasma storage, preparation, and LC-MS/MS analysis was performed

Table 4-1 Dose formulations and amounts for 10 drugs administered i.v. and p.o. to Beagle dogs

					i.v. Dose			p.o.		
Compound	**i.v. Formulation**	**p.o. Formulation**	**MW**	**Salt MW**	**mg/kg**	**µmol/kg**	**Volume ml/kg**	**mg/kg**	**µmol/kg**	**Volume ml/kg**
Buspirone[a]	Saline	Propylene Glycol	385.51	421.97	0.78	2.00	2.00	1.57	4.00	2.00
Diltiazem[a]	Saline	Propylene Glycol	414.52	450.98	0.82	2.00	2.00	1.66	4.00	2.00
Ipriflavone[c]	5% DMSO:95% (25%w/v Cyclodextrin:UPH2O)	Propylene Glycol	280.32	280.32	1.00	3.57	2.00	2.00	7.13	2.00
Losartan[a]	Saline	Propylene Glycol	422.92	461	1.00	2.17	2.00	2.00	4.34	2.00
Midazolam[a]	Saline	Propylene Glycol	325.77	362.23	0.50	1.38	2.00	0.50	1.38	2.00
Nicardipine[a]	Saline	Propylene Glycol	479.53	515.99	1.03	2.00	2.00	2.06	4.00	2.00
Pirenzepine[d]	0.1% Tween 80; 0.5%HPMC	Citrate buffer (pH5)	351.41	376.72	3.00	8.54	2.00	3.00	8.837	2.00
Raloxifene[a]	5% DMSO: 35%TEG:60% UPH_20	Propylene Glycol	473.59	510.04	1.02	2.00	2.00	2.04	4.00	2.00
Sildenafil[b]	Saline	Propylene Glycol	474.58	666.71	1.00	1.50	2.00	2.00	3.00	2.00
Verapamil[a]	Saline	Propylene Glycol	454.61	555.45	0.56	1.00	2.00	2.22	4.00	2.00

a:1 male and 1 female dog i.v. and p.o matched. , b: 2 male dogs i.v. and p.o matched, c: 2 male dogs i.v. and p.o, 1 dog matched, d: dosed as part of a separate study, unknown sex of i.v., 3 male p.o.

identically to the rat (**Section 3.2.5**). Estimates of i.v. systemic clearance ($CL_{i.v}$) and oral bioavailability (F) were determined using **Equation 3-5** and **Equation 3-6** using i.v. and p.o. *vs.* concentration data input into Pheonix Winnonlin v6.2. R_b values were determined using **Equation 3-4**. Estimates of F_H and $Fa.F_G$ were made as described previously **(Equation 3-7** to **Equation 3-9)**.

4.3.8. Physiologically based pharmacokinetic modelling on dog F_G

As a means of comparing the predictive power of F_G based on the Q_{gut} model to a dog PBPK model, Simcyp v12 animal (Cetara, Sheffiled, UK) was used to make F_G estimates. Files were created for each compound using measures of R_b, fu_p, determined as described previously, and in house database values of logP, pKa, molecular weight. Compound specific parameters are summarised in **Appendix Table 7-7**. Predicted Fa and Q_{gut} measures were input as estimated for the Q_{gut} model. *In vivo* measures of renal clearance were included for each compound. DIM and regional DIM CL_{int} metabolism was also incorporated for each compound. It should be noted that to prevent a correction applied to elution based DIM within the v.12 software, CL_{int} was input as scraping prepared microsomes. The model species was modified to include the measured liver and regional intestinal scaling factors and mucosal (i.e. enterocyte) yields. An example input for midazolam is included in **Appendix Table 7-8**.

4.3.9. Data analysis

Scatter plots of CL_{int} and F_G were complied in Matlab (2012a). Tests comparing means using Student's t-test to test for statistical significance at a level of 5% was applied using SPSS Statistics version 20. Tests for bias and precision of estimated $Fa.F_G$ (gmfe and rmse) and qualitative zoning of predicted low F_G values were applied as described previously in the rat (**Chapter 3**).

4.4. Results

4.4.1. Male and female dog intestinal characteristics

Demographic data for the dogs utilised in this study is presented in **Table 4-2** along with information of liver and intestinal organ weights, and intestinal mucosal and homogenate yields. The average length of intestine for male (n=3) and female (n=12) dogs were 392 ±10 and 311 ±41 cm respectively ($p<0.01$). Average small intestinal weights were 353 ±51 and 294 ±42 g for male and female dogs. Distribution of gut weight per cumulative length of intestine is shown in **Figure 4-2**. In both male and females the highest weight per cm of intestine was found in the proximal segment (duodenum), falling sharply to a baseline value, until rising slightly in the distal ileum. Yield of mucosa showed no differences between sex or regions, and ranged between 0.16 to 0.29 g/cm (**Figure 4-3**). Similar observations were apparent in total protein homogenate yields, however mean segment 6 homogenate yield was 5.9 mg/cm, whereas proximal homogenate yields in segments 1-3 were 12.0 mg/cm (**Figure 4-4**).

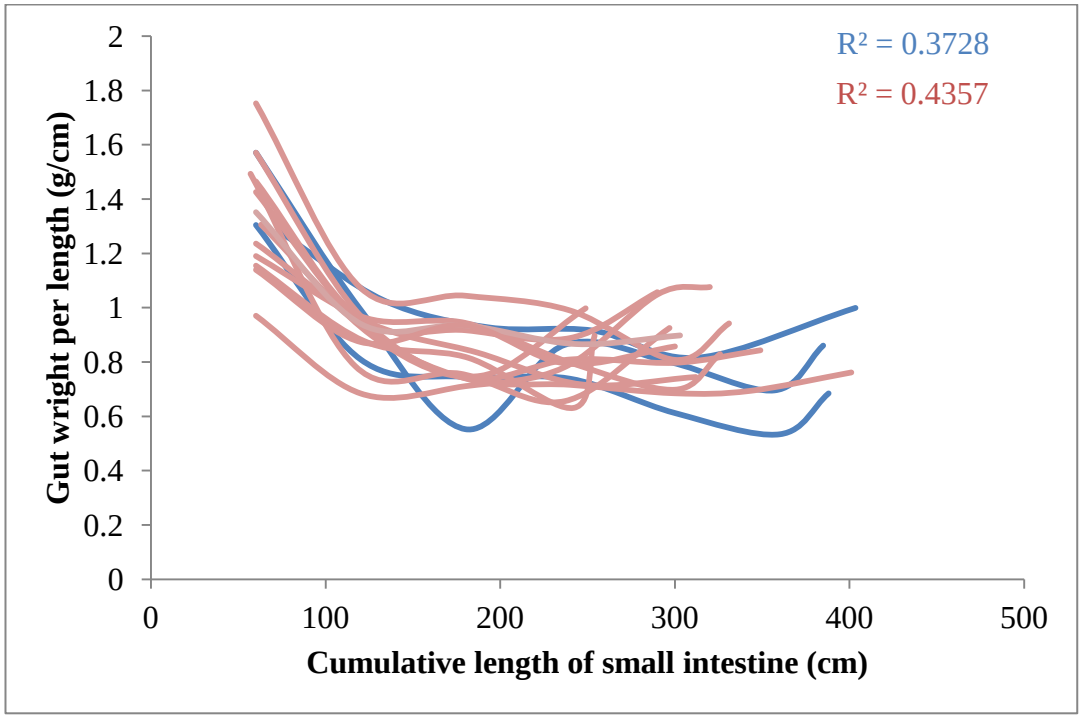

Figure 4-2 Intestinal weight as a function of cumulative length of beagle dog intestine.

Male (Blue lines) n=3 and Female (Red lines) n=12.

Table 4-2 Mean dog donor details for male (n=3) and female (n=12) dogs.

Sex	Mean Body Weight (kg)	Mean Age (months)	Mean Liver Weight (g)	Mean Total Intestine Weight	% BW	Mean Total Intestine Length (cm)
Male	13.9 (±2.9)	47 (±2)	466 (±98)	353 (±51)	2.57 (±0.31)	392 (±10)
Female	12.6 (±2.6)	104 (±20)	428 (±112)	294 (±42)	2.37 (±0.39)	311 (±41)

Table 4-3 Mean segment weights and mucoasl and homogenate yields and for male (n=3) and female (n=12) dogs.

Sex	Segment	Mean segment weight (g/cm)	Mean mucosal yield (g/g intestine)	Mean homogenate protein yield (mg/g intestine)
Male	1	1.39 (±0.16)	0.16 (±0.05)	10.5 (±4.0)
	2	0.94 (±0.12)		
	3	0.74 (±0.19)		
	4	0.84 (±0.09)		
	5	0.74 (±0.11)		
	6	0.74 (±0.24)		
Female	1	1.34 (±0.22)	0.19 (±0.04)	8.6 (±2.4)
	2	0.91 (±0.10)	0.21 (±0.08)	12.2 (±4.8)
	3	0.84 (±0.11)	0.29 (±0.04)	23.1 (±10.8)
	4	0.80 (±0.12)		
	5	0.86 (±0.13)		
	6	0.88 (±0.14)	0.29 (±0.10)	8.8 (±2.1)

Mucosal and homogenate yields represent n=3 for each segment.

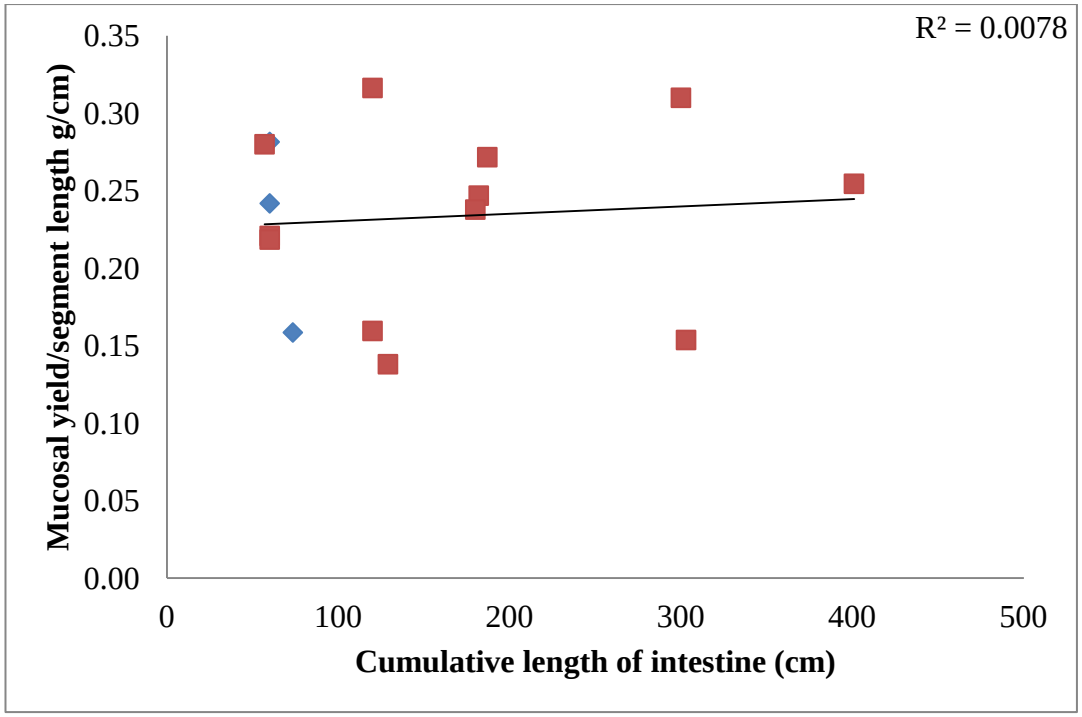

Figure 4-3 Mucoasl yields in male (◆) and female (■) beagle dog intestines as a function of cumulative length of intestine.

Data represents n=3 for segment 1 of male intestine, and n=3 for segments 1, 2, 3 and 6 of female intestine

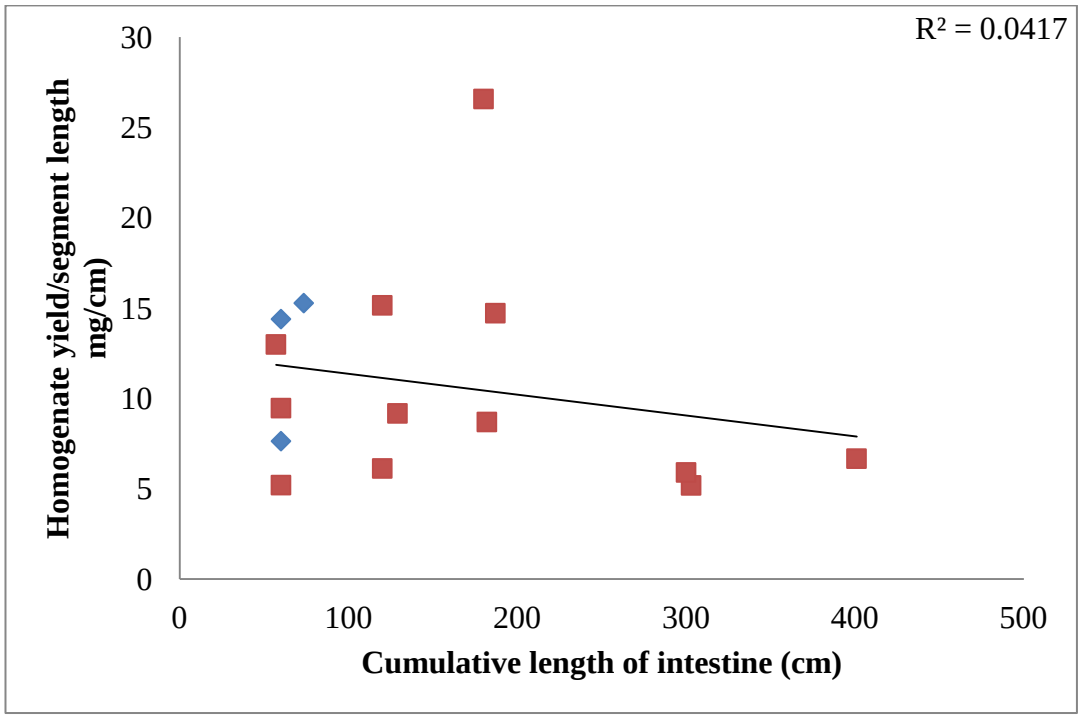

Figure 4-4 Homogenate yields in male (◆) and female (■) beagle dog intestines as a function of cumulative length of intestine.

Data represents n=3 for segment 1 of male intestine, and n=3 for segments 1, 2, 3 and 6 of female intestine

4.5. Dog microsomal preparation

4.5.1. Comparison of male and female hepatic and proximal intestine scalars

Comparison of microsomal liver and intestinal recoveries, scalars and metabolic activities are shown in **Table 4-4**. Results shown are from the preparation of one liver sample and the proximal intestine (Segment 1) from each male (n=3) and female (n=3) dog. Comparison of the microsomal recoveries is shown in **Figure 4-5**. Recovery was 2.2- to 4.3-fold higher in male and female dogs in hepatic tissue relative to intestine, however no trends were observed comparing either individual or sex (R^2=0.006).

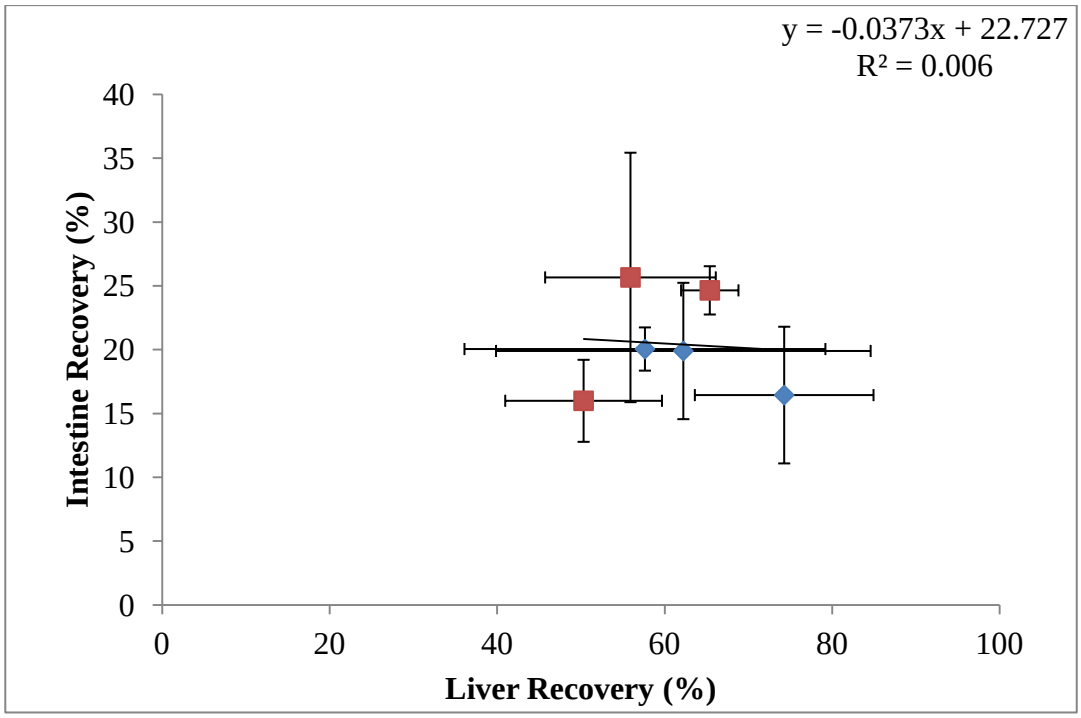

Figure 4-5 Comparison of intestinal and hepatic microsomal recoveries obtained from the same in male (◆) (n=3) and female (■) (n=3) beagle dogs.

Data represent mean ±stdev of 3 microsomal marker based recoveries of CYP content and CYP and UGT activities for each sample preparation.

Corrected mean scalars where higher in both tissues for male *vs.* female (43.6 *vs.* 36.3 mg/g) but were not statistically significant (p=0.13). Mean 6β-OH TEST activities in male and female liver microsomes were 1.29 and 1.05 nmol/min/mg. 16α-OH TEST was also a major metabolite formed in the DLM which rivalled 6β-OH TEST formation (**Table 4-4**). Mean 4-NP gluc activities were 62.5 and 74.4 nmol/min/mg. Activities in both male and

female liver microsomes towards CYP and UGT marker probes showed no significant differences (p=0.13 and 0.22 respectively).

By means of assessing the impact of inter-operator variability in the microsome preparation method, liver microsomes from a separate tissue sample from the same lobe were also prepared. Mean values of male and female MPPGL for each operator are shown in **Table 4-4**. No significant difference was observed between operators in recovery or corrected (p=0.12, p=0.46 for male and female respectively) values of MPPGL. Again whilst corrected scalars showed a mean value higher in male, no significant difference was observed (p=0.17). The mean CV between corrected liver microsomal scalars for the two operators was 20.3%.

Correlations between liver and proximal intestinal scalars are shown in **Figure 4-6**. When the intestinal scalar is expressed in terms of per gram mucosa, the values are near equivalent to the corresponding hepatic values. Good correlations was observed between the values of scalar obtained for liver and proximal intestine from the same dogs, regardless of sex for both MPPGI *vs.* MPPGL (R^2=0.91, p<0.01) or MPPGM *vs.* MPPGL (R^2=0.81, p<0.01).

In segment 1 of male and female beagle dog intestine, mean 6β-OH TEST (0.3 *vs.* 0.8 nmol/min/mg), and 4-NP gluc formation (0.69 and 1.25 nmol/min/mg) was highest in female *vs.* male proximal intestine but not statistically significant (p=0.24 and 0.08). 16α-OH TEST was not a metabolite formed in segment 1 intestinal microsomes (**Appendix Figure 7-1**).

Table 4-4 Comparison of microsomal hepatic and proximal intestinal microsomal activities and scalars.

		Liver					Segment 1 Intestine					
Dog #	Sex	Recovery[a] (%)	MPPGL[a] (mg/g)	CYP content (nmol/mg)	6β-OH TEST activity (nmol/min/mg)	4-NP gluc activity (nmol/min/mg)	Recovery[a] (%)	MPPGI[a] (mg/g)	MPPGM[a] (mg/g)	CYP content (nmol/mg)	6β-OH TEST activity (nmol/min/mg)	4-NP gluc activity (nmol/min/mg)
1	Male	74.3 (±10.7)	35.6 (±4.7)	0.73	1.14	79.01	16.4 (±5.4)	4.2 (±1.2)	35.5 (±9.8)	0.07	0.38	1.11
2	Male	57.7 (±21.5)	54.0 (±25.5)	0.48	1.61	54.18	20.1 (±1.7)	11.2 (±0.9)	52.0 (±4.4)	0.05	0.23	0.37
3	Male	62.2 (±22.4)	41.2 (±13.5)	0.68	1.11	54.34	19.9 (±5.3)	4.5 (±1.4)	29.0 (±9.1)	0.08	0.28	0.59
Mean		**64.7 (±8.6)**	**43.6 (±9.5)**	**0.63 (±0.13)**	**1.29 (±0.28)**	**62.51 (±14.29)**	**18.8 (±2.0)**	**6.7 (±3.9)**	**38.8 (±11.9)**	**0.07 (±0.02)**	**0.30 (±0.07)**	**0.69 (±0.38)**
4	Female	65.4 (±2.0)	33.5 (±1.8)	0.71	1.1	74.34	24.6 (±1.9)[Δ]	2.7 (±0.2)[Δ]	18.0 (±1.4) [Δ]	0.07	1.29	1.1
5	Female	50.3 (±8.5)	45.0 (±8.5)	0.50	0.83	72.60	16.0 (±3.8)	6.2 (±1.2)	33.1 (±6.3)	0.07	0.86	1.21
6	Female	55.9 (±8.3)	30.5 (±5.9)	0.75	1.23	76.15	25.7 (±10.2)	2.2 (±1.1)	12.2 (±4.9)	0.06	0.32	1.44
Mean		**57.2 (±7.6)**	**36.3 (±7.7)**	**0.65 (±0.15)**	**1.05 (±0.20)**	**74.36 (±1.77)**	**22.1 (±5.3)**	**3.9 (±2.0)**	**21.1 (±10.8)**	**0.07 (±0.00)**	**0.82 (±0.49)***	**1.25 (±0.17)**

a:represent mean (±stdev) of 3 microsomal correction for losses markers of CYP content, and CYP and UGT activity. Δ mean of CYP and UGT activities only.

Table 4-5 Inter-operator variability in preparation of matched dog male and female liver samples.

	Operator 1					Operator 2				
Sex	6β-OH TEST (nmol/min/mg)	16α-OH TEST (nmol/min/mg)	4-NP Gluc (nmol/min/mg)	Recovery (%)	MPPGL (mg/g)	6β-OH TEST (nmol/min/mg)	16α-OH TEST (nmol/min/mg)	4-NP Gluc (nmol/min/mg)	Recovery (%)	MPPGL (mg/g)
Male	1.29 (±0.28)	1.14 (±0.10)	62.51 (±14.29)	64.7 (±18.0)	43.8 (±15.6)	0.75 (±0.16)	0.81 (±0.15)	63.2 (±24.7)	46.1 (±12.3)	54.2 (±20.8)
Female	1.05 (±0.20)	1.53 (±0.20)	74.36 (±1.77)	57.2 (±9.7)	36.9 (±8.1)	1.2 (±0.31)	1.62 (±0.14)	63.22 (±10.17)	60.5 (±16.8)	41.1 (±10.9)

Data represent mean (±stdev) of n=3

4.5.2. Female regional intestinal characterisation

Comparison of the regional distributions of CYP content, CYP and UGT activities, as well as scalars observed in female dogs is shown in **Table 4-6**. Representative plots for regional intestinal CYP content and CYP and UGT activity, and scalars are shown in **Figure 4-7** and **Figure 4-8** respectively. Regional changes in testosterone 6β-OH TEST indicated the maximal activities occurring in segments 1 and 3 (823.7 and 810.8 pmol/min/mg). The lowest activity was observed in segment 6 (153.0 pmol/min/mg) (**Table 4-6**). 6β-OH TEST formation indicated a distal reduction in CYP3A activity indicated a modest decline distally (**Figure 4-8B**). However, CYP activity in the third segment rivalled that of the proximal segment (**Figure 4-8B)**. 4-NP gluc formation fell sharply along the course of the intestine. A significantly reduced activity in the distal *vs.* proximal segment ($p<0.05$) was observed (**Figure 4-8C**).

Regional distributions of scalars, either expressed per gram intestine tissue, per gram of mucosa (effectively enterocyte yeild), or alternatively per cm of length of intestine, for all the markers for correction indicated a increasing microsomal scalar from the first until the third segment (**Figure 4-8**). For example, when expressed per gram of mucosa, mean scalars for the first, second and third segments were 21.5 (±10. 8), 30.9 (±8.0) and 37.2 (±17.2) respectively. Distal scalars fell to near proximal segment levels (18.7 ±6.3 MPPGM) (**Table 4-6**).

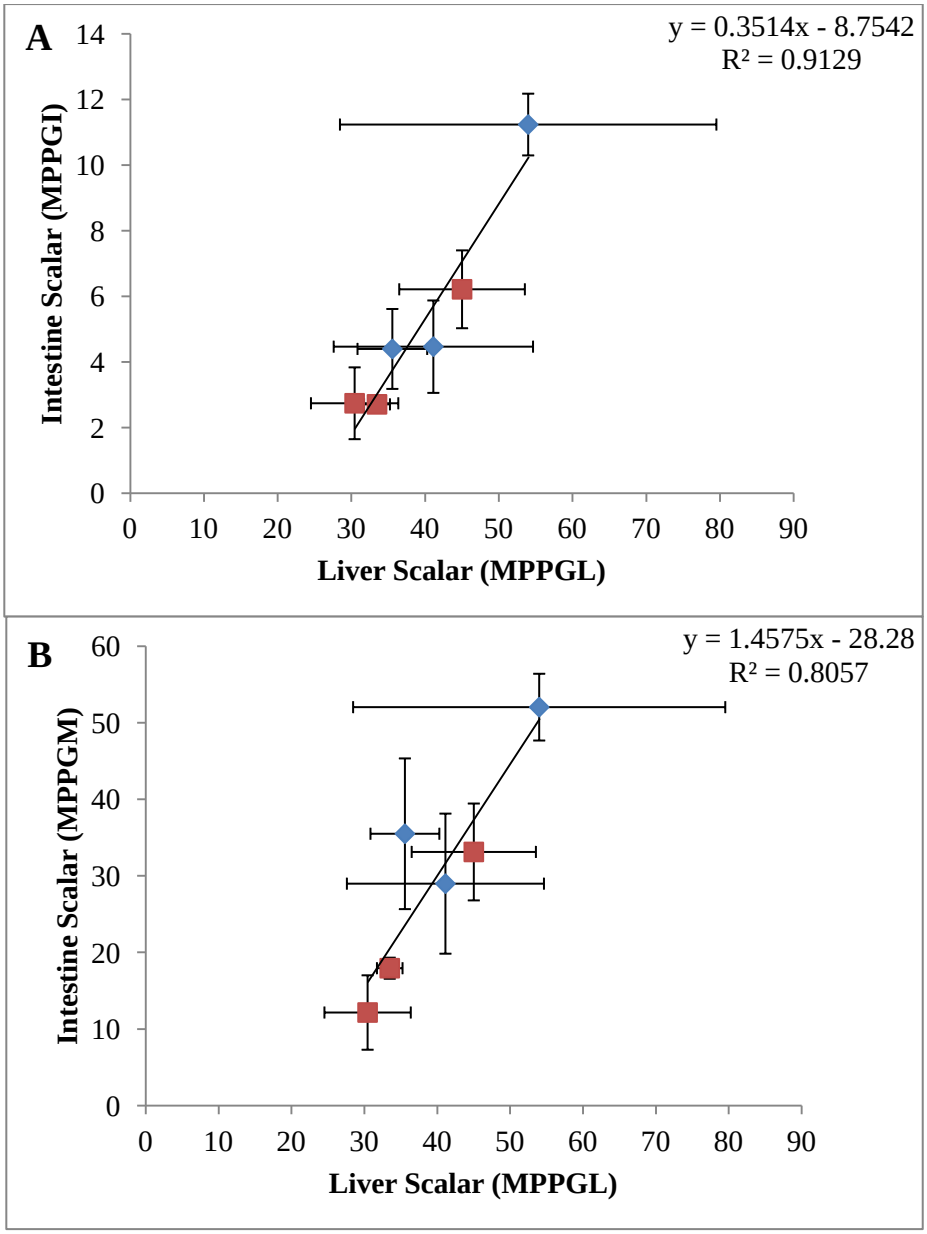

Figure 4-6 Correlation between values of matched individual male (◆) and female (■) hepatic and intestinal scalars expressed per gram of organ (A) or per gram mucosa (B). N=3 per sex.

Table 4-6 Comparison of regional CYP contents, CYP and UGT activities and scalars in the female dog intestine.

Sex	Segment	Mean CYP content (pmol/mg) [a]	6β-OH TEST Max Rate of Formation (pmol/min/mg) [a]	4-NP Gluc Max Rate of Formation (nmol/min/mg) [a]	Recovery (%)	MPPGI (mg/g intestine)	MPPGM (mg/g mucosa)	MPPcm (mg/cm)
Female	1	69.5 (±4.2)	823.7 (488.7)	1.25 (±0.17)	21.8 (±7.3)	4.1 (±2.0)	21.5 (±10.8)	5.5 (±3.4)
Female	2	51.4 (±9.2)	381.30 (±332.2)	0.86 (±0.53	26.0 (±9.6)	6.6 (±2.7)	30.9 (±8.0)	6.4 (±3.2)
Female	3	55.6 (±27.2)	810.8 (±265.6)	0.51 (±0.15)	19.6 (±5.6)	10.2 (±3.5)	37.2 (±17.2)	9.3 (±3.9)
Female	6	51.2 (±15.3)	153.0 (±45.3)	0.42 (±0.06)	21.4 (±6.5)	5.2 (±1.8)	18.7 (±6.3)	4.2 (±1.3)

n=3 for each segment for unmatched donors. a, represents per mg of microsomal protein.

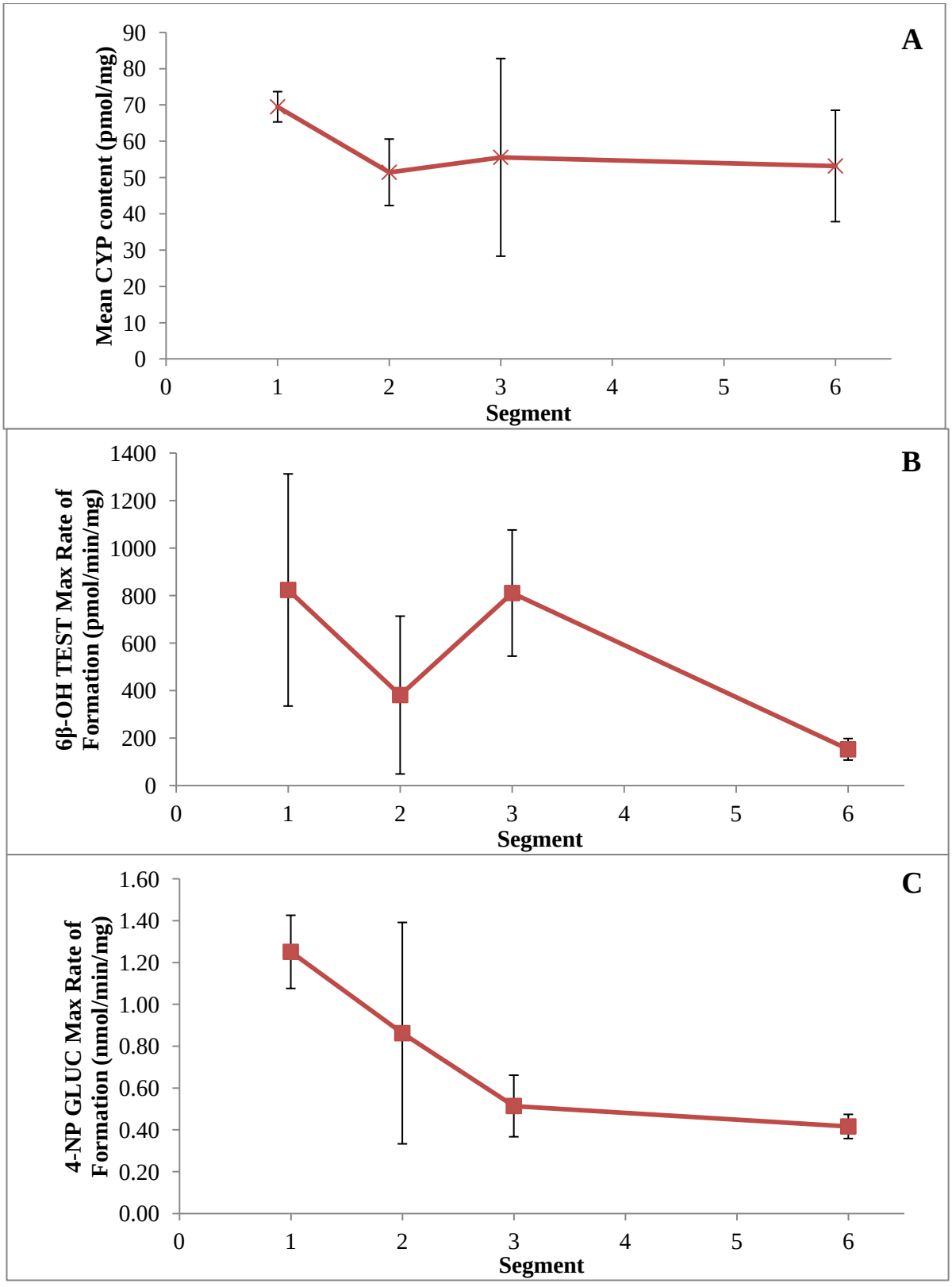

Figure 4-7 Regional distribution of CYP content and CYP 6β-OH TEST formation (B) and UGT 4-NP gluc formation (C) activities female DIM from intestinal segments 1,2,3 and 6. N=3 per segment.

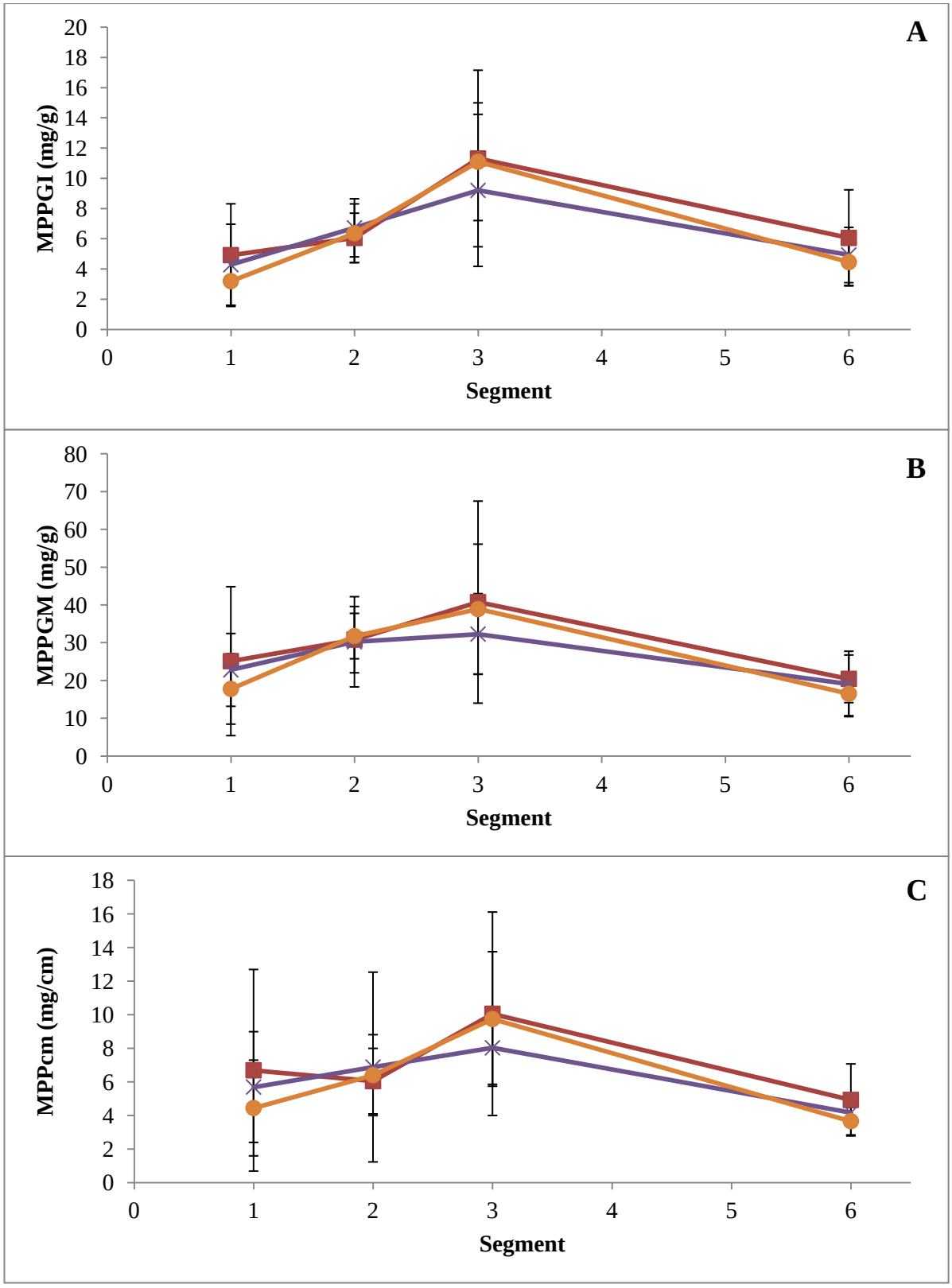

Figure 4-8 Regional distributions of intestinal microsomal protein in the female dog Corrected for microsomal markers of CYP content (■) and CYP activity (×)and UGT activity (●). A: MPPGI, B: MPPGM, C: MPPcm. Data represents n=3 per segment.

4.5.3. *In vitro* microsomal protein binding and intrinsic clearance in dog liver and proximal intestinal microsomes

Values of mean fu_{inc} and $CL_{int,u}$ in either pooled or individual microsomes are shown in **Table 4-7**. Terfendine showed the lowest measure fu_{inc} (0.01 and 0.02, respectively) in both liver and intestinal microsomes. Minimal non-specific protein binding (fu_{inc} >0.98) was observed in DLM for 43% of the compounds studied. A greater than 2-fold difference in value of fu_{inc} between liver and microsomes was observed for cyclosporine.

Highest mean $CL_{int,u}$ was seen in liver tissue *vs.* the intestine in both male and female. Values of $CL_{int,u}$ in DLM ranged from 4.4 (pirenzepine) and 13064 (saquinavir) µl/min/mg. Values in DIM ranged from 1.2 (pirenzepine) to 3924 (saquinavir) µl/min/mg. Mean CV for male liver, segment 1 and female liver, segment 1, were 78, 119, 70 and 87% respectively.

Sex differences in the relative importance of hepatic and intestinal metabolism was highlighted for omeprazole, nitrendipine, terfenadine and ipriflavone where in male dogs, the dominant route of metabolism was hepatic. However, in female dogs the intestinal component near rivalled that of the hepatic component.

Values of hepatic and segment 1 $CL_{int,u}$ for CYP3A substrate compounds normalised for literature reported CYP3A12 content (Heikkinen et al., 2012) are shown in **Figure 4-9**. Values normalised for mean testosterone 6β-OH TEST formation rates for male and female liver and intestinal microsomes (**Table 4-4**) is shown in **Figure 4-10**. Positive correlations for CYP3A substrates are shown between the liver and intestine was observed for both CYP3A content normalisation (R^2=0.64 and 0.94 for male and female respectively) and activity (R^2=0.64 and 0.94 for male and female respectively). Values corrected for CYP3A activity were closer to unity *vs.* normalisation by reported CYP3A12 content (**Table 4-8**).

Table 4-7 $CL_{int,u}$ and fu_{inc} determined for n=24 compounds in male and female DLM and DIM.

Compound		fu_{inc}		$CL_{int,u}$ (µl/min/mg)						
				Male		Female				
				DLM [b]	DIM	DLM [b]	DIM			
Study #	Name	DLM [a]	DIM [a]		Segment 1[b]		Segment 1 [b]	Segment 2[c]	Segment 3 [c]	Segment 6 [c]
1	7-Hydroxycoumarin	1.00		640.4	36.8	285.2	91.7	152.2	357.9	18.1
4	Bisporolol	1.00		7.8	2.6	1.6	0.9	2.0	1.3	6.2
6	Buspirone	0.99		136.9	3.9	148.0	24.5	18.3	15.8	3.1
7	Cimetidine	1.00		11.8	8.8	6.8	14.9	8.9	7.1	2.3
8	Cyclosporine A	0.86	0.33	15.1	10.4	10.7	5.0	4.5	3.8	2.1
10	Diltiazem	0.72		78.4	6.0	63.7	17.1	12.8	15.4	7.7
11	Domperidone	0.37		58.6	5.2	46.6	11.7	24.2	30.4	5.4
12	Felodipine	1.00		5.9	1.8	21.6	17.5	21.7	16.8	7.1
13	Furosemide	1.00	0.63	51.4	27.7	24.9	41.6	2.0	11.1	25.8
14	Indomethacin	0.82		14.8	11.0	14.1	12.6	1.8	8.7	0.4
15	Ipriflavone	0.40	0.40	2330.0	66.1	1852.7	837.6	53.8	69.5	29.0
16	Irbesartan	1.00		26.6	5.5	20.6	3.8	2.8	10.8	3.0
17	Losartan	1.00		40.1	3.5	32.3	6.3	7.2	14.3	2.6
18	Midazolam	0.74	0.99	193.7	163.2	237.5	331.9	277.2	276.7	38.9
19	Nicardipine	0.16	0.08	8552.0	942.5	8042.9	3544.1	2775.1	3273.2	585.4
19	Nitredipine	0.22		751.9	55.7	766.1	288.3	109.0	88.7	90.8
21	Omeprazole	1.00		183.1	22.3	164.8	146.4	37.7	44.0	17.6
22	Pirenzepine	1.00		4.4	1.2	6.9	5.0	9.3	11.5	0.8
23	Raloxifene	0.15	0.06	4868.8	763.2	5688.1	1098.9	324.4	244.2	45.8
24	Saquinavir	0.22	0.12	13064.4	593.8	13035.8	3924.9	1877.0	2061.9	442.0
25	Sildenafil	0.87	1.00	34.4	16.1	32.1	22.4	19.2	29.1	1.5
27	Tacrolimus	0.22	0.21	1261.1	406.1	1742.9	947.7	557.9	1896.6	516.4
28	Terfenadine	0.02	0.01	1610.5	496.1	1154.3	1186.8	1082.6	1554.1	697.1
29	Verapamil		0.60	191.7	4.8	149.4	19.6	41.9	49.0	5.9

A: Data represent n=2 of triplicate incubations in pooled DIM and DLM microsomes at 1 mg/ml, b: Data represent a n=3 occasion mean from duplicate incubations at 1 mg/ml in DIM and DLM microsomes from individual donors after correction for fu_{inc}

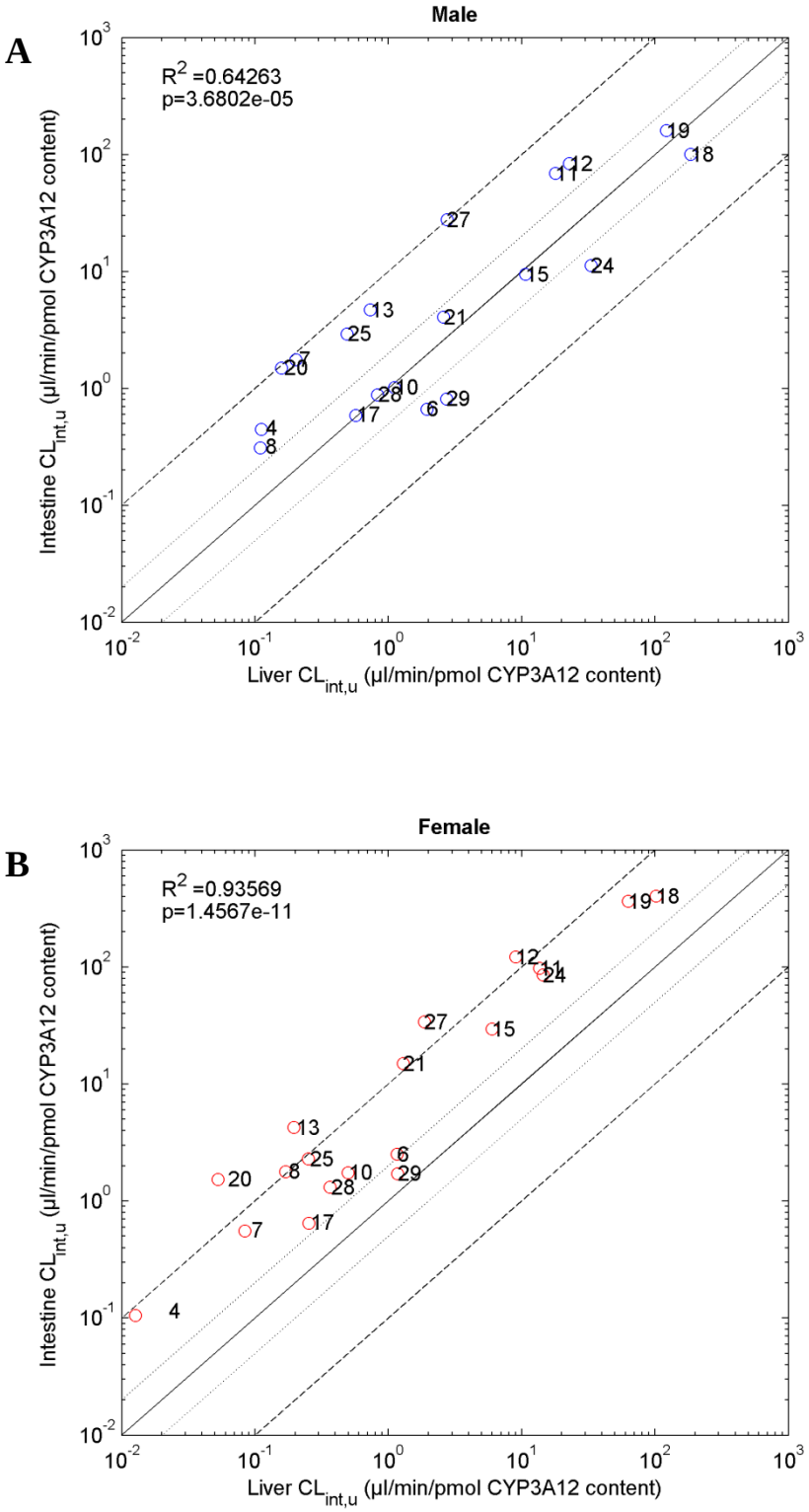

Figure 4-9 Dog Male (A) and Female (B) liver and intestinal $CL_{int,u}$ correlations for CYP3A substrates normalised for reported intestinal and hepatic CYP3A content (Heikkinen et al., 2012).

Solid line represents line of unity, dotted lines 2-fold, and dashed lines 10 fold. Study numbers correspond to compounds in **Table 4-7**.

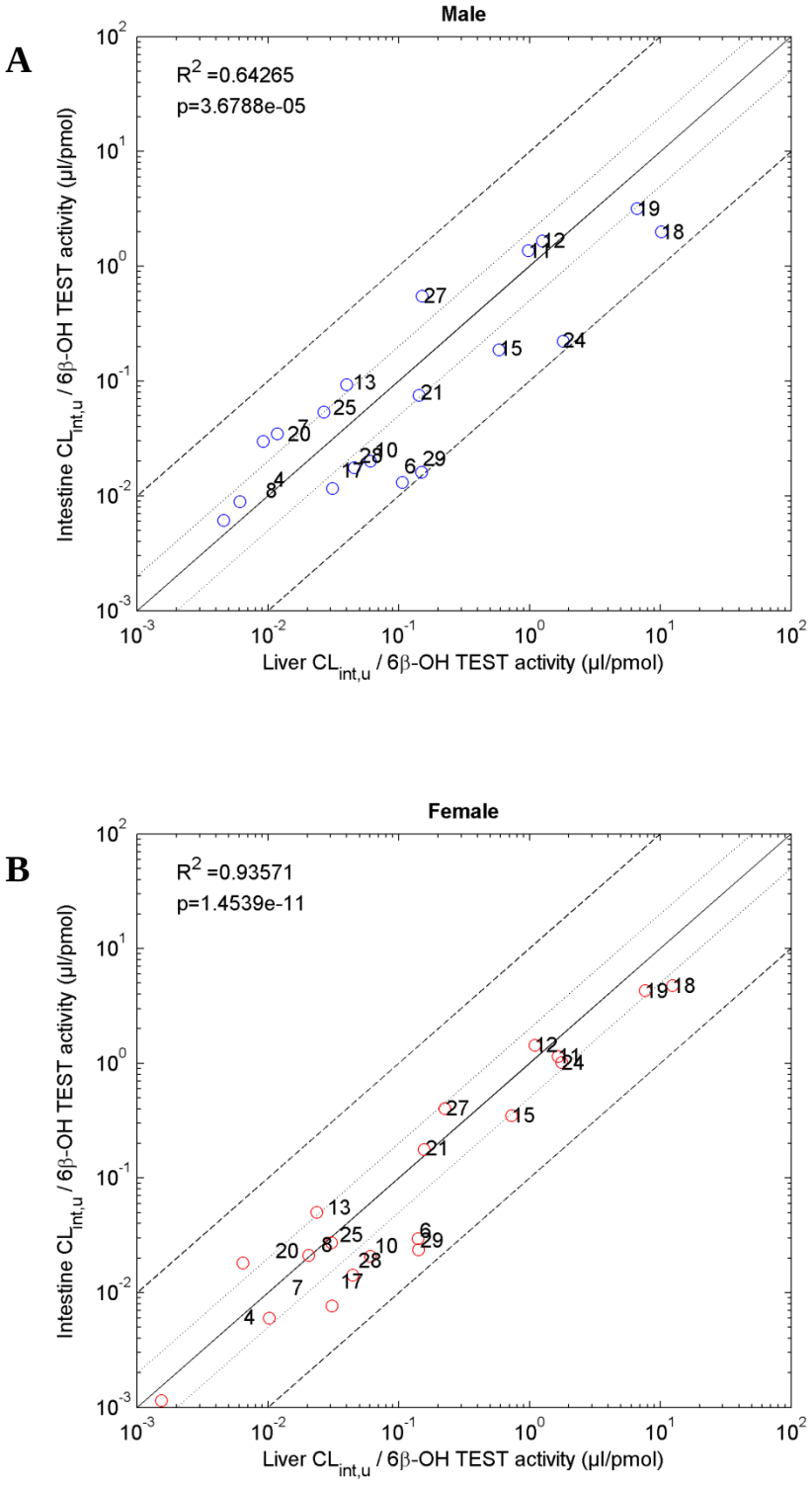

Figure 4-10 Dog Male (A) and Female (B) liver and intestinal $CL_{int,u}$ correlations for CYP3A substrates normalised for measure intestinal and hepatic CYP3A testosterone 6β-OH TEST activity.

Solid line represents line of unity, and dotted lines 2-fold, and dashed lines 10 fold. Study numbers correspond to compounds in **Table 4-7**

Table 4-8 Assessment of liver and intestinal normalisation through literature reported CYP3A content or in house measured activity.

	$CL_{int,u}$ CYP3A content normalised		$CL_{int,u}$ CYP3A activity normalised	
	Male	**Female**	**Male**	**Female**
gmfe	1.93	6.75	0.70	0.65
rmse	28.53	80.63	1.96	1.81
>5-fold (%)	25.00	58.33	16.67	4.17
> 2-fold (%)	62.50	95.83	66.67	50.00

gmfe: geometric mean fold error, rmse: root mean standard error.

4.5.4. Regional intestinal *in vitro* intrinsic clearance

The regional $CL_{int,u}$ for n=24 compounds in each segment is shown in **Table 4-7**. The highest metabolism was observed in CYP3A substrates in segment 1. Coefficient of variation for segments 2, 3 and 6 were 53, 64, and 85% respectively The lowest mean $CL_{int,u}$ for all substrates was observed in segment 6, were mean activity was 4.9-fold lower than segment 1. The largest fold changes between segments 1 and 6 were observed for CYP3A substrate ipriflavone (29-fold), CYP2C substrate indomethacin (30-fold), as well as UGT substrate raloxifene (24-fold). The compounds which displayed the highest metabolism in all regions were saquinavir, terfenadine, tacrolimus and nicardipine.

4.5.5. IVIVE of dog hepatic and intestinal microsomal clearance

The microsomal and organ specific scalars for extrapolating *in vitro* CL_{int} from hepatic and segment intestinal microsomes are shown in (**Table 4-9**). Liver scalars ranged from 30.5 to 54.0mg/g and segment 1 intestinal scalars from 2.7 to 11.2 mg/g. Liver weights ranged from 410.9 to 545.3 g, and segment 1 intestine 58.2 to 94.2 g. Regional intestinal scalars based on pools from each segments are shown in **Table 4-10**. The highest intestinal microsomal scalar was observed in segment 3 (10.2 mg/g) and lowest in segment 6 (5.2 mg/g).

Table 4-9 Microsomal Scalars and organ weights utilised for male and female beagle dog hepatic and segment 1 intestinal metabolism.

	Liver		Intestine Segment 1	
Dog	MPPGL (mg/g)	Organ Weight (g)	MPPGI (mg/g)	Organ Weight (g)
Male 1	35.6	545.3	4.4	94.1
Male 2	54.0	357.2	11.2	78.3
Male 3	41.2	496.3	4.5	94.2
Female 1	33.5	415.6	2.7	87.9
Female 2	45.0	435.3	6.2	85.1
Female 3	30.5	410.9	2.7	58.2

Scalars based on mean of three markers for correction for losses.

Table 4-10 Microsomal Scalars and organ weights utilised for female beagle dog intestinal segments 2, 3 and 6.

Segment	MPPGI (mg/g)	Organ Weight (g)
2	6.5	60.3
3	10.2	51.9
4	5.2	50.4

Scalars based on mean of three markers for correction for losses. Mean of n=3 preparations for pooled segments 2, 3 and 6.

Table 4-11 shows measured P_{app} A-B Caco-2 values (unless stated) which were scaled to make estimates of Q_{gut}. Values of P_{app} ranged from 0.1 (pirenzipine) to $121x10^{-6}$.cm/s (indomethacin).Scaled measures of F_G and F_H in segment 1 and hepatic microsomes for male and female dogs, and comparison to literature or in house estimates of F_G and F_H based on comparison of p.o.and i.v. dosing are shown in **Table 4-12**. Reported F_G cover a range from 0.0) (raloxifene) to 1 (diltizem, buspirone, ipriflavone, verapermil and nicardipine), with 8 compounds with an F_G lower than 0.5.

Plots showing *in vitro* estimates of F_G in both male and female segment 1 based on both Caco-2 or physicochemical based relationships are displayed in **Figure 4-11** and **Figure 4-12**, respectively, alongside estimates of F_H. Underprediction of *in vitro* F_G is observed for CYP3A substrates midazolam, saquinavir, tacrolimus, ipriflavone and nicardipine. The degree of prediction accuracy is described in. Poor prediction of F_H was observed for diltizem, buspirone, verapamil ipriflavone. Prediction accuracies were similar for both Caco-2 and physicochemical based scaling of F_G. Similar estimates of F_H were observed using Simcyp animal v12 ADAM PBPK model, however poorer estimates of $Fa.F_G$ were made (**Figure 4-14**, **Table 4-13**, **Table 4-14**).

Table 4-11 Measured Caco-2 P_{app} and estimates of Peff, Q_{gut} and Fa in the dog intestine

	Physicochemical				Caco-2			
Compound	**PSA**	**HBD**	**Q_{gut} (l/h)**	**Fa[b]**	**P_{app} A-B ($x10^{-6}$cm/s)**	**P_{eff} ($x10^{-4}$ cm/s)**	**Q_{gut} (l/h)**	**Fa[b]**
7-Hydroxycoumarin	51	1	1.25	1.00	61.7	7.41	1.91	1.00
Bisporolol Fumerate	64	2	0.55	1.00	5.8	1.34	0.48	1.00
Buspirone	60	0	1.70	1.00	9.8	1.96	0.68	1.00
Cimetidine	82	3	0.20	0.95	0.6	0.26	0.10	0.80
Cyclosporine A	290	5	0.00	0.01	NV	NV	NV	NV
Diltiazem	56	0	1.82	1.00	10.5	2.06	0.71	1.00
Domperidone	67	2	0.52	1.00	6.7	1.49	0.53	1.00
Felodipine	69	1	0.87	1.00	3.3	0.89	0.33	0.99
Furosemide	130	4	0.03	0.42	0.3	0.16	0.06	0.64
Indomethacin	69	1	0.87	1.00	121	12.06	2.57	1.00
Ipriflavone	37	0	2.46	1.00	57.4	7.03	1.85	1.00
Irbesartan	82	1	0.65	1.00	13.3	2.44	0.82	1.00
Losartan K	87	2	0.32	0.99	1.9	0.60	0.23	0.96
Midazolam HCl	20	0	3.06	1.00	36.2	5.04	1.46	1.00
Nicardipine	114	1	0.31	0.99	26.5	4.02	1.23	1.00
Nitrendipine	113	1	0.32	0.99	84.8	9.32	2.21	1.00
Omeprazole	71	1	0.83	1.00	NV	NV	NV	NV
Pirenzepine HCl	64	1	0.96	1.00	0.2	0.12	0.05	0.54
Raloxifene HCl	74	2	0.44	1.00	4.9	1.19	0.43	1.00
Saquinavir Mesylate	179	6	0.00	0.04	3.3	0.89	0.33	0.99
Sildenafil	105	1	0.38	0.99	40.3	5.44	1.55	1.00
Tacrolimus	186	3	0.01	0.23	73.6	8.42	2.08	1.00
Terfenadine	46	2	0.83	1.00	9	1.84	0.64	1.00
Verapamil	56	0	1.82	1.00	15.7	2.75	0.91	1.00

NV: no value.

Table 4-12 Literature reported observed and in house predicted F, F_G and F_H from IVIVE of male and female dog segment 1 DIM and DLM and Q_{gut} and Fa predictions from either Caco-2 data or physicochemical based permeability

		F	Fa.F_G					F_H			
Compound				Caco-2		Phys					
Study #	Name	Ob	Ob	M	F	M	F	Ob	M	F	Observed Reference
1	7-Hydroxycoumarin	0.48	0.54	0.67	0.65	0.59	0.6	0.89	0.47	0.67	(Ritschel and Grummich, 1981)
4	Bisporolol	0.86	0.94	0.89	0.96	0.90	0.96	0.92	0.97	0.99	(Beddies et al., 2008)
6	Buspirone	0.02	1.00	0.86	0.62	0.93	0.78	0.00	0.49	0.53	In house
7	Cimetidine	0.75	0.95	0.42	0.37	0.58	0.54	0.79	0.93	0.97	(Le Traon et al., 2009)
8	Cyclosporine A	0.46	0.51	NV	NV	0.00	0.00	0.90	NV	NV	(Mealey et al., 2010)
10	Diltiazem	0.19	1.00	0.85	0.71	0.93	0.85	0.00	0.58	0.72	In house
11	Domperidone	0.20	0.32	0.81	0.72	0.81	0.71	0.62	0.78	0.82	(Heykants et al., 1981b)
12	Felodipine	0.17	0.35	0.90	0.59	0.95	0.78	0.49	1.00	1.00	(Baarnhielm et al., 1986)
13	Furosemide	0.47	0.54	0.13	0.12	0.07	0.05	0.87	0.91	0.94	(Yakatan et al., 1979)
14	Indomethacin	NV	NV	0.91	0.94	0.80	0.87	NV	0.99	0.97	
15	Ipriflavone	0.01	1.00	0.57	0.35	0.63	0.38	0.00	0.45	0.54	In house
16	Irbesartan	NV	NV	0.87	0.92	0.85	0.90	NV	0.96	0.95	
17	Losartan	0.41	0.56	0.75	0.66	0.80	0.73	0.73	0.96	0.94	(Lo et al., 1995)
18	Midazolam	0.02	0.04	0.35	0.24	0.48	0.37	0.51	0.63	0.61	(Nishimura et al., 2007)
19	Nicardipine	0.06	1.00	0.11	0.05	0.08	0.01	0.00	0.16	0.29	(Kadono et al., 2010)
20	Nitrendipine	0.29	0.48	0.66	0.42	0.30	0.11	0.61	0.39	0.44	(Krause et al., 1988)
21	Omeprazole	0.15	0.17	NV	NV	0.65	0.32	0.89	NV	NV	
22	Pirenzepine	0.60	0.67	0.46	0.27	0.97	0.89	0.90	0.98	0.98	In house
23	Raloxifene	0.00	0.00	0.12	0.03	0.12	0.03	0.48	0.25	0.30	(Kosaka et al., 2011)
24	Saquinavir	0.08	0.17	0.10	0.01	0.00	0.00	0.50	0.03	0.16	(Tam-Zaman et al., 2004)
25	Sildenafil	0.34	0.56	0.81	0.79	0.60	0.53	0.60	0.79	0.82	(Walker et al., 1999)
27	Tacrolimus	0.07	0.07	0.26	0.18	0.01	0.00	0.98	0.50	0.38	(Jacobson et al., 2001)
28	Terfenadine	NV	NV	0.15	0.05	0.17	0.06	NV	0.21	0.26	
29	Verapamil	0.13	1.00	0.91	0.87	0.95	0.92	0.00	0.41	0.62	(Toffoli et al., 1997)

Ob: Observed *in vivo*, Caco-2: Caco-2 based permeability scaling, Phys: Physicochemical permeability based scaling, NV: no value.

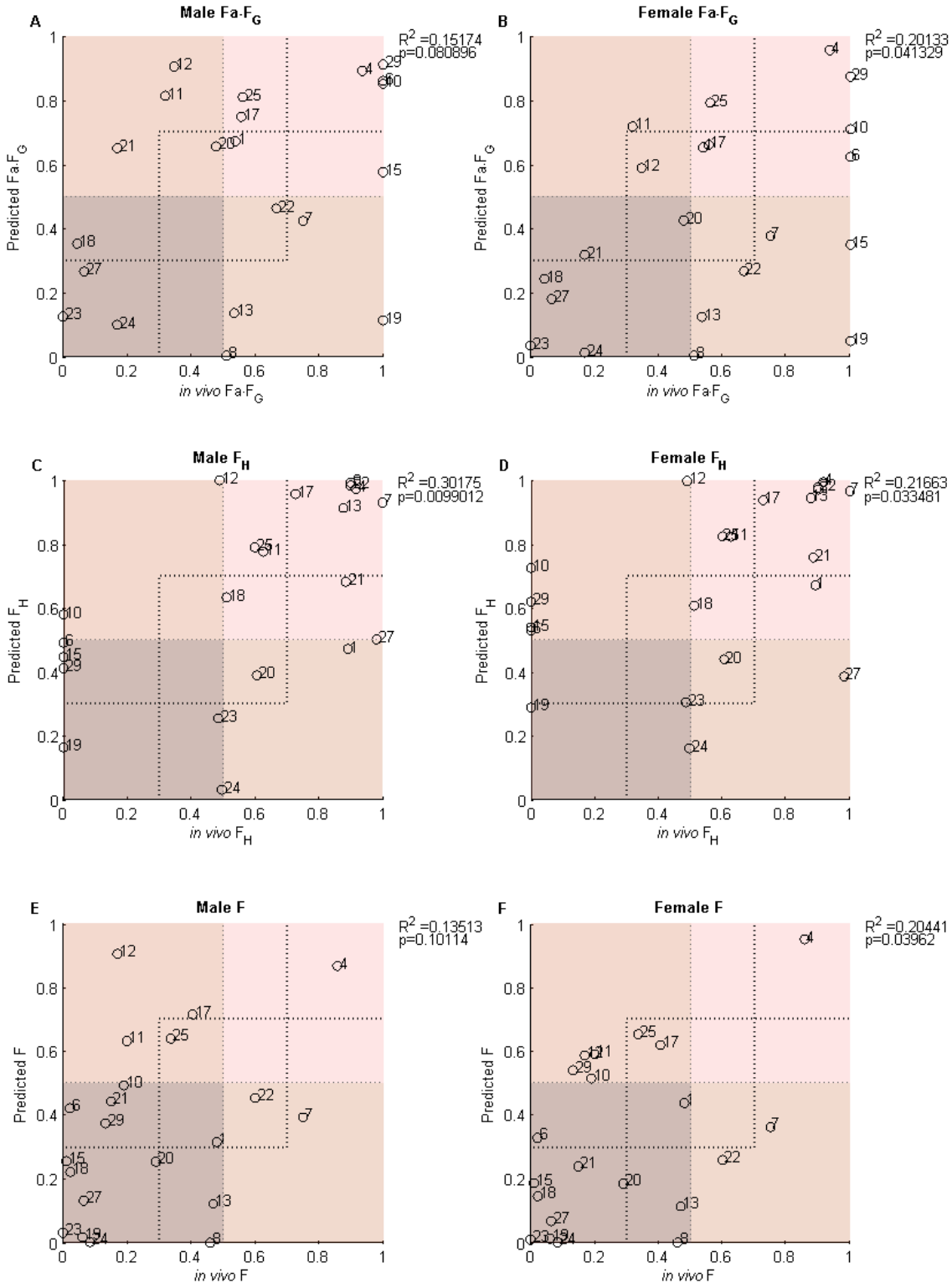

Figure 4-11 Comparison of predicted and observed measures of Fa.F_G F_H and F based on Caco-2 permeability extrapolated from DIM and DLM. Male Fa.F_G (A) and female Fa.F_G (B) based on Q_{gut} model, male F_H (C) and female F_H (D) based 'well-stirred' liver model, male F (E) and female F (F) based on F_H and Fa.F_G predictions.

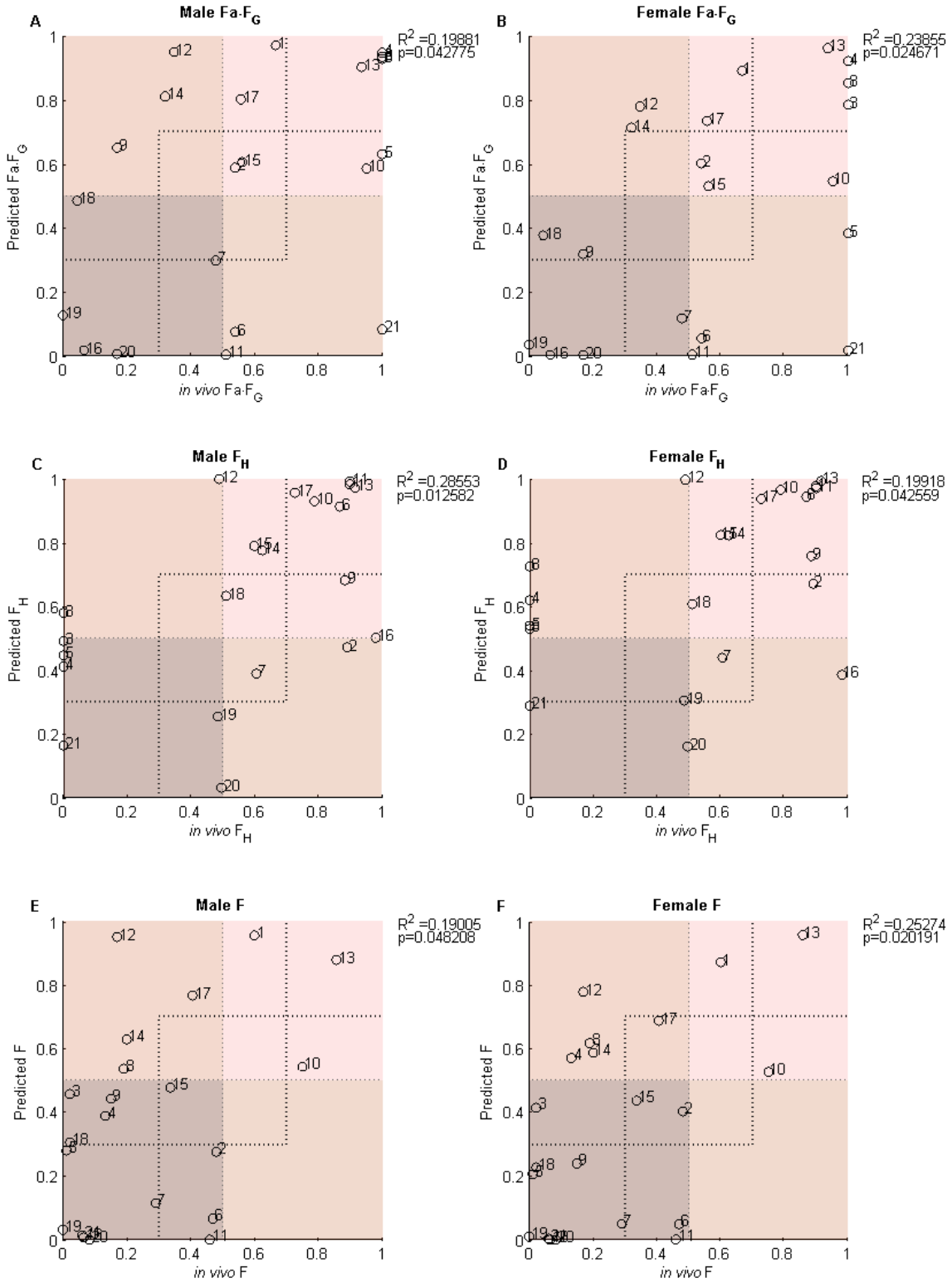

Figure 4-12 Comparison of predicted and observed measures of $Fa.F_G$ F_H and F based on compound physiochemical based permeability extrapolated from DIM and DLM. Male $Fa.F_G$ (A) and female $Fa.F_G$ (B) based on Q_{gut} model, male F_H (C) and female F_H (D) based 'well-stirred' liver model, male F (E) and female F (F) based on F_H and $Fa.F_G$ predictions.

TN and TP categorisation for Q_{gut} approaches were similar between sexes and between physicochemical and Caco-2 based scaling techniques, with $Fa.F_G$, F_H and F in the male using Caco-2 of 63%, 76% and 68% respectively. Similar predictions were observed in the female, however the accuracy in F_H was reduced (67%). The model estimates of $Fa.F_G$, F_H and F using the ADAM model, were 76%, 71% and 62% respectively.

Precision accuracy asseed using the ratio of observed and predicted $Fa.F_G$, F_H and F is shown in **Figure 4-13**. Precision accuracy was within 2-fold for 58% and 47% of compounds for male and female Caco-2 based $Fa.F_G$ predictions. Similar accuracy was sheen in physicochemical based estimates (52% and 48% for male and female respectiuvely). Highest prediction accuraracy was observed for FH estimates 66% and 61% for male and female, respectively. Estimates of F were low, with highest prediction accuracies seen using $Fa.F_G$ predictions based on Caco-2 based scaling. Highest inaccuracies were seen for compounds with low observed bioavailability. Highest underprediction in $Fa.F_G$ was observed for saquinavir, ipriflavone, nicardipine and furosemide. Overprediction was observed for raloxifene, midazolam and tacrolimus based on Caco-2 scaling. Overprediction for the ADAM model was for saquinavir and raloxifene. Underprediction was observed for nitrendipine and ipriflavone.

Assesment using the narrow rage of $Fa.F_G$, F_H and F ($FM_{,<0.3}$, $FM_{,0.3\text{-}0.7}$ and $FM_{,>0.7}$) classifications is shown in **Table 4-15**. Correct classification was more frequently observed using Caco-2 over physicochemical based scaling stratergies (52% *vs.* 43% and 58% *vs.* 43% for male and female respectively). Similar results were shown for F (52% *vs.* 38% and 58% *vs.* 58% for male and female respectively). ADAM classifications are shown in **Table 4-16**. Correct categorisation was observed for 57% of compounds for $Fa.F_G$. Incidence of $Fa.F_{G,<0.3}$, $Fa.F_{G,0.3\text{-}0.7}$ and $Fa.F_{G,>0.7}$ was 19%, 14% and 24%. In all, 80% of $Fa.F_{G,<0.3}$ compounds were accurately predicted using the ADAM model. Correct prediction of F_H and F accounted for 48% and 57% respectively, although $F_{,<0.3}$ accounted for 67%.

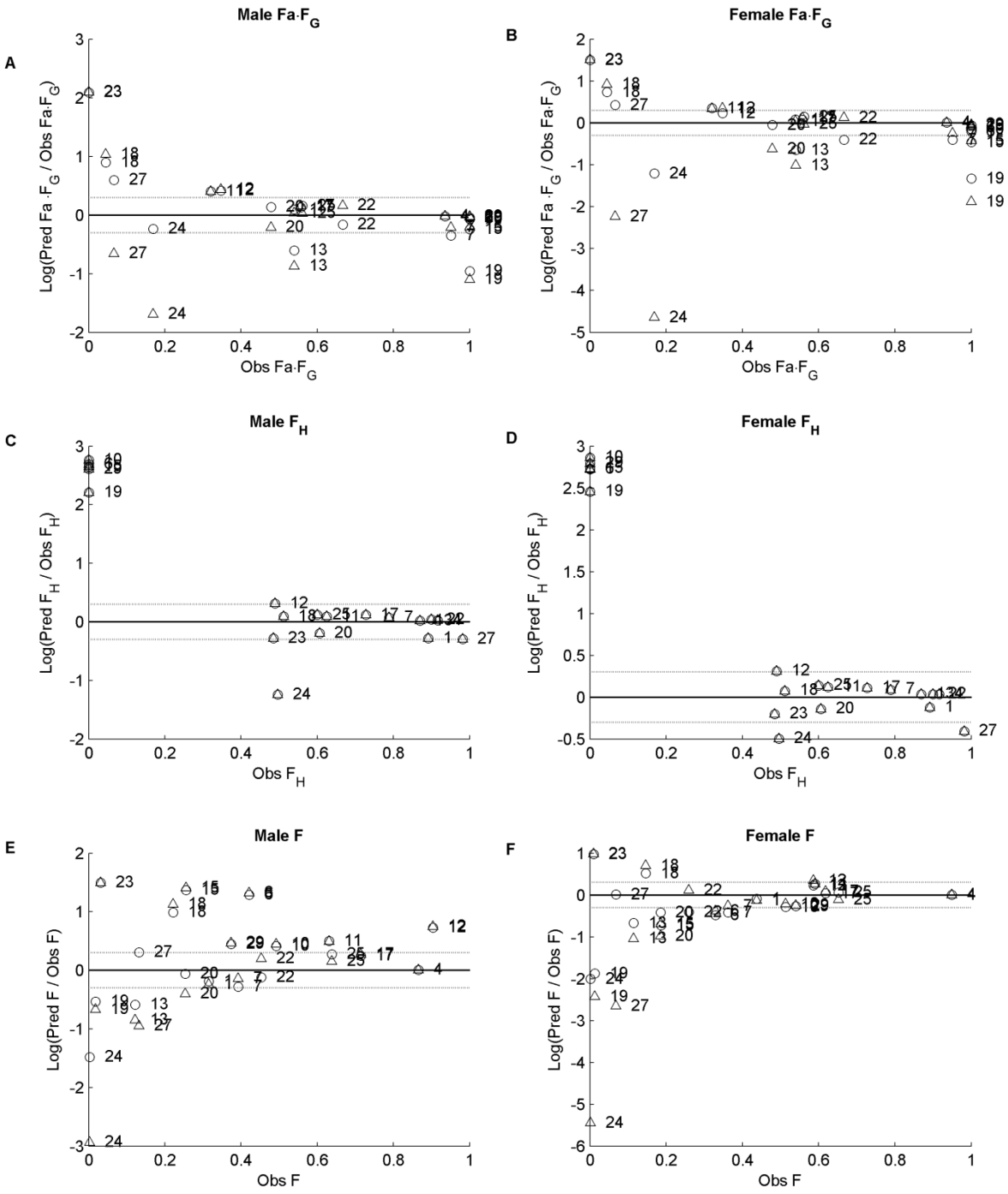

Figure 4-13 Precision of predictions for Male (A,C,E), Female (B,D,F) of Fa.F_G, F_H and F using form physicochemical (Δ) and Caco-2 (o) based scaling of *in vitro* dog intestinal metabolic data.

The dotted lines at ±0.3 log units represents 50% underprediction and 100% overprediction precision limits.

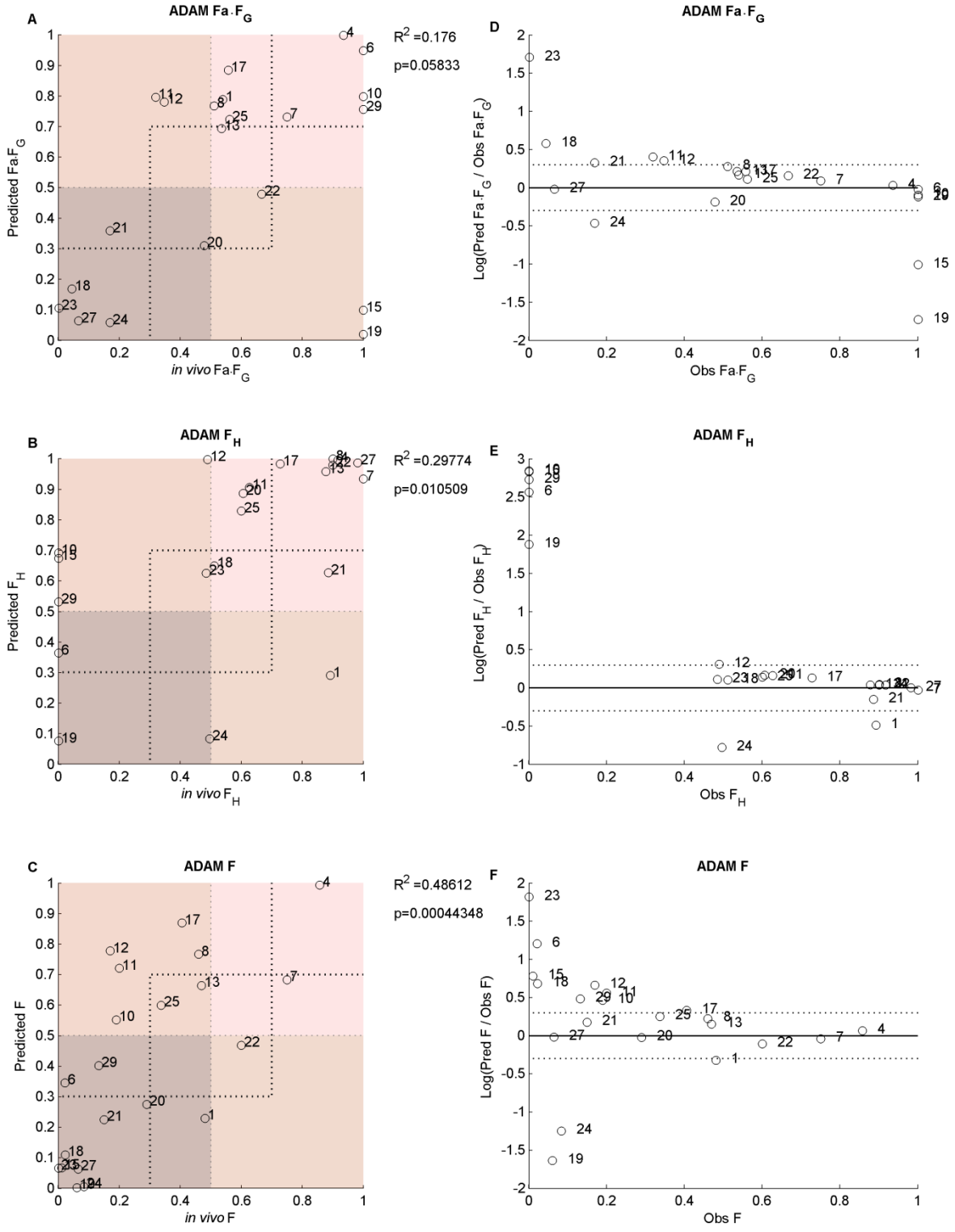

Figure 4-14 Comparison of predicted and observed measures of Fa.F_G F_H and F using the ADAM model. Fa.F_G (A) F_H (B), and F (C). Graphs of the precision accuracy of predictions based on the ratio of observed over predicted Fa.FG (D), FH (E) and F (H)

Input parameters can be found in **Appendix Table 7-7** and **Appendix Table 7-8**. The dotted lines for D, E and F at ±0.3 log units represents 50% underprediction and 100% overprediction precision limits.

Table 4-13 Prediction accuracy of F_G and F_H and for all compounds, and compounds with a fraction metabolized less than 0.5 using Q_{gut} and 'well-stirred' models and ADAM model estimates

		Q_{gut}				'Well-Stirred' Model		ADAM Model	
		Caco-2 $Fa.F_G$[a]		Physicochemical $Fa.F_G$		F_H			
		Male	Female	Male	Female	Male	Female	$Fa.F_G$	F_H
All compounds	n	19	19	21	21	21	21	21	21
	>2-fold (%)	47.4	31.6	47.6	33.3	33.3	9.5	38.1	38.1
	<2-fold (%)	52.6	68.4	52.4	66.7	66.7	90.5	61.9	61.9
	gmfe	1.30	0.85	0.74	0.33	3.51	4.20	1.06	4.05
	rmse	0.35	0.37	0.37	0.37	0.32	0.35	0.36	0.35
in vivo FM<0.5	n	7	7	8	8	8	8	8	8
	>2-fold (%)	85.7	14.3	87.5	37.5	87.5	12.5	75.0	87.5
	<2-fold (%)	14.3	85.7	12.5	62.5	12.5	87.5	25.0	12.5
	gmfe	1.27	1.92	1.37	0.28	29.06	41.52	2.36	36.2
	rmse	0.56	0.21	0.54	0.28	0.5	0.54	0.28	0.47

FM: Fraction metabolised. a: Cyclosporine (8) and omeprazole (21) were not included in calculations as these were estimated based on physicochemical properties only

Table 4-14 Prediction accuracy of low FM or F categorisation for all compounds using Q_{gut} and 'well-stirred' models and ADAM model estimates

Male						Female						ADAM		
Categorisation of low $Fa.F_G$						Categorisation of low $Fa.F_G$						Categorisation of low $Fa.F_G$		
Physicochemical			Caco-2[a]			Physicochemical			Caco-2[a]			Fa.FG		
Class	n	%	Class	n	%	Class	n	%	Class	n	%	Class	n	%
TP	6	28.6	TP	5	23.8	TP	6	28.6	TP	6	28.6	TP	6	28.7
TN	9	42.9	TN	10	47.6	TN	9	42.9	TN	9	42.8	TN	10	47.6
FP	3	14.3	FP	3	14.3	FP	4	19.1	FP	4	19.1	FP	3	14.2
FN	3	14.3	FN	3	14.3	FN	2	9.5	FN	2	9.5	FN	2	9.5
Categorisation of low F_H						Categorisation of low F_H						Categorisation of low F_H		
Well-stirred						Well-stirred						F_H		
Class	n	%				Class	n	%				Class	N	%
TP	6	28.6				TP	3	14.3				TP	3	14.3
TN	11	52.4				TN	11	52.4				TN	12	57.1
FP	2	9.5				FP	2	9.5				FP	1	4.8
FN	2	9.5				FN	5	23.8				FN	5	23.8
Categorisation of low F						Categorisation of low F						Categorisation of low F		
Physicochemical			Caco-2[a]			Physicochemical			Caco-2[a]			F		
Class	n	%	Class	n	%	Class	n	%	Class	n	%	Class	N	%
TP	14	66.7	TP	14	66.7	TP	12	57.1	TP	12	57.1	TP	11	52.4
TN	3	14.3	TN	1	4.8	TN	3	14.3	TN	1	4.8	TN	2	9.5
FP	0	0.00	FP	2	9.5	FP	0	0.00	FP	2	9.5	FP	1	4.8
FN	4	19.1	FN	4	19.1	FN	6	28.6	FN	6	28.6	FN	7	33.3

a: Cyclosporine (8) and omeprazole (21) were not included in calculations as these were estimated based on physicochemical properties only.

Table 4-15 Incidence of $FM_{,<0.3}$, $FM_{,0.3-0.7}$ and $FM_{,>0.7}$ correct and incorrect categorisation for predicted and observed $Fa.F_G$, F_H and F using metabolism data and either physicochemical or Caco-2 based scaling methodologies.

Male

$Fa.F_G$

	Physicochemical					Caco-2				
		Correct		Incorrect			Correct		Incorrect	
	$Fa.F_G$<0.3	3	14.3%	2	9.5%	$Fa.F_G$<0.3	3	15.8%	1	5.3%
	$Fa.F_G$ 0.3-0.7	2	9.5%	7	33.3%	$Fa.F_G$ 0.3-0.7	3	15.8%	5	26.3%
	$Fa.F_G$>0.7	4	19.0%	3	14.3%	$Fa.F_G$>0.7	4	21.1%	3	15.8%
∑	21	9	42.9%	12	57.1%	19	10	52.6%	9	47.4%

F_H

		Correct		Incorrect		
	F_H<0.3	1	4.8%	4	19.0%	
	F_H 0.3-0.7	2	9.5%	5	23.8%	
	F_H>0.7	6	28.6%	3	14.3%	
∑	21	9	42.9%	12	57.1%	

F

	Physicochemical					Caco-2				
		Correct		Incorrect			Correct		Incorrect	
	F<0.3	6	28.6%	7	33.3%	F<0.3	7	33.3%	6	28.6%
	F 0.3-0.7	1	4.8%	5	23.8%	F 0.3-0.7	3	14.3%	3	14.3%
	F>0.7	1	4.8%	1	4.8%	F>0.7	1	4.8%	1	4.8%
∑	21	8	38.1%	13	61.9%	21	11	52.4%	10	47.6%

Female

$Fa.F_G$

	Physicochemical					Caco-2				
		Correct		Incorrect			Correct		Incorrect	
	$Fa.F_G$<0.3	3	14.3%	2	9.5%	$Fa.F_G$<0.3	4	21.1%	0	0.0%
	$Fa.F_G$ 0.3-0.7	2	9.5%	7	33.3%	$Fa.F_G$ 0.3-0.7	4	21.1%	4	21.1%
	$Fa.F_G$>0.7	4	19.0%	3	14.3%	$Fa.F_G$>0.7	3	15.8%	4	21.1%
∑	21	9	42.9%	12	57.1%	19	11	57.9%	8	42.1%

F_H

		Correct		Incorrect	
	F_H<0.3	1	4.8%	4	19.0%
	F_H 0.3-0.7	3	14.3%	4	19.0%
	F_H>0.7	7	33.3%	2	9.5%
∑	21	11	52.4%	10	47.6%

F

	Physicochemical					Caco-2				
		Correct		Incorrect			Correct		Incorrect	
	F<0.3	8	38.1%	5	23.8%	F<0.3	7	36.8%	5	26.3%
	F 0.3-0.7	3	14.3%	3	14.3%	F 0.3-0.7	3	15.8%	2	10.5%
	F>0.7	1	4.8%	1	4.8%	F>0.7	1	5.3%	1	5.3%
∑	21	12	57.1%	9	42.9%	19	11	57.9%	8	42.1%

Table 4-16 Incidence of $FM_{,<0.3}$, $FM_{,0.3-0.7}$ and $FM_{,>0.7}$ correct and incorrect categorisation for predicted and observed $Fa.F_G$, F_H and F using metabolism data and theADAM model.

		ADAM			
		$Fa.F_G$			
		Correct		Incorrect	
	$Fa.F_G$<0.3	4	19.0%	1	4.8%
	$Fa.F_G$ 0.3-0.7	3	14.3%	6	28.6%
	$Fa.F_G$>0.7	5	23.8%	2	9.5%
∑	21	12	57.1%	9	42.9%
		F_H			
		Correct		Incorrect	
	F_H<0.3	1	4.8%	4	19.0%
	F_H 0.3-0.7	2	9.5%	5	23.8%
	F_H>0.7	7	33.3%	2	9.5%
∑	21	10	47.6%	11	52.4%
		F			
		Correct		Incorrect	
	F<0.3	8	38.1%	5	23.8%
	F 0.3-0.7	3	14.3%	3	14.3%
	F>0.7	1	4.8%	1	4.8%
∑	21	12	57.1%	9	42.9%

4.5.6. Regional intestinal metabolism in the female beagle dog.

The predicted regional E_G is shown in **Table 4-17**. The rank order for intestinal metabolism was segment 1<=segment 2<segment3>>segment 6 ($p<0.05$). Intestinal extraction in segment 1 was in general lower in male *vs.* female but not statistically significant. The regional distribution of E_G in segment 1 of male and segments 1, 2, 3 and 6 of female beagle intestine is shown in **Figure 4-15**. Lowest mean E_G is observed in the distal segment for both CYP3A and UGT compounds, with segment 1 and 3 showing the highest mean E_G.

Table 4-17 Regional estimates of intestinal E_G in segment one of male and segments 1, 2, 3 and 6 for female dogs from Caco-2 based Q_{gut} estimates

	Male	Female			
Compound	**Segment 1[b]**	**Segment 1[b]**	**Segment 2[c]**	**Segment 3[c]**	**Segment 6[c]**
7-Hydroxycoumarin	0.33	0.35	0.65	0.62	0.09
Bisporolol	0.11	0.04	0.08	0.07	0.16
Buspirone	0.14	0.38	0.39	0.41	0.07
Cimetidine	0.47	0.53	0.64	0.45	0.20
Cyclosporine A	0.80	0.71	0.50	0.50	0.50
Diltiazem	0.15	0.29	0.29	0.38	0.14
Domperidone	0.18	0.28	0.51	0.64	0.12
Felodipine	0.08	0.41	0.61	0.60	0.24
Furosemide	0.79	0.81	0.31	0.65	0.80
Indomethacin	0.08	0.06	0.02	0.09	0.00
Ipriflavone	0.43	0.65	0.41	0.54	0.19
Irbesartan	0.15	0.10	0.09	0.26	0.06
Losartan K	0.22	0.31	0.43	0.47	0.13
Midazolam	0.65	0.76	0.82	0.86	0.29
Nicardipine	0.89	0.95	0.98	0.99	0.88
Nitredipine	0.34	0.58	0.53	0.53	0.35
Omeprazole	0.35	0.68	0.51	0.61	0.23
Pirenzepine	0.15	0.51	0.60	0.67	0.13
Raloxifene	0.88	0.97	0.90	0.92	0.54
Saquinavir	0.90	0.99	0.99	0.99	0.95
Sildenafil	0.19	0.21	0.22	0.36	0.02
Tacrolimus	0.74	0.82	0.44	0.97	0.68
Terfenadine	0.85	0.95	0.97	0.99	0.94
Verapamil	0.09	0.13	0.52	0.62	0.09

a: based on Physchem properties b: Data represent a n=3 occasion mean from duplicate incubations in DIM microsomes from individual donors c: Data represent a n=2 occasion mean from duplicate incubations

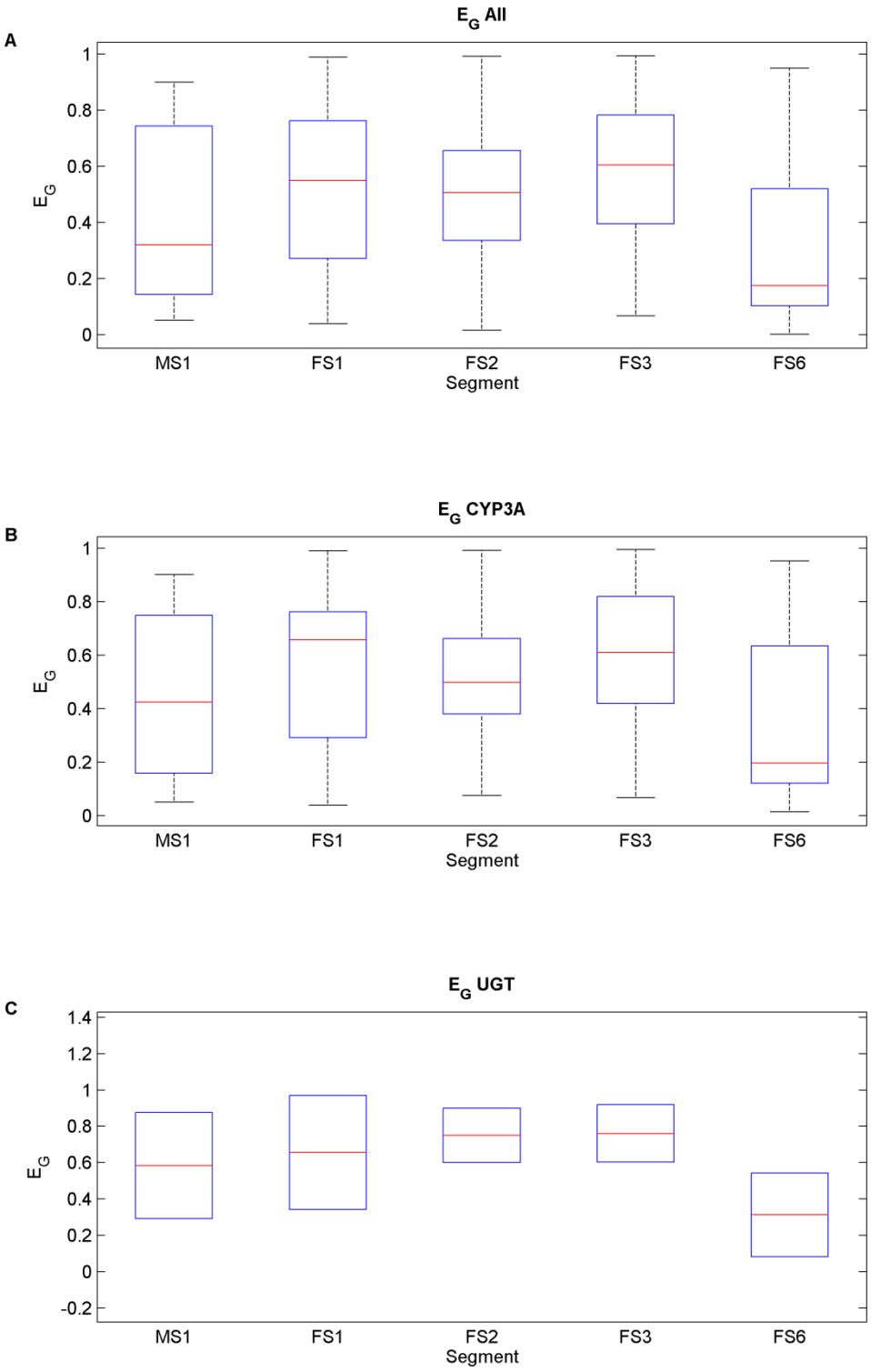

Figure 4-15 Regional predicted E_G in segment 1 of male and segments 1, 2,3 and 6 in female beagle dog intestine for all 24 compounds (A) and CYP3A (B) (n=12) and UGT (C) (n=2) substrate compounds.

4.6. Discussion

The primary aims of this chapter were to derive intestinal and hepatic scalars for male and female dogs, and to characterise regional gradients in scalars. Secondly, the focus was to characterise the regional activities of intestinal microsomes towards marker probes and a diverse range of compounds to assess both metabolic contributions and to estimate scaled up measures of intestinal extraction (E_G).

4.6.1. Male and female dog intestinal characteristics

Comparing both male and female dogs, both the length and weight of total intestine was longer in male dogs. In terms of weight of tissue per cm length, the main proportion of the intestine was uniform, with higher weight per gram in the proximal and distal segments. These most likely represent the duodenum (i.e. segment 1) and ileum (i.e. segment 6), and are in line with these being reported in the dog to being relatively short segments in comparison to the jejunum (Kararli, 1995). Observed mucosal yields (0.16 to 0.29 g/cm) did not indicate any significant regional changes, suggesting that changes in weight are not related to changes in enterocyte number, rather more likely changes other cell types (e.g. smooth muscle). Similar yields have also been recently reported to be observed in beagle dogs (0.16 to 0.45 g/cm) (Heikkinen et al., 2012). Homogenate yields in the distal segment (segment 6) were slightly lower (5.9 *vs.* 12.0) than mean proximal yield (segments 1-3), however this may in part be due to the increased mucus content in the distal portion of the small intestine (Koropatkin et al., 2012), and its effect of trapping protein during centrifugation (Stohs et al., 1976). The addition of heparin to the initial elution buffer and subsequent low speed centrifugation steps to dilute out mucus content utilised in the method (**Chapter 2**) was incorporated in mind to reduce the aggregation of proteins caused by the presence of mucus. This may be harder to prevent in distal portions of the intestine, and future work should investigate increasing the heparin concentration further. However, comparison of recoveries between segments was equivalent between all segments, suggesting that mucus contamination was not responsible (see below).

4.6.2. Male and female hepatic and proximal intestine scalar comparisons

Comparing dog intestinal microsomes prepared from segment 1 of male and female dogs to those of the liver prepared from matched donors did not indicate any trends in terms of inter-individual specific factors which influence the recovery of microsomal protein.

Recovery was between 2.2-4.3 fold higher in the liver *vs.* intestine, reflective of the difficulties in isolating microsomes from intestinal tissue.

Male and female hepatic microsomal scalars from frozen tissue where 43.0 (±16.9) and 36.9 (±8.1) mg/g liver respectively and were within values reported in the literature. Previously reported hepatic scalars where corrections for losses had been applied where 43 in male liver (Baarnhielm et al., 1986). Smith et al (2008) reported in microsomes prepared from fresh liver homogenate values of 59 (48-70) (n=5) and 52 (42-62) mg/g liver (n=4) in male and female dogs respectively. Values from frozen homogenate were 27(20-34) and 33 (24-42) mg/g liver. Most recently values of 43.5 (±20.5) and 72.5 (±47.4) (n=2) have been reported using similar corrections for losses based on CYP content and testosterone 6β-hydroxylation (Heikkinen et al., 2012). Assessment of inter-operator variability revealed no significant differences in values of matched corrected or uncorrected microsomal scalars or recoveries indicating that the method was highly reproducible.

Reproducibility between separate operators on liver samples from the same animal in this study was high (CV 20%), suggesting low inter-operator variability. Weighted mean of combining the results from this study and these previous studies reveals MPPGL scaling factors of 47.7 (n=12), 38.8 (n=10), and 43.7 (n=22) mg/g for female, male and mixed populations.

Mean activities towards testosterone 6β-hydroxylation in DLM were similar to literature values (1.12nmol/min/mg and 1.07 nmol/min/mg for male and female liver microsomes, respectively) (Kyokawa et al., 2001). 4-NP gluc was however 4-fold lower than reported previously in dog liver microsomes (Kaivosaari et al., 2002).

CYP content in dog liver microsomes (0.62 nmol/mg microsomal protein in both male and female dogs) was within the range of previously reported values of 0.78 and 0.77 nmol P450/mg microsomal protein (Smith et al., 2008), 0.51 and 0.48 nmol/mg (Kyokawa et al., 2001) and 0.45 and 47 nmol/mg (Nishibe et al., 1998) from freshly prepared male and female livers. Values of 0.40 and 0.61 nmol/mg in microsomes prepared from frozen male and female respectively livers have also been reported recently (Heikkinen et al., 2012).

In comparison to the liver, intestinal values of CYP content were 10-fold lower (0.07 nmol/mg in both male and female). Previously reported values of 38 and 37 pmol/mg have been reported in dog duodenal male and female intestinal microsomes (Kyokawa et al.,

2001). These values are 2-fold lower than those observed in these studies, likely to be because these were prepared through the less optimal method of intestinal scrapping, shown to induce more damage and contamination to enzymes resulting in lower enzyme contents and activities (Mohri and Uesawa, 2001; Galetin and Houston, 2006). 6β-OH TEST and 4-NP gluc rates in this study were also over 10-fold higher than those prepared by intestinal scraping (Prueksaritanont et al., 1996; Kyokawa et al., 2001). Activity of testosterone 6β-hydroxylation rate of formation differed between male and female segment 1 microsomes, where in the lowest was seen in males, but female activity rivalled that of the liver. Formation of 4-nitrophenol glucuronide was similar between the sexes.

Scaling factors based on values of microsomal protein per weight of tissue where 4.5- to 12.5- fold lower in the intestine compared to the liver, but within 2.5-fold when expressed on a gram mucosa (enterocytes) basis. A strong positive correlation was observed between values of hepatic and proximal intestinal scalars (R^2=0.91 and R^2=0.81 for gram intestine or gram mucosal normalised scalars). No known correlations between matched donor liver and intestinal scaling factors have been previously published. The importance of these relationships may drive future estimates of inter-individual scaling factors for estimating intestinal extraction based on known liver scaling factors and metabolism.

4.6.3. Female regional intestinal characterisation

In comparison to the literature, values of intestinal CYP content were higher than reported in the literature (Kyokawa et al., 2001) presumably for the reasons stated above with regard to the elution *vs.* scraping preparation method. 6β-OH TEST formation indicated a distal reduction in CYP3A activity (**Figure 4-8B**). However, CYP activity in the third segment rivalled that of the proximal segment (**Figure 4-8B)**. This regional distribution is similar to that recorded for formation rate of the CYP3A substrate temazepam, where the highest activities were observed in segments 1 and 3 (**Figure 4-1**) (Heikkinen et al., 2012). An identical pattern of CYP3A12 measured through mass spectrometry based expression is observed as reported in the same study **Figure 1-4** (Heikkinen et al., 2012). Mean microsomal total CYP was consistent along the intestine for the segments tested (**Figure 4-7**). The full complement of CYP enzymes is not known for the dog intestine, but it is likely that more distal portions of the intestine have alternative dominant CYP isoform expression, similar to CYP2J2 in human intestine (Paine et al., 2006) to account for the lack of change in overall CYP content observed.

4-NP gluc formation fell sharply along the course of the intestine. A significantly reduced activity was observed in the distal *vs.* proximal segment ($p<0.05$). 4-NP has been reported to be a substrate for UGT1A6 in mice rats and humans (Shiratani et al., 2008), and an observed decreased distal activity is similar to what has been reported on an mRNA level in dog small intestines (Haller et al., 2012). No information of UGT protein expression in dog small intestine has been reported in the literature.

Regional distributions of intestinal scalars in female dogs expressed per unit length or unit weight of intestine or mucosa showed a mean increase from segments 1-3 for all the markers for correction for losses. A similar peak of microsomal scalar was reported in segment 4 in dog intestinal microsomes (**Figure 1-4**)(Heikkinen et al., 2012). Reported scalars were 2- to 3-fold higher than those observed in these studies, and may reflect higher mucus contamination. However this may be explained through a longer elution time (45 *vs.* 30 minutes) which may increase non-microsomal protein contamination of the microsome pellet. This may be evidenced through lower observed testosterone 6β-hydroxylation (0.03-0.12 nmol/min/mg protein) (Heikkinen, A., personal communication). Recoveries for dog intestinal microsomes were equivalent for all segments studied, indicating that any effect of mucus contamination effecting microsomal preparation was equivalent in all segments.

4.6.4. *In vitro* intrinsic clearance in dog liver and proximal intestinal microsomes

In terms of measured values of $CL_{int,u}$, an interesting observation was that whilst mean values in liver microsomes were equivalent in both male and female, the relative contributions of intestinal metabolic capability was much lower in male *vs.* female. The relative importance of sex differences hepatic and intestinal metabolism was especially highlighted for omeprazole, nitrendipine, terfenadine and ipriflavone where in male dogs, the dominant route of metabolism was hepatic. However, in female dogs the intestinal component near rivalled that of the hepatic component. All these compounds are substrates for CYP3A dependant metabolism. This corresponds to the decreased 6β-OH TEST formation seen in male *vs.* female segment 1 intestinal microsomes, and furthermore the capability of female intestinal microsome activity to rival that of the liver.

Normalising the observed $CL_{int,u}$ to measured testosterone activities in respective hepatic and intestinal microsomes produced the most unified statistically significant positive relationship to that of both respective tissues. Normalisation based on reported CYP

content (Heikkinen et al., 2012) also produced a positive correlation, however these relationships were further removed from unity. This may in part be a limitation of using measured enzyme content from only 2 donors per sex, and intestinal microsomes prepared in another lab.

4.6.5. Regional intestinal *in vitro* intrinsic clearance

The metabolic capabilities of segments 2, 3 and 6 where compared to that of segment 1 in female. $CL_{int,u}$ metabolic activities were similar in the proximal 3 segments, and lowest in the distal segment. This was true of all the substrates studied, and reflects both the gradients in probe CYP and UGT activities along the course of the intestine and reported enzyme expression levels (Haller et al., 2012; Heikkinen et al., 2012).

4.6.6. IVIVE of dog hepatic and intestinal clearance

Limited data on intestinal contributions in of the dog has been reported in the literature. Estimates of F_G and F_H were made form data available from i.v. and p.o. dosing wither in house or from literature searching. Comparing scaled up estimates of F_G based on individual scaling of metabolism and extrapolation of either measured Caco-2 permeability or permeabilities based on physiochemical properties of the compounds indicated near equivalent prediction success. A consistent observation between methods was underestimation of F_G (overestimation of intestinal metabolism). The worst prediction success was observed for CYP3A substrates: midazolam, saquinavir, tacrolimus, ipriflavone and nicardipine. Predictions were worsened using a PBPK model using drug and species specific inputs, however the reasons for this underprediction of F_G is unknown. Estimates of F_H were similar using both models suggesting it was related to a marginalisation of the intestinal component. Nicardipine, ipriflavone and saquinavir display low solubility (<10µM, **Appendix Table 7-7**) and may also drive the higher F_G observed *in vivo*. Further work would be required to see if incorporation of solubility which was not applied in this case since it was presumed that dissolution would be minimal following administration of solution, and when in house PK was preformed, p.o. solutions were tested for dissolution following acid addition.

TN and TP categorisation for Q_{gut} approaches was successful between sexes and between physicochemical and Caco-2 based scaling techniques, with $Fa.F_G$, F_H and F in the male using Caco-2 of 71%, 81% and 71% respectively. Similar predictions were observed in the

female dog, however the accuracy in F_H was reduced. Similar model estimates of $Fa.F_G$ and F were seen using ADAM model estimates, of 76%, 71% and 62% respectively.

Precision accuracy asseed using the ratio of observed and predicted $Fa.F_G$, F_H and F is shown in **Figure 4-13** and **Figure 4-14**. Precision accuracy was within 2-fold for 58% and 47% of compounds for male and female Caco-2 based $Fa.F_G$ predictions. Similar accuracy was seen in physicochemical based estimates (52% and 48% for male and female respectiuvely). Highest prediction accuraracy was observed for F_H estimates 66% and 61% for male and female, respectively. Estimates of F were low, with highest prediction accuracies seen using $Fa.F_G$ predictions based on Caco-2 based scaling. Highest inaccuracies were seen for compounds with low observed bioavailability. Highest underprediction in $Fa.F_G$ was observed for saquinavir, ipriflavone, nicardipine and furosemide. Overprediction was observed for raloxifene, midazolam and tacrolimus based on Caco-2 scaling. Overprediction for the ADAM model was reduced in line with an increase in compounds within 2-fold (62%), but still observed for saquinavir and raloxifene. Underprediction was observed for nitrendipine and ipriflavone.

Assesment using the narrow rage of $Fa.F_G$, F_H and F ($FM_{,<0.3}$, $FM_{,0.3\text{-}0.7}$ and $FM_{,>0.7}$) classifications is shown in **Table 4-15**. Correct classification was more frequently observed using Caco-2 over physicochemical based scaling stratergies (52% *vs.* 43% and 58% *vs.* 43% for male and female respectively). Similar results were shown for F (52% *vs.* 38% and 58% *vs.* 58% for male and female respectively). ADAM classifications are shown in **Table 4-16**. Correct categorisation was observed for 57% of compounds for $Fa.F_G$. Incidence of $Fa.F_{G,<0.3}$, $Fa.F_{G,0.3\text{-}0.7}$ and $Fa.F_{G,>0.7}$ was 19%, 14% and 24%, and within $Fa.F_{G,<0.3}$ for the female dog based in caco-2 scaling, 100% of compounds were correctly classified. In all, 80% of $Fa.F_{G,<0.3}$ compounds were accurately predicted using the ADAM model. Correct prediction of F_H and F accounted for 48% and 57% respectively, although $F_{,<0.3}$ accounted for 67%.

In general, prediction accuracy was similar between approaches, however worst predictions were generally observed using physicochemical based Qgut scaling approiaches *vs.* either Caco-2 based Q_{gut} or ADAM scaling. PBPK modelling using the ACAT model has been applied in the dog using intestinal and hepatic enzyme expression and distributions through emerging mass spec (MS) based measures of enzyme abundance, and application has shown improved estimations of intestinal metabolism (with 1.5 fold)

and F in the dog for a limited set (n=5) of compounds (Heikkinen et al., 2012; Heikkinen et al., 2013). Furthermore, the *in vivo* extraction ranged from 0.42 to 0.90 and predictions ranged for 0.60 to 0.96, and so the predictive limits of the model were not pushed to compounds with high intestinal extraction since, when F_G is >0.5, it is not possible to overpredict F_G by more than 2-fold. In this in house study the predicted and observed $Fa.F_G$ covered the complete range (0.00 to 1.00). Reported estimates overlapping compounds of sildenafil, domparidone, felodipine and nitrendipine were 0.96, 0.54, 0.75 and 0.72 which were similar to estimates in this study, except for nitrendipine which appeared to fit with better in house to *in vivo* $Fa.F_G$ estimates.

Prediction success for intestinal metabolism is in part dependant on reliable measures of the absolute *in vivo* metabolic component. The method used to estimate intestinal metabolism in this work was an indirect measure through comparing i.v and p.o. dosing. Using this technique, the choice of a low administered dose is preferable in order to prevent saturation of intestinal metabolism (Lin et al., 1999). One of the primary assumptions of this method is that there is negligible metabolism in enterocytes following i.v. administration and that systemic clearance of a drug after i.v. dose (corrected for renal excretion) reflects only hepatic elimination (E_H). However, in instances of compounds with a high observed blood clearance, the integrity of this assumption may not be entirely valid, as illustrated in the case of midazolam where an average 8% extraction ratio after an i.v. dosed midazolam has been reported in anhepatic patients (and up to 26% in one patient) (Galetin et al., 2010). In these cases, overestimation of E_H lowers estimated of E_G, compounding prediction success. A low percentage of drugs (19%) had an *in vivo* F_G less than 0.5, highlighting either the low contribution of the dog intestine, or more likely E_H overestimation, since all the compounds which have low prediction success also demonstrate high i.v. clearance in the dog (**Table 4-12**). Poor F_H prediction using the 'well-stirred' liver model was observed for high hepatic extraction compounds diltiazem, buspirone, verapamil and ipriflavone.

Finally, because of the inherent difficulties of separating out both Fa and F_G components of oral bioavailability, to limit the effect of Fa it is important that as in these studies, the dose administered was in solution. However in reality is by making indirect measures of F_H and F_G, the *in vivo* F_G is a combined effect of both F_G and Fa ($Fa.F_G$) (Lin et al., 1999). Fa is dependent on both absorption and actions of efflux transporters (e.g. P-gp), as well as physiochemical considerations such as solubility and pKa, which are important to consider

when assessing the absorption potential of drugs in the gastrointestinal tract, with respect to pH gradients along the course of the intestine. Importantly when considering inter-species comparisons, the dog pH is at least 1 log unit higher than that of human (Chiou et al., 2000). The impact of Fa was not fully addressed in this work and would be required to make more reliable estimates of F_G.

Oral bioavailability *in vivo* is also dependent on the region where the compound is absorbed, and as such the impact of regional metabolism may be important either for drugs not absorbed in the proximal intestine (e.g. delayed release formulations), or alternatively those undergoing enterohepatic recirculation and efflux from the bile back into the gastrointestinal tract (Paine et al., 1997; Dressman and Reppas, 2000). Assessment of regional E_G in the female dog intestine revealed the rank order for intestinal metabolism of segment 1<=segment 2<segment3>>segment 6($p<0.05$). These results were in line both with observed activities, as well as published gradients of both enzyme expression and activity (Haller et al., 2012; Heikkinen et al., 2012) as previously discussed.

4.7. Conclusions

Intestinal and hepatic scaling factors were described for both male and female dogs. A unique correlation between proximal intestinal scaling factors and those in the liver were described which may be important in future estimations of inter-individual variability within dog populations. Normalisation of $CL_{int,u}$ to measured liver and intestinal testosterone 6β-hydroxylation revealed good correlations between hepatic and intestinal metabolism. Scaling of intestinal metabolism revealed that lowest prediction success was for CYP3A compounds where overestimation (i.e. underestimation of CYP3A activity) of *in vitro* determined F_G was observed. This may be in part be driven by limitations in estimates of *in vivo* F_G for high clearance compounds. Similar estimates were seen using PBPK models (ADAM) model compared to the Q_{gut} model.

5. Human intestinal microsome preparation and characterisation, and comparison and correlation of species differences in intestinal metabolism to human

5.1. Introduction

Drug R & D programmes look to design and optimise compounds to have acceptable PK properties to engage the specific target site of action for the required duration, in order to elicit a desired PD effect. A key element in determining the probability of success of a given drug series for driving investment decisions (i.e. first in man studies) is the predictions of efficacious human dose, MAD and therapeutic safety margin. These assessments are driven by both *in vitro* and preclinical *in vivo* data predictions of human i.v. and p.o. drug clearance profiles. Predictions in human are driven both from *in vitro* methods and animal data. Given the known poor correlations between animal and human bioavailability (Grass and Sinko, 2002; Musther et al., 2013), therefore more emphasis is placed on IVIVE, for example using human liver microsomes or hepatocytes (Obach, 2001; Houston and Galetin, 2008; Hallifax et al., 2012).

A recent PhRMA collaborative study, reported however, that whilst estimates of F_H may have relative predictive success for estimating i.v. clearance (with a 69% high prediction accuracy), oral clearance estimates are poor (23% high prediction accuracy) (Poulin et al., 2011). As in this study, frequently the intestinal component is ignored since estimates of the contribution of the intestine to oral clearance are limited by a lack of established *in vitro* tools, scaling factors and understanding of intestinal species differences (Cubitt et al., 2009; Kostewicz et al., 2013). Incorporation of the intestinal component however cannot be ignored.

Scaling of human intestinal metabolism based on total CYP3A content has been applied using either a minimal Q_{gut} model or PBPK approaches; however, this is in part limited by its application to CYP3A substrates only (Gertz et al., 2010; Gertz et al., 2011) due to availability of CYP abundance data in both intestine and liver. Alternative approaches have utilised published values based on microsomal scaling factors derived from microsomes prepared using intestinal scraping (Paine et al., 1997; Cubitt et al., 2009). However, limitations to intestinal scaling are the number of studies and donors between the liver and intestine. Scaling based on intestinal CYP3A abundance is based on 31 donors (Paine et al., 2006), corrected microsomal scalars are only available from 20 donors, and only available from microsome prepared by intestinal scraping (Paine et al., 1997) for which activities are reported to be lower (Galetin and Houston, 2006). In contrast, estimates of liver CYP3A are based on 219 livers (Rowland Yeo et al., 2003), and microsomal scalars

are based on covariate analysis 108 livers (Barter et al., 2007). Furthermore, since reduced CYP activities are observed comparing scraping to elution based isolation of intestinal enterocytes (Galetin and Houston, 2006), the impact of elution on the resulting microsomal scaling factors is however unknown. This may therefore impact estimates of both CYP and UGT scaling based on microsomal scaling factors, and similar discrepancies exist in scaling based on cytosolic scaling factors. However this is further limited by no reported cytosolic regional protein expression (Cubitt et al., 2009; Cubitt et al., 2011). Considering the regional distributions of intestinal metabolic enzymes, regional differences in activities and scalars requires further understanding in order to assist PBPK based approaches to predicting intestinal metabolism (Kostewicz et al., 2013). Therefore, further confidence in human intestinal scaling is required.

5.2. Aims

The principle aims of this chapter are to derive scalars for human intestinal tissue, and to look at regional aspects of both scaling factors, CYP content and CYP and UGT activities. Furthermore, differences in metabolic activity between intestinal regions will be assessed by screening a broad range of compounds using combined CYP and UGT cofactors and a substrate depletion approach. In vitro-*in vivo* extrapolation of generated CL_{int} data will be performed using defined scalars to predict human F_G. Comparison to *in vivo* measures of human F_G will also be discussed, and compared to previous rat and dog estimates.

5.3. Materials and Methods

5.3.1. Source of human tissue

Collection of human intestinal tissues was from surgical resections and their use was approved by the regional Ethical Committee in Gothenburg (Sweden). Donors were hospitalized at Östra Sahlgrenska University Hospital, Gothenburg, and an informed written consent was obtained from each patient prior to tissue collection. Resections of jejunum intestinal segments were from two female and one male donors aged 36-43 years old, undergoing laparoscopic Roux-en-Y gastric bypass. Ileum samples were obtained from two colon cancer patients, one male and one female 77 and 78 years old. Donor details for each pool are shown in **Table 5-1**.

Table 5-1 Summary of jejunum and ileum donor pools

Intestinal Region	Gender	Age (yr)	Medication
Jejunum	Male	43	Tramadol, Metformin, Citalopram
Jejunum	Female	36	None
Jejunum	Female	43	Losartan
Ileum	Female	78	Calcium carbonate, Primidone*, Clonazepam, Levetiracetam
Ileum	Male	77	None

* known CYP3A4 inducer (Monaco and Cicolin, 1999)

Directly after surgical removal, the tissues were stored in ice-cold, constantly carbogenated (95 % O_2, 5% CO_2) Krebs-Ringer buffer (pH 7.4, made up in house), with 5 mM glucose (Simga, #G0350500), and transported to the laboratory within 30 min. On arrival to the lab, samples were opened out and flushed with ice cold wash buffer as described previously. Samples were blotted dry and weighed, before flash freezing in liquid nitrogen and storage at -80^{o}C.

5.3.2. Microsomal preparation and characterisation

On the day of preparation, either jejunum or ileum segment samples where thawed in wash buffer, and pinned down with the mucosal side exposed to silicon (Sylgard® 184 silicone elastomer kit, Dow Corning, Michigan, USA) moulded into a sealable container, similar to the method of von Richter et al., (2004). Samples were pooled based on section considering the small size of the samples (5-10 cm) and the limited yields of microsomes.

Samples were incubated three times for 15 minutes to obtain enterocytes (total 45 minutes). A longer incubation time was required than rat or dog tissue on account of the increased folded structure of the intestine. Loose mucosa trapped in intestinal folds at the end of the incubation where gently teased out using a metal spatula. Preparation of intestinal microsomes was as previously described in the rat and dog (**Chapter 2**), except that sonication of mucosa was achieved using a 250 sonifier (Branson Ultrasonics, Danbury, CT, USA). An output of 30W was set, calculated using the power output chart supplied. Following preparation both homogenate and microsomal samples were analysed for CYP content as described previously in the rat and dog at concentrations of 2 mg/ml in order to correct for losses in preparation. Following analysis, microsomes were immediately stored at -80^{o}C pending transfer and subsequent storage in the UK. In addition to CYP content, testosterone metabolite and 4-NP gluc formation in microsome and homogenate pools were used as markers to correct for losses in the isolation process, as analogous to work described previously in the rat and dog. In all the cases microsomes used underwent 1 freeze thaw cycle. Calculation of microsomal scalers was performed as described previously (**Equation 2-3, Equation 2-4, Equation 2-5**).

5.3.3. Human jejunum and ileum CL_{int} determination and microsomal binding

Microsomal CL_{int} determination was undertaken with incubations of 40 minutes at 1mg/ml protein concentration, and using combined CYP and UGT cofactors, as described previously in the rat and dog. The reaction was initiated following 5 minute incubation of cofactors at 37^{o}C and shaking at 900 rpm by addition of compound (1μM final concentration). The compounds studied in human intestinal jejunum microsomes (HIJM) were the same 23 as used for the dog, with the exception of cimetidine (**Appendix Table 7-1**). Incubations with human intestinal ileum microsomes (HIIM) were with a reduced set of 8 compounds (7-hydroxycoumarin, buspirone, ipriflavone, midazolam, raloxifene, saquinavir, sildenafil and tacrolimus) due to low microsomal yields. All incubations were in duplicate, and results represent mean observations from incubations on 2 separate occasions.

Measures of fu_{inc} were not undertaken in human intestinal microsomes due to the limited amount of protein, and therefore unless the human fu_{inc} value was available in the literature from microsomes prepared by elution procedures, measures obtained from dog intestinal microsomes at the same protein concentration were used as a surrogate.

5.3.4. Prediction of human intestinal F_G and Fa

Measures of $CL_{int,u}$ were scaled up to measures of $CL_{u,gut}$ (**Equation 3-13**) using mean values of MPPGI scaling factors and regional weights of mean values from 20 intestines of 411 and 319g for jejunum and ileum respectively, as reported in Paine et al., (1997). Predicted F_G based on $CL_{int,u}$ obtained in jejunum microsomes were compared to observed *in vivo* F_G values which were either calculated from *in vivo* p.o and i.v data (as described in **Chapter 3**), or reported previously using the same method (Gertz et al., 2010); the assumption was that proximal jejunum was the site of compound absorption and metabolism. Value of hepatic blood flow was set at 20.7 ml/min/kg (Gertz et al., 2010) for estimation of *in vivo* F_H to calculate subsequently F_G where required.

P_{eff} were predicted using the P_{app} data obtained in the Caco-2 in the absence of transport inhibitors, or from compound physicochemical properties as described previously. The individual permeability data for both input methods are as listed previously in **Table 3-7**. Reported *in vivo* P_{eff} was used for cyclosporine (Lennernas, 2007b). Prediction of Fa were made using the relationship between radius of the intestine and small intestine transit time as performed previously for the prediction in dog, using the transit time of 3.32 h and radius of 1.75 cm (Yu and Amidon, 1999)(**Equation 4-3**). Estimates of CL_{perm} were calculated based on the cylindrical surface area of the intestine (0.66 m^2) using the same radius and an intestinal length of 6 m (Yang et al., 2007; Gertz et al., 2010)(**Equation 3-14**). This is since P_{eff} accounts for surface area amplifications of the fold of Kerkering, villi and microvilli. Predictions of Q_{gut} and F_G were made using a villus blood flow of 18 l/h (Yang et al., 2007) (**Equation 3-15** and **Equation 3-16**).

5.3.5. Data analysis

Scatter plots observed *vs.* predicted F_G were complied in Matlab (2012a). Tests for bias and precision of estimated Fa.F_G (gmfe and rmse) and qualitative zoning of predicted low F_G values were applied as described previously in the rat (**Chapter 3**).

5.4. Results

5.4.1. Human intestinal microsome characterisation

CYP spectrum scan of homogenate and microsomal samples is shown in **Figure 5-1**. Characteristic of the ileum samples (**Figure 5-2B**) was an increase in peak situated a 424 nm and 558nm. Formation of 6β-OH TEST and 4-NP Gluc metabolites is shown for both HIJM and HIIM in **Figure 5-2**. A summary of characteristics of region human intestinal pool CYP and UGT activities and CYP contents is shown in **Table 5-2**. Human intestinal microsomes displayed a similar CYP content in ileum and jejunum microsomes, with slightly increased levels in the ileum. The only major testosterone metabolite observed in human intestinal microsome incubations was 6β-OH TEST. The formation of 6β-OH TEST was however 3.6-fold higher in the jejunum pool. Androstenedione formations and 4-NP glucuronidation was highest in ileum *vs.* jejunum pools (1.91 *vs.* 1.37 nmol/min/mg).

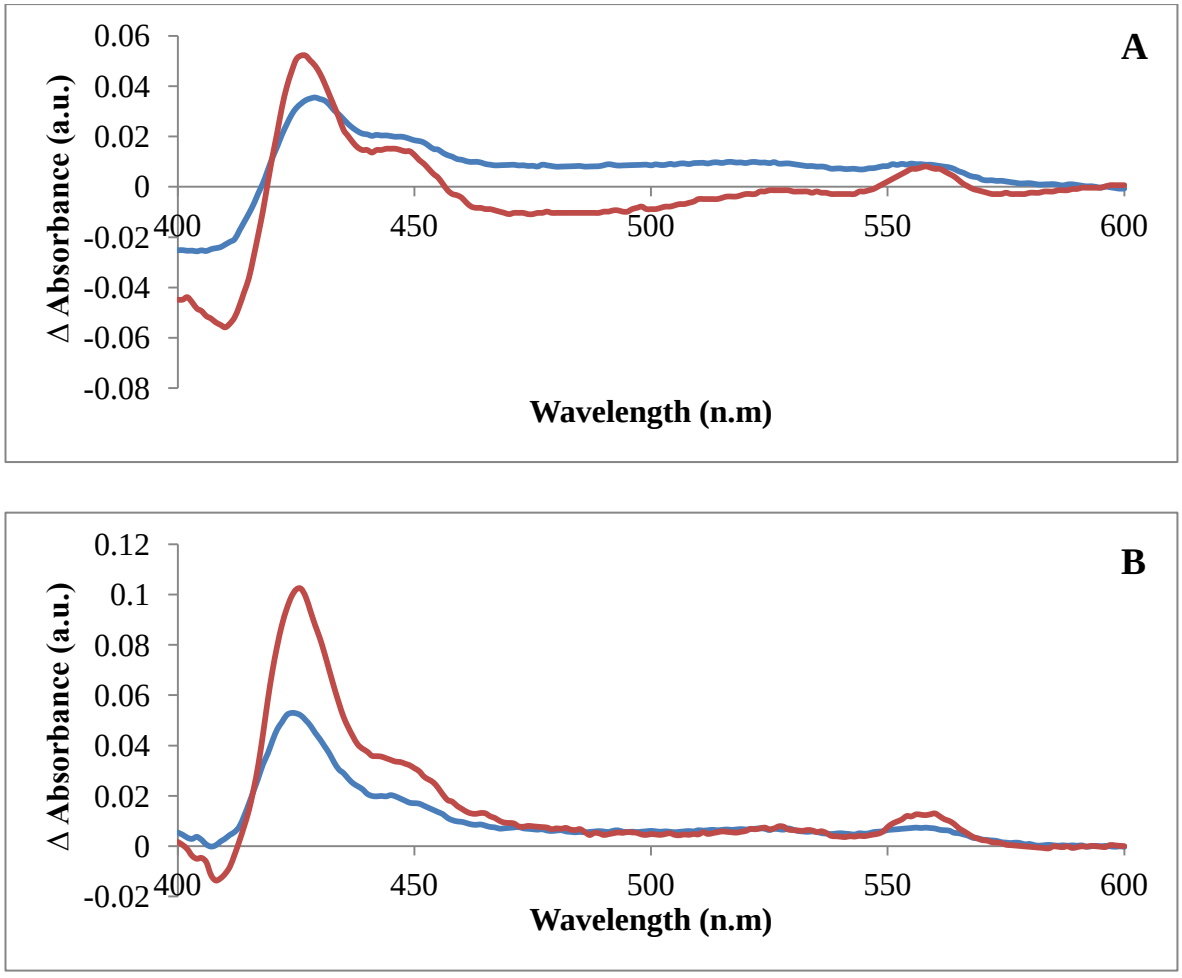

Figure 5-1 CYP wavelength spectrum scan from 600 to 400nm for homogenate (blue) and microsomes (red) prepared from jejunum (A) and ileum (B) intestinal tissue. Data shown represent mean of triplicate scans on 1 occasion.

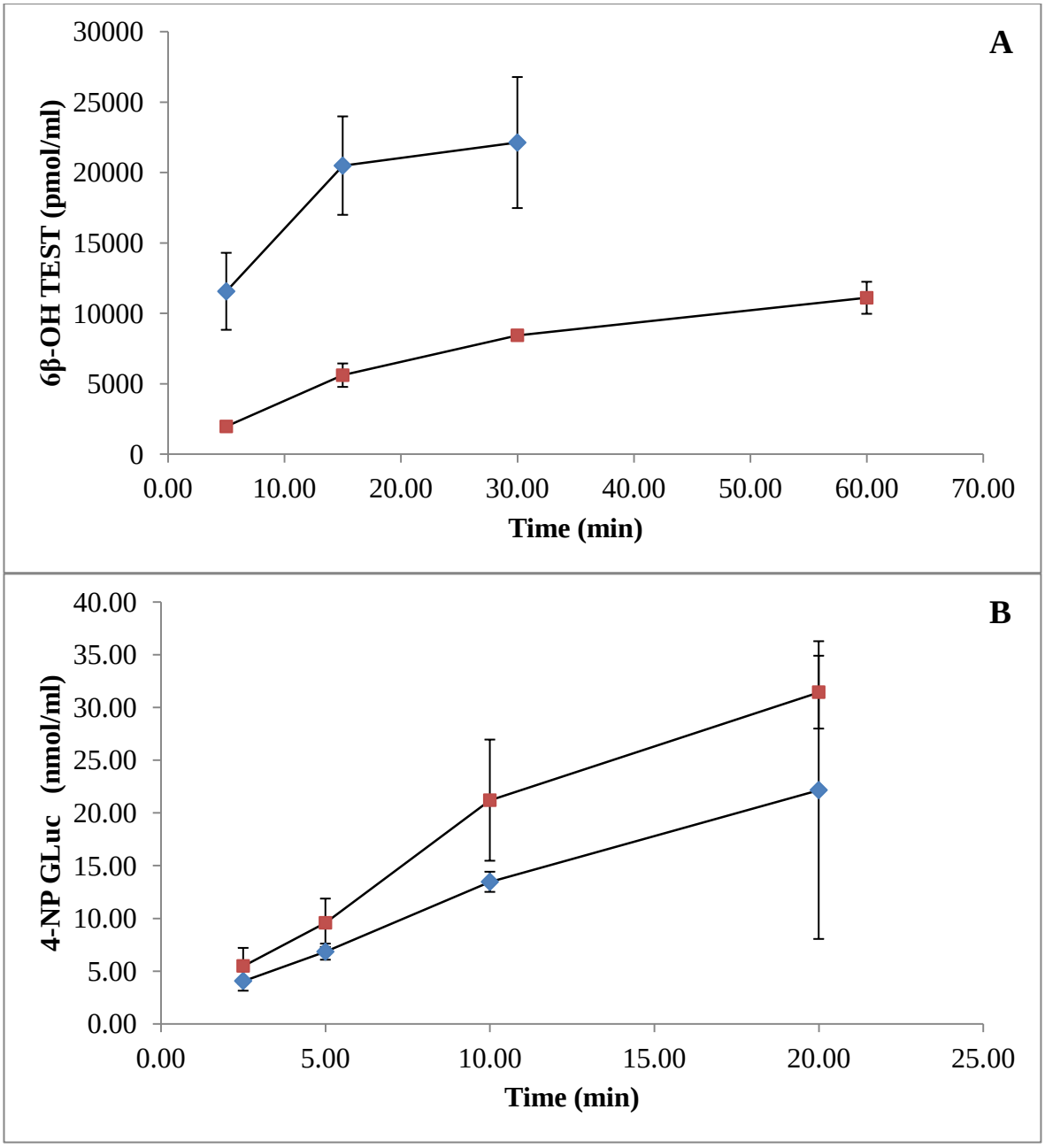

Figure 5-2 Formation of 6β-OH TEST (A) and 4-NP Gluc (B) in HIJM (■) and HIIM (◆). Data represent mean ±stdev of incubations in triplicate on 1 occasion.

Table 5-2 Summary of human mucosal yield, and jejunum and ileum microsomal pools CYP content and maximal 6β-OH TEST and 4-NP Gluc formation rates.

Region Pool	Mucosal yield (g mucosa / g intestine)	CYP Content (pmol/mg)[a]	6β-OH TEST (pmol/min/mg)[a]	Androstenedione (pmol/min/mg)[a]	4-NP Gluc (nmol/min/mg)[a]
Jejunum	0.39	111.4	1366.1	138.98	1.37
Ileum	0.44	138.1	374.2	313.22	1.91

a: Results represent mean of 3 replicates on 1 occasion. All results represent per mg of microsomal protein

Microsomal recoveries and scalars derived from the three microsomal markers for ileum and jejunum microsome pools are shown in **Table 5-3**. Mean recovery in jejunum and ileum pools were similar (36% and 38% respectively). Recoveries were comparable across the microsomal markers especially for CYP and 4-NP gluc, with highest recoveries observed using 6β-OH TEST as a microsomal marker. Scalars were highest in jejunum tissue *vs.* the ileum (6.4 and 3.3 mg/g intestine).

Table 5-3 Microsomal recoveries and scalars using three microsomal markers in human jejunum and ileum pools.

Jejunum Pool[a]				Ileum Pool[b]			
Marker	Recovery (%)	MPPGI (mg/g tissue)	MPPGM (mg/g mucosa)	Marker	Recovery (%)	MPPGI (mg/g tissue)	MPPGM (mg/g mucosa)
CYP Content	28.5	7.8	20.1	**CYP Content**	31.1	3.8	8.6
6β-OH TEST	402	5.5	14.2	**6β-OH TEST**	48.7	2.4	5.5
4-NP Gluc	37.9	5.9	15.1	**4-NP Gluc**	33.2	3.6	8.0
Mean	35.5	6.4	16.5	**Mean**	37.6	3.26	7.3
Stdev	6.2	1.2	3.2	**Stdev**	9.6	0.73	1.7

a: n=3 donors, b: n=2 donors, Stdev: standard deviation

5.4.2. Human intestinal $CL_{int,u}$

The $CL_{int,u}$ values obtained for the dataset of 23 drugs are shown in **Table 5-4**, ranging from 0.1 (pirenzepine) to 2220 µl/min/mg microsomal protein (terfenadine) for HIJM pools, and from 3.31 (buspirone) to 3014 µl/min/mg microsomal protein (raloxifene) in HIIM pools, respectively. Comparison of the same compounds between HIJM and HIIM pools showed that metabolism of CYP3A substrates was the highest in the jejunum (buspirone, ipriflavone, midazolam, saquinavir and sildenafil and tacrolimus) whilst UGT metabolised compounds showed more pronounced metabolism in the HIIM microsomes (7-hydroxycoumarin, raloxifene). The greatest fold difference was observed for raloxifene, where a 39.4-fold increase in metabolism was observed in HIIM relative to data obtained in HIJM. Metabolism of 7-hydroxycoumarin was similar between pools (1.4-fold higher in HIIM). The mean fold difference between HIJM and HIIM for CYP3A compounds was 3.1-fold.

5.4.3. Prediction of human Q_{gut} and Fa

Q_{gut} was predicted for all the compounds investigated using metabolism data obtained in pooled HIJM. Use of P_{eff} values based on Caco-2 data in conjunction with metabolism resulted in predicted Q_{gut} of 0.21 (furosemide) and 11.05 l/h (indomethacin) (**Table 5-5**).

The lowest Fa was also predicted for furosemide (0.28). Out of all the compounds, 87% were predicted to show good absorption (Fa>0.90). Estimates for Q_{gut} using physicochemical based permeability estimates ranged from 0.00 (cyclosporine) and 12.48 l/h (midazolam). Using physicochemical based estimates of Fa, 83% of compounds were predicted to shown good intestinal absorption (Fa>0.90).

Table 5-4 Intrinsic clearance and non-specific binding in HIJM and HIIM

Compound			$CL_{int,u}$ (µl/min/mg microsomal protein)[d]	
#	Name	fu_{inc}[d]	HIJM Pool	HIIM Pool
1	7-Hydroxycoumarin	1.00[a]	131.69	179.97
4	Bisporolol	0.89[b]	0.11	
6	Buspirone	0.84[c]	23.40	3.31
8	Cyclosporine A	0.42[c]	22.69	
10	Diltiazem	0.72[a]	11.98	
11	Domperidone	0.37[a]	35.58	
12	Felodipine	0.19[c]	101.10	
13	Furosemide	1.00[a]	16.21	
14	Indomethacin	0.88[b]	4.62	
15	Ipriflavone	0.40[b]	33.89	22.29
16	Irbesartan	0.79[b]	6.49	
17	Losartan	0.87[b]	13.87	
18	Midazolam	0.69[c]	105.53	40.37
19	Nicardipine	0.16[a]	1813.80	
20	Nitrendipine	1.00[a]	32.49	
21	Omeprazole	0.90[b]	11.24	
22	Pirenzepine	1.00[b]	0.10	
23	Raloxifene	0.15[a]	76.57	3014.32
24	Saquinavir	0.71[c]	1021.87	308.18
25	Sildenafil	0.79[c]	28.08	11.90
27	Tacrolimus	0.33[c]	520.18	360.43
28	Terfenadine	0.03[c]	2219.68	
29	Verapamil	0.57[c]	92.54	

a: in house dog value, b: in house rat value, c: Gertz et al.,(2010)

Table 5-5 Predictions of Q_{gut}, Fa and F_G using estimates based on Caco-2 and physicochemically derived predictions of P_{eff} and scaled $CL_{int,u}$

		Predicted									Observed	
		Permeability					F_G					
Compound		Caco-2			Physicochemical		Caco-2		Physicochemical			
#	Name	Peff cm-4/s	Qgut (l/h)	Fa	Qgut (l/h)	Fa	HJM	HIM	HJM	HIM	FG	Reference
1	7-HC	7.41	8.90	1.00	6.34	1.00	0.30	0.45	0.23	0.37		
4	Bisporolol	1.51	2.99	0.98	3.08	0.99	0.99		0.99		0.96	(Leopold, 1986; Leopold et al., 1986; Le Jeunne et al., 1991)
6	Buspirone	2.13	3.95	1.00	8.12	1.00	0.52	0.95	0.69	0.98	0.21	(Gertz et al., 2010)
8	Cyclosporine A	1.61[a]	3.15	0.99	0.00	0.00	0.53		0.00		0.44	(Gertz et al., 2010)
10	Diltiazem	1.93	3.65	0.99	8.57	1.00	0.66		0.82		0.52	(Hoglund and Nilsson, 1988)
11	Domperidone	2.38	5.65	1.00	2.89	0.98	0.45		0.36		0.28	(Heykants et al., 1981a; Meuldermans et al., 1981)
12	Felodipine	0.89	2.11	0.94	4.61	1.00	0.27		0.27		0.45	(Gertz et al., 2010)
13	Furosemide	0.16	0.37	0.44	0.19	0.26	0.26		0.19		0.87	(Smith et al., 1980; Hammarlund et al., 1984)
14	Indomethacin	12.06	11.05	1.00	4.61	1.00	0.94		0.86		1.00	(Yeh et al., 1982)
15	Ipriflavone	7.03	8.66	1.00	10.71	1.00	0.62	0.86	0.67	0.89		
16	Irbesartan	2.44	4.39	1.00	3.58	0.99	0.82		0.79		0.95	(Kostis et al., 2001)
17	Losartan	0.78	1.67	0.91	1.86	0.93	0.43		0.46		0.70	(Lo et al., 1995)
18	Midazolam	5.04	7.19	1.00	12.48	1.00	0.30	0.74	0.43	0.83	0.51	(Gertz et al., 2010)
19	Nicardipine	4.02	6.24	1.00	1.79	0.93	0.02		0.01		0.23	(Guerret et al., 1989)
20	Nitrendipine	9.32	22.14	1.00	1.83	0.93	0.67		0.30		1.00	(Mikus et al., 1987; Soons and Breimer, 1991)
21	Omeprazole	NV	NV	NV	4.44	1.00	NV		0.75		0.93	(Regardh et al., 1985; Regardh et al., 1990)
22	Pirenzepine	0.12	0.28	0.35	5.06	1.00	0.95		1.00		1.00	(Carmine and Brogden, 1985)
23	Raloxifene	1.41	2.83	0.98	2.48	0.97	0.25	0.04	0.22	0.03	0.07	(Kosaka et al., 2011)
24	Saquinavir	0.61	1.34	0.86	0.02	0.02	0.01	0.07	0.00	0.00	0.18	(Gertz et al., 2010)
25	Sildenafil	5.44	7.52	1.00	2.19	0.96	0.64	0.91	0.35	0.75	0.54	(Gertz et al., 2010)
27	Tacrolimus	8.42	9.47	1.00	0.09	0.13	0.14	0.30	0.00	0.00	0.14	(Gertz et al., 2010)
28	Terfenadine	1.33	2.69	0.98	4.42	1.00	0.01		0.01		0.40	(Gertz et al., 2010)
29	Verapamil	2.36	4.28	1.00	8.57	1.00	0.24		0.39		0.65	(Gertz et al., 2010)

a:Lennernäs et al., (2007b)

5.4.4. Human intestinal regional F_G and assessment of jejunum F_G predictions

Predictions of F_G *vs.* observed *in vivo* of F_G are presented visually in **Figure 5-3**, and measures of prediction bias and success are shown in **Table 5-6**. F_G estimates based on Caco-2 estimates and $CL_{int,u}$ from HIJM resulted in the strongest correlation with *in vivo* data (R^2=0.51, p<0.001 *vs.* 0.42, p<0.002) and the lowest observed rmse (0.24 *vs.* 0.31) *vs.* physicochemical based estimates. Furthermore prediction success was highest, with 67% of compounds with an F_G<0.5 predicted within 2-fold (rmse 0.23 *vs.* 0.29). Overprediction of F_G was observed for buspirone and raloxifene, where as underprediction was observed for saquinavir, nicardipine, terfenadine, felodipine, verapamil and furosemide. A lower number of FP's were observed (20 *vs.*29%), and a slightly increased prediction success of TN's (35% *vs.* 29%). However, incidence of FN's were increased (10 *vs.* 5%), and a slight decrease in TP's was observed (35 *vs.* 38%). Overall TN and TP predictions success of F_G was high (70% in Caco-2 based approaches and 67% in physicochemical based scaling).

Table 5-6 Observation of prediction bias and categorisation of low F_G for observed *vs.* predicted F_G in human jejunum microsomes

Prediction Bias						Categorisation of low F_G					
Physicochemical			Caco-2			Physicochemical			Caco-2		
	n	21		n	20	**Class**	**n**	**%**	**Class**	**n**	**%**
	>2-fold (%)	33		>2-fold (%)	30	TP	8	38	TP	7	35
	<2-fold (%)	67		<2-fold (%)	70	TN	6	29	TN	7	35
	gmfe	0.27		gmfe	0.58	FP	6	29	FP	4	20
	rmse	0.31		rmse	0.24	FN	1	5	FN	2	10
F_G<0.5	n	9	F_G<0.5	n	19						
	>2-fold (%)	56		>2-fold (%)	33						
	<2-fold (%)	44		<2-fold (%)	67						
	gmfe	0.08		gmfe	0.44						
	rmse	0.29		rmse	0.23						

Incidence of $F_{G,<0.3}$, $F_{G,0.3\text{-}0.7}$ and $F_{G,>0.7}$ for physicochemical and Caco-2 based scaling is shown in **Table 5-7**. Correct categorisation was observed for 62% and 65% of compounds respectively for physicochemical and Caco-2 scaling repectively. 67% of compound with $F_{G,<0.3}$ was 67% for both approaches.

Ratio of prediction accuracy is shown in **Figure 5-4**. Overprediction was observed for ipriflavone, losartan and indomethacin. Underprediction was shown for buspirone, and raloxifene. Highest observation of precision accuracy was observed for Caco-2 scaling where 60% of compounds were within 2-fold, *vs.*57% for physicochemical scaling.

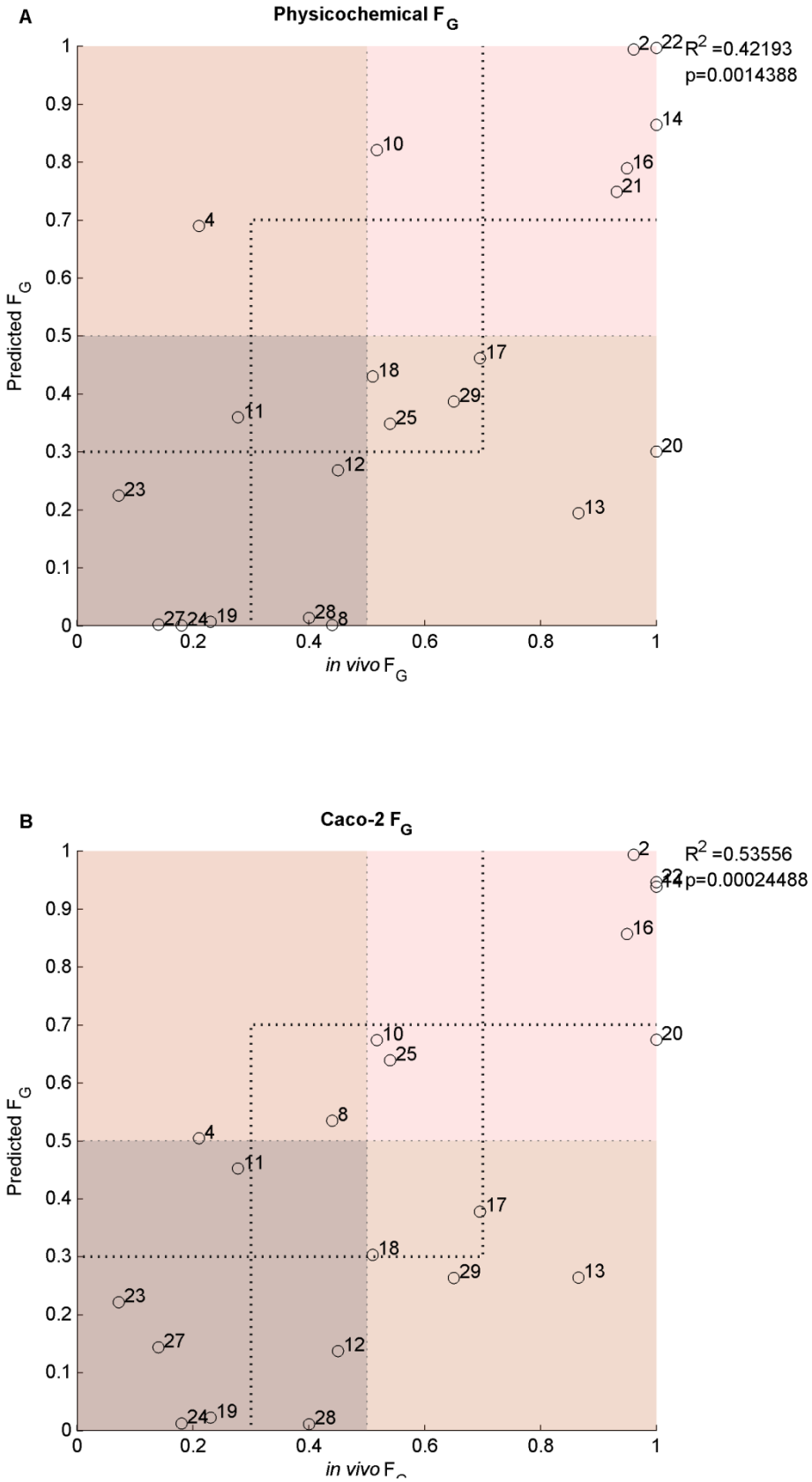

Figure 5-3 Correlation between observed and predicted F_G in human jejunum microsomes using either physicochemical (A) or Caco-2 (B) based permeability estimates.

Compound numbers relate to **Table 5-4**.

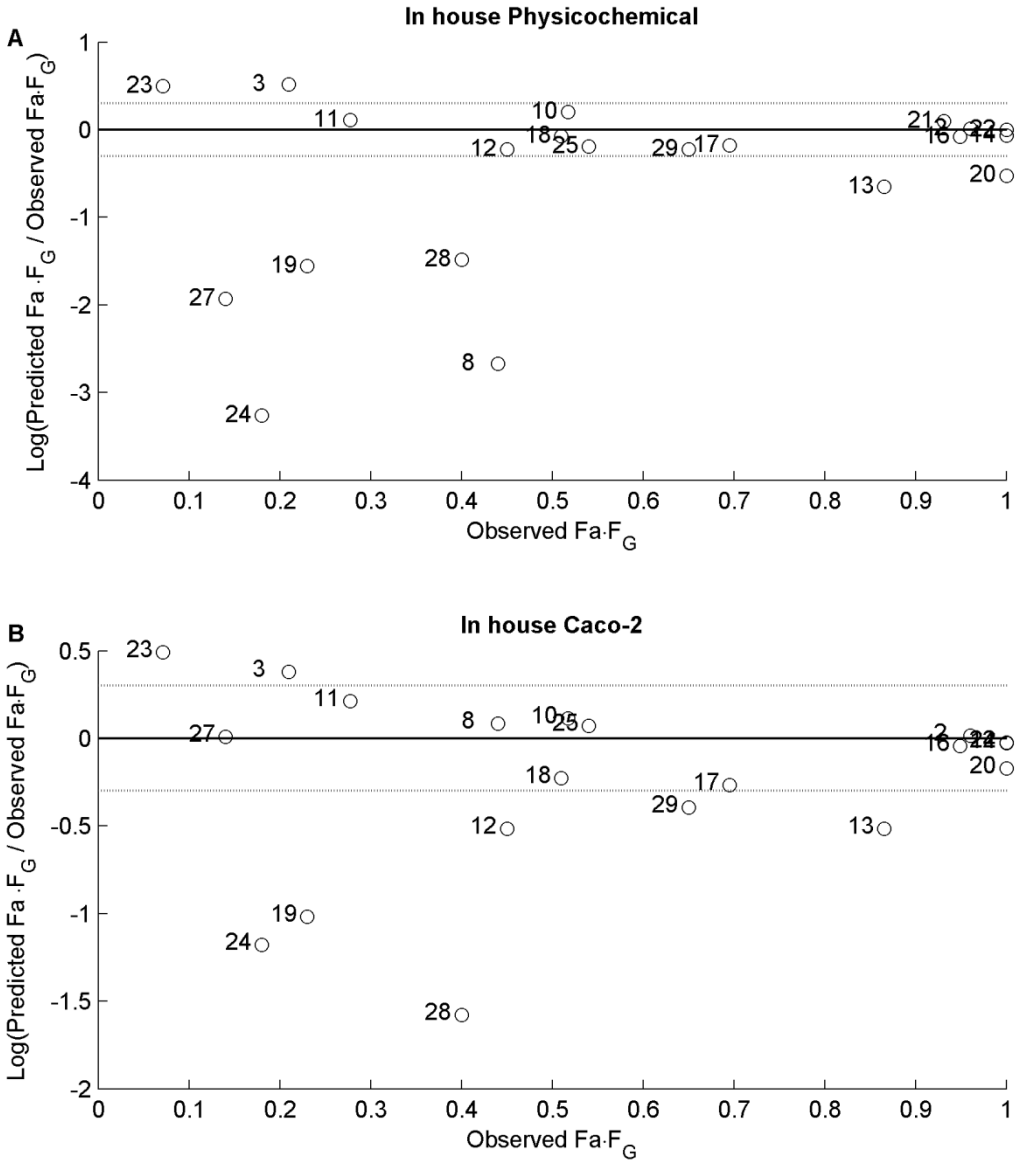

Figure 5-4 Precision of predictions of F_G using physicochemical (A) and Caco-2 (B) based scaling of in vtro rat intestinal metabolic data.

The dotted lines at ±0.3 log units represents 50% underprediction and 100% overprediction precision limits.

Table 5-7 Incidence of $F_{G,<0.3}$, $F_{G,0.3\text{-}0.7}$ and $F_{G,>0.7}$ correct and incorrect categorisation for predicted and observed F_G using metabolism data and either physicochemical or Caco-2 based scaling methodologies.

		Fa.F_G								
		Physicochemical					**Caco-2**				
			Correct		**Incorrect**			**Correct**		**Incorrect**	
	$F_{G<0.3}$		4	19%	2	10%	$F_{G<0.3}$	4	20%	2	10%
	$F_{G\ 0.3\text{-}0.7}$		4	19%	4	19%	$F_{G\ 0.3\text{-}0.7}$	5	25%	3	15%
	$F_{G>0.7}$		5	24%	2	10%	$F_{G>0.7}$	4	20%	2	10%
∑		21	13	62%	8	38%	20	13	65%	7	35%

5.5. Comparison of intestinal metabolism between species

In order to compare intestinal metabolism between species, predictions of E_G are compared from both preclinical species (rat and dog) and human in **Table 5-8**, alongside rank order of intestinal metabolism observed. E_G in the rat was generally highest and ranged from 0.1 (bisoprolol) to 1 (terfenadine and saquinavir). Female dog generally showed increased intestinal metabolism over male dog, ranging from 0.04 (bisoprolol) to 0.99 (saquinavir) and 0.06 (felodipine) to 0.90 (saquinavir) respectively. Human intestinal metabolism rivalled the rat and ranged from 0.05 (pirenzepine) and 0.99 (terfenadine and saquinavir). Saquinavir and terfenadine metabolism was highly metabolised in all species, whilst bisoprolol showed low intestinal metabolism across all the species studied. Midazolam demonstrated comparable metabolism in the dog to human, but lower metabolism in the rat.

Table 5-8 Comparison of predicted E_G in preclinical species and human for 23 compounds investigated across preclinical species and human.

#	Compound Name	Rat	Dog Male	Dog Female	Human	E_G Rank Order
1	7-Hydroxycoumarin	0.75	0.33	0.35	0.70	rat>human>female dog>male dog
2	Bisprolol	0.10	0.11	0.04	0.01	male dog >rat>female dog>human
4	Buspirone	0.40	0.14	0.38	0.48	human>rat>female dog>male dog
8	Cyclosporine A	0.35	0.80[a]	0.70[a]	0.47	male dog>female dog>human>rat
10	Dilitiazem	0.45	0.15	0.30	0.34	rat>human>female dog>male dog
11	Domperidone	NV	0.18	0.28	0.55	human>>female dog>male dog
12	Felodipine	NV	0.08	0.41	0.86	human>>female dog>male dog
13	Furosemide	0.30	0.79	0.81	0.74	female dog=male dog>human>>rat
14	Indomethacin	0.07	0.09	0.06	0.06	male dog>female dog>rat=human
15	Ipriflavone	0.87	0.43	0.66	0.38	rat>female dog>male dog>human
16	Irbesartan	0.48	0.13	0.08	0.18	rat>>human>male dog>female dog
17	Losartan	0.61	0.22	0.32	0.57	rat>human>female dog>male dog
18	Midazolam	0.29	0.65	0.76	0.70	female dog>human>male dog>rat
19	Nicardipine	0.98	0.89	0.95	0.98	rat>human>female dog>male dog
20	Nitrendipine	NV	0.34	0.58	0.33	female dog>male dog>human
21	Omeprazole	0.57[a]	0.35[a]	0.69[a]	0.25[a]	female dog>rat>>male dog>human
22	Pirenzepine	0.49	0.19	0.51	0.05	female dog>rat>>male dog>human
23	Raloxifene	0.98	0.88	0.97	0.75	rat>female dog>male dog>human
24	Saquinavir	1.00	0.90	0.99	0.99	rat>human=female dog>male dog
25	Sildenafil	0.27	0.19	0.21	0.36	human>rat>female dog>male dog
27	Tacrolimus	0.88	0.74	0.83	0.86	rat>human>female dog>male dog
28	Terfenadine	1.00	0.85	0.95	0.99	rat>human>male dog>female dog
29	Verapamil	0.49	0.09	0.13	0.76	human>>rat>female dog>male dog

a: results estimated from physicochemical permeability estimates. All other predictions are based on the metabolism and Caco-2 permeability data generated in the current study, as detailed in previous sections.

Plots displaying estimates of E_G compared between preclinical species and human is shown in **Figure 5-5**. Estimates for the entire compound set show similar correlations in both rat and human, with R^2 values of 0.49, 0.34 and 0.39 for rat, female dog and male dog respectively. The strongest correlation in CYP3A substrates was observed between rat and human predicted values (R^2=0.61, p<0.001), where 70% of compounds were observed within 2-fold (**Table 5-9**). The weakest relationship for CYP3A substrates was observed between male dog and human (R^2=0.26, p=0.08), however 54% of compounds were still within two fold. In general however, the incidence of high metabolism in the dog for CYP3A compounds was lower than in human.

Table 5-9 Comparison of percentage of all compounds studied and CYP3A substrates only within two fold of Human F in rat and dog

	Rat	**Dog (M)**	**Dog (F)**
N All compounds	20	23	23
>2-fold (%)	35.0	39.1	30.4
<2-fold (%)	65.0	60.9	69.6
N CYP 3A substrates	10	13	13
>2-fold (%)	30.0	46.2	23.1
<2-fold (%)	70.0	53.8	76.9

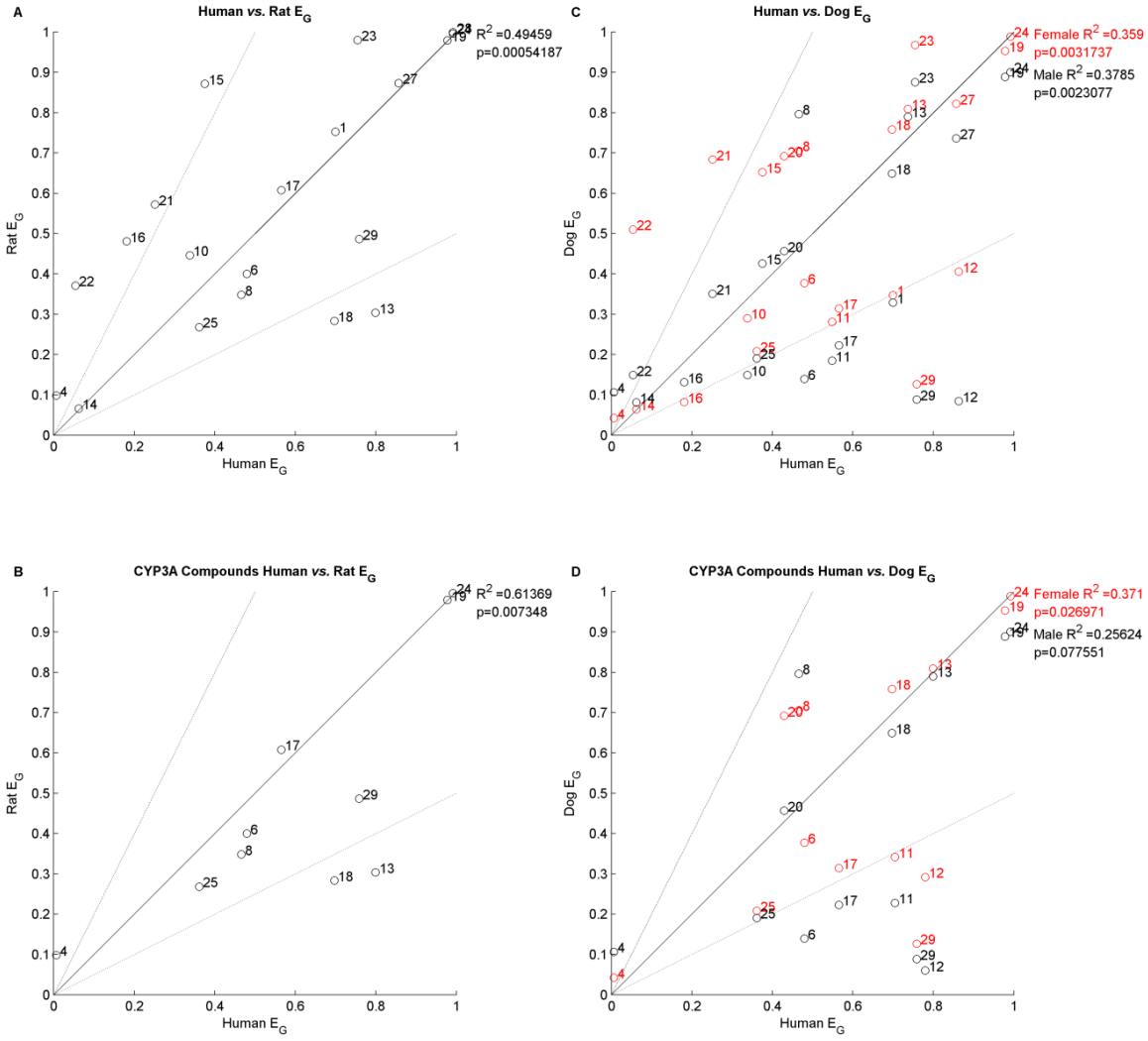

Figure 5-5 Correlations between Human and preclinical species predicted E_G values for the whole set of 20 overlapping compounds in the rat, and 23 in the dog studied compounds (A and C) and CYP3A substrates only (n= 10, B and D).

Rat predictions are shown in panels A and C and dog in B and D. E_G estimates based on HIJM metabolism data and Caco-2 permeability, with the exception of omeprazole in all species, and cyclosporine in dog, where physicochemical estimates were utilised. Solid line represents the line of unity and dashed lines are 2-fold. Compound numbers relate to listing in **Table 5-8**. Percentage within 2-fold is shown in **Table 5-9**.

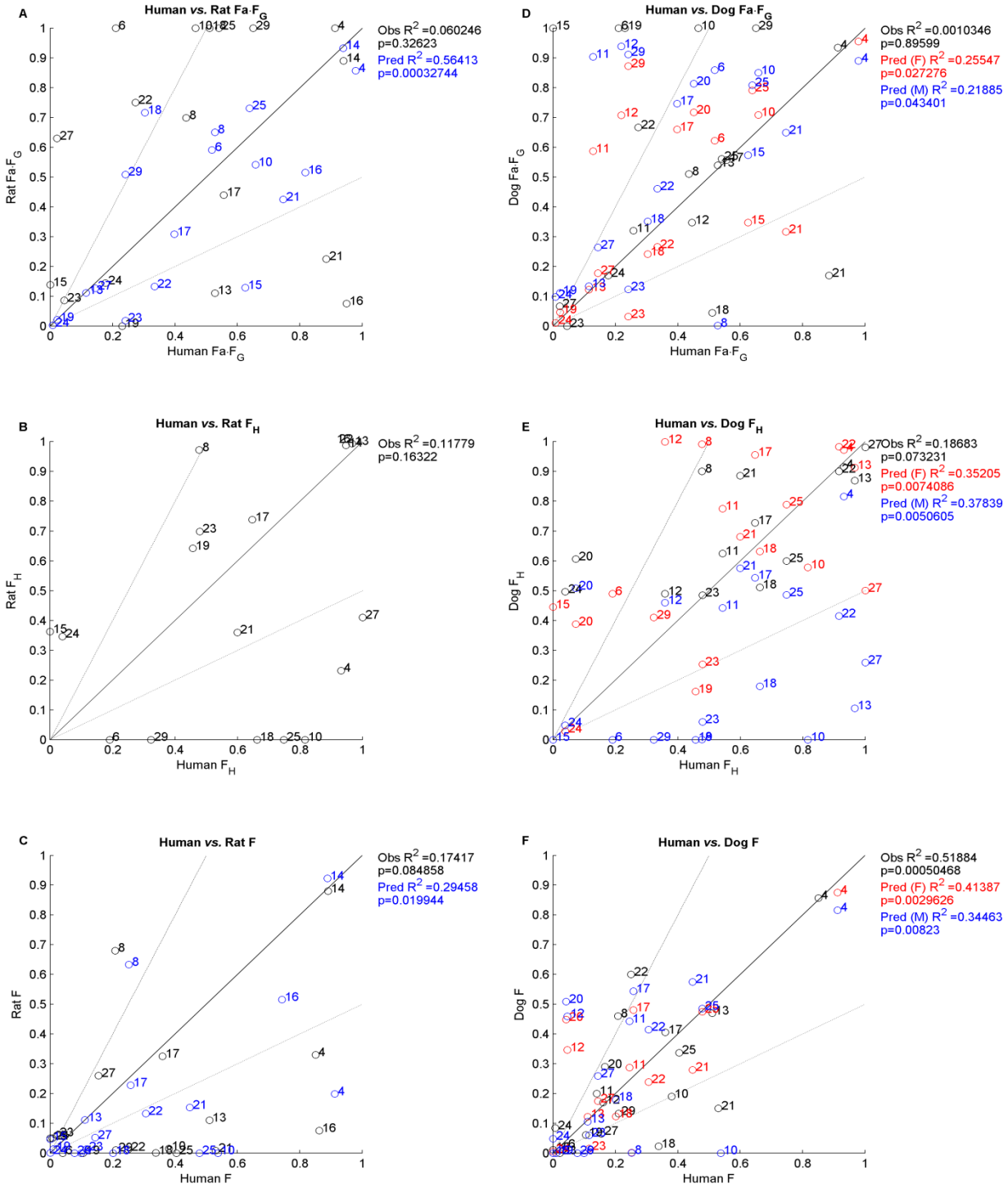

Figure 5-6 Comparison of relationships between observed or predicted values of Fa.F_G, F_H and F in rat (A,B,C) (n=18 compounds) and dog (D,E,F)(n=19 compounds) in comparison to human. Estimates of F were made using *in vivo* F_H estimates.

5.5.1. Relationships between intestinal and hepatic metabolic contributions and absorption to bioavailability between species

Rank order of E_G between species suggested that human showed dominant metabolism for CYP3A compounds. Human CYP3A E_G was highly correlated to the observed E_G in rat

(R^2=0.61, p<0.01). Human *vs.* dog E_G showed weaker relationships than the rat *vs.* human for either all compounds or CYP3A only (**Figure 5-6**). Correlations of both F_H and F were for between the rat and human (R^2=0.16). Stronger relationships in F were observed in the dog (R^2=0.51 for observed F). Predictions of F showed similar % within 2-fold of human, with 29% band 32% for observed *vs*. predicted, and 65% , 52 and 57% for observed vs male and female predicted, respectively (**Table 5-10**).

Table 5-10 Observed and predicted relationships between F in preclinical species and in human in study compounds

	Rat *in vivo*	**Rat Predicted**	**Dog *in vivo***	**Dog Predicted (M)**	**Dog Predicted (F)**
n	14	19	17	21	21
>2 fold (%)	71.4	68.4	35.3	47.6	42.9
<2 fold (%)	28.6	31.6	64.7	52.4	57.1

M: male , F: Female

Correlation of predicted Fa between human and either rat or dog indicated a strong relationship in both species, but an incidence of higher Fa in the dog (**Figure 5-7**).

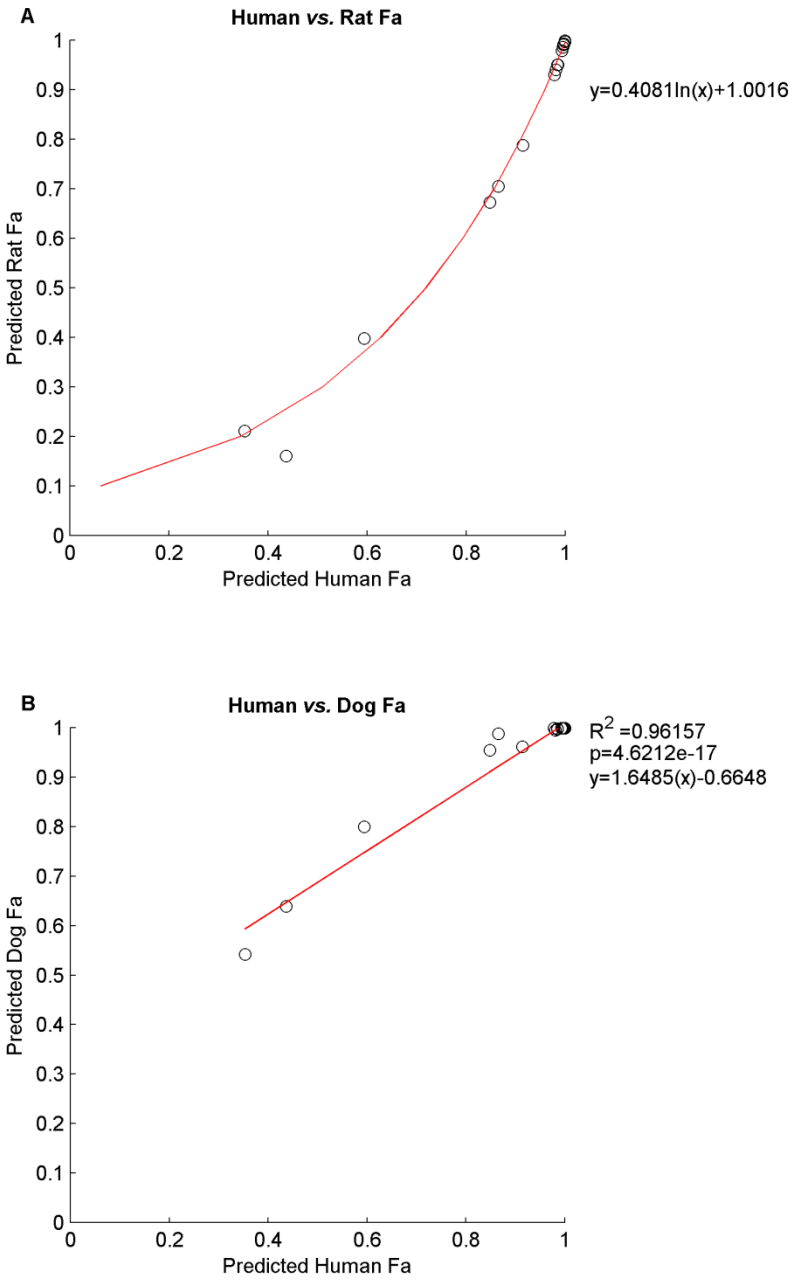

Figure 5-7 Relationship between predicted Fa between human and either the rat (A) and dog (B).

Estimates based on Caco-2 permeabilities and the relationships between P_{eff} and F_a reported in Amidon et al., (1988) for the rat, and Yu and Amidon, (1999) for dog and human. Data shows the Fa estimates in rat dog and human for the same set of compounds with in house permeability data (n=24).

5.5.2. Sensitivity analysis of the Q_{gut} model to system parameters

The sensitivity of the Q_{gut} model using the model input parameters of P_{eff} and $CL_{int,u}$ for each species (**Table 5-11**) is shown in **Figure 5-8**. Compounds with a low permeability displayed a significant increase in E_G over a narrow range of $CL_{int,u}$. Of note, similar distributions were seen for rat and human, however in the dog, for highly permeable compounds (P_{eff} >10 cm/s^{-4}), maximal E_G was around 0.6, where as in human in rat a higher E_G up to 0.8 could still occur.

Table 5-11 Input parameters for Q_{gut} sensitivity analysis for each rat, dog and human

Species	Q_{villi} (l/h)	Scalar (MPPGI)	Segment Weight (g)	Surface Area (m^2)
Rat	0.3	9.6	5.3[a]	0.016
Dog	5.6	4.0[b]	77.1[a]	0.109
Human	18.0	6.4	411.0[c]	0.660

a: proximal 60cm segment, b: female dog scalar, c:jejunum weight from Paine et al., (1997).

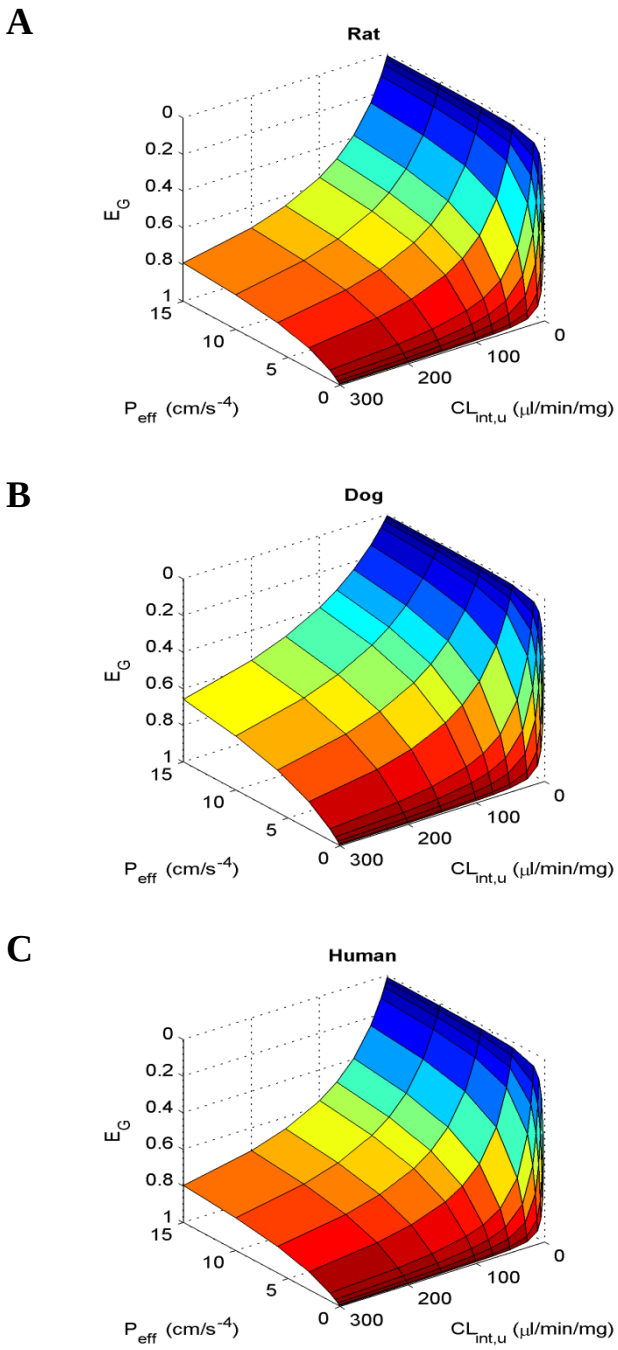

Figure 5-8 Q_{gut} model sensitivity in prediction of E_G towards $CL_{int,u}$ and P_{eff} input parameters for rat (A), dog (B) and human (C).

Species specific model parameters are shown in **Table 5-11**.

5.6. Discussion

Human intestinal microsomes prepared from jejunum and ileum tissue demonstrated regional differences with respect to both intestinal scalars as well as activities. Recoveries of microsomal protein were similar using the 3 microsomal markers, and comparable between intestinal regions (36 *vs.* 38% for jejunum and ileum, respectively). Microsomal scalars were highest in jejunum tissue, approximately 2- fold higher than the distal ileum. Expression of scalars in comparison to literature reported scalars is summarised in **Table 5-12**. The only known reports of corrected microsomal scalar in human intestinal tissue prepared by scraping were similar but showed less gradiation between the intestinal regions (Paine et al., 1997). Scalars for MPPGM for matched regions were similar in the jejunum, however were 3.2-fold lower to those reported in the ileum (Paine et al., 1997; Cubitt et al., 2009) (**Table 5-12**). This confirms earlier observations in the rat that scalars based on yield of mucosa are more sensitive to the methodology employed, and as such extrapolate poorly between labs. It should be noted that, due to the low number of samples (n=3 for jejunum pool, and 2=2 for ileum pool, both prepared on 1 occasion), firm conclusions of regional human scalars or species relationships is limited.

Table 5-12 Comparison of reported and in house measured regional human intestinal scalars

	Region				
Scalar	**Duodenum**	**Jejunum**	**Ileum**	**Weighted Scalar**	**Study**
MPPGI	3.33	3.27	2.83	3.11	(Paine et al., 1997)
		6.39	3.26		This study
MPPGM	14.54	20.49	23.55	20.56	(Paine et al., 1997; Cubitt et al., 2009)
		16.46	7.34		This study

Microsomal CYP content was similar between both jejunum and ileum microsomes. Similar trends in total CYP levels have been observed in human jejunum and ileum intestinal microsomes, where reported median CYP contents were 70 and 50 pmol/mg respectively (Paine et al., 1997). Mean levels of CYP in microsomes prepared in this study were at least 2-fold higher than literature reports (Paine et al., 1997; Paine et al., 2006; Bruyere et al., 2010), most likely related to the differences influenced by the enterocyte elution *vs.* scraping preparation methods (Mohri and Uesawa, 2001; Galetin and Houston, 2006) as described previously.

Similar to the Paine et al., (1997) study, CYP3A metabolite formation was not correlated to total CYP content. Median maximum rate of formation (V_{max}) of the midazolam metabolite 1'-hydroxymidazolam was previously reported to be 426 and 68 pmol/min/mg for jejunum and ileum microsomes, respectively. This represented a 6-fold reduction in activity between the regions. The observed fold difference in 6β-OH TEST formation in this study was 3.6-fold, and both are correlated to the reported reduced CYP3A content in the jejunum *vs.* the ileum (30.6 *vs.* 16.6 pmol/mg) (Paine et al., 1997). Given that total CYP levels were unchanged; this fits with other CYP enzymes being expressed in distal segments of the intestine, e.g. CYP2J2 (Zeldin et al., 1997). Since testosterone is not a CYP2J2 metabolite it was not possible to monitor any changes in activity between the regions.

An increased expression of cytochrome b_5 was reported previously in the ileum *vs.* the duodenum and jejunum (0.25 nmol/mg *vs.* 0.19 nmol/mg in duodenum and jejunum) (Paine et al., 1997) and corresponds to the increased 427 and 558 nm peaks observed in the wavelength spectrum scans observed in this study. Since the measurement of absolute abundance is based on the Omura and Sato (1964) technique, it was not possible to calculate concentration of cytochrome b_5 using the wavelength scans produced in this study.

Activity of HIJM towards 6β-OH TEST formation (1.37 nmol/min/mg) was within the range of reported proximal duodenum/jejunum microsomes prepared via elution methods 0.36 – 5.88 nmol/min/mg (Obach et al., 2001; Gertz et al., 2011). Values were similar to those in observed to those in Gertz et al., (Gertz et al., 2010) (1.84 nmol/min/mg) and 3-fold lower than mean values reported in Gertz et al., (2011), based on commercial intestinal microsomal pool. Of note, similar mean values to this study have been obtained from microsomes prepared from scrapped jejunum microsomes, however considerable variability is observed (1.58 ±1.56 nmol/min/mg, CV 98%) (Prueksaritanont et al., 1996). Similar to the fold differences in 6β-OH TEST formation, a mean 3.1 fold regional difference was observed between HIJM and HIIM for CYP3A compounds, where an increased metabolism was observed in the proximal intestine. It should be noted for one ilum donor, primidone a known CYP3a4 inducer (primidone (Monaco and Cicolin, 1999))was included in the medication, and so caution should be applied. The limited number of samples also limits the abitity to form firm conclusions from this study.

Activities for the formation of UGT1A6 and UGT1A9 (Hanioka et al., 2001b) metabolite 4-NP Gluc have also been previously reported in scrapping prepared microsomes

(0.80±0.68 nmol/min/mg, CV 85%) demonstrating similar variation to their reported 6β-OH TEST formation (Prueksaritanont et al., 1996). Microsomes prepared by elution in this study revealed 4-NP gluc activities of 1.37 nmol/min/mg. Activities were slightly increased (1.4-fold) in the distal ileum microsomes (1.91 nmol/min/mg) suggesting the role of phase II glucuronidation in the more distal regions of the human intestine. Similar trends were also seen for 7-hydroxycoumarin CL_{int} data. However, the difference in CL_{int} between regions was more pronounced in the case of raloxifene (39 fold). Raloxifene is a UGT 1A10 and UGT1A8 substrate, and since UGT1A10 is reported to be selectively expressed in the human intestine and is a major route in the metabolism of raloxifene (raloxifene 4'-β-glucuronide), it is implicated in the observed low bioavailability in human (Jeong et al., 2005). Given the extent of metabolism in the ileum *vs.* the jejunum, and only utilising jejunum data for prediction of F_G in this study, it is likely that this is responsible for the slight overprediction of F_G for this compound (F_G= 0.25 *vs.* 0.07 for predicted *vs.* observed). Greater than 2-fold overprediction of F_G was also observed for buspirone in line with previous observations of underprediction of the hepatic clearance component (Gertz et al., 2010).

Prediction of F_G was well correlated to *in vivo* estimates, with the strongest correlation observed using for Caco-2 *vs.* permeability estimates based on physicochemical properties (R^2=0.51 *vs.* 0.42). Prediction of TN and TP low F_G compounds was high (70%). 65% of compounds were correctly predicted using a stricter F_G classification system, and 60% of compounds assessed on the ratio of observed to predicted F_G based on Caco-2 scaling.

Underprediction of F_G was observed for saquinavir, nicardipine, terfenadine, felodipine, verapamil and furosemide. Since nicardipine and terfenadine are highly bound to microsomal protein, small changes in CL_{int} or erroneous fu_{inc} determination might have subsequently affected the *in vitro* estimate of its clearance. Saquinavir and verapamil are CYP3A inhibitors, and whilst no inhibition was observed in the depletion profiles (**Appendix Figure 7-2** and **Appendix Figure 7-3**) this may bias estimates of F_G. *In vivo* estimates of F_G of furosemide may be compromised by the poor absorption of the compound. Furthermore, saquinavir, verapamil, terfenadine, furosemide, tacolimus and raloxifene are P-gp inhibitors; however, incorporation of the Caco-2 data in the presence of transport inhibitors worsened their F_G predictions. In the case of terfenadine, improved predictions have been observed using PBPK modelling (Gertz et al., 2011). Given the low expression of CYP3A (1% of hepatic) (Paine et al., 2006) and P-gp in the intestine, it is likely that concentrations above K_m in the intestine following oral dosing may lead to

enzyme and transporter saturation *in vivo* which does not occur at the concentrations observed *in vitro*, therefore reducing the effects of CYP3A and P-gp and leading to *in vitro* underprediction of F_G. Furthermore, solubility was not accounted for the in Q_{gut} model, and may account for the underprediction of F_G for saquinavir, verapamil and nicardipine.

Given the small size of the microsome pool (n=3 donors), it is likely that it is not fully representative the true population. Correlations of R^2=0.38 have been observed using total intestinal CYP3A based scaling using midazolam Q_{gut} calibrated Caco-2 F_G estimates (Gertz et al., 2010). Of note, the generated CL_{int} from the n=10 microsome pool in the Gertz et al., (2010) study, intestinal microsomes were on average 3-fold higher for matched compounds (range of 0.7-fold for terfenadine, to 11.6-fold for felodipine). Fold difference in midazolam $CL_{int,u}$ was 3.2-fold. The intestinal microsomes used in study by Gertz et al (2010) were commercial (Xenotech) and prepared from proximal sections of the small intestine, but the exact preparation method used is unknown. From initial work in the rat it is clear that preparation method influences both CYP contents (and therefore activity) as well as value of microsomal scalar (**Chapter 2**), therefore it is interesting that improved correlations were observed by correction of the derived in house (IH) jejunum scalar by the fold difference in activities between the reported study and IH midazolam $CL_{int,u}$ (**Equation 5-1**), without the requirement for midazolam Q_{gut} correction (R^2=0.43). It should be noted that reported 6β-OH TEST formation was only 1.35-fold higher than in this study.

Equation 5-1

$$Study\ corrected\ Scaling\ factor = IH\ Scaling\ factor \cdot \frac{Midazolam\ CLint,u_{IH}}{Midazolam\ CLint,u_{study}}$$

5.6.1. Species differences in intestinal metabolism

Metabolism and permeability data was obtained for an overlapping set of 20 compounds between rat and dog preclinical species and human. These were used for the prediction of intestinal availability and compare the predicted extent of intestinal extraction across species, and asses the preclinical species with the closest prediction to human.

Rank order of E_G between species suggested that human showed dominant metabolism for CYP3A compounds. Human CYP3A E_G was highly correlated to the observed E_G in rat (R^2=0.61, p<0.01). Human *vs.* dog E_G showed weaker relationships than the rat *vs.* human for either all compounds or CYP3A only. Despite this observation however, lower midazolam metabolism was observed in the rat, whilst more comparable metabolism was

displayed in the dog and human. Highest E_G in the dog over rat and human was observed for compounds generally associated with dominant hepatic elimination (e.g. buspirone, indomethacin). Saquinavir and terfenadine, as well as raloxifene which all display high microsomal protein binding were highly metabolised in all species. Bisoprolol displayed low metabolism in all species studied. Given the extent of 4-NP glucuronidation in the rat (**Chapter 3**) it was not surprising that for UGT substrates, greatest E_G was observed of all studied species.

Previous reports of relationships between $Fa.F_G$ in rat *vs.* human from *in vivo* estimates have been poor (Bueters et al., 2013), however it is likely that difficulties in calculating the $Fa.F_G$ component via indirect i.v and p.o. measures play a role, especially for compounds with high hepatic extraction. Relationships between $Fa.F_G$ between species however were generally improved using predictions rather than *in vivo* estimations. A strong relationship was observed in predicted rat *vs.* human. Comparison of the Q_{gut} model sensitivities for rat, dog and human (**Figure 5-8**) highlighted similarities between the human and rat. However, in the dog, the extent of E_G for matched CL_{int} and P_{eff} values was reduced. This low extraction was in line with a general observation rank order of E_G between species.

Correlation of predicted Fa between human and either rat or dog indicated a strong relationship in the rat, but an incidence of higher Fa in the dog (**Figure 5-7**). This is in agreement with previous successful predictions based on rat data (Chiou and Barve, 1998; Cao et al., 2006) and poor relationships from the dog (Chiou et al., 2000).

Improved F_H relationships were observed in the dog using predicted rather than observed relationships to the human. This is again likely to be related to the difficulties in determining F_H and $Fa.F_G$ *in vivo* through indirect i.v. and p.o. dosing for compounds with high hepatic extraction, as previously discussed. In general however, the relationships between $Fa.F_G$, F_H and F between species were poor, especially in the rat. This was expected as the reported F relationships between species are poor (Musther et al., 2013), and relationships between clearance in either dog and rat and human are weak compared to other species, e.g. monkeys (Ward and Smith, 2004; Ward et al., 2005) .

5.7. Conclusions

Microsomal scaling factors were calculated for both jejunum and ileum human intestinal segments. A decrease in both value of microsomal scalar, and activity towards CYP3A activity was observed. UGT activity towards either 4-NP Gluc formation of 7-hydroxycoumarin depletion was marginally increased, however a large increase in raloxifene metabolism was observed, indicating an increase in UGT1A10 expression in the distal intestine. Good prediction of *in vivo* F_G was observed using scaled up values of metabolism in jejunum microsomes. Application of the scalar corrected for testosterone activity between studies appeared to make correction for any differences in preparation. The extent of intestinal metabolism for $Fa.F_G$ was well correlated between rat and human especially for CYP3A compounds.

6. Final Discussion

The role of the intestine in determining the oral bioavailability of drugs has been recognised and extensively studied (Paine et al., 1996; Thummel et al., 1996; Lin et al., 1999). However, the difficulties in establishing reliable *in vitro* tools, scaling factors for IVIVE, and understanding of species differences in intestinal metabolism, have limited both absolute quantification, and translation from observations in preclinical species to man.

The application of methods of microsomal preparation established in the liver to extrahepatic tissues is not straightforward. In the case of the intestine, this has been hindered due to its long and folded structure, its multitude of cell types, and its complex role as a barrier to the external environment (DeSesso and Jacobson, 2001; van de Kerkhof et al., 2007b; Thelen and Dressman, 2009). However, through the combined understandings of the impact of scraping or elution of enterocytes, the action of intestinal proteases on degradation of CYP enzymes (Komura et al., 2002), the "tough" enterocytic structure and its implications for homogenisation (Lindeskog et al., 1986), and the effect of contaminants of mucus and no-enterocytic cell types (Hulsmann et al., 1974a; Lin et al., 1999), progress on microsomal preparation has been made. In this study, an optimised method was developed, analysing key steps in enterocyte elution and microsome preparation, focusing principally on enterocyte incubation conditions, homogenisation intensities and buffer constituents. Intestinal microsomal scaling factors were obtained in preclinical species and human, accounting for regional differences. In the dog, comparison was also performed to hepatic scaling factors obtained in the matched animals. In addition, metabolic activities of intestinal microsomes of different species were assessed using the same drug set. Predictive success of generated metabolic data was investigated by integrating obtained metabolic data with generated permeability data in Caco-2 and comparing to collated or in house obtained *in vivo* estimates of $F_{G.}$

6.1. Intestinal microsome preparation: Establishing methods and reproducibility

The rat was initially selected as a source of intestinal tissue in order to optimise microsomal preparation considering the ease of access and the extent of comparative literature data available for quantitative comparisons (Dawson and Bridges, 1981; Emoto et al., 2000; Takemoto et al., 2003; Bruyere et al., 2009). During the optimisation process in the current study two main findings were apparent with respect to the yields of both protein and enzymatic content. Firstly, microsomal recoveries, scaling factors and CYP levels in intestinal microsomes are primarily influenced by the initial enterocyte

preparation method. Secondly, the overall protein yields are affected by the degree of homogenisation of the sample (**Chapter 2**). Previous reports had highlighted the advantage of the utilisation of elution techniques over the use of scraping of the intestinal tissue since this resulted in increased CYP activities (Mohri and Uesawa, 2001; Galetin and Houston, 2006). This finding was also evident in the current analysis, as CYP3A activity was reduced in microsomes prepared by scraping compared to elution, although data were only available for a single batch of rat intestinal microsomes (**Chapter 3**). In line with analogous comparisons in human intestinal microsomes (Galetin and Houston, 2006), alternative CYP pathways were less susceptible to damage using scraping techniques. UGT activity also appeared to be unaffected.

The final essential stage of the intestinal microsomal preparation prior to its use in metabolic stability studies in rat, dog and human was to clarify the roles of glycerol and heparin in microsomal preparation, and ultimately to ensure reproducibility of the method. Mucus is an important aggregator of ingested material in the intestine, however, it impedes microsomal preparation (Stohs et al., 1976). Heparin added in the initial preparation procedure aided both enterocytic isolation and helped remove mucus contamination. Its use in later stages of the preparation interfered with appropriate microsomal pellet formation. Glycerol addition resulted in mean increases in CYP content as observed previously (Stohs et al., 1976), however at the expense of method reproducibility. Given that reproducibility of the method was key for understanding intestinal metabolism with increased confidence, it was important to establish the reliability of matched preparations. Good reproducibility and low variation in activity and in microsomal scalars was demonstrated using two pools of intestinal microsomes produced in the rat. Furthermore, validation of the CYP and UGT cofactor approach enabled greater utility for assessing both CYP and UGT mediated activites and allowed for sequential metabolism (e.g. amitriptyline).

6.2. Species differences in intestinal microsomal recoveries and scalars

In the case of the liver, significant work has been undertaken in order to establish scaling factors for human and preclinical species using correction for losses experiments (Houston, 1994). For example, human estimates of liver scalars are established on covariate analysis of 108 livers (Barter et al., 2007). In contrast, in the human intestine, only one principle study has identified scalars through correction for losses from 20 donors (Paine et al., 1997; Paine et al., 2006). This however is based on the less optimal scraping preparation procedure. Estimates for the dog intestine are only recently available, from 4 donors

(Heikkinen et al., 2012). Rat intestinal values based on corrections for losses in microsome preparation were not available prior to this study.

This was the first known study to collate values of intestinal scalars from rat, dog and human within the same lab. Correction for losses in rat intestinal microsomes was achieved using CYP as a specific microsomal marker. However, pools utilised in dog and human intestinal tissues were smaller than that of the rat. Therefore, in order to increase confidence in values of intestinal scalars in dog and human, two additional activity markers were measured in homogenates and microsomes of testosterone metabolite formation, and 4-NP glucuronidation, in addition to CYP content.

Mean intestinal microsomal recoveries were similar in rat and human, as shown in **Table 6-1**. Recovery in dog intestine was low, in agreement with previous studies (Heikkinen et al., 2012), most likely related to an increased content of mucus in the intestine. This is probable, since similar recoveries were observed in rat when no heparin was included to remove mucus. Expression of mucus secreting goblet cell expression or basal mucus levels have however not knowingly been compared between species.

Table 6-1 Summary of intestinal scalars in rat, dog and human proximal intestine and dog liver.

	Recovery (%)		MPPGT (mg/g)	
Species	**Intestine**	**Liver**	**Intestine**	**Liver**
Rat (n=18)	33.1 ± 7.9		9.6 ± 3.5	
Dog (M) (n=3)	18.7 ± 3.8	55.4 ± 14.1	6.9 ± 3.6	48.9 ± 11.8
Dog (F) (n=3)	21.1 ± 7.4	58.9 ± 9.7	4.2 ± 2.1	38.7 ± 6.8
Human (pool=3)	35.5 ± 6.2		6.3 ± 1.2	

MPPGT: microsomal protein per gram tissue.

Recoveries in liver were high compared to the intestine, in matched liver samples for 3 male and 3 female dogs in which microsomes from the proximal intestine were also prepared (**Table 6-1**). Values of liver microsomal scalar in the beagle dog were comparable with previous observations where corrections for losses were applied (Baarnhielm et al., 1986; Smith et al., 2008; Heikkinen et al., 2012). Reproducibility between separate operators on liver samples from the same animal in this study was high (CV 20%), suggesting low inter-operator variability. Weighted mean of combining the

results from this study and these previous studies reveals MPPGL scaling factors of 47.7 (n=12), 38.8 (n=10), and 43.7 (n=22) mg/g for female, male and mixed populations.

This study represents the largest analysis to date of dog liver and intestinal scalars from the same animal (n=6). Values of microsomal scalar observed in the proximal intestine and liver demonstrated a strong positive correlation (**Figure 4-6**), and were not influenced by sex. This relationship therefore has potential for forming a basis for making population estimates and incorporating variability for intestinal scalars based on known population liver scaling factors. Such a relationship was not observed in a smaller pool of 4 dogs using matched liver and intestinal tissue, but this may be related to differences in the elution preparation methods, and the fact that intestinal tissue was shipped overnight rather than prepared fresh on the day of removal (Heikkinen et al., 2012).

Regional distributions of intestinal scalars were studied in both the dog and human. Recoveries in female segments of dog intestine were uniform. However, scaling factors varied from segment to segment, increasing in the first three proximal segments of the dog intestine. Values in the distal segment were comparable to the first segment of small intestine (**Table 4-6**). Whilst these values are on average 2-fold lower on a gram of tissue basis to the only other literature study, identical regional distributions have been observed in mean regional scaling factors in both male and female dogs (Heikkinen et al., 2012).

Whist values of human intestinal microsome recoveries were higher than observed in the dog, similarly, recoveries were observed to be identical in the ileum compared to the proximal jejunum (**Table 5-3**, **Table 6-1**). Values of scaling factors were however 2-fold lower in the distal small intestine. Reports of human corrected intestinal scalars in 20 donors using intestinal microsomes prepared via scraping were almost 2-fold lower in to values observed in this study for the jejunum, but similar to ileum values. In the Paine et al., (1997) study, distribution of microsomal scalars was more uniform along the intestine. The results from this study are limited in terms of pool size (n=3 for jejunum and n=2 for ileum) and the small size of the segments utilised (circa. 5-10cm) *vs.* microsomes prepared from the whole intestine (Paine et al., 1997). Furthermore, it is possible that a reduction in values of microsomal protein are reduced with age, analogous to reported values of liver microsomal scalars (Barter et al., 2007). In this study, jejunum microsomes were prepared from an age group or 36-43 years old, whilst ileum microsomal donors were 77-78 years old. It should be notes that using MPPGM, the fold difference was 2.2 fold reduced in ileumj samples *vs.* jejunum.

6.3. Validity of intestinal microsomes for intestinal scaling

The validity of intestinal microsomes compared to alternative *in vitro* approaches, e.g. use of intestinal slices has been brought into question as an *in vitro* tool to describe *in vivo* intestinal metabolism (Martignoni et al., 2006). For example, microsomal activity scaled up to per mg of intestinal protein level has been reported to show significantly lower metabolism than intestinal slices for the same dataset (Martignoni et al., 2006). However, in this case, whilst comparison of homogenate and microsomal protein were used to provide a microsomal scaling factor, no correction for losses based on a microsomal specific marker was applied, meaning that the total homogenate protein measurement contained non microsomal protein. Application of mean recovery (33%) in rat from this study from the microsomal marker CYP, whilst not being specific for this studies method of preparation, made a much more comparable outcome. Furthermore, as demonstrated in this study, extrapolation of total intestinal metabolism can be applied from microsomal data to make *in vivo* estimates of E_G. Successful applications have also been applied to make F_G predictions in either CYP3A or UGT compounds using enzyme abundance or reported microsomal scalars, respectively (Cubitt et al., 2009; Gertz et al., 2010)

In this study, metabolism data obtained in intestinal microsomes from selected compounds were extrapolated in the rat, the dog and human using the derived microsomal scalars. Compounds in each set were chosen on the basis of varying degrees of intestinal metabolism, and their varied physicochemical properties and various routes of metabolism. A total of 20 overlapping drugs were studied in all 3 species in order to make comparisons of intestinal metabolism between species, making this the largest known comparison of E_G in preclinical species and man within the same lab.

6.4. Species differences in intestinal metabolism

In the rat, the main metabolites observed were 6β-OH TEST, 16α-OH TEST, 16β-OH TEST and androstenedione. These corresponded to the activities of CYP3A (6β-OH TEST), and CYP2B and CYP2C (16α-OH TEST, 16β-OH TEST and androstenedione). These corresponded to observed protein expression in Wistar rats (Mitschke et al., 2008), where CYP2B expression is reported to rival CYP3A (Mitschke et al., 2008). Similar activities were observed in commercially available HW intestinal microsomes, except that androstenedione activity was reduced. Activity towards testosterone in commercially available SD rat intestinal microsomes was similar, although 16α-OH TEST activity was almost 2-fold higher than the commercial HW microsomes, most likely related to differences in CYP2C activities between the strains. This was in line with reported CYP2C

activity observed in SD intestinal microsomes (Sohlenius-Sternbeck and Orzechowski, 2004). UGT activity towards 4-NP was similar in both strains, but lower than in house prepared microsomes.

Activity towards testosterone metabolite and 4-NP Gluc formation was performed in all species in order to characterise each species in the same lab using the identical preparation method. Previously, comparisons between species have been based on cross study comparisons, and as such were limited by the differences in preparation techniques employed. In contrast to the rat, the main testosterone metabolite formed in dog and human intestinal microsomes was 6β-OH TEST, corresponding to CYP3A activity. Activity in DLM showed activity of 16α-OH TEST formation corresponding to CYP2B which rivalled CYP3A 6β-OH TEST formation, highlighting the different enzyme activities between organs.

Activity of CYP and UGT was the highest in the dog liver, and similar between both male and female individuals. However, activity of 6β-OH TEST and 4-NP gluc in the dog intestine was highest in the female *vs.* male, perhaps indicating a greater role of the intestine in metabolism in the female dog. In both male and females, normalisation of $CL_{int,u}$ in liver and intestine for a broad range of CYP3A compounds by either reported CYP3A abundance (Heikkinen et al., 2012) or 6β-OH TEST formation in the liver or intestine for either male or female respectively, demonstrated a strong positive correlation (**Figure 4-9** and **Figure 4-10**). Good correlations have been previously observed in human liver and intestinal metabolism normalised of CYP3A abundance (Galetin and Houston, 2006; Gertz et al., 2010), and therefore application of scaling metabolism based on CYP3A abundance has been applied successfully (Gertz et al., 2010). However, care must be taken when using this scaling approach since there are differences in metabolic activities between the organs, (e.g. CYP2B in the dog liver), which mean this approach is not applicable for compounds with differing metabolic routes of elimination unless the compound is known to only be a CYP3A substrate.

Mean 6β-OH TEST activity in the human jejunum microsomes was the highest of all species studied, although similar activity was observed in the female dog intestine (**Figure 6-1A**). A 5-fold higher activity was observed in human *vs.* rat, as has been previously observed using intestinal slices (25 pmol/min/mg protein vs 107 pmol/min/mg protein) (Martignoni et al., 2006; van de Kerkhof et al., 2006). Androstenedione formation was highest in the rat compared to human. This is likely to be realted to the dominant role of the cyctoslic enzyme 17β-Hydroxysteroid dehydrogenase (van de Kerkhof et al., 2006)

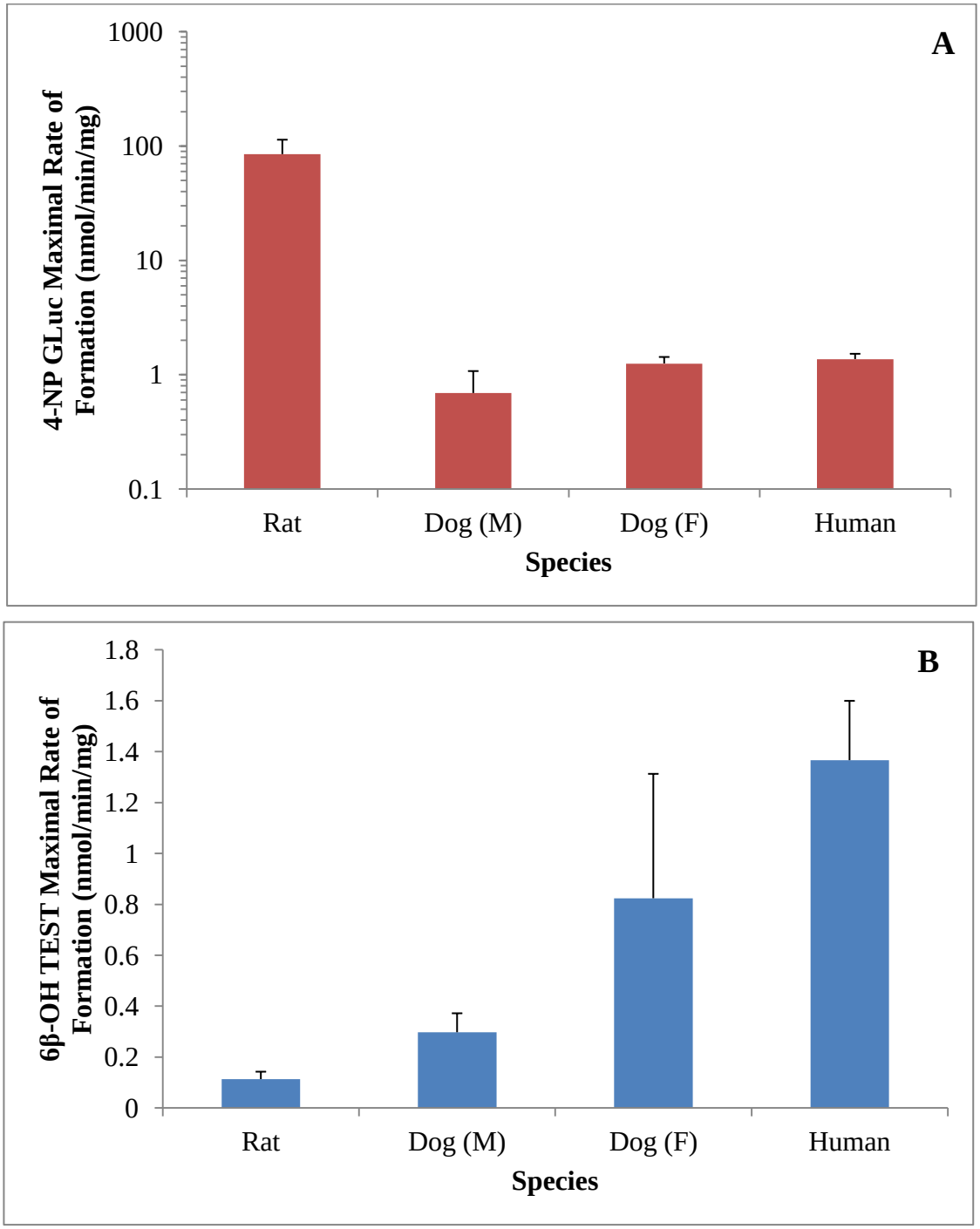

Figure 6-1 Species differences in CYP 6β-OH TEST (A) and 4-NP Gluc (B) maximal rate of formation in RIM, male and female segment 1DIM and HIJM

which is not present in microsomes. Androstenedione formation was not quantifiable in the dog. Activity of 4-NP glucuronidation was similar in human jejunum microsomes and segment 1 in both the male and female dog (**Figure 6-1B**). However, the dominant role of UGT in the rat intestine was indicated by the significant activity of 4-NP Gluc formation which was around 70 fold higher than in the dog and human (**Figure 6-1B**). The differing importance of other enzyme routes of CYP (e.g. importance of CYP2B as well as CYP3A)

and UGT elimination in the rat were reflected in the poor correlations between E_G rat and human, in line with previous observations (Cao et al., 2006; Bueters et al., 2013). However, when only CYP3A eliminated compounds were selected, the correlation was significantly stronger (**Figure 5-5**), suggesting good prediction of human E_G from the rat for this category of compounds.

In all species, overprediction of F_G was observed for compounds with high hepatic clearance, and this trend was particularly evident in the dog. This in part highlights the limitations of the indirect approach for estimating intestinal metabolism, since high hepatic clearance may mask the intestinal component. Greater confidence of *in vivo* $Fa.F_G$ estimates has been achieved in the rat using cannulation of the portal vein (Kuze et al., 2009; Matsuda et al., 2012). For example estimates of midazolam F_G in the rat are improved. Estimates of indomethacin and raloxifene were similar to those derived from cannulation based methods, and most likely due to the low hepatic contributions which reduces the masking of the intestinal component. Therefore, a cannulation based approach would only be recommended for drugs which display high hepatic clearance, since this is limited in its applicability to routine high throughput application in drug development programs.

6.5. Prediction success of Q_{gut} scaling of intestinal metabolism

Extrapolation of rat intestinal metabolism to estimate F_G demonstrated good correlation, with low (30%) CV between the 2 pools using either physicochemical or Caco-2 based permeability estimates for Q_{gut} scaling. In general, estimation of P_{eff} based on physicochemical properties was limited by the PSA of the compound. For example, cyclosporine had a very low predicted P_{eff} *vs.* observed *in vivo*. Therefore, caution should be applied when utilising physicochemical based P_{eff} for large PSA (>100Å) compounds, in agreement with previous observations (Gertz et al., 2010). Prediction of F_G based on Caco-2 (either Q_{gut} or ADAM model in dog) demonstrated the strongest success in the rat, dog and human. In general in all cases, worst estimates were observed for compounds with low F_G. Whilst general over and underprediction was reduced using the ADAM model, the approach requires a greater input of data more approapriate to later stage development of the drug, where as the Q_{gut} approach offered a more screening approach to F_G estimation.

PBPK modelling of intestinal metabolism is in its infancy especially with regard to preclinical species, however with increasing knowledge on enzyme expression and distributions through emerging MS based measures of enzyme abundance (e.g. MRM MS),

and application has shown improved estimations of intestinal metabolism and F in the dog (within 1.5-fold) (Heikkinen et al., 2012; Heikkinen et al., 2013). However, the number of compounds studied was low, and the observed range in was biased towards compounds with high F_G and so the limits of the model have not been fully tested and therefore requires further validation. Emerging technologies (e.g. QconCAT) (Ohtsuki et al., 2012) may also help fill the gaps in terms of both enzyme and transporter intestinal abundance, as well as in other tissues, and lead to increased confidence in PBPK scaling strategies.

Underprediction of intestinal metabolism was generally observed for 3 sets of sometimes overlapping compound properties: P-gp substrates, CYP3A inhibitors and high microsomal protein binding. In the case of high microsomal binding, small changes of CL_{int} or fu_{inc} would make large differences in E_G estimates, making predictions for this class of compounds unreliable. For example, by only comparing raw estimates of CL_{int}, when the 2 pools were compared in the rat, estimates of E_G for compounds with a fu_{inc} <0.3 *vs.* >0.3, CV was 35% and 18%, respectively.

The incubation protein concentrations used in this study were low and incubations short (maximum 40 minutes), as such that enzyme inhibition was not observed over the time course of the depletion experiments. However, with regard to the P-gp substrates and CYP3A inhibitors (e.g. saquinavir, nicardipine, raloxifene), the limitations of the Q_{gut} model are that is a minimal model, and as such unable to accommodate the impact of time or mechanistic based inhibition, or furthermore saturation of either enzymes or transporters which may occur *in vivo*. Furthermore, the impact of low P_{eff} (e.g. as a result of P-pg efflux) can have a significant effect on E_G over a narrow range of change in CL_{int} (when CLint is low)(**Figure 5-8**). Therefore, best practice would be to utilise data from cellular permeability data in the presence of transport inhibitors to get a raw measure of passive cellular permeability. Furthermore, this would limit the impact in differences in transporter expression in the cellular model *vs.* the respective species studied. However, for the compounds in this study which underwent P-gp transport (e.g. saquinavir, raloxifene), the observed $CL_{int,u}$ was already high, meaning that estimates of *in vivo* F_G were low , and therefore that there was minimal change in E_G prediction, in agreement with results from a Q_{gut} sensitivity analysis (**Figure 5-8**). Of note, for compounds with with higher expected F_G (e.g. 0.32 for terfenadine), improved predictions have been demonstrated using a PBPK approach towards prediction human intestinal metabolism by incorporating regional absorption (Gertz et al., 2011).

It should be noted that whist solubility was high for the majority (60% of measured compounds) of compounds studied (**Appendix Table 7-7**), it was observed to be low for terfenadine, verapamil, simvastatin, raloxifene, nicardipine and ipriflavone. This was not modelled in the dog and was not possible to consider using the Q_{gut} model in all species, and may also be a reason for the poor prediction of *in vivo* F_G observed in these species. More comprehensive modelling taking into account solubility may improve *in vitro* predictions for these compounds and requires further investigation.

The use of the Q_{gut} model as a categorisation indicated a high degree of success. In the rat 82% of compounds were correctly allocated with $Fa.F_G$ of either TP or TN. 70% F_G correct allocation was observed in human, and 71% in dog. This therefore has significant application as a screening tool in early compound development, especially when there is limited data available for reliable PBPK scaling approaches.

6.6. Regional intestinal activity

In the dog, rather than a multiple pool approach from the same region as applied in the rat, the regional variations in scaling factors and activity were assessed (**Chapter 4**). Therefore, in order to cross validate values of microsomal scalars, multiple microsomal markers based on CYP content and CYP and UGT activity for correction for losses were applied, and were highly reproducible.

Regional differences in dog intestinal segments indicated that whilst mean CYP contents were relatively uniform, activities differed dramatically. Highest CYP activity in the female intestine was observed in the proximal first and third segments, whilst lowest activity was observed in the final distal segment. These reflected activity gradients analogous to those previously reported, with an increase in CYP activity until the third proximal region, and a decreased activity in the distal small intestine (Heikkinen et al., 2012). Reported expressions of CYP3A12 and CYP211B content also follow these gradient patterns in the dog intestine (Heikkinen et al., 2012); however, in this study only CYP3A seemed the major CYP enzyme in terms of testosterone metabolite formation. Regional activities towards UGT substrates and the probe 4-NP suggested a general distal decline in UGT activity across the regions studied.

In contrast to the dog, activity towards 4-NP glucuronidation and observed depletion of 7-hydroxycoumarin was marginally increased in the human ileum compared to jejunum by similar proportions. However, the distal UGT activity in human ileum intestinal microsomes was significantly higher compared to the jejunum for raloxifene, and was the

likely reason for the underprediction of E_G in human using only jejunum metabolism data. Given that this compound is a P-gp substrate and has low aqueous solubility, it is likely therefore that it may be present at more distal regions of the intestine. This would furthermore coincide with a very low observed bioavailability of raloxifene in human (Jeong et al., 2005). Reports of human UGT activity regional gradients are conflicting, however finding from this study suggest that expression of certain isoforms (e.g. UGT1A6 and 1A9) may be more uniform, whilst expression of UGT1A10 may be increased distally. These conclusions are however a limited reflection of the general population in light of the relative disease state of the donors, as well as the limited number of samples and requires further investigation using a larger number of UGT substrates.

In the human, analogous to the dog, total measured CYP content was uniform between the proximal and distal small intestine, however CYP3A activity was decreased distally. This therefore suggests the expression of alternative CYP enzymes in the distal intestine in both species. For example, CYP2J2 has been reported in distal regions of the human small intestine (Zeldin et al., 1997), however, it was not possible to monitor activity of this CYP using the testosterone metabolite formation assay or using the substrates investigated in this study.

6.7. Prediction of oral bioavailability in preclinical species and man

Comparison of the Q_{gut} model sensitivities for rat, dog and human (**Figure 5-8**) highlighted that whilst similarities are observed for the human and rat, in the dog, the extent of E_G for matched CL_{int} and P_{eff} values is reduced. This low extraction was in line with a general observation rank order of E_G between species, with highest extractions generally observed in rat and human.

The correlation of predicted Fa between human and either rat or dog indicated a strong relationship in the rat, but an incidence of higher Fa in the dog (**Figure 5-7**). This is in agreement with previous successful predictions based on rat data (Chiou and Barve, 1998; Cao et al., 2006) and poor relationships from the dog (Chiou et al., 2000). In the dog, it is postulated that despite the similarities in physiology and anatomy between the dog and human, absorption of compounds is greater and transit time is shorter. Reasons for this increased absorption have been suggested to be related to several characteristics of the dog intestine, including the longer length of villi, the impact of an increased bile salt concentration on membrane structure and permeability, the presence and number of tight junctions to facilitate paracellular transport, the impact of a reduced gastrointestinal pH (1

log unit *vs.* human) on weak base absorption, and increased protein binding (Chiou et al., 2000). However, since these factors were not factored into these estimates of Fa, and since P_{eff} inputs were identical in all species, this may therefore be associated with the relationship between small intestine transit time and intestinal radius (Amidon et al., 1988).

These poor relationships of E_G predictions and/or Fa observed in this study between the rat and dog and human go some way as to explaining the disconnect between observed F in preclinical species and in man (Musther et al., 2013). Relationships, between $Fa.F_G$ in preclinical species and human especially in the rat were improved using *in vitro* predictions over *in vivo* estimates, most likely as a result of the limitations of the indirect method for $Fa.F_G$ estimation for reasons stated above. Overall estimates of human $Fa.F_G$ or F are poor, however conversely to what may be expected, estimates from the dog were improved *vs.* the rat, possibly based on improved relationships between F_H in dog and human (**Figure 5-5**).

The prediction of F within each species is shown in **Figure 6-2** using *in vivo* estimates of F_H, and $Fa.F_G$ predicted from *in vitro* data. High confidence in F prediction was observed in all species, with good confidence in human estimates of oral bioavailability (67% within 2-fold) (**Table 6-2**). In the rat, predictions were within 2-fold of observed values was observed for 70% of compounds. Estimates for dog were slightly worse in both male and female (57%). It should be noted that the observed oral F of the compounds studied were generally low, in part based on their original selection for intestinal metabolism potential, and the likelihood that if metabolised in the intestine, liver metabolism would also be high. In this respect the data set is biased since in the rat, dog and human, the majority of compounds studied have observed low bioavailability (80%, 85% and 81% respectively had an observed F< 50%).

Table 6-2 Comparison of F predictions to observed F in each species for compounds studied

	Rat	**Dog (M)**	**Dog (F)**	**Human**
n	**23**	**21**	**21**	**21**
>2-fold (%)	**30.4**	**38.1**	**42.9**	**33.3**
<2-fold (%)	**69.6**	**61.9**	**57.1**	**66.7**

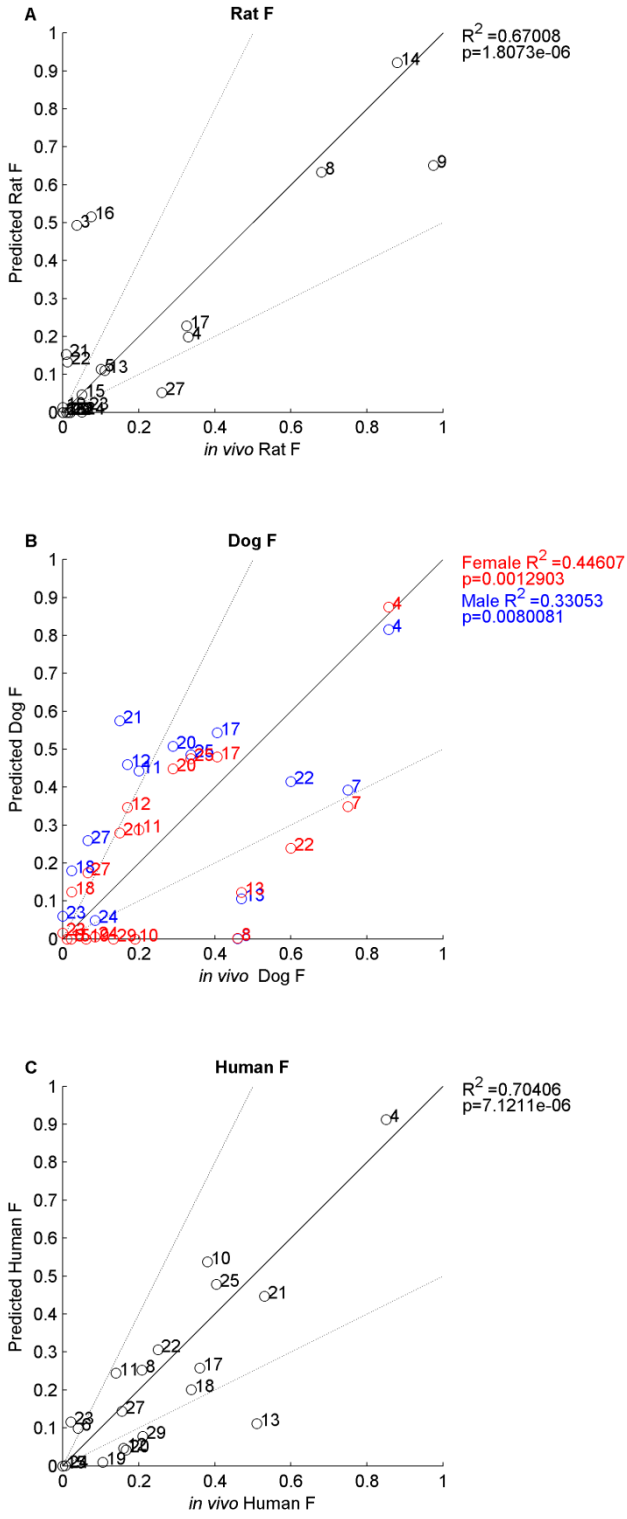

Figure 6-2 F predictions for rat (A), dog (B) and human (C). Estimates were made based on Fa.F_G *in vitro* estimates based on Caco-2 permeability estimates, and indirectly determined *in vivo* F_H.

Solid line: line of unity, dashed lines: 2-fold. Compound numbers refer to **Appendix Table 7-1.**

6. Final conclusions and future work

Intestinal metabolism has historically been hard to extrapolate due to limitations in both *in vitro* tools and *in vitro* to *in vivo* relationships. It was observed that changes to the preparation method can impact the enzyme contents and microsomal scaling factors, so it is important that in house measures are applied in order to gain confidence in values of microsomal scalars. As was observed, values normalised based per gram mucosa showed the most sensitivity between labs so it is recommended a MPPGI scalar approach is more appropriate when the scalar is unknown. Microsomal scaling using liver microsomes as a surrogate for intestinal metabolism should be treated with caution due to the metabolic differences in enzyme expression, however it is apparent for CYP3A substrates in the dog that certain trends exist when activities in each tissue are normalised similar to observations in the human. Furthermore, liver scalars and intestinal scalars showed strong correlations.

Estimates of *in vivo* F_G are limited when hepatic extraction is high, so in these cases it is recommended that cannulation is used to determine the exact hepatic component. Compounds with low hepatic extraction show similar estimates of F_G to cannulation studies when using indirect measures.

This was the largest know study to define intestinal scaling factors and metabolism for preclinical species (rat and dog) and human. Regional variations in scaling factors where studied comprehensively in the female dog, and correlations between liver and proximal scalars in male and female dogs. CYP content as well as CYP and UGT activities were explored in theses preparartions, however further work would be required to analyse absolute enzyme abundances in order to provide confidence in PBPK approaches, as well as e.g. anaylisng liver and intestinal CYP3A abundance normalised activities.

Proximal scalars were obtained in the rat model used for establishing of the microsomal preparation method, and for measuring losses from homogenisation to microsomal isolation. However losses in protein from initial starting intestinal tissue to homogenate was not assessed. Whilst there was no general trend for under or over prediction which would suggest this would be a significant loss, however for complete confidence in scaling this would need to be addressed.

A combined cofactor approach was validated, enabling for more efficient use of intestinal tissue as well as allowing for sequential metabolism. Extrapolation of F_G showed comparable success for Caco-2 and physicochemical based scaling, however stronger relationships were observed using Caco-2 permeability estimates. Poor prediction was observed for compounds which are CYP3A inhibitors, P-gp substrates and/or showed high protein binding, PBPK model approaches may be more appropriate for these compounds, but this requires further work and further characterisations of regional enzyme and transporter expressions. However these were correctly allocated as low F_G compounds in this study using a categorisation approach. This Q_{gut} approach was therefore successful as a screening tool for assessing likely F_G potential. More thorough examination of the data would be required in order to assess the benefit of more advanced PBPK approaches. The impact of the value fu_{gut} on Q_{gut} F_G estimates was not assessed, and a default value of 1 was applied as per a previous analysis in human (Yang et al., 2007). Future work should look at the influence on this prerameter on these F_G estimates.

Work in the human was limited to 3 and 2 donors for jejunum and ileum, only. Therefore in order to provide greater confidence in values of human intestinal scaling factors, as well as regional trends, futher work should include a larger cohort of donors.

Correlations between CYP3A E_G in rat and human were observed, however in general, relationships to human were poor. Using intestinal estimates of F_G however, in the compounds studied, within each species, good confidence in estimates of bioavailability were made. Further work would be required using a broader range of compounds with higher observed F given the low F bias for the compounds in this study.

7. Appendix

Appendix Table 7-1 Overview of compound molecular properties and investigational species studied.

Compound		Molecular Properties				Metabolic Route of Elimination (Human)		Species Studied		
Study #	**Compound**	**Ion Class**	**MW (Da)**	**PSA (Å²)**	**HBD**	**CYP Pathway**	**UGT Pathway**	**Rat[a]**	**Dog[b]**	**Human[c]**
1	7-Hydroxycoumarin	Neutral	162.14	51	1		UGT	Y	Y	Y[d]
2	Amitriptyline	Base	277.41	1	0	3A		Y		
3	Atorvastatin	Acid	558.65	119	4	3A		Y		
4	Bisprolol	Base	325.45	64	3	3A, 2D		Y	Y	Y
5	Bumetanide	Acid	364.42	130	4	2C		Y	Y	Y
6	Buspirone	Base	385.51	60	0	3A		Y	Y	Y[d]
7	Cimetidine	Base	252.34	82	3	3A			Y	
8	Cyclosporine A	Neutral	1202.62	290	5	3A	2B	Y	Y	Y
9	Diclofenac	Acid	296.15	55	2	2C	UGT	Y	Y	Y
10	Dilitiazem	Base	414.52	56	0	3A, 2D6		Y	Y	Y
11	Domperidone	Base	425.92	67	2	3A			Y	Y
12	Felodipine	Neutral	384.26	69	1	3A			Y	Y
13	Furosemide	Acid	330.75	130	4	3A		Y	Y	Y
14	Indomethacin	Acid	357.79	69	1	2C		Y	Y	Y
15	Ipriflavone	Neutral	280.32	37	0	3A, 1A, 2C	UGT	Y	Y	Y[d]
16	Irbesartan	Zwitterion	428.54	82	1	2C	1A6	Y	Y	Y
17	Losartan	Acid	422.92	87	2	3A, 2C		Y	Y	Y
18	Midazolam	Neutral	325.77	20	0	3A	UGT1A	Y	Y	Y[d]
19	Nicardipine	Neutral	360.36	113	1	3A		Y	Y	Y
20	Nitrendipine	Base	479.53	114	1	3A			Y	Y
21	Omeprazole	Neutral	345.42	71	1		1A8/10	Y	Y	Y
22	Pirenzepine	Base	351.41	64	1	3A, 2C		Y	Y	Y
23	Raloxifene	Base	473.59	74	2	1A, 2C		Y	Y	Y[d]
24	Saquinavir	Base	670.85	179	6	3A		Y	Y	Y[d]
25	Sildenafil	Base	474.58	105	1	3A, 2C		Y	Y	Y[d]
26	Simvastatin	Neutral	418.57	77	1	3A		Y		
27	Tacrolimus	Neutral	804.02	186	3	3A	UGT2B	Y	Y	Y[d]
28	Terfenadine	Base	471.68	46	2	3A		Y	Y	Y
29	Verapamil	Base	454.61	56	0	3A		Y	Y	Y

PSA: Polar surface area, HBD: hydrogen bond donors, a: studied in proximal rat intestine, b: studied in intestinal segment 1 and liver of male and female dog, and segments 2,3 and 6 of female dog intestine and liver c: studied in human jejunum microsomes, d: Studied in human ileum microsomes

7.1. References for Figure 2-1

Cotreau, M.M., et al., Methodologies to study the induction of rat hepatic and intestinal cytochrome P450 3A at the mRNA, protein, and catalytic activity level. J Pharmacol Toxicol Methods, 2000. 43(1): p. 41-54.
Warrington, J.S., D.J. Greenblatt, and L.L. von Moltke, Age-related differences in CYP3A expression and activity in the rat liver, intestine, and kidney. J Pharmacol Exp Ther, 2004. 309(2): p. 720-9. Kotegawa, T., et al., In vitro, pharmacokinetic, and pharmacodynamic interactions of ketoconazole and midazolam in the rat. J Pharmacol Exp Ther, 2002. 302(3): p. 1228-37.
Watkins, P.B., et al., Identification of glucocorticoid-inducible cytochromes P-450 in the intestinal mucosa of rats and man. J Clin Invest, 1987. 80(4): p. 1029-36.
Emoto, C., et al., Characterization of cytochrome P450 enzymes involved in drug oxidations in mouse intestinal microsomes. Xenobiotica, 2000. 30(10): p. 943-53.
Damre, A., S.R. Mallurwar, and D. Behera, Preparation and characterization of rodent intestinal microsomes: comparative assessment of two methods. Indian J Pharm Sci, 2009. 71(1): p. 75-7.
Bruyere, A., et al., Development of an optimized procedure for the preparation of rat intestinal microsomes: comparison of hepatic and intestinal microsomal cytochrome P450 enzyme activities in two rat strains. Xenobiotica, 2009. 39(1): p. 22-32.
Mohri, K. and Y. Uesawa, Enzymatic activities in the microsomes prepared from rat small intestinal epithelial cells by differential procedures. Pharm Res, 2001. 18(8): p. 1232-6.
Jones, D.P., R. Grafstrom, and S. Orrenius, Quantitation of hemoproteins in rat small intestinal mucosa with identification of mitochondrial cytochrome P-450. J Biol Chem, 1980. 255(6): p. 2883-90.
Bruyere, A., et al., Effect of Variations in the Amounts of P-Glycoprotein (ABCB1), BCRP (ABCG2) and CYP3A4 along the Human Small Intestine on PBPK Models for Predicting Intestinal First Pass. Mol Pharm.
Dawson, J.R. and J.W. Bridges, Intestinal microsomal drug metabolism: A comparison of rat and guinea-pig enzymes, and of rat crypt and villous tip cell enzymes Biochemical Pharmacology, 1981. 30(17): p. 2415-2420.
Zhang, Q.Y., et al., Characterization of human small intestinal cytochromes P-450. Drug Metab Dispos, 1999. 27(7): p. 804-9.
de Waziers, I., et al., Cytochrome P 450 isoenzymes, epoxide hydrolase and glutathione transferases in rat and human hepatic and extrahepatic tissues. J Pharmacol Exp Ther, 1990. 253(1): p. 387-94.

Paine, M.F., et al., Characterization of interintestinal and intraintestinal variations in human CYP3A-dependent metabolism. J Pharmacol Exp Ther, 1997. 283(3): p. 1552-62.
Powell, M., Kinetics of Cytochrome P450 Enzymes in the Canine Liver and Small Intestine, in School of Pharmacy and Pharmaceutical Sciences. 2006, University of Manchester.
Takemoto, K., et al., Catalytic activities of cytochrome P450 enzymes and UDP-glucuronosyltransferases involved in drug metabolism in rat everted sacs and intestinal microsomes. Xenobiotica, 2003. 33(1): p. 43-55.
Koster, A.S. and J. Noordhoek, Glucuronidation in the rat intestinal wall. Comparison of isolated mucosal cells, latent microsomes and activated microsomes. Biochem Pharmacol, 1983. 32(5): p. 895-900.
Prueksaritanont, T., et al., Comparative studies of drug-metabolizing enzymes in dog, monkey, and human small intestines, and in Caco-2 cells. Drug Metab Dispos, 1996. 24(6): p. 634-42.
Shiratani, H., et al., Species differences in UDP-glucuronosyltransferase activities in mice and rats. Drug Metab Dispos, 2008. 36(9): p. 1745-52.
Paine, M.F., et al., The human intestinal cytochrome P450 "pie". Drug Metab Dispos, 2006. 34(5): p. 880-6.
Mouly, S. and M.F. Paine, P-glycoprotein increases from proximal to distal regions of human small intestine. Pharm Res, 2003. 20(10): p. 1595-9.
Komura, H., et al., Species difference in nisoldipine oxidation activity in the small intestine. Drug Metab Pharmacokinet, 2002. 17(5): p. 427-36.
Bock, K.W., et al., Tissue-specific regulation of canine intestinal and hepatic phenol and morphine UDP-glucuronosyltransferases by beta-naphthoflavone in comparison with humans. Biochem Pharmacol, 2002. 63(9): p. 1683-90.
Weiser, M.M., Intestinal epithelial cell surface membrane glycoprotein synthesis. I. An indicator of cellular differentiation. J Biol Chem, 1973. 248(7): p. 2536-41.
Hubscher, G., G.R. West, and D.N. Brindley, Studies on the fractionation of mucosal homogenates from the small intestine. Biochem J, 1965. 97(3): p. 629-42.
Borm, P., A. Frankhuijzen-Sierevogel, and J. Noordhoek, Time and dose dependence of 3-methylcholanthrene-induced metabolism in rat intestinal mucosal cells and microsomes. Biochem Pharmacol, 1982. 31(22): p. 3707-10.
Borm, P.J., A. Frankhuijzen-Sierevogel, and J. Noordhoek, Kinetics of *in vitro* O-deethylation of phenacetin and 7-ethoxycoumarin by rat intestinal mucosal cells and microsomes. The effect of induction with 3-methylcholanthrene and inhibition with alpha-naphthoflavone. Biochem Pharmacol, 1983. 32(10): p. 1573-80.

Fasco, M.J., et al., Rat small intestinal cytochromes P450 probed by warfarin metabolism. Mol Pharmacol, 1993. 43(2): p. 226-33.
Pacifici, G.M., et al., Tissue distribution of drug-metabolizing enzymes in humans. Xenobiotica, 1988. 18(7): p. 849-56.
Stohs, S.J., et al., The isolation of rat intestinal microsomes with stable cytochrome P-450 and their metabolism of benzo(alpha) pyrene. Arch Biochem Biophys, 1976. 177(1): p. 105-16.
Lindeskog, P., et al., Isolation of rat intestinal microsomes: partial characterization of mucosal cytochrome P-450. Arch Biochem Biophys, 1986. 244(2): p. 492-501.
Hoensch, H., et al., Oxidative metabolism of foreign compounds in rat small intestine: cellular localization and dependence on dietary iron. Gastroenterology, 1976. 70(6): p. 1063-70.
Shirkey, R.S., J. Chakraborty, and J.W. Bridges, Comparison of the drug metabolising ability of rat intestinal mucosal microsomes with that of liver. Biochem Pharmacol, 1979. 28(18): p. 2835-9.
Zhang, Q.Y., et al., Characterization of rat small intestinal cytochrome P450 composition and inducibility. Drug Metab Dispos, 1996. 24(3): p. 322-8.
Bonkovsky, H.L., et al., Cytochrome P450 of small intestinal epithelial cells. Immunochemical characterization of the increase in cytochrome P450 caused by phenobarbital. Gastroenterology, 1985. 88(2): p. 458-67.
von Richter, O., et al., Cytochrome P450 3A4 and P-glycoprotein expression in human small intestinal enterocytes and hepatocytes: a comparative analysis in paired tissue specimens. Clin Pharmacol Ther, 2004. 75(3): p. 172-83.
Pinkus, L.M. and H.G. Windmueller, Phosphate-dependent glutaminase of small intestine: localization and role in intestinal glutamine metabolism. Arch Biochem Biophys, 1977. 182(2): p. 506-17.
Yoon, I.S., et al., Pharmacokinetics and first-pass elimination of metoprolol in rats: contribution of intestinal first-pass extraction to low bioavailability of metoprolol. Xenobiotica, 2011. 41(3): p. 243-51.
Lampen, A., et al., Metabolism and transport of the macrolide immunosuppressant sirolimus in the small intestine. J Pharmacol Exp Ther, 1998. 285(3): p. 1104-12.
Fitzsimmons, M.E. and J.M. Collins, Selective biotransformation of the human immunodeficiency virus protease inhibitor saquinavir by human small-intestinal cytochrome P4503A4: potential contribution to high first-pass metabolism. Drug Metab Dispos, 1997. 25(2): p. 256-66.
Lu, X., C. Li, and D. Fleisher, Cimetidine sulfoxidation in small intestinal microsomes. Drug Metab Dispos, 1998. 26(9): p. 940-2.

Keelan, M., et al., Dietary omega 3 fatty acids and cholesterol modify enterocyte microsomal membrane phospholipids, cholesterol content and phospholipid enzyme activities in diabetic rats. Lipids, 1994. 29(12): p. 851-8.

Eeckhoudt, S.L., Y. Horsmans, and R.K. Verbeeck, Differential induction of midazolam metabolism in the small intestine and liver by oral and intravenous dexamethasone pretreatment in rat. Xenobiotica, 2002. 32(11): p. 975-84.

Kanazu, T., et al., Assessment of the hepatic and intestinal first-pass metabolism of midazolam in a CYP3A drug-drug interaction model rats. Xenobiotica, 2005. 35(4): p. 305-17.

Kurosawa, S., et al., Effect of ursodeoxycholic acid on the pharmacokinetics of midazolam and CYP3A in the liver and intestine of rats. Xenobiotica, 2009. 39(2): p. 162-70.

Chhabra, R.S., R.J. Pohl, and J.R. Fouts, A comparative study of xenobiotic-metabolizing enzymes in liver and intestine of various animal species. Drug Metab Dispos, 1974. 2(5): p. 443-7.

Hirunpanich, V., K. Murakoso, and H. Sato, Inhibitory effect of docosahexaenoic acid (DHA) on the intestinal metabolism of midazolam: *in vitro* and *in vivo* studies in rats. Int J Pharm, 2008. 351(1-2): p. 133-43.

Appendix Table 7-2 Age, body weight and intestinal sample weights of rats used in this study.

Condition	Sex	Age (weeks)	Body Weight (g)	60cm intestine weight (g)	Intestine weight (g/cm)[a]
1	M	9	307 ±75	4.62 ±0.32	0.077 ±0.005
2	M	9	283 ±25	4.52 ±0.43	0.075 ±0.007
3	M	9	266 ±13	4.19 ±0.28	0.069 ±0.005
4	M	9	275 ±22	4.61 ±0.34	0.077 ±0.006
5	M	10	305 ±30	4.97 ±0.42	0.083 ±0.007
6	M	10	308 ±11	5.37 ±0.41	0.090 ±0.007
7	M	9	279 ±13	4.82 ±0.52	0.080 ±0.009
8	M	9	294 ±21	5.53 ±0.10	0.092 ±0.002
Mean			289 ±21	4.83 ±0.13	0.080 ±0.002

Data represents mean +/-stdev of n=3.a: normalized for 60cm length of intestine. M:Male

Appendix Table 7-3 Testosterone hydroxy metabolite elution times and LLOQ

Metabolite	MW	MS Mass (Da)	LLOQ (pmol/ml) Method A	LLOQ (pmol/ml) Method B	Mean Retention Time (min) Method A	Mean Retention Time (min) Method B	Internal Standard
2-α	304	305	100	50	5.42	5.31	11-beta
2-β	304	305	100	50	5.80	5.55	11-beta
6- α	304	305	100	50	2.48	2.71	11-beta
6- β	304	305	100	100	3.05	3.21	11-beta
7- α	304	305	100	100	3.45	3.63	11-beta
11- α	304	305	100	50	5.21	4.73	11-beta
11- β	304	305	-	-	4.78	5.21	-
15- α	304	305	100	100	3.18	3.44	11-beta
15- β	304	305	100	50	2.55	2.83	11-beta
16- α	304	305	100	100	4.18	4.27	11-beta
16- β	304	305	100	50	4.48	4.58	11-beta
Androstenedione	286	287	100	50	6.32	6.63	11-beta

LLOQ: Lower Limit of quntification

Appendix Table 7-4 Elution gradients for rate of formation studies in RIM, DIM, DLM and HIM with testosterone and 4-nitrophenol.

Testosterone method A					Testosterone method B					4-nitrophenol				
Event	Time (min)	A%	B%	Flow (ml/min)	Event	Time (min)	A%	B%	Flow (ml/min)	Event	Time (min)	A%	B%	Flow (ml/min)
1	0	95	5	1.0	1	0	70	30	0.5	1	0	95	5	0.5
2	0.65	66	34	1.0	2	8	45	55	0.5	2	2.5	5	95	0.5
3	4.5	60	40	1.0	3	8.01	5	95	0.5	3	5	5	95	0.5
4	5.5	50	50	1.0	4	9.5	5	95	0.5	4	5.01	95	5	0.5
5	7.5	23	77	1.0	5	9.51	70	30	0.5	5	8	95	5	0.5
6	8.5	5	95	1.0	6	12	70	30	0.5					
7	10.5	5	95	1.0										
8	11	95	5	1.0										
9	12.5	95	5	1.0										

Appendix Figure 7-1 Representative Elution profile for Testosterone hydroxylation metabolites in example method B top standard from DLM (A), RIM (B), DIM (C), DLM (D), method A top standard (E) and HIM (F)

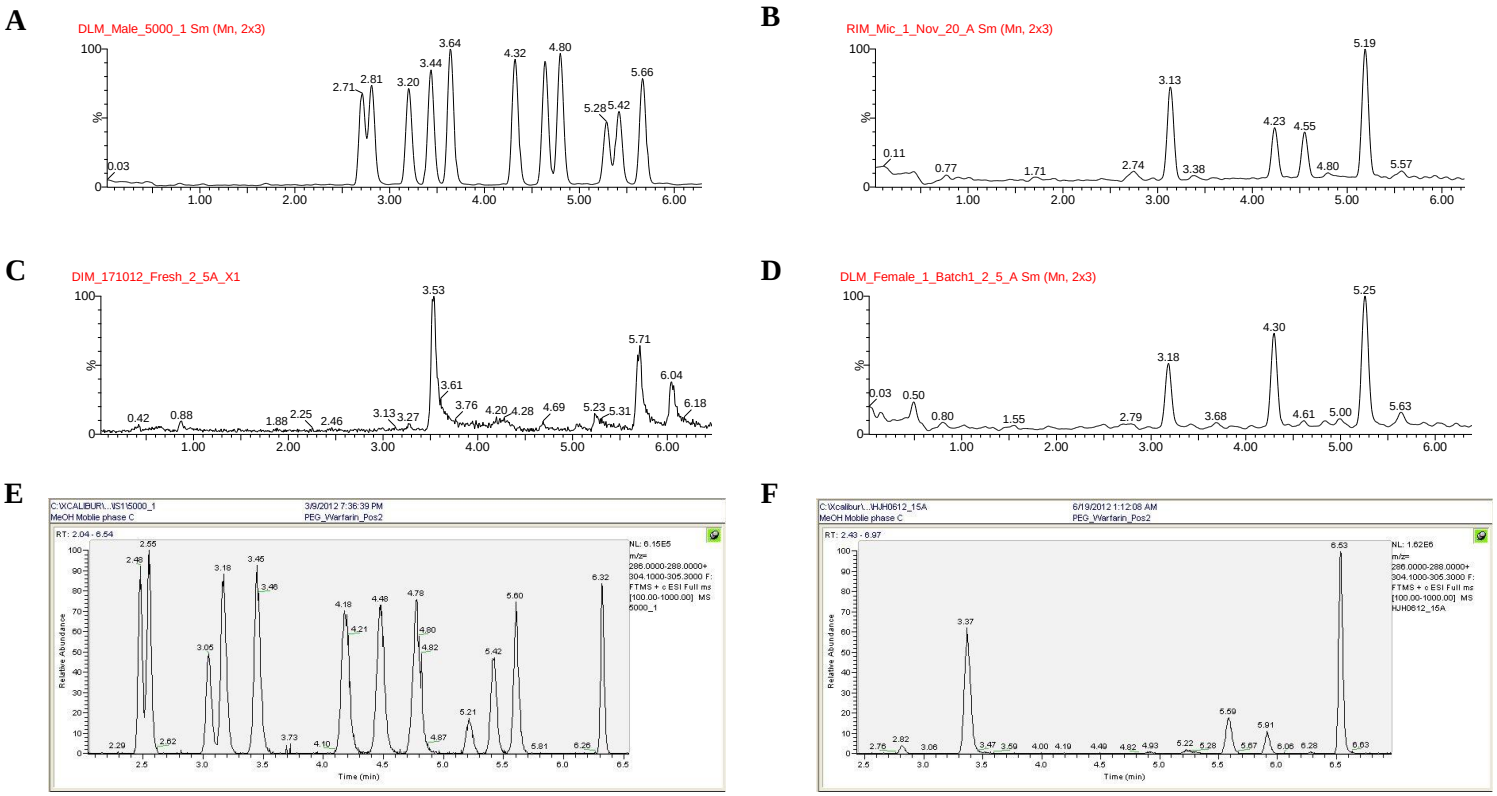

HIM determined using method A, RIM, DIM, DLM determined using method B.

Appendix Table 7-5 MS transitions for compounds in depletion studies in RIM, DIM, DLM and HIM, and pharmacokinetic studies in rat and dog blood and plasma.

Compound	Ion Class	MW (Da)	Transition (Da)	Col Voltage (V)	Col. Energy	Retention Time (min)
Internal Standard AZ1	Base	407.48	408.18>207.54	35	22	1.33
7-Hydroxycoumarin	Neutral	162.14	163.04 > 107.05	35	10	1.22
Amitryptiline	Base	277.41	278.19 > 91.23	40	22	1.77
Atorvastatin	Acid	558.65	559.26 > 440.60	25	22	1.71
Bisporolol Fumerate	Base	325.45	326.23 > 116.03	35	10	1.28
Bumetamide	Acid	364.42	365.12 > 184.17	40	22	1.00
Buspirone	Base	385.51	386.26 > 122.02	35	22	1.26
Cimetidine	Base	252.34	253.22 > 159.66	55	12	0.94
Cyclosporine A	Neutral	1202.62	1204.08 > 1206.50	35	22	1.51
Diclofenac	Acid	296.15	294.00 > 250.00	40	10	1.57
Diltiazem	Base	414.52	415.17 > 177.99	35	22	1.33
Domperidone	Base	425.91	426.17 > 175.06	35	22	1.28
Felodipine	Base	384.25	385.23 > 339.83	35	12	1.46
Furosemide[a]	Acid	330.75	332.07 > 90.90	35	25	1.47
Indomethacin	Acid	357.79	358.09>139.91	35	22	1.47
Ipriflavone	Neutral	280.32	281.22 > 239.66	35	12	1.48
Irbesartan	Zwitterion	428.54	429.24 > 207.01	35	22	1.33
Losartan K	Acid	422.92	424.35 > 406.96	35	12	1.4
Midazolam HCl	Neutral	325.77	326.50 > 291.50	35	22	1.36
Nicardipine	Base	479.53	480.21 > 315.21	35	22	1.34
Nitrendipine	Base	360.13	361.35 > 315.74	55	12	1.44
Omeprazole	Neutral	345.42	346.25 > 182.04	35	12	1.2
Pirenzepine HCl	Base	351.41	352.18 > 113.11	35	22	1.33
Raloxifene HCl	Base	473.59	474.35 > 112.71	95	36	1.31
Saquinavir Mesylate	Base	670.85	671.39 > 570.42	35	34	1.4
Sildenafil	Base	474.58	475.21 > 100.08	35	22	1.33
Simvastatin	Neutral	418.57	419.28 > 199.06	35	10	1.49
Tacrolimus	Neutral	804.02	804.49 > 768.62	35	10	1.34
Terfenadine	Base	471.68	472.32 > 437.17	55	24	1.41
Verapamil	Base	454.61	455.35 > 190.16	35	24	1.33

a: Detected using electrospray in negative mode (method B)

Appendix Table 7-6 Elution gradients for microsomal depletion and rat and dog pharmacokinetic studies

Method A				
Event	**Time(min)**	**Flow Rate (ml/min)**	**%A**	**%B**
1	Initial	0.4	95	5
2	0.2	0.4	95	5
3	1	0.4	100	0
4	1.5	0.4	100	0
5	1.51	0.4	95	2
6	2	0.4	95	5

Method B				
Event	**Time(min)**	**Flow Rate (ml/min)**	**%A**	**%B**
1	Initial	0.725	95	5
2	0.3	0.725	95	5
3	1.4	0.725	5	95
4	1.9	0.725	5	95
5	2	0.725	95	5

Run Time: 2.00 min, Target Column Temperature: 60ºC, A: 0.1% Formic acid in UPH2O, B: 0.1% Formic acid in MeOH. All compounds except Furosemide were detected using method A.

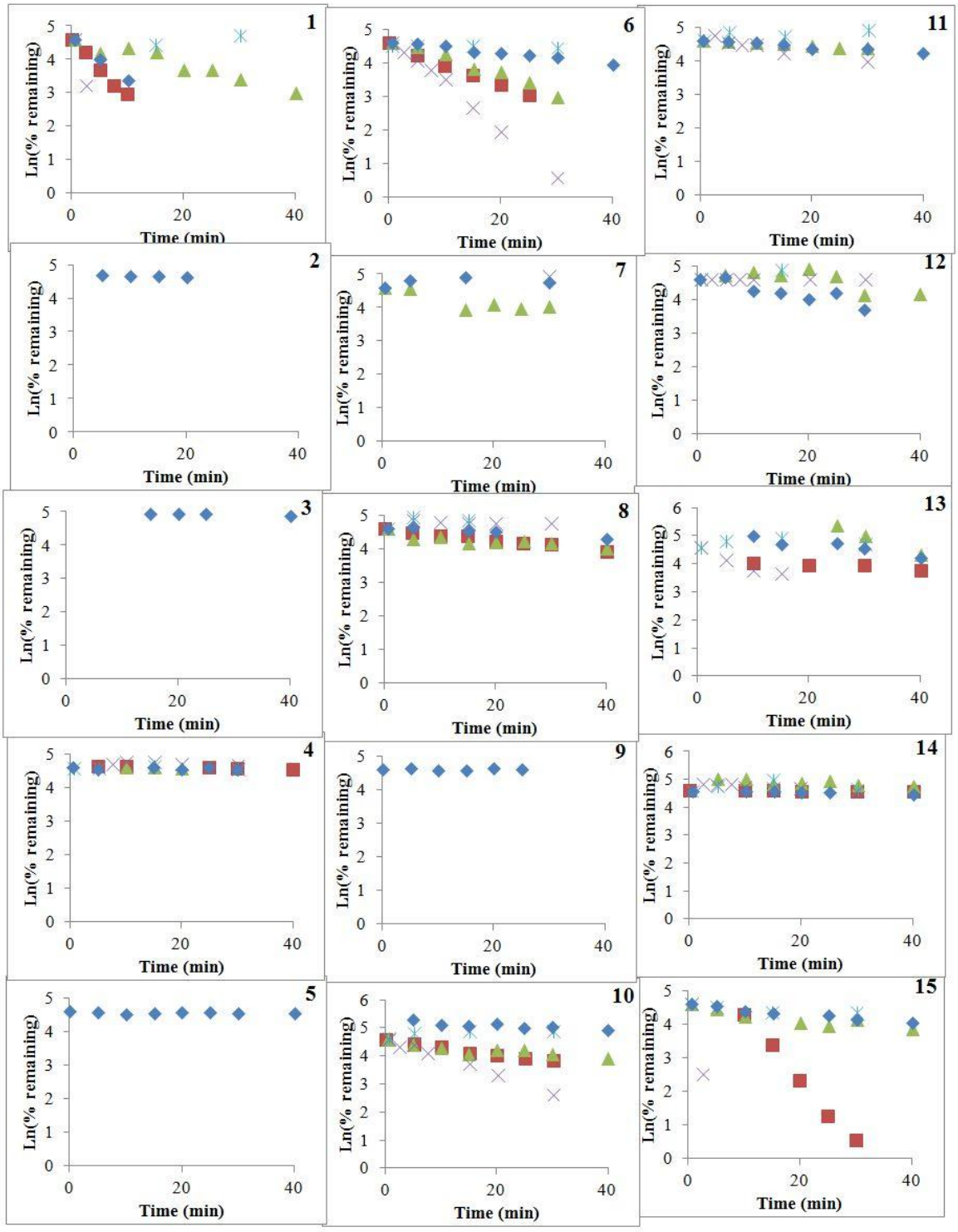

Appendix Figure 7-2 Sample depletion profiles for compounds 1-15 used in this study at incubations at 1mg/ml and concentrations of 1µM in RIM (■), DIM (▲), DLM (×), DLM (no cofactors) (✳)and HIM(◆).

Compound numbers correspond to Appendix Table 7-1.

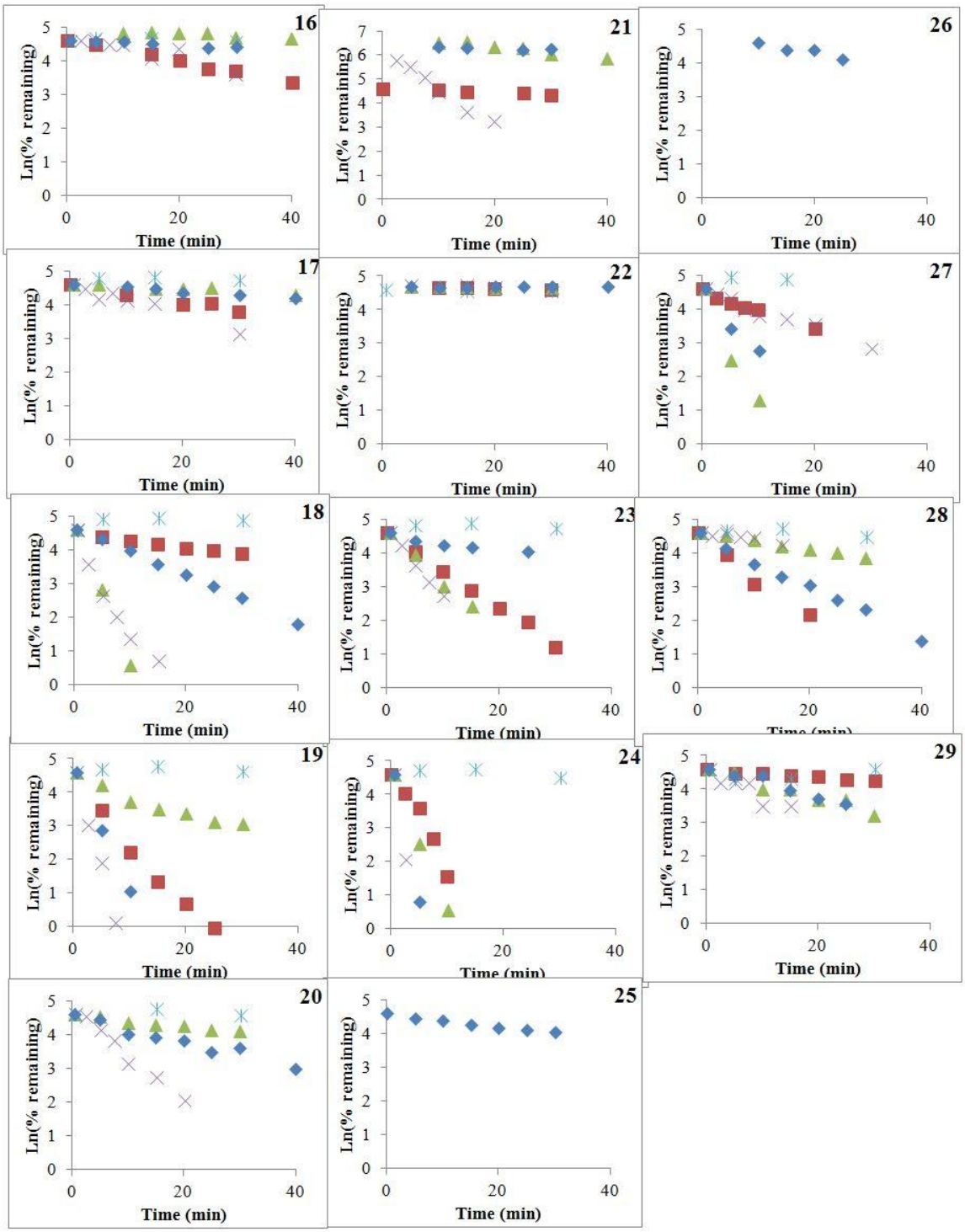

Appendix Figure 7-3 Sample depletion profiles for compounds 16-29 used in this study at incubations at 1mg/ml and concentrations of 1µM in RIM (■), DIM (▲), DLM (×), DLM (no cofactors) (✳)and HIM(◆).

Compound numbers correspond to Appendix Table 7-1.

Appendix Table 7-7 Compound specific input parameters for PBPK modeling in the beagle dog using Simcyp animal v12 ADAM model and for assessing safe dosing levels prior to dosing in dog from rat PK data.

#	Compound	LogP	pKa (Acid 1)	pKa (Acid 2)	pKa (Base 1)	pKa (Base 2)	Solubility (µM)[a]	Dog Plasma % free	Rat Plasma % free	Caco-2 P_{app} ($1E^{-6}$.cm/s)	Caco-2 P_{app} + transporter inhibitors[b] ($1E^{-6}$.cm/s)
1	7-Hydroxycoumarin	1.58	7.9				2113	19.16	5.81	61.70	52.95
2	Amitriptyline	4.41			9.2		2458	9.19	14.84	13.70	13.84
3	Atorvastatin	3.85	13.6	4.3	0.4		>2688	5.585	5.15	18.49	11.54
4	Bisprolol Fumarate	1.89	13.9		9.4		2308	>14.690	>14.820	5.80	10.16
5	Bumetanide	2.88	10.1	3.2	4.5		1495	9.69	2.31	1.73	1.78
6	Buspirone	1.59			7.7	4.3	1449	33.245	32.375	9.80	12.78
7	Cimetidine	-0.07			7.1	2.6	5418	>27.300	>27.530	0.60	NV
8	Cyclosporine A	2.79	13.3	13.4						NV	NV
9	Diclofenac	4.55	4.2				>5364	0.475	0.565	111.60	NV
10	Diltiazem	4.73			8.9		>1374	26.925	>27.530	10.50	8.91
11	Domperidone	4.05	11.1	12.2	9	0.4				6.72	12.84
12	Felodipine	4.76			2.7		2.073			3.30	3.22
13	Furosimide	2.3	3	9.8			4129	7.23	0.64	0.30	0.59
14	Indomethacin	4.25	4				2830	2.223	0.253	121.00	105.50
15	Ipriflavone	4.25					2.757	0.89	1.495	57.40	63.14
16	Irbesartan	5.25	4.2		2.6	0.6	893.4	4.87	2.62	13.31	23.18
17	Losartan	3.46	13.7	4.2	4.4	0.6	>2678	4.14		1.90	2.91
18	Midazolam	3.8			6	1	72.03			36.20	30.79
19	Nicardipine	4.89			7.3	2.6	7.453	0.44	0.935	26.50	26.62
19	Nitredipine	3.81			2.8					84.79	76.96
21	Omeprazole	2.45	8.5		4.7	2.6	947.2	NV	NV	NV	NV
22	Pirenzepine	0.21	11.3		7.4	2.1	>3683	>14.690	>49.880	0.20	NV
23	Raloxifene	4.57	8.8	9.2	8.5		9.054	0.485	0.74	4.90	0.15
24	Saquinavir	5.08	11		6.3	1.6	36.54			3.30	5.83
25	Sildenafil	2.47	10.1		6	0.9	19.85	25.645	11.91	40.3	48.04
26	Simvastatin	4.72	13.5				2.501	NV	NV	6.80	NV
27	Tacrolimus	4.79	13.8	10				NV	NV	73.6	NV
28	Terfenadine	5.62	13.3		9.4		<8.185	0.33	0.59	9.00	7.33
29	Verapamil	4.02			9		>2.061	18.88	21.245	15.7	12.53

a: solubility is provided however this was not used for PBPK modeling for simplicity since it was assumed that dissolution would be minimal following administration of solution and stability testing following acid addition prior to p.o. administration. b: P_{app} measured at 10µM substrate concentration in the presence Inhibitors (50 µM quinidine (P-gp), 20 µM sulfasalazine (BCRP), and 30 µM benzbromarone (MRP2).

Appendix Table 7-8 Sample compound and beagle dog input parameters for ADAM model in Simcyp® Animal v12

Simcyp Dog Simulator

Release 1 (30/07/2012)

Substrate	
Compound Name	Dog-Midazolam_Oli
Route	Oral
Dose Type	mg/kg
Dose	0.500
Start Day	1.000
Start Time	09h:00m
Dosing Regimen	Single Dose
PhysChem and Blood Binding	
Mol Weight (g/mol)	325.800
log P	3.530
Compound Type	Ampholyte
pKa 1	10.950
pKa 2	6.200
B/P	0.870
fu	0.089
Absorption	
Absorption Model	ADAM
Input Type	Predicted
fu(Gut)	1.000
Peff,Dog Type	Entered
Entered Peff,Dog (10-4 cm/s)	5.040
Degradation Rate Stomach (1/h)	0.000

Trial Design	
Species name	Olis_good_doggy_MPPGI
Seed	Fixed
Seed Value	1.000
Integration error tolerance	0.020
State variable accuracy	0.000
Number of Time Samples	200.000
Fasted/Fed	Fasted
Fluid intake with dose (mL)	50.000
Study Duration (h)	24.000
No of Subjects	Species Representative
Sub : Route	Oral
Sub : Dose Type	mg/kg
Sub : Dose	0.500
Sub : Dosing	Single Dose
Sub : Dose Interval	n/a
Sub : NoDoses	1.000
Differential Solver	5th-order Runge-Kutta
Maximum number of steps	1000000.000
Relative Tolerance	0.000
Relative Tolerance when ADAM is used	0.000
Integration error tolerance	0.020

Software Version Detail	
Source File Location	C:\Program Files\Simcyp\Simcyp Simulator V12
Data Path Location	C:\Users\Public\Documents
SimAnimal.exe	
File Version	12.0.79.0
Date Modified	30/07/2012
File Size (bytes)	4222464
SimDB.dll	
File Version	12.0.79.0
Date Modified	30/07/2012
File Size (bytes)	6124032
SimAnimalExcel.dll	
File Version	12.0.79.0
Date Modified	30/07/2012
File Size (bytes)	3128832
Windows Version	Version 6.0 (Build 6002: Service Pack 2)
Excel Version	2007
Simulation Duration(seconds)	0.000

Peff,Dog Duodenum (10E-4 cm/s)	1.627				
Degradation Rate Duodenum (1/h)	0.000				
Peff,Dog Jejunum I (10E-4 cm/s)	1.913				
Degradation Rate Jejunum I (1/h)	0.000				
Peff,Dog Jejunum II (10E-4 cm/s)	1.913				
Degradation Rate Jejunum II (1/h)	0.000				
Peff,Dog Jejunum III (10E-4 cm/s)	1.913				
Degradation Rate Jejunum III (1/h)	0.000				
Peff,Dog Jejunum i.v. (10E-4 cm/s)	1.913				
Degradation Rate Jejunum i.v. (1/h)	0.000				
Peff,Dog Ileum I (10E-4 cm/s)	1.913				
Degradation Rate Jejunum V (1/h)	0.000				
Peff,Dog Ileum II (10E-4 cm/s)	0.859				
Degradation Rate Ileum (1/h)	0.000				
Peff,Dog Colon (10E-4 cm/s)	0.890				
Degradation Rate Colon (1/h)	0.000				
Input Form	Solution				
Distribution					
Distribution Model	Full PBPK Model				
Vss mode	Predicted				
Vss (L/kg)	9.878				
Prediction Method	Method 2				
log Po:w	3.530				
logP vo:w	Predicted				
logP vo:w value	2.586				
Compound Type	Ampholyte				
pKa 1	10.950				
pKa 2	6.200				
Adipose Input Type	Predicted				
Adipose Value	21.496				
Bone Input Type	Predicted				
Bone Value	5.007				
Brain Input Type	Predicted				
Brain Value	11.248				
Gut Input Type	Predicted				
Gut Value	11.911				
Heart Input Type	Predicted				
Heart Value	5.383				

Kidney Input Type	Predicted				
Kidney Value	5.541				
Liver Input Type	Predicted				
Liver Value	6.083				
Lung Input Type	Predicted				
Lung Value	6.353				
Muscle Input Type	Predicted				
Muscle Value	3.618				
Skin Input Type	Predicted				
Skin Value	17.434				
Spleen Input Type	Predicted				
Spleen Value	3.221				
Elimination					
Clearance Type	Whole Organ Metabolic Clearance				
Liver Clearance Type	DLM				
Use Saturable Kinetics	No				
DLM CLint (µL/min/mg)	234.000				
DLM fu inc	0.990				
DLM Use Metabolite	No				
Intestine Clearance Type	DIM (Scrapings)				
Use Saturable Kinetics	No				
DIM CLint (µL/min/mg)	245.000				
DIM fu inc	0.740				
DIM Use Metabolite	No				
Reg Diff (Duodenum)	0.800				
Reg Diff (Jejunum I)	1.000				
Reg Diff (Jejunum II)	1.000				
Reg Diff (Jejunum III)	1.000				
Reg Diff (Jejunum i.v.)	0.500				
Reg Diff (Jejunum V)	0.500				
Reg Diff (Ileum)	0.100				
Active Uptake into Hepatocyte	1.000				
Biliary Clearance (µL/min/10^6)	0.000				
Percentage available for re-absorption (%)	100.000				
CL R (mL/min)	0.280				
Additional Systemic Clearance (mL/min)	0.000				

Liver & GI Tract		Tissue Volumes & Composition		Tissue Blood Flow Rates	
Liver		Adipose Volume (mL)	2437.000	Cardiac output (mL/min)	2049.000
		Bone Volume (mL)	472.000	Adipose (% of Qc)	6.500
HPGL (10^6 hepatocytes/g liver)	170.000	Brain Volume (mL)	70.000	Bone (% of Qc)	9.200
MPPGL (mg/g liver)	38.700	Gut Volume (mL)	452.000	Brain (% of Qc)	2.800
Liver Density (g/mL)	1.080	Heart Volume (mL)	76.000	Stomach (% of Qc)	3.200
Liver Weight (g)	325.080	Kidney Volume (mL)	47.000	SI (% of Qc)	9.300
% Hepatic Bile Entering Gallbladder Mean	70.000	Liver Volume (mL)	301.000	Villi (% of Qc)	3.900
% Hepatic Bile Entering Gallbladder CV (%)	32.000	Lung Volume (mL)	87.000	LI (% of Qc)	2.700
IMMC Cycle Time Mean (h)	2.110	Muscle Volume (mL)	4239.000	Heart (% of Qc)	4.400
IMMC Cycle Time CV (%)	12.000	Skin Volume (mL)	1068.000	Kidney (% of Qc)	15.900
Fasted Gallbladder Release Constant Mean (1/h)	0.180	Spleen Volume (mL)	29.000	Liver (Art) (% of Qc)	7.000
Fasted Gallbladder Release Constant CV (%)	30.000	Plasma Volume (mL)	481.000	Liver (Port) (% of Qc)	20.400
Fed Gallbladder Release Constant Mean (1/h)	0.480	RBC Volume (mL)	379.000	Lung (% of Qc)	100.000
Fed Gallbladder Release Constant CV (%)	19.000	Adipose : EW (%)	29.600	Muscle (% of Qc)	32.900
Fasted Gallbladder Residual Volume Mean (%)	79.400	Adipose : NL (%)	66.570	Skin (% of Qc)	6.800
Fasted Gallbladder Residual Volume CV (%)	13.000	Adipose : NP (%)	0.130	Spleen (% of Qc)	4.700
Fed Gallbladder Residual Volume Mean (%)	59.900	Bone : EW (%)	9.600	Splanchnic Blood Flow Fed/Fasted ratio	2.510
Fed Gallbladder Residual Volume CV (%)	40.000	Bone : NL (%)	1.700		
		Bone : NP (%)	0.170		
GI Tract		Brain : EW (%)	20.000		
		Brain : NL (%)	3.900		
Fasted Mean gastric emptying time (h)	0.370	Brain : NP (%)	0.150		
Fasted Mean gastric emptying time CV (%)	69.000	Gut : EW (%)	29.500		
Fed Mean gastric emptying time (h)	0.590	Gut : NL (%)	3.800		
Fed Mean gastric emptying time CV (%)	52.000	Gut : NP (%)	1.250		
Initial volume of stomach fluid (mL) - Fasted	20.000	Heart : EW (%)	23.700		
Initial volume of stomach fluid CV (%) - Fasted	0.000	Heart : NL (%)	1.400		
Initial volume of stomach fluid (mL) - Fed	400.000	Heart : NP (%)	1.570		
Initial volume of stomach fluid CV (%) - Fed	0.000	Kidney : EW (%)	29.400		
Small intestinal transit time (h)	2.390	Kidney : NL (%)	1.200		
Small intestinal transit time CV (%)	65.000	Kidney : NP (%)	2.420		
Colon transit time (h)	7.540	Liver : EW (%)	38.100		
Colon transit time CV (%)	24.000	Liver : NL (%)	1.400		

MPPGI (mg protein/g gut)	4.200	Liver : NP (%)	2.400		
Enterocyte volume (mL)	20.000	Lung : EW (%)	33.800		
Duodenum Length (cm)	23.000	Lung : NL (%)	1.810		
Jejunum Length (cm)	291.000	Lung : NP (%)	1.340		
Ileum Length (cm)	13.000	Muscle : EW (%)	8.100		
Duodenum Diameter (cm)	1.060	Muscle : NL (%)	1.000		
Jejunum Diameter (cm)	1.060	Muscle : NP (%)	0.840		
Ileum Diameter (cm)	1.060	Skin : EW (%)	41.700		
Duodenum Blood Flow (Qvilli %)	8.850	Skin : NL (%)	6.000		
Duodenum Transit Time (% Total)	8.000	Skin : NP (%)	0.440		
Duodenum Wet Weight (g/cm)	1.340	Spleen : EW (%)	20.500		
Jejunum I Blood Flow (Qvilli %)	17.250	Spleen : NL (%)	0.770		
Jejunum I Transit Time (% Total)	17.600	Spleen : NP (%)	1.130		
Jejunum I Wet Weight (g/cm)	0.910	Plasma : EW (%)	93.000		
Jejunum II Blood Flow (Qvilli %)	17.250	Plasma : NL (%)	0.220		
Jejunum II Transit Time (% Total)	17.600	Plasma : NP (%)	0.260		
Jejunum II Wet Weight (g/cm)	0.840	RBC : EW (%)	0.000		
Jejunum III Blood Flow (Qvilli %)	17.250	RBC : NL (%)	0.240		
Jejunum III Transit Time (% Total)	17.600	RBC : NP (%)	0.220		
Jejunum III Wet Weight (g/cm)	0.800	Adipose : IW (%)	3.700		
Jejunum i.v. Blood Flow (Qvilli %)	17.250	Adipose : AP (mg/g)	0.400		
Jejunum i.v. Transit Time (% Total)	17.600	Adipose : KpALB	0.049		
Jejunum i.v. Wet Weight (g/cm)	0.860	Adipose : KpLPP	0.068		
Jejunum V Blood Flow (Qvilli %)	17.250	Bone : IW (%)	33.300		
Jejunum V Transit Time (% Total)	17.600	Bone : AP (mg/g)	0.670		
Jejunum V Wet Weight (g/cm)	0.860	Bone : KpALB	0.100		
Ileum Blood Flow (Qvilli %)	4.900	Bone : KpLPP	0.050		
Ileum Transit Time (% Total)	4.000	Brain : IW (%)	55.700		
Ileum Wet Weight (g/cm)	0.880	Brain : AP (mg/g)	0.400		
Stomach pH Fasted	3.500	Brain : KpALB	0.048		
Stomach pH Fasted CV (%)	37.000	Brain : KpLPP	0.041		
Stomach pH Fed	2.100	Gut : IW (%)	49.800		
Stomach pH Fed CV (%)	18.000	Gut : AP (mg/g)	2.410		
Duodenum pH Fasted	6.100	Gut : KpALB	0.158		
Duodenum pH Fasted CV (%)	11.000	Gut : KpLPP	0.141		
Duodenum pH Fed	6.700	Heart : IW (%)	54.200		
Duodenum pH Fed CV (%)	11.000	Heart : AP (mg/g)	2.920		
Jejunum I pH Fasted	6.100	Heart : KpALB	0.157		
Jejunum I pH Fasted CV (%)	11.000	Heart : KpLPP	0.160		

Jejunum I pH Fed	6.100	Kidney : IW (%)	52.100		
Jejunum I pH Fed CV (%)	11.000	Kidney : AP (mg/g)	5.030		
Jejunum II pH Fasted	6.100	Kidney : KpALB	0.130		
Jejunum II pH Fasted CV (%)	13.000	Kidney : KpLPP	0.137		
Jejunum II pH Fed	6.100	Liver : IW (%)	39.100		
Jejunum II pH Fed CV (%)	13.000	Liver : AP (mg/g)	4.560		
Jejunum III pH Fasted	6.600	Liver : KpALB	0.086		
Jejunum III pH Fasted CV (%)	7.000	Liver : KpLPP	0.161		
Jejunum III pH Fed	6.600	Lung : IW (%)	44.800		
Jejunum III pH Fed CV (%)	7.000	Lung : AP (mg/g)	2.220		
Jejunum i.v. pH Fasted	6.800	Lung : KpALB	0.212		
Jejunum i.v. pH Fasted CV (%)	7.000	Lung : KpLPP	0.168		
Jejunum i.v. pH Fed	6.800	Muscle : IW (%)	63.800		
Jejunum i.v. pH Fed CV (%)	7.000	Muscle : AP (mg/g)	1.220		
Jejunum V pH Fasted	6.400	Muscle : KpALB	0.064		
Jejunum V pH Fasted CV (%)	25.000	Muscle : KpLPP	0.059		
Jejunum V pH Fed	6.400	Skin : IW (%)	8.200		
Jejunum V pH Fed CV (%)	25.000	Skin : AP (mg/g)	1.320		
Ileum pH Fasted	6.600	Skin : KpALB	0.277		
Ileum pH Fasted CV (%)	25.000	Skin : KpLPP	0.096		
Ileum pH Fed	6.600	Spleen : IW (%)	57.300		
Ileum pH Fed CV (%)	25.000	Spleen : AP (mg/g)	3.180		
Colon pH Fasted	6.500	Spleen : KpALB	0.097		
Colon pH Fasted CV (%)	12.000	Spleen : KpLPP	0.207		
Colon pH Fed	6.500	Plasma : IW (%)	0.000		
Colon pH Fed CV (%)	12.000	Plasma : AP (mg/g)	0.090		
Stomach CMC Fasted (mM)	1.000	RBC : IW (%)	65.100		
Stomach Bile Fasted (mM)	0.290	RBC : AP (mg/g)	0.450		
Stomach Bile Fasted CV (%)	141.000	Local pH : Plasma	7.400		
Stomach CMC Fed (mM)	1.000	Local pH : EW	7.400		
Stomach Bile Fed (mM)	0.290	Local pH : IW	7.120		
Stomach Bile Fed CV (%)	100.000	Local pH : IWRBC	7.220		
Duodenum CMC Fasted (mM)	1.000				
Duodenum Bile Fasted (mM)	3.310				
Duodenum Bile Fasted CV (%)	97.000				
Duodenum CMC Fed (mM)	1.000				
Duodenum Bile Fed (mM)	8.740				
Duodenum Bile Fed CV (%)	79.000				
Jejunum I CMC Fasted (mM)	1.000				
Jejunum I Bile Fasted (mM)	4.910				
Jejunum I Bile Fasted CV (%)	79.00				

	0				
Jejunum I CMC Fed (mM)	1.000				
Jejunum I Bile Fed (mM)	14.350				
Jejunum I Bile Fed CV (%)	28.000				
Jejunum II CMC Fasted (mM)	1.000				
Jejunum II Bile Fasted (mM)	4.910				
Jejunum II Bile Fasted CV (%)	79.000				
Jejunum II CMC Fed (mM)	1.000				
Jejunum II Bile Fed (mM)	14.350				
Jejunum II Bile Fed CV (%)	28.000				
Jejunum III CMC Fasted (mM)	1.000				
Jejunum III Bile Fasted (mM)	4.910				
Jejunum III Bile Fasted CV (%)	79.000				
Jejunum III CMC Fed (mM)	1.000				
Jejunum III Bile Fed (mM)	14.350				
Jejunum III Bile Fed CV (%)	28.000				
Jejunum i.v. CMC Fasted (mM)	1.000				
Jejunum i.v. Bile Fasted (mM)	4.910				
Jejunum i.v. Bile Fasted CV (%)	79.000				
Jejunum i.v. CMC Fed (mM)	1.000				
Jejunum i.v. Bile Fed (mM)	14.350				
Jejunum i.v. Bile Fed CV (%)	28.000				
Jejunum V CMC Fasted (mM)	1.000				
Jejunum V Bile Fasted (mM)	4.910				
Jejunum V Bile Fasted CV (%)	79.000				
Jejunum V CMC Fed (mM)	1.000				
Jejunum V Bile Fed (mM)	14.350				
Jejunum V Bile Fed CV (%)	28.000				
Ileum CMC Fasted (mM)	1.000				
Ileum Bile Fasted (mM)	1.250				
Ileum Bile Fasted CV (%)	30.000				
Ileum CMC Fed (mM)	1.000				
Ileum Bile Fed (mM)	5.960				
Ileum Bile Fed CV (%)	65.000				
Colon CMC Fasted (mM)	1.000				
Colon Bile Fasted (mM)	0.600				
Colon Bile Fasted CV (%)	50.000				
Colon CMC Fed (mM)	1.000				
Colon Bile Fed (mM)	0.600				
Colon Bile Fed CV (%)	50.00				

	0				
Duodenum Villi Channel Depth Mean (µm)	935.850				
Duodenum Villi Channel Depth CV (%)	26.000				
Duodenum Villi Channel Width Mean (µm)	26.870				
Duodenum Villi Channel Width CV (%)	30.000				
Duodenum Villi Thickness Mean (µm)	197.700				
Duodenum Villi Thickness CV (%)	14.000				
Duodenum Fold Expansion Mean	1.000				
Duodenum Fold Expansion CV (%)	0.000				
Duodenum Pore Radius Mean	12.900				
Duodenum Pore Radius CV (%)	0.000				
Jejunum I Villi Channel Depth Mean (µm)	717.500				
Jejunum I Villi Channel Depth CV (%)	21.000				
Jejunum I Villi Channel Width Mean (µm)	26.870				
Jejunum I Villi Channel Width CV (%)	30.000				
Jejunum I Villi Thickness Mean (µm)	191.800				
Jejunum I Villi Thickness CV (%)	14.670				
Jejunum I Fold Expansion Mean	1.000				
Jejunum I Fold Expansion CV (%)	0.000				
Jejunum I Pore Radius Mean	12.900				
Jejunum I Pore Radius CV (%)	0.000				
Jejunum II Villi Channel Depth Mean (µm)	717.500				
Jejunum II Villi Channel Depth CV (%)	21.000				
Jejunum II Villi Channel Width Mean (µm)	26.870				
Jejunum II Villi Channel Width CV (%)	30.000				
Jejunum II Villi Thickness Mean (µm)	191.800				
Jejunum II Villi Thickness CV (%)	14.670				
Jejunum II Fold Expansion Mean	1.000				
Jejunum II Fold Expansion CV (%)	0.000				
Jejunum II Pore Radius Mean	12.900				
Jejunum II Pore Radius CV (%)	0.000				
Jejunum III Villi Channel Depth Mean (µm)	717.500				
Jejunum III Villi Channel Depth CV (%)	21.000				
Jejunum III Villi Channel Width Mean (µm)	26.870				
Jejunum III Villi Channel Width CV (%)	30.000				
Jejunum III Villi Thickness Mean (µm)	191.800				
Jejunum III Villi Thickness CV (%)	14.670				

Jejunum III Fold Expansion Mean	**1.000**				
Jejunum III Fold Expansion CV (%)	**0.000**				
Jejunum III Pore Radius Mean	**12.900**				
Jejunum III Pore Radius CV (%)	**0.000**				
Jejunum i.v. Villi Channel Depth Mean (µm)	**717.500**				
Jejunum i.v. Villi Channel Depth CV (%)	**21.000**				
Jejunum i.v. Villi Channel Width Mean (µm)	**26.870**				
Jejunum i.v. Villi Channel Width CV (%)	**30.000**				
Jejunum i.v. Villi Thickness Mean (µm)	**191.800**				
Jejunum i.v. Villi Thickness CV (%)	**14.670**				
Jejunum i.v. Fold Expansion Mean	**1.000**				
Jejunum i.v. Fold Expansion CV (%)	**0.000**				
Jejunum i.v. Pore Radius Mean	**12.900**				
Jejunum i.v. Pore Radius CV (%)	**0.000**				
Jejunum V Villi Channel Depth Mean (µm)	**717.500**				
Jejunum V Villi Channel Depth CV (%)	**21.000**				
Jejunum V Villi Channel Width Mean (µm)	**26.870**				
Jejunum V Villi Channel Width CV (%)	**30.000**				
Jejunum V Villi Thickness Mean (µm)	**191.800**				
Jejunum V Villi Thickness CV (%)	**14.670**				
Jejunum V Fold Expansion Mean	**1.000**				
Jejunum V Fold Expansion CV (%)	**0.000**				
Jejunum V Pore Radius Mean	**12.900**				
Jejunum V Pore Radius CV (%)	**0.000**				
Ileum Villi Channel Depth Mean (µm)	**527.350**				
Ileum Villi Channel Depth CV (%)	**17.000**				
Ileum Villi Channel Width Mean (µm)	**21.820**				
Ileum Villi Channel Width CV (%)	**30.000**				
Ileum Villi Thickness Mean (µm)	**181.470**				
Ileum Villi Thickness CV (%)	**15.000**				
Ileum Fold Expansion Mean	**1.000**				
Ileum Fold Expansion CV (%)	**0.000**				
Ileum Pore Radius Mean	**12.900**				
Ileum Pore Radius CV (%)	**0.000**				
Colon Fold Expansion Mean	**1.000**				
Colon Fold Expansion CV (%)	**0.000**				
Colon Pore Radius Mean	**12.900**				
Colon Pore Radius CV (%)	**0.000**				

Duodenum Unstirred Layer Thickness Mean (µm)	**170.000**				
Duodenum Unstirred Layer Thickness CV (%)	**22.350**				
Duodenum Unstirred Layer pH Mean	**6.500**				
Duodenum Unstirred Layer pH CV (%)	**0.500**				
Jejunum I Unstirred Layer Thickness Mean (µm)	**123.000**				
Jejunum I Unstirred Layer Thickness CV (%)	**3.000**				
Jejunum I Unstirred Layer pH Mean	**6.500**				
Jejunum I Unstirred Layer pH CV (%)	**0.500**				
Jejunum II Unstirred Layer Thickness Mean (µm)	**123.000**				
Jejunum II Unstirred Layer Thickness CV (%)	**3.000**				
Jejunum II Unstirred Layer pH Mean	**6.500**				
Jejunum II Unstirred Layer pH CV (%)	**0.500**				
Jejunum III Unstirred Layer Thickness Mean (µm)	**123.000**				
Jejunum III Unstirred Layer Thickness CV (%)	**3.000**				
Jejunum III Unstirred Layer pH Mean	**6.500**				
Jejunum III Unstirred Layer pH CV (%)	**0.500**				
Jejunum i.v. Unstirred Layer Thickness Mean (µm)	**123.000**				
Jejunum i.v. Unstirred Layer Thickness CV (%)	**3.000**				
Jejunum i.v. Unstirred Layer pH Mean	**6.500**				
Jejunum i.v. Unstirred Layer pH CV (%)	**0.500**				
Jejunum V Unstirred Layer Thickness Mean (µm)	**123.000**				
Jejunum V Unstirred Layer Thickness CV (%)	**3.000**				
Jejunum V Unstirred Layer pH Mean	**6.500**				
Jejunum V Unstirred Layer pH CV (%)	**0.500**				
Ileum Unstirred Layer Thickness Mean (µm)	**480.000**				
Ileum Unstirred Layer Thickness CV (%)	**10.000**				
Ileum Unstirred Layer pH Mean	**6.500**				
Ileum Unstirred Layer pH CV (%)	**0.500**				
Colon Unstirred Layer Thickness Mean (µm)	**830.000**				
Colon Unstirred Layer Thickness CV (%)	**13.000**				
Colon Unstirred Layer pH Mean	**6.500**				
Colon Unstirred Layer pH CV (%)	**0.500**				

8. References

Agoram B, Woltosz WS and Bolger MB (2001) Predicting the impact of physiological and biochemical processes on oral drug bioavailability. *Adv Drug Deliv Rev* **50 Suppl 1:**S41-67.

Akabane T, Tabata K, Kadono K, Sakuda S, Terashita S and Teramura T (2010) A comparison of pharmacokinetics between humans and monkeys. *Drug Metab Dispos* **38:**308-316.

Amidon GL, Sinko PJ and Fleisher D (1988) Estimating human oral fraction dose absorbed: a correlation using rat intestinal membrane permeability for passive and carrier-mediated compounds. *Pharm Res* **5:**651-654.

Arlotto MP, Trant JM and Estabrook RW (1991) Measurement of steroid hydroxylation reactions by high-performance liquid chromatography as indicator of P450 identity and function. *Methods Enzymol* **206:**454-462.

Baarnhielm C, Dahlback H and Skanberg I (1986) In vivo pharmacokinetics of felodipine predicted from in vitro studies in rat, dog and man. *Acta Pharmacol Toxicol (Copenh)* **59:**113-122.

Bae SK, Yang KH, Aryal DK, Kim YG and Lee MG (2009) Pharmacokinetics of amitriptyline and one of its metabolites, nortriptyline, in rats: little contribution of considerable hepatic first-pass effect to low bioavailability of amitriptyline due to great intestinal first-pass effect. *J Pharm Sci* **98:**1587-1601.

Balimane PV and Chong S (2005) Cell culture-based models for intestinal permeability: a critique. *Drug Discov Today* **10:**335-343.

Barr WH and Riegelman S (1970) Intestinal drug absorption and metabolism. I. Comparison of methods and models to study physiological factors of in vitro and in vivo intestinal absorption. *J Pharm Sci* **59:**154-163.

Barter ZE, Bayliss MK, Beaune PH, Boobis AR, Carlile DJ, Edwards RJ, Houston JB, Lake BG, Lipscomb JC, Pelkonen OR, Tucker GT and Rostami-Hodjegan A (2007) Scaling factors for the extrapolation of in vivo metabolic drug clearance from in vitro data: reaching a consensus on values of human microsomal protein and hepatocellularity per gram of liver. *Curr Drug Metab* **8:**33-45.

Bartholow M (2012) Top 200 Drugs of 2011.

Beddies G, Fox PR, Papich MD, Kanikanti VR, Krebber R and Keene BW (2008) Comparison of the pharmacokinetic properties of bisoprolol and carvedilol in healthy dogs. *Am J Vet Res* **69:**1659-1663.

Benet LZ and Cummins CL (2001) The drug efflux-metabolism alliance: biochemical aspects. *Adv Drug Deliv Rev* **50 Suppl 1:**S3-11.

Bertera FM, Mayer MA, Opezzo JA, Taira CA, Bramuglia GF and Hocht C (2007) Pharmacokinetic-pharmacodynamic modeling of diltiazem in spontaneously hypertensive rats: a microdialysis study. *J Pharmacol Toxicol Methods* **56:**290-299.

Bjorkman S, Stanski DR, Harashima H, Dowrie R, Harapat SR, Wada DR and Ebling WF (1993) Tissue distribution of fentanyl and alfentanil in the rat cannot be described by a blood flow limited model. *J Pharmacokinet Biopharm* **21:**255-279.

Blanchard J (1981) Evaluation of the relative efficacy of various techniques for deproteinizing plasma samples prior to high-performance liquid chromatographic analysis. *J Chromatogr* **226:**455-460.

Boase S and Miners JO (2002) In vitro-in vivo correlations for drugs eliminated by glucuronidation: investigations with the model substrate zidovudine. *Br J Clin Pharmacol* **54:**493-503.

Bock KW, Bock-Hennig BS, Munzel PA, Brandenburg JO, Kohle CT, Soars MG, Riley RJ, Burchell B, von Richter O, Eichelbaum MF, Swedmark S and Orzechowski A (2002) Tissue-specific regulation of canine intestinal and hepatic phenol and morphine UDP-glucuronosyltransferases by beta-naphthoflavone in comparison with humans. *Biochem Pharmacol* **63:**1683-1690.

Bonkovsky HL, Hauri HP, Marti U, Gasser R and Meyer UA (1985) Cytochrome P450 of small intestinal epithelial cells. Immunochemical characterization of the increase in cytochrome P450 caused by phenobarbital. *Gastroenterology* **88:**458-467.

Borm P, Mingels MJ, Hulshoff A, Frankhuyzen-Sierevogel A and Noordhoek J (1983a) Rapid formation of N-hydroxymethylpentamethylmelamine by mitochondria from rat small intestinal epithelium. *Life Sci* **33:**2113-2119.

Borm PJ, Frankhuijzen-Sierevogel A and Noordhoek J (1983b) Kinetics of in vitro O-deethylation of phenacetin and 7-ethoxycoumarin by rat intestinal mucosal cells and microsomes. The effect of induction with 3-methylcholanthrene and inhibition with alpha-naphthoflavone. *Biochem Pharmacol* **32:**1573-1580.

Borm PJ, Koster AS, Frankhuijzen-Sierevogel A and Noordhoek J (1983c) Comparison of two cell isolation procedures to study in vitro intestinal wall biotransformation in control and 3-methyl-cholanthrene pretreated rats. *Cell Biochem Funct* **1:**161-167.

Brown RP, Delp MD, Lindstedt SL, Rhomberg LR and Beliles RP (1997) Physiological parameter values for physiologically based pharmacokinetic models. *Toxicol Ind Health* **13:**407-484.

Bruneau P (2001) Search for predictive generic model of aqueous solubility using Bayesian neural nets. *J Chem Inf Comput Sci* **41:**1605-1616.

Bruyere A (2011) Personal Communication.

Bruyere A, Decleves X, Bouzom F, Ball K, Marques C, Treton X, Pocard M, Valleur P, Bouhnik Y, Panis Y, Scherrmann JM and Mouly S Effect of Variations in the Amounts of P-Glycoprotein (ABCB1), BCRP (ABCG2) and CYP3A4 along the Human Small Intestine on PBPK Models for Predicting Intestinal First Pass. *Mol Pharm*.

Bruyere A, Decleves X, Bouzom F, Ball K, Marques C, Treton X, Pocard M, Valleur P, Bouhnik Y, Panis Y, Scherrmann JM and Mouly S (2010) Effect of variations in the amounts of P-glycoprotein (ABCB1), BCRP (ABCG2) and CYP3A4 along the human small intestine on PBPK models for predicting intestinal first pass. *Mol Pharm* **7:**1596-1607.

Bruyere A, Decleves X, Bouzom F, Proust L, Martinet M, Walther B and Parmentier Y (2009) Development of an optimized procedure for the preparation of rat intestinal microsomes: comparison of hepatic and intestinal microsomal cytochrome P450 enzyme activities in two rat strains. *Xenobiotica* **39:**22-32.

Buckley DB and Klaassen CD (2007) Tissue- and gender-specific mRNA expression of UDP-glucuronosyltransferases (UGTs) in mice. *Drug Metab Dispos* **35:**121-127.

Bueters T, Juric S, Sohlenius-Sternbeck AK, Hu Y and Bylund J (2013) Rat poorly predicts the combined non-absorbed and presystemically metabolized fractions in the human. *Xenobiotica*.

Buhring KU, Sailer H, Faro HP, Leopold G, Pabst J and Garbe A (1986) Pharmacokinetics and metabolism of bisoprolol-14C in three animal species and in humans. *J Cardiovasc Pharmacol* **8 Suppl 11:**S21-28.

Burke MD and Orrenius S (1979) Isolation and comparison of endoplasmic reticulum membranes and their mixed function oxidase activities from mammalian extrahepatic tissues. *Pharmacol Ther* **7:**549-599.

Caccia S, Conti I, Vigano G and Garattini S (1986) 1-(2-Pyrimidinyl)-piperazine as active metabolite of buspirone in man and rat. *Pharmacology* **33:**46-51.

Caccia S, Muglia M, Mancinelli A and Garattini S (1983) Disposition and metabolism of buspirone and its metabolite 1-(2-pyrimidinyl)-piperazine in the rat. *Xenobiotica* **13:**147-153.

Cao X, Gibbs ST, Fang L, Miller HA, Landowski CP, Shin HC, Lennernas H, Zhong Y, Amidon GL, Yu LX and Sun D (2006) Why is it challenging to predict intestinal drug absorption and oral bioavailability in human using rat model. *Pharm Res* **23:**1675-1686.

Carmine AA and Brogden RN (1985) Pirenzepine. A review of its pharmacodynamic and pharmacokinetic properties and therapeutic efficacy in peptic ulcer disease and other allied diseases. *Drugs* **30:**85-126.

Casado J, Pastor-Anglada M and Remesar X (1987) Hepatic uptake of amino acids at mid-lactation in the rat. *Biochem J* **245:**297-300.

Chen M, Xu D, Hu XL and Wang H (2008) Effects of liver fibrosis on verapamil pharmacokinetics in rats. *Clin Exp Pharmacol Physiol* **35:**287-294.

Chiou WL and Barve A (1998) Linear correlation of the fraction of oral dose absorbed of 64 drugs between humans and rats. *Pharm Res* **15:**1792-1795.

Chiou WL and Buehler PW (2002) Comparison of oral absorption and bioavailablity of drugs between monkey and human. *Pharm Res* **19:**868-874.
Chiou WL, Jeong HY, Chung SM and Wu TC (2000) Evaluation of using dog as an animal model to study the fraction of oral dose absorbed of 43 drugs in humans. *Pharm Res* **17:**135-140.
Choi DH, Chang KS, Hong SP, Choi JS and Han HK (2008) Effect of atorvastatin on the intravenous and oral pharmacokinetics of verapamil in rats. *Biopharm Drug Dispos* **29:**45-50.
Choi JS, Piao YJ and Han HK (2006) Pharmacokinetic interaction between fluvastatin and diltiazem in rats. *Biopharm Drug Dispos* **27:**437-441.
Chou CC and Grassmick B (1978) Motility and blood flow distribution within the wall of the gastrointestinal tract. *Am J Physiol* **235:**H34-39.
Chovan JP, Ring SC, Yu E and Baldino JP (2007) Cytochrome P450 probe substrate metabolism kinetics in Sprague Dawley rats. *Xenobiotica* **37:**459-473.
Christians U, Schmitz V and Haschke M (2005) Functional interactions between P-glycoprotein and CYP3A in drug metabolism. *Expert Opin Drug Metab Toxicol* **1:**641-654.
Chung HJ, Kang HE, Yang KH, Kim SY and Lee MG (2009) Ipriflavone pharmacokinetics in mutant Nagase analbuminemic rats. *Biopharm Drug Dispos* **30:**294-304.
Chung JW, Yang SH and Choi JS (2010) Effects of lovastatin on the pharmacokinetics of nicardipine in rats. *Biopharm Drug Dispos* **31:**436-441.
Cong D, Doherty M and Pang KS (2000) A new physiologically based, segregated-flow model to explain route-dependent intestinal metabolism. *Drug Metab Dispos* **28:**224-235.
Cotreau MM, von Moltke LL, Beinfeld MC and Greenblatt DJ (2000) Methodologies to study the induction of rat hepatic and intestinal cytochrome P450 3A at the mRNA, protein, and catalytic activity level. *J Pharmacol Toxicol Methods* **43:**41-54.
Cubitt HE, Houston JB and Galetin A (2009) Relative importance of intestinal and hepatic glucuronidation-impact on the prediction of drug clearance. *Pharm Res* **26:**1073-1083.
Cubitt HE, Houston JB and Galetin A (2011) Prediction of human drug clearance by multiple metabolic pathways: integration of hepatic and intestinal microsomal and cytosolic data. *Drug Metab Dispos* **39:**864-873.
Damre A, Mallurwar SR and Behera D (2009) Preparation and characterization of rodent intestinal microsomes: comparative assessment of two methods. *Indian J Pharm Sci* **71:**75-77.
Darwich AS, Neuhoff S, Jamei M and Rostami-Hodjegan A (2010) Interplay of metabolism and transport in determining oral drug absorption and gut wall metabolism: a simulation assessment using the "Advanced Dissolution, Absorption, Metabolism (ADAM)" model. *Curr Drug Metab* **11:**716-729.
Davi H, Tronquet C, Miscoria G, Perrier L, DuPont P, Caix J, Simiand J and Berger Y (2000) Disposition of irbesartan, an angiotensin II AT1-receptor antagonist, in mice, rats, rabbits, and macaques. *Drug Metab Dispos* **28:**79-88.
Davies B and Morris T (1993) Physiological parameters in laboratory animals and humans. *Pharm Res* **10:**1093-1095.
Dawson JR and Bridges JW (1981) Intestinal microsomal drug metabolism: A comparison of rat and guinea-pig enzymes, and of rat crypt and villous tip cell enzymes *Biochemical Pharmacology* **30:**2415-2420.
de Graaf IA, de Kanter R, de Jager MH, Camacho R, Langenkamp E, van de Kerkhof EG and Groothuis GM (2006) Empirical validation of a rat in vitro organ slice model as a tool for in vivo clearance prediction. *Drug Metab Dispos* **34:**591-599.
De Kanter R, Monshouwer M, Draaisma AL, De Jager MH, de Graaf IA, Proost JH, Meijer DK and Groothuis GM (2004) Prediction of whole-body metabolic clearance of drugs through the combined use of slices from rat liver, lung, kidney, small intestine and colon. *Xenobiotica* **34:**229-241.
de Waziers I, Cugnenc PH, Yang CS, Leroux JP and Beaune PH (1990) Cytochrome P 450 isoenzymes, epoxide hydrolase and glutathione transferases in rat and human hepatic and extrahepatic tissues. *J Pharmacol Exp Ther* **253:**387-394.
Deguchi T, Watanabe N, Kurihara A, Igeta K, Ikenaga H, Fusegawa K, Suzuki N, Murata S, Hirouchi M, Furuta Y, Iwasaki M, Okazaki O and Izumi T (2011) Human pharmacokinetic

prediction of UDP-glucuronosyltransferase substrates with an animal scale-up approach. *Drug Metab Dispos* **39:**820-829.
Delp MD, Evans MV and Duan C (1998) Effects of aging on cardiac output, regional blood flow, and body composition in Fischer-344 rats. *J Appl Physiol* **85:**1813-1822.
Delp MD, Manning RO, Bruckner JV and Armstrong RB (1991) Distribution of cardiac output during diurnal changes of activity in rats. *Am J Physiol* **261:**H1487-1493.
DeSesso JM and Jacobson CF (2001) Anatomical and physiological parameters affecting gastrointestinal absorption in humans and rats. *Food Chem Toxicol* **39:**209-228.
DeSesso JM, Williams AL and John EM (2008) Chapter 21 Contrasting the Gastrointestinal Tracts of Mammals: Factors that Influence Absorption, in: *Annual Reports in Medicinal Chemistry*, pp 353-371, Academic Press.
Ding X and Kaminsky LS (2003) Human extrahepatic cytochromes P450: function in xenobiotic metabolism and tissue-selective chemical toxicity in the respiratory and gastrointestinal tracts. *Annu Rev Pharmacol Toxicol* **43:**149-173.
Dressman J (1986) Comparison of Canine and Human Gastrointestinal Physiology. *Pharmaceutical Research* **3:**123-131.
Dressman JB and Reppas C (2000) In vitro-in vivo correlations for lipophilic, poorly water-soluble drugs. *Eur J Pharm Sci* **11 Suppl 2:**S73-80.
Eade MN, Reid IR and Quinn JP (1977) Intestinal blood flow in the dog measured by indicator fractionation without tissue samples. *Clin Exp Pharmacol Physiol* **4:**235-245.
Ekins S, Maenpaa J and Wrighton SA (1999) *In vitro metabolism: subcellular fractions*. Marcel Dekker, New York:.
Emoto C, Yamazaki H, Yamasaki S, Shimada N, Nakajima M and Yokoi T (2000) Characterization of cytochrome P450 enzymes involved in drug oxidations in mouse intestinal microsomes. *Xenobiotica* **30:**943-953.
Fahmi OA, Maurer TS, Kish M, Cardenas E, Boldt S and Nettleton D (2008) A combined model for predicting CYP3A4 clinical net drug-drug interaction based on CYP3A4 inhibition, inactivation, and induction determined in vitro. *Drug Metab Dispos* **36:**1698-1708.
Fasco MJ, Silkworth JB, Dunbar DA and Kaminsky LS (1993) Rat small intestinal cytochromes P450 probed by warfarin metabolism. *Mol Pharmacol* **43:**226-233.
FDA Approved Drug Products (2012).
Fisher MB, Campanale K, Ackermann BL, VandenBranden M and Wrighton SA (2000) In vitro glucuronidation using human liver microsomes and the pore-forming peptide alamethicin. *Drug Metab Dispos* **28:**560-566.
Fisher MB and Labissiere G (2007) The role of the intestine in drug metabolism and pharmacokinetics: an industry perspective. *Curr Drug Metab* **8:**694-699.
Fisher MB, Paine MF, Strelevitz TJ and Wrighton SA (2001) The role of hepatic and extrahepatic UDP-glucuronosyltransferases in human drug metabolism. *Drug Metab Rev* **33:**273-297.
Fromm MF, Busse D, Kroemer HK and Eichelbaum M (1996) Differential induction of prehepatic and hepatic metabolism of verapamil by rifampin. *Hepatology* **24:**796-801.
Galetin A (2007) Intestinal first-pass metabolism: bridging the gap between in vitro and in vivo. *Curr Drug Metab* **8:**643-644.
Galetin A, Gertz M and Houston JB (2008) Potential role of intestinal first-pass metabolism in the prediction of drug-drug interactions. *Expert Opin Drug Metab Toxicol* **4:**909-922.
Galetin A, Gertz M and Houston JB (2010) Contribution of intestinal cytochrome p450-mediated metabolism to drug-drug inhibition and induction interactions. *Drug Metab Pharmacokinet* **25:**28-47.
Galetin A and Houston JB (2006) Intestinal and hepatic metabolic activity of five cytochrome P450 enzymes: impact on prediction of first-pass metabolism. *J Pharmacol Exp Ther* **318:**1220-1229.
Ganapathy V, Gupta N and Martindale RG (2006) *Protein Digestion and Absorption*. Elsevier Academic Press, Burlington, Mass. ; London.
Gertz M, Davis JD, Harrison A, Houston JB and Galetin A (2008a) Grapefruit juice-drug interaction studies as a method to assess the extent of intestinal availability: utility and limitations. *Curr Drug Metab* **9:**785-795.

Gertz M, Harrison A, Houston JB and Galetin A (2010) Prediction of human intestinal first-pass metabolism of 25 CYP3A substrates from in vitro clearance and permeability data. *Drug Metab Dispos* **38:**1147-1158.

Gertz M, Houston JB and Galetin A (2011) Physiologically based pharmacokinetic modeling of intestinal first-pass metabolism of CYP3A substrates with high intestinal extraction. *Drug Metab Dispos* **39:**1633-1642.

Gertz M, Kilford PJ, Houston JB and Galetin A (2008b) Drug lipophilicity and microsomal protein concentration as determinants in the prediction of the fraction unbound in microsomal incubations. *Drug Metab Dispos* **36:**535-542.

Gill KL, Houston JB and Galetin A (2012) Characterization of in vitro glucuronidation clearance of a range of drugs in human kidney microsomes: comparison with liver and intestinal glucuronidation and impact of albumin. *Drug Metab Dispos* **40:**825-835.

Glaeser H, Bailey DG, Dresser GK, Gregor JC, Schwarz UI, McGrath JS, Jolicoeur E, Lee W, Leake BF, Tirona RG and Kim RB (2007) Intestinal drug transporter expression and the impact of grapefruit juice in humans. *Clin Pharmacol Ther* **81:**362-370.

Goon D and Klaassen CD (1992) Effects of microsomal enzyme inducers upon UDP-glucuronic acid concentration and UDP-glucuronosyltransferase activity in the rat intestine and liver. *Toxicol Appl Pharmacol* **115:**253-260.

Grace RF, Edwards SR, Mather LE, Lin Y and Power I (2000) Central and peripheral tissue distribution of diclofenac after subcutaneous injection in the rat. *Inflammopharmacology* **8:**43-54.

Grams B, Harms A, Braun S, Strassburg CP, Manns MP and Obermayer-Straub P (2000) Distribution and inducibility by 3-methylcholanthrene of family 1 UDP-glucuronosyltransferases in the rat gastrointestinal tract. *Arch Biochem Biophys* **377:**255-265.

Granger DN, Richardson PD, Kvietys PR and Mortillaro NA (1980) Intestinal blood flow. *Gastroenterology* **78:**837-863.

Grass GM and Sinko PJ (2002) Physiologically-based pharmacokinetic simulation modelling. *Adv Drug Deliv Rev* **54:**433-451.

Groothuis GM and de Graaf IA (2013) Precision-cut intestinal slices as in vitro tool for studies on drug metabolism. *Curr Drug Metab* **14:**112-119.

Guerret M, Cheymol G, Hubert M, Julien-Larose C and Lavene D (1989) Simultaneous study of the pharmacokinetics of intravenous and oral nicardipine using a stable isotope. *Eur J Clin Pharmacol* **37:**381-385.

Haller S, Schuler F, Lazic SE, Bachir-Cherif D, Kramer SD, Parrott NJ, Steiner G and Belli S (2012) Expression profiles of metabolic enzymes and drug transporters in the liver and along the intestine of beagle dogs. *Drug Metab Dispos* **40:**1603-1610.

Hallifax D, Turlizzi E, Zanelli U and Houston JB (2012) Clearance-dependent underprediction of in vivo intrinsic clearance from human hepatocytes: comparison with permeabilities from artificial membrane (PAMPA) assay, in silico and caco-2 assay, for 65 drugs. *Eur J Pharm Sci* **45:**570-574.

Hammarlund MM and Paalzow LK (1982) Dose-dependent pharmacokinetics of furosemide in the rat. *Biopharm Drug Dispos* **3:**345-359.

Hammarlund MM, Paalzow LK and Odlind B (1984) Pharmacokinetics of furosemide in man after intravenous and oral administration. Application of moment analysis. *Eur J Clin Pharmacol* **26:**197-207.

Han KS, Lee SH, Lee MG and Kim ND (1993) Pharmacokinetics and pharmacodynamics of bumetanide after intravenous and oral administration to spontaneously hypertensive rats and DOCA-salt induced hypertensive rats. *Biopharm Drug Dispos* **14:**533-548.

Hanioka N, Jinno H, Tanaka-Kagawa T, Nishimura T and Ando M (2001a) Determination of UDP-glucuronosyltransferase UGT1A6 activity in human and rat liver microsomes by HPLC with UV detection. *J Pharm Biomed Anal* **25:**65-75.

Hanioka N, Ozawa S, Jinno H, Ando M, Saito Y and Sawada J (2001b) Human liver UDP-glucuronosyltransferase isoforms involved in the glucuronidation of 7-ethyl-10-hydroxycamptothecin. *Xenobiotica* **31:**687-699.

Hashimoto Y, Sasa H, Shimomura M and Inui K (1998) Effects of intestinal and hepatic metabolism on the bioavailability of tacrolimus in rats. *Pharm Res* **15:**1609-1613.
He YL, Murby S, Warhurst G, Gifford L, Walker D, Ayrton J, Eastmond R and Rowland M (1998) Species differences in size discrimination in the paracellular pathway reflected by oral bioavailability of poly(ethylene glycol) and D-peptides. *J Pharm Sci* **87:**626-633.
Heikkinen AT, Fowler S, Gray L, Li J, Peng Y, Yadava P, Railkar A and Parrott N (2013) In vitro to in vivo extrapolation and physiologically based modeling of cytochrome P450 mediated metabolism in beagle dog gut wall and liver. *Mol Pharm* **10:**1388-1399.
Heikkinen AT, Friedlein A, Lamerz J, Jakob P, Cutler P, Fowler S, Williamson T, Tolando R, Lave T and Parrott N (2012) Mass spectrometry-based quantification of CYP enzymes to establish in vitro/in vivo scaling factors for intestinal and hepatic metabolism in beagle dog. *Pharm Res* **29:**1832-1842.
Hellriegel ET, Bjornsson TD and Hauck WW (1996) Interpatient variability in bioavailability is related to the extent of absorption: implications for bioavailability and bioequivalence studies. *Clin Pharmacol Ther* **60:**601-607.
Hewitt NJ, Lechon MJ, Houston JB, Hallifax D, Brown HS, Maurel P, Kenna JG, Gustavsson L, Lohmann C, Skonberg C, Guillouzo A, Tuschl G, Li AP, LeCluyse E, Groothuis GM and Hengstler JG (2007) Primary hepatocytes: current understanding of the regulation of metabolic enzymes and transporter proteins, and pharmaceutical practice for the use of hepatocytes in metabolism, enzyme induction, transporter, clearance, and hepatotoxicity studies. *Drug Metab Rev* **39:**159-234.
Heykants J, Hendriks R, Meuldermans W, Michiels M, Scheygrond H and Reyntjens H (1981a) On the pharmacokinetics of domperidone in animals and man. IV. The pharmacokinetics of intravenous domperidone and its bioavailability in man following intramuscular, oral and rectal administration. *Eur J Drug Metab Pharmacokinet* **6:**61-70.
Heykants J, Knaeps A, Meuldermans W and Michiels M (1981b) On the pharmacokinetics of domperidone in animals and man. I. Plasma levels of domperidone in rats and dogs. Age related absorption and passage through the blood brain barrier in rats. *Eur J Drug Metab Pharmacokinet* **6:**27-36.
Higuchi S and Shiobara Y (1980) Metabolic fate of nicardipine hydrochloride, a new vasodilator, by various species in vitro. *Xenobiotica* **10:**889-896.
Hirunpanich V, Katagi J, Sethabouppha B and Sato H (2006) Demonstration of docosahexaenoic acid as a bioavailability enhancer for CYP3A substrates: in vitro and in vivo evidence using cyclosporin in rats. *Drug Metab Dispos* **34:**305-310.
Hoensch H, Woo CH, Raffin SB and Schmid R (1976) Oxidative metabolism of foreign compounds in rat small intestine: cellular localization and dependence on dietary iron. *Gastroenterology* **70:**1063-1070.
Hoensch HP, Hutt R and Hartmann F (1979) Biotransformation of xenobiotics in human intestinal mucosa. *Environ Health Perspect* **33:**71-78.
Hoensch HP, Hutzel H, Kirch W and Ohnhaus EE (1985) Isolation of human hepatic microsomes and their inhibition by cimetidine and ranitidine. *Eur J Clin Pharmacol* **29:**199-206.
Hoglund P and Nilsson LG (1988) Physiological disposition of intravenously administered 14C-labeled diltiazem in healthy volunteers. *Ther Drug Monit* **10:**401-409.
Holtbecker N, Fromm MF, Kroemer HK, Ohnhaus EE and Heidemann H (1996) The nifedipine-rifampin interaction. Evidence for induction of gut wall metabolism. *Drug Metab Dispos* **24:**1121-1123.
Houston JB (1994) Utility of in vitro drug metabolism data in predicting in vivo metabolic clearance. *Biochem Pharmacol* **47:**1469-1479.
Houston JB and Carlile DJ (1997) Prediction of hepatic clearance from microsomes, hepatocytes, and liver slices. *Drug Metab Rev* **29:**891-922.
Houston JB and Galetin A (2008) Methods for predicting in vivo pharmacokinetics using data from in vitro assays. *Curr Drug Metab* **9:**940-951.
Hu N, Xie S, Liu L, Wang X, Pan X, Chen G, Zhang L, Liu H, Liu X, Xie L and Wang G (2011) Opposite effect of diabetes mellitus induced by streptozotocin on oral and intravenous pharmacokinetics of verapamil in rats. *Drug Metab Dispos* **39:**419-425.

Hulsmann WC, van den Berg JW and de Jonge HR (1974a) Isolation of intestinal mucosa cells. *Methods Enzymol* **32:**665-673.
Hulsmann WC, van den Berg JW and de Jonge HR (1974b) Isolation of intestinal mucosa cells. *Methods Enzymol* **32:**665-673.
Ito K and Houston JB (2004) Comparison of the use of liver models for predicting drug clearance using in vitro kinetic data from hepatic microsomes and isolated hepatocytes. *Pharm Res* **21:**785-792.
Ito K and Houston JB (2005) Prediction of human drug clearance from in vitro and preclinical data using physiologically based and empirical approaches. *Pharm Res* **22:**103-112.
Iwatsubo T, Hirota N, Ooie T, Suzuki H, Shimada N, Chiba K, Ishizaki T, Green CE, Tyson CA and Sugiyama Y (1997) Prediction of in vivo drug metabolism in the human liver from in vitro metabolism data. *Pharmacol Ther* **73:**147-171.
Jacobson P, Ng J, Ratanatharathorn V, Uberti J and Brundage RC (2001) Factors affecting the pharmacokinetics of tacrolimus (FK506) in hematopoietic cell transplant (HCT) patients. *Bone Marrow Transplant* **28:**753-758.
Jamei M, Turner D, Yang J, Neuhoff S, Polak S, Rostami-Hodjegan A and Tucker G (2009) Population-based mechanistic prediction of oral drug absorption. *AAPS J* **11:**225-237.
Jeong EJ, Liu Y, Lin H and Hu M (2005) Species- and disposition model-dependent metabolism of raloxifene in gut and liver: role of UGT1A10. *Drug Metab Dispos* **33:**785-794.
Jones HM and Houston JB (2004) Substrate depletion approach for determining in vitro metabolic clearance: time dependencies in hepatocyte and microsomal incubations. *Drug Metab Dispos* **32:**973-982.
Kadono K, Akabane T, Tabata K, Gato K, Terashita S and Teramura T (2010) Quantitative prediction of intestinal metabolism in humans from a simplified intestinal availability model and empirical scaling factor. *Drug Metab Dispos* **38:**1230-1237.
Kaivosaari S, Salonen JS and Taskinen J (2002) N-Glucuronidation of some 4-arylalkyl-1H-imidazoles by rat, dog, and human liver microsomes. *Drug Metab Dispos* **30:**295-300.
Kaminsky LS and Fasco MJ (1991) Small intestinal cytochromes P450. *Crit Rev Toxicol* **21:**407-422.
Kaminsky LS and Zhang QY (2003) The small intestine as a xenobiotic-metabolizing organ. *Drug Metab Dispos* **31:**1520-1525.
Kararli TT (1995) Comparison of the gastrointestinal anatomy, physiology, and biochemistry of humans and commonly used laboratory animals. *Biopharm Drug Dispos* **16:**351-380.
Katashima M, Yamamoto K, Sugiura M, Sawada Y and Iga T (1995) Comparative pharmacokinetic/pharmacodynamic study of proton pump inhibitors, omeprazole and lansoprazole in rats. *Drug Metab Dispos* **23:**718-723.
Kato M, Chiba K, Hisaka A, Ishigami M, Kayama M, Mizuno N, Nagata Y, Takakuwa S, Tsukamoto Y, Ueda K, Kusuhara H, Ito K and Sugiyama Y (2003) The intestinal first-pass metabolism of substrates of CYP3A4 and P-glycoprotein-quantitative analysis based on information from the literature. *Drug Metab Pharmacokinet* **18:**365-372.
Kawai R, Mathew D, Tanaka C and Rowland M (1998) Physiologically based pharmacokinetics of cyclosporine A: extension to tissue distribution kinetics in rats and scale-up to human. *J Pharmacol Exp Ther* **287:**457-468.
Kilford PJ, Stringer R, Sohal B, Houston JB and Galetin A (2009) Prediction of drug clearance by glucuronidation from in vitro data: use of combined cytochrome P450 and UDP-glucuronosyltransferase cofactors in alamethicin-activated human liver microsomes. *Drug Metab Dispos* **37:**82-89.
Kim EJ, Han KS and Lee MG (2000a) Gastrointestinal first-pass effect of furosemide in rats. *J Pharm Pharmacol* **52:**1337-1343.
Kim EJ, Han KS and Lee MG (2000b) Intestinal first-pass effect of bumetanide in rats. *Int J Pharm* **194:**193-199.
Kim SH, Choi YM and Lee MG (1993) Pharmacokinetics and pharmacodynamics of furosemide in protein-calorie malnutrition. *J Pharmacokinet Biopharm* **21:**1-17.

Kim SH and Lee MG (2002) Pharmacokinetics of ipriflavone, an isoflavone derivative, after intravenous and oral administration to rats hepatic and intestinal first-pass effects. *Life Sci* **70:**1299-1315.

Kim YC, Oh EY, Kim SH and Lee MG (2006) Pharmacokinetics of diclofenac in rat model of diabetes mellitus induced by alloxan or steptozotocin. *Biopharm Drug Dispos* **27:**85-92.

Klemm K and Moody FG (1998) Regional intestinal blood flow and nitric oxide synthase inhibition during sepsis in the rat. *Ann Surg* **227:**126-133.

Klingenberg M (2003) Pigments of rat liver microsomes. *Arch Biochem Biophys* **409:**2-6.

Klippert P, Borm P and Noordhoek J (1982) Prediction of intestinal first-pass effect of phenacetin in the rat from enzyme kinetic data--correlation with in vivo data using mucosal blood flow. *Biochem Pharmacol* **31:**2545-2548.

Kolars JC, Awni WM, Merion RM and Watkins PB (1991) First-pass metabolism of cyclosporin by the gut. *Lancet* **338:**1488-1490.

Kolars JC, Lown KS, Schmiedlin-Ren P, Ghosh M, Fang C, Wrighton SA, Merion RM and Watkins PB (1994) CYP3A gene expression in human gut epithelium. *Pharmacogenetics* **4:**247-259.

Komura H and Iwaki M (2008) Species differences in in vitro and in vivo small intestinal metabolism of CYP3A substrates. *J Pharm Sci* **97:**1775-1800.

Komura H and Iwaki M (2011) In vitro and in vivo small intestinal metabolism of CYP3A and UGT substrates in preclinical animals species and humans: species differences. *Drug Metab Rev*.

Komura H, Yasuda M, Yoshida NH and Sugiyama Y (2002) Species difference in nisoldipine oxidation activity in the small intestine. *Drug Metab Pharmacokinet* **17:**427-436.

Koropatkin NM, Cameron EA and Martens EC (2012) How glycan metabolism shapes the human gut microbiota. *Nat Rev Microbiol* **10:**323-335.

Kosaka K, Sakai N, Endo Y, Fukuhara Y, Tsuda-Tsukimoto M, Ohtsuka T, Kino I, Tanimoto T, Takeba N, Takahashi M and Kume T (2011) Impact of intestinal glucuronidation on the pharmacokinetics of raloxifene. *Drug Metab Dispos* **39:**1495-1502.

Koster AS and Noordhoek J (1983) Glucuronidation in the rat intestinal wall. Comparison of isolated mucosal cells, latent microsomes and activated microsomes. *Biochem Pharmacol* **32:**895-900.

Kostewicz ES, Arrons L, Bergstrand M, Bolger MB, Galetin A, Hatley O, Jamei M, Lloyd R, Pepin X, Rostami-Hodjegan A, Sjogren E, Tannergren C, Turner DB, Wagner C, Weitschies W and Dressman JB (2013) PBPK Models for the prediction of in vivo performance of oral dosage forms. *European Journal of Pharmaceutical Sciences* **in press**.

Kostis JB, Vachharajani NN, Hadjilambris OW, Kollia GD, Palmisano M and Marino MR (2001) The pharmacokinetics and pharmacodynamics of irbesartan in heart failure. *J Clin Pharmacol* **41:**935-942.

Krause HP, Ahr HJ, Beermann D, Siefert HM, Suwelack D and Weber H (1988) The pharmacokinetics of nitrendipine. I. Absorption, plasma concentrations, and excretion after single administration of [14C]nitrendipine to rats and dogs. *Arzneimittelforschung* **38:**1593-1599.

Kuze J, Mutoh T, Takenaka T, Morisaki K, Nakura H, Hanioka N and Narimatsu S (2009) Separate evaluation of intestinal and hepatic metabolism of three benzodiazepines in rats with cannulated portal and jugular veins: comparison with the profile in non-cannulated mice. *Xenobiotica* **39:**871-880.

Kyokawa Y, Nishibe Y, Wakabayashi M, Harauchi T, Maruyama T, Baba T and Ohno K (2001) Induction of intestinal cytochrome P450 (CYP3A) by rifampicin in beagle dogs. *Chem Biol Interact* **134:**291-305.

Lapple F, von Richter O, Fromm MF, Richter T, Thon KP, Wisser H, Griese EU, Eichelbaum M and Kivisto KT (2003) Differential expression and function of CYP2C isoforms in human intestine and liver. *Pharmacogenetics* **13:**565-575.

Lau YY, Okochi H, Huang Y and Benet LZ (2006) Pharmacokinetics of atorvastatin and its hydroxy metabolites in rats and the effects of concomitant rifampicin single doses:

relevance of first-pass effect from hepatic uptake transporters, and intestinal and hepatic metabolism. *Drug Metab Dispos* **34:**1175-1181.

Le Ferrec E, Chesne C, Artusson P, Brayden D, Fabre G, Gires P, Guillou F, Rousset M, Rubas W and Scarino ML (2001) In vitro models of the intestinal barrier. The report and recommendations of ECVAM Workshop 46. European Centre for the Validation of Alternative methods. *Altern Lab Anim* **29:**649-668.

Le Jeunne C, Poirier JM, Cheymol G, Ertzbischoff O, Engel F and Hugues FC (1991) Pharmacokinetics of intravenous bisoprolol in obese and non-obese volunteers. *Eur J Clin Pharmacol* **41:**171-174.

Le Traon G, Burgaud S and Horspool LJ (2009) Pharmacokinetics of cimetidine in dogs after oral administration of cimetidine tablets. *J Vet Pharmacol Ther* **32:**213-218.

Lee DY, Chung HJ, Choi YH, Lee U, Kim SH, Lee I and Lee MG (2009) Pharmacokinetics of ipriflavone and its two metabolites, M1 and M5, after the intravenous and oral administration of ipriflavone to rat model of diabetes mellitus induced by streptozotocin. *Eur J Pharm Sci* **38:**465-471.

Lee DY, Lee I and Lee MG (2007) Pharmacokinetics of omeprazole after intravenous and oral administration to rats with liver cirrhosis induced by dimethylnitrosamine. *Int J Pharm* **330:**37-44.

Lee SH, Lee MG and Kim ND (1994) Pharmacokinetics and pharmacodynamics of bumetanide after intravenous and oral administration to rats: absorption from various GI segments. *J Pharmacokinet Biopharm* **22:**1-17.

Lee YH, Park KH and Ku YS (2000) Pharmacokinetic changes of cyclosporine after intravenous and oral administration to rats with uranyl nitrate-induced acute renal failure. *Int J Pharm* **194:**221-227.

Lennernas H (2003) Clinical pharmacokinetics of atorvastatin. *Clin Pharmacokinet* **42:**1141-1160.

Lennernas H (2007a) Animal data: the contributions of the Ussing Chamber and perfusion systems to predicting human oral drug delivery in vivo. *Adv Drug Deliv Rev* **59:**1103-1120.

Lennernas H (2007b) Modeling gastrointestinal drug absorption requires more in vivo biopharmaceutical data: experience from in vivo dissolution and permeability studies in humans. *Curr Drug Metab* **8:**645-657.

Leopold G (1986) Balanced pharmacokinetics and metabolism of bisoprolol. *J Cardiovasc Pharmacol* **8 Suppl 11:**S16-20.

Leopold G, Pabst J, Ungethum W and Buhring KU (1986) Basic pharmacokinetics of bisoprolol, a new highly beta 1-selective adrenoceptor antagonist. *J Clin Pharmacol* **26:**616-621.

Letelier ME, Lagos F, Faundez M, Miranda D, Montoya M, Aracena-Parks P and Gonzalez-Lira V (2007) Copper modifies liver microsomal UDP-glucuronyltransferase activity through different and opposite mechanisms. *Chem Biol Interact* **167:**1-11.

Lin JH, Chiba M and Baillie TA (1999) Is the role of the small intestine in first-pass metabolism overemphasized? *Pharmacol Rev* **51:**135-158.

Lin JH and Lu AY (2001) Interindividual variability in inhibition and induction of cytochrome P450 enzymes. *Annu Rev Pharmacol Toxicol* **41:**535-567.

Lindeskog P, Haaparanta T, Norgard M, Glaumann H, Hansson T and Gustafsson JA (1986) Isolation of rat intestinal microsomes: partial characterization of mucosal cytochrome P-450. *Arch Biochem Biophys* **244:**492-501.

Lo MW, Goldberg MR, McCrea JB, Lu H, Furtek CI and Bjornsson TD (1995) Pharmacokinetics of losartan, an angiotensin II receptor antagonist, and its active metabolite EXP3174 in humans. *Clin Pharmacol Ther* **58:**641-649.

Lown KS, Kolars JC, Thummel KE, Barnett JL, Kunze KL, Wrighton SA and Watkins PB (1994) Interpatient heterogeneity in expression of CYP3A4 and CYP3A5 in small bowel. Lack of prediction by the erythromycin breath test. *Drug Metab Dispos* **22:**947-955.

Lown KS, Mayo RR, Leichtman AB, Hsiao HL, Turgeon DK, Schmiedlin-Ren P, Brown MB, Guo W, Rossi SJ, Benet LZ and Watkins PB (1997) Role of intestinal P-glycoprotein (mdr1) in interpatient variation in the oral bioavailability of cyclosporine. *Clin Pharmacol Ther* **62:**248-260.

Luke DR, Brunner LJ and Vadiei K (1990) Bioavailability assessment of cyclosporine in the rat. Influence of route of administration. *Drug Metab Dispos* **18:**158-162.
Malik AB, Kaplan JE and Saba TM (1976) Reference sample method for cardiac output and regional blood flow determinations in the rat. *J Appl Physiol* **40:**472-475.
Mandal S, Mandal SS and Sawant KK (2010) Design and development of microemulsion drug delivery system of atorvastatin and study its intestinal permeability in rats. *International Journal of Drug Delivery* **2:**69-75.
Martignoni M, Groothuis G and de Kanter R (2006) Comparison of mouse and rat cytochrome P450-mediated metabolism in liver and intestine. *Drug Metab Dispos* **34:**1047-1054.
Matsubara T, Koike M, Touchi A, Tochino Y and Sugeno K (1976) Quantitative determination of cytochrome P-450 in rat liver homogenate. *Anal Biochem* **75:**596-603.
Matsuda Y, Konno Y, Satsukawa M, Kobayashi T, Takimoto Y, Morisaki K and Yamashita S (2012) Assessment of intestinal availability of various drugs in the oral absorption process using portal vein-cannulated rats. *Drug Metab Dispos* **40:**2231-2238.
McEntee K, Clercx C, Pypendop B, Peeters D, Balligand M, D'Orio V and Henroteaux M (1996) Cardiac performance in conscious healthy dogs during dobutamine infusion. *Res Vet Sci* **61:**234-239.
Mealey KL, Waiting D, Raunig DL, Schmidt KR and Nelson FR (2010) Oral bioavailability of P-glycoprotein substrate drugs do not differ between ABCB1-1Delta and ABCB1 wild type dogs. *J Vet Pharmacol Ther* **33:**453-460.
Meuldermans W, Hurkmans R, Swysen E, Hendrickx J, Michiels M, Lauwers W and Heykants J (1981) On the pharmacokinetics of domperidone in animals and man III. Comparative study on the excretion and metabolism of domperidone in rats, dogs and man. *Eur J Drug Metab Pharmacokinet* **6:**49-60.
Mikus G, Fischer C, Heuer B, Langen C and Eichelbaum M (1987) Application of stable isotope methodology to study the pharmacokinetics, bioavailability and metabolism of nitrendipine after i.v. and p.o. administration. *Br J Clin Pharmacol* **24:**561-569.
Mistry M and Houston JB (1985) Quantitation of extrahepatic metabolism. Pulmonary and intestinal conjugation of naphthol. *Drug Metab Dispos* **13:**740-745.
Mitschke D, Reichel A, Fricker G and Moenning U (2008) Characterization of cytochrome P450 protein expression along the entire length of the intestine of male and female rats. *Drug Metab Dispos* **36:**1039-1045.
Mizuma T, Kawashima K, Sakai S, Sakaguchi S and Hayashi M (2005) Differentiation of organ availability by sequential and simultaneous analyses: intestinal conjugative metabolism impacts on intestinal availability in humans. *J Pharm Sci* **94:**571-575.
Mohri K and Uesawa Y (2001) Enzymatic activities in the microsomes prepared from rat small intestinal epithelial cells by differential procedures. *Pharm Res* **18:**1232-1236.
Molpeceres J, ChacÃ³n M, Berges L, Pedraz JL, GuzmÃ¡n M and Aberturas MR (1998) Age and sex dependent pharmacokinetics of cyclosporine in the rat after a single intravenous dose. *International Journal of Pharmaceutics* **174:**9-18.
Monaco F and Cicolin A (1999) Interactions between anticonvulsant and psychoactive drugs. *Epilepsia* **40 Suppl 10:**S71-76.
Moon CH, Lee HJ, Jung YS, Lee SH and Baik EJ (1998) Pharmacokinetics of losartan and its metabolite, EXP3174, after intravenous and oral administration of losartan to rats with streptozotocin-induced diabetes mellitus. *Res Commun Mol Pathol Pharmacol* **101:**147-158.
Moon Y, Kim SY, Ji HY, Kim YK, Chae HJ, Chae SW and Lee HS (2007) Characterization of cytochrome P450s mediating ipriflavone metabolism in human liver microsomes. *Xenobiotica* **37:**246-259.
Mouly S and Paine MF (2003) P-glycoprotein increases from proximal to distal regions of human small intestine. *Pharm Res* **20:**1595-1599.
Murakami T, Nakanishi M, Yoshimori T, Okamura N, Norikura R and Mizojiri K (2003) Separate assessment of intestinal and hepatic first-pass effects using a rat model with double cannulation of the portal and jugular veins. *Drug Metab Pharmacokinet* **18:**252-260.

Murray GI, Barnes TS, Sewell HF, Ewen SW, Melvin WT and Burke MD (1988) The immunocytochemical localisation and distribution of cytochrome P-450 in normal human hepatic and extrahepatic tissues with a monoclonal antibody to human cytochrome P-450. *Br J Clin Pharmacol* **25:**465-475.

Musther H, Olivares-Morales A, Hatley OJD, Liu B and Rostami-Hodjegan A (2013) Animal verses human oral drug bioavailability: Do they correleate? *European Journal of Pharmaceutical Sciences* **in press**.

Nakamura T, Sakaeda T, Ohmoto N, Tamura T, Aoyama N, Shirakawa T, Kamigaki T, Kim KI, Kim SR, Kuroda Y, Matsuo M, Kasuga M and Okumura K (2002) Real-time quantitative polymerase chain reaction for MDR1, MRP1, MRP2, and CYP3A-mRNA levels in Caco-2 cell lines, human duodenal enterocytes, normal colorectal tissues, and colorectal adenocarcinomas. *Drug Metab Dispos* **30:**4-6.

Nakanishi Y, Matsushita A, Matsuno K, Iwasaki K, Utoh M, Nakamura C and Uno Y (2010) Regional distribution of cytochrome p450 mRNA expression in the liver and small intestine of cynomolgus monkeys. *Drug Metab Pharmacokinet* **25:**290-297.

Nakanishi Y, Matsushita A, Matsuno K, Iwasaki K, Utoh M, Nakamura C and Uno Y (2011) Regional distribution of drug-metabolizing enzyme activities in the liver and small intestine of cynomolgus monkeys. *Drug Metab Pharmacokinet* **26:**288-294.

Nishibe Y, Wakabayashi M, Harauchi T and Ohno K (1998) Characterization of cytochrome P450 (CYP3A12) induction by rifampicin in dog liver. *Xenobiotica* **28:**549-557.

Nishimura T, Amano N, Kubo Y, Ono M, Kato Y, Fujita H, Kimura Y and Tsuji A (2007) Asymmetric intestinal first-pass metabolism causes minimal oral bioavailability of midazolam in cynomolgus monkey. *Drug Metab Dispos* **35:**1275-1284.

Obach RS (2001) The prediction of human clearance from hepatic microsomal metabolism data. *Curr Opin Drug Discov Devel* **4:**36-44.

Obach RS (2011) Predicting clearance in humans from in vitro data. *Curr Top Med Chem* **11:**334-339.

Obach RS, Baxter JG, Liston TE, Silber BM, Jones BC, MacIntyre F, Rance DJ and Wastall P (1997) The prediction of human pharmacokinetic parameters from preclinical and in vitro metabolism data. *J Pharmacol Exp Ther* **283:**46-58.

Obach RS, Zhang QY, Dunbar D and Kaminsky LS (2001) Metabolic characterization of the major human small intestinal cytochrome p450s. *Drug Metab Dispos* **29:**347-352.

Ohno S and Nakajin S (2009) Determination of mRNA expression of human UDP-glucuronosyltransferases and application for localization in various human tissues by real-time reverse transcriptase-polymerase chain reaction. *Drug Metab Dispos* **37:**32-40.

Ohtsuki S, Schaefer O, Kawakami H, Inoue T, Liehner S, Saito A, Ishiguro N, Kishimoto W, Ludwig-Schwellinger E, Ebner T and Terasaki T (2012) Simultaneous absolute protein quantification of transporters, cytochromes P450, and UDP-glucuronosyltransferases as a novel approach for the characterization of individual human liver: comparison with mRNA levels and activities. *Drug Metab Dispos* **40:**83-92.

Omura T and Sato R (1964) The Carbon Monoxide-Binding Pigment of Liver Microsomes. I. Evidence for Its Hemoprotein Nature. *J Biol Chem* **239:**2370-2378.

Pacifici GM, Franchi M, Bencini C, Repetti F, Di Lascio N and Muraro GB (1988) Tissue distribution of drug-metabolizing enzymes in humans. *Xenobiotica* **18:**849-856.

Paine MF, Hart HL, Ludington SS, Haining RL, Rettie AE and Zeldin DC (2006) The human intestinal cytochrome P450 "pie". *Drug Metab Dispos* **34:**880-886.

Paine MF, Khalighi M, Fisher JM, Shen DD, Kunze KL, Marsh CL, Perkins JD and Thummel KE (1997) Characterization of interintestinal and intraintestinal variations in human CYP3A-dependent metabolism. *J Pharmacol Exp Ther* **283:**1552-1562.

Paine MF, Leung LY, Lim HK, Liao K, Oganesian A, Zhang MY, Thummel KE and Watkins PB (2002) Identification of a novel route of extraction of sirolimus in human small intestine: roles of metabolism and secretion. *J Pharmacol Exp Ther* **301:**174-186.

Paine MF, Shen DD, Kunze KL, Perkins JD, Marsh CL, McVicar JP, Barr DM, Gillies BS and Thummel KE (1996) First-pass metabolism of midazolam by the human intestine. *Clin Pharmacol Ther* **60:**14-24.

Pang KS (2003) Modeling of intestinal drug absorption: roles of transporters and metabolic enzymes (for the Gillette Review Series). *Drug Metab Dispos* **31:**1507-1519.
Panorchan P, Thompson MS, Davis KJ, Tseng Y, Konstantopoulos K and Wirtz D (2006) Single-molecule analysis of cadherin-mediated cell-cell adhesion. *J Cell Sci* **119:**66-74.
Pappenheimer JR (1998) Scaling of dimensions of small intestines in non-ruminant eutherian mammals and its significance for absorptive mechanisms. *Comp Biochem Physiol A Mol Integr Physiol* **121:**45-58.
Peris-Ribera JE, Torres-Molina F, Garcia-Carbonell MC, Aristorena JC and Pla-Delfina JM (1991) Pharmacokinetics and bioavailability of diclofenac in the rat. *J Pharmacokinet Biopharm* **19:**647-665.
Perrier L, Bourrie M, Marti E, Tronquet C, Masse D, Berger Y, Magdalou J and Fabre G (1994) In vitro N-glucuronidation of SB 47436 (BMS 186295), a new AT1 nonpeptide angiotensin II receptor antagonist, by rat, monkey and human hepatic microsomal fractions. *J Pharmacol Exp Ther* **271:**91-99.
Piao YJ and Choi JS (2008) Effects of morin on the pharmacokinetics of nicardipine after oral and intravenous administration of nicardipine in rats. *J Pharm Pharmacol* **60:**625-629.
Pinkus LM and Windmueller HG (1977) Phosphate-dependent glutaminase of small intestine: localization and role in intestinal glutamine metabolism. *Arch Biochem Biophys* **182:**506-517.
Poulin P, Jones RD, Jones HM, Gibson CR, Rowland M, Chien JY, Ring BJ, Adkison KK, Ku MS, He H, Vuppugalla R, Marathe P, Fischer V, Dutta S, Sinha VK, Bjornsson T, Lave T and Yates JW (2011) PHRMA CPCDC initiative on predictive models of human pharmacokinetics, part 5: Prediction of plasma concentration-time profiles in human by using the physiologically-based pharmacokinetic modeling approach. *J Pharm Sci*.
Powell M (2006) Kinetics of Cytochrome P450 enzymes in the canine liver and small intestine, in: *School of Pharmacy and Pharmaceutical Sciences*, University of Manchester.
Prueksaritanont T, Gorham LM, Hochman JH, Tran LO and Vyas KP (1996) Comparative studies of drug-metabolizing enzymes in dog, monkey, and human small intestines, and in Caco-2 cells. *Drug Metab Dispos* **24:**634-642.
Quinney SK, Galinsky RE, Jiyamapa-Serna VA, Chen Y, Hamman MA, Hall SD and Kimura RE (2008) Hydroxyitraconazole, formed during intestinal first-pass metabolism of itraconazole, controls the time course of hepatic CYP3A inhibition and the bioavailability of itraconazole in rats. *Drug Metab Dispos* **36:**1097-1101.
Regardh CG, Andersson T, Lagerstrom PO, Lundborg P and Skanberg I (1990) The pharmacokinetics of omeprazole in humans--a study of single intravenous and oral doses. *Ther Drug Monit* **12:**163-172.
Regardh CG, Gabrielsson M, Hoffman KJ, Lofberg I and Skanberg I (1985) Pharmacokinetics and metabolism of omeprazole in animals and man--an overview. *Scand J Gastroenterol Suppl* **108:**79-94.
Reyes-Gordillo K, Muriel P, Castaneda-Hernandez G and Favari L (2007) Pharmacokinetics of diclofenac in rats intoxicated with CCL4, and in the regenerating liver. *Biopharm Drug Dispos* **28:**415-422.
Riches Z, Stanley EL, Bloomer JC and Coughtrie MW (2009) Quantitative evaluation of the expression and activity of five major sulfotransferases (SULTs) in human tissues: the SULT "pie". *Drug Metab Dispos* **37:**2255-2261.
Ritschel WA and Grummich KW (1981) Pharmacokinetics of coumarin and 7-hydroxycoumarin upon i.v. and p.o. administration in the euthyroid and hypothyroid beagle dog. *Arzneimittelforschung* **31:**643-649.
Ritter JK (2007) Intestinal UGTs as potential modifiers of pharmacokinetics and biological responses to drugs and xenobiotics. *Expert Opin Drug Metab Toxicol* **3:**93-107.
Rostami-Hodjegan A and Tucker GT (2007) Simulation and prediction of in vivo drug metabolism in human populations from in vitro data. *Nat Rev Drug Discov* **6:**140-148.
Rowland A, Knights KM, Mackenzie PI and Miners JO (2008) The "albumin effect" and drug glucuronidation: bovine serum albumin and fatty acid-free human serum albumin enhance

the glucuronidation of UDP-glucuronosyltransferase (UGT) 1A9 substrates but not UGT1A1 and UGT1A6 activities. *Drug Metab Dispos* **36:**1056-1062.
Rowland M and Tozer TN (2010) *Clinical pharmacokinetics and pharmacodynamics : concepts and applications*. Lippincott Williams & Wilkins, Philadelphia, Pa. ; London.
Rowland Yeo K, Rostami-Hodjegan A and Tucker GT (2003) Abundace of cytochrome P450 in humna liver: a meta analysis. *British Journal of CLinical Pharmacology* **57:**687-688.
Russell WMS and Burch RL (1959) *The Principles of Humans Experimental Technique*. Methuen, London.
Sangalli L, Bortolotti A, Jiritano L and Bonati M (1988) Cyclosporine pharmacokinetics in rats and interspecies comparison in dogs, rabbits, rats, and humans. *Drug Metab Dispos* **16:**749-753.
Sheiner LB and Beal SL (1981) Some suggestions for measuring predictive performance. *J Pharmacokinet Biopharm* **9:**503-512.
Shelby MK, Cherrington NJ, Vansell NR and Klaassen CD (2003) Tissue mRNA expression of the rat UDP-glucuronosyltransferase gene family. *Drug Metab Dispos* **31:**326-333.
Shibata N, Gao W, Okamoto H, Kishida T, Iwasaki K, Yoshikawa Y and Takada K (2002) Drug interactions between HIV protease inhibitors based on physiologically-based pharmacokinetic model. *J Pharm Sci* **91:**680-689.
Shin HC, Kim HR, Cho HJ, Yi H, Cho SM, Lee DG, Abd El-Aty AM, Kim JS, Sun D and Amidon GL (2009a) Comparative gene expression of intestinal metabolizing enzymes. *Biopharm Drug Dispos* **30:**411-421.
Shin HC, Kim HR, Cho HJ, Yi H, Cho SM, Lee DG, El-Aty AM, Kim JS, Sun D and Amidon GL (2009b) Comparative gene expression of intestinal metabolizing enzymes. *Biopharm Drug Dispos* **30:**411-421.
Shin HS, Bae SK and Lee MG (2006) Pharmacokinetics of sildenafil after intravenous and oral administration in rats: hepatic and intestinal first-pass effects. *Int J Pharm* **320:**64-70.
Shiratani H, Katoh M, Nakajima M and Yokoi T (2008) Species differences in UDP-glucuronosyltransferase activities in mice and rats. *Drug Metab Dispos* **36:**1745-1752.
Shirkey RJ, Chakraborty J and Bridges JW (1979) An improved method for preparing rat small intestine microsomal fractions for studying drug metabolism. *Anal Biochem* **93:**73-81.
Smith DE, Lin ET and Benet LZ (1980) Absorption and disposition of furosemide in healthy volunteers, measured with a metabolite-specific assay. *Drug Metab Dispos* **8:**337-342.
Smith PK, Krohn RI, Hermanson GT, Mallia AK, Gartner FH, Provenzano MD, Fujimoto EK, Goeke NM, Olson BJ and Klenk DC (1985) Measurement of protein using bicinchoninic acid. *Anal Biochem* **150:**76-85.
Smith R, Jones RD, Ballard PG and Griffiths HH (2008) Determination of microsome and hepatocyte scaling factors for in vitro/in vivo extrapolation in the rat and dog. *Xenobiotica* **38:**1386-1398.
Sohlenius-Sternbeck AK and Orzechowski A (2004) Characterization of the rates of testosterone metabolism to various products and of glutathione transferase and sulfotransferase activities in rat intestine and comparison to the corresponding hepatic and renal drug-metabolizing enzymes. *Chem Biol Interact* **148:**49-56.
Sonderfan AJ, Arlotto MP and Parkinson A (1989) Identification of the cytochrome P-450 isozymes responsible for testosterone oxidation in rat lung, kidney, and testis: evidence that cytochrome P-450a (P450IIA1) is the physiologically important testosterone 7 alpha-hydroxylase in rat testis. *Endocrinology* **125:**857-866.
Soons PA and Breimer DD (1991) Stereoselective pharmacokinetics of oral and intravenous nitrendipine in healthy male subjects. *Br J Clin Pharmacol* **32:**11-16.
Stohs SJ, Grafstrom RC, Burke MD, Moldeus PW and Orrenius SG (1976) The isolation of rat intestinal microsomes with stable cytochrome P-450 and their metabolism of benzo(alpha) pyrene. *Arch Biochem Biophys* **177:**105-116.
Strassburg CP, Kneip S, Topp J, Obermayer-Straub P, Barut A, Tukey RH and Manns MP (2000) Polymorphic gene regulation and interindividual variation of UDP-glucuronosyltransferase activity in human small intestine. *J Biol Chem* **275:**36164-36171.

Tahara K, Saigusa K, Kagawa Y, Taguchi M and Hashimoto Y (2006) Pharmacokinetics and pharmacodynamics of bisoprolol in rats with bilateral ureter ligation-induced renal failure. *Drug Metab Pharmacokinet* **21:**389-394.

Takada K, Usuda H, Oh-Hashi M, Yoshikawa H, Muranishi S and Tanaka H (1991) Pharmacokinetics of FK-506, a novel immunosuppressant, after intravenous and oral administrations to rats. *J Pharmacobiodyn* **14:**34-42.

Takano M, Yumoto R and Murakami T (2006) Expression and function of efflux drug transporters in the intestine. *Pharmacology & Therapeutics* **109:**137-161.

Takemoto K, Yamazaki H, Tanaka Y, Nakajima M and Yokoi T (2003) Catalytic activities of cytochrome P450 enzymes and UDP-glucuronosyltransferases involved in drug metabolism in rat everted sacs and intestinal microsomes. *Xenobiotica* **33:**43-55.

Tam-Zaman N, Tam YK, Tawfik S and Wiltshire H (2004) Factors responsible for the variability of saquinavir absorption: studies using an instrumented dog model. *Pharm Res* **21:**436-442.

Tanaka C, Kawai R and Rowland M (2000) Dose-dependent pharmacokinetics of cyclosporin A in rats: events in tissues. *Drug Metab Dispos* **28:**582-589.

Taylor GL, Patel B and Sullivan AT (2007) Evaluation of blood flow parameters in addition to blood pressure and electrocardiogram in the conscious telemetered beagle dog. *Journal of Pharmacological and Toxicological Methods* **56:**212-217.

Thelen K and Dressman JB (2009) Cytochrome P450-mediated metabolism in the human gut wall. *J Pharm Pharmacol* **61:**541-558.

Thummel KE, O'Shea D, Paine MF, Shen DD, Kunze KL, Perkins JD and Wilkinson GR (1996) Oral first-pass elimination of midazolam involves both gastrointestinal and hepatic CYP3A-mediated metabolism. *Clin Pharmacol Ther* **59:**491-502.

Toffoli G, Robieux I, Fantin D, Gigante M, Frustaci S, Nicolosi GL, De Cicco M and Boiocchi M (1997) Non-linear pharmacokinetics of high-dose intravenous verapamil. *Br J Clin Pharmacol* **44:**255-260.

Tortora GJ and Derrickson B (2006) *Principles of anatomy and physiology*. Wiley, New York, N.Y. ; Chichester.

Traber PG, Wang W and Yu L (1992) Differential regulation of cytochrome P-450 genes along rat intestinal crypt-villus axis. *Am J Physiol* **263:**G215-223.

Tukey RH and Strassburg CP (2001) Genetic multiplicity of the human UDP-glucuronosyltransferases and regulation in the gastrointestinal tract. *Mol Pharmacol* **59:**405-414.

Valentin J (2002) Basic anatomical and physiological data for use in radiological protection: Reference values. Oxford: Pergamon.

van de Kerkhof EG, de Graaf IA, de Jager MH and Groothuis GM (2007a) Induction of phase I and II drug metabolism in rat small intestine and colon in vitro. *Drug Metab Dispos* **35:**898-907.

van de Kerkhof EG, de Graaf IA, de Jager MH, Meijer DK and Groothuis GM (2005) Characterization of rat small intestinal and colon precision-cut slices as an in vitro system for drug metabolism and induction studies. *Drug Metab Dispos* **33:**1613-1620.

van de Kerkhof EG, de Graaf IA and Groothuis GM (2007b) In vitro methods to study intestinal drug metabolism. *Curr Drug Metab* **8:**658-675.

van de Kerkhof EG, de Graaf IA, Ungell AL and Groothuis GM (2008) Induction of metabolism and transport in human intestine: validation of precision-cut slices as a tool to study induction of drug metabolism in human intestine in vitro. *Drug Metab Dispos* **36:**604-613.

van de Kerkhof EG, Ungell AL, Sjoberg AK, de Jager MH, Hilgendorf C, de Graaf IA and Groothuis GM (2006) Innovative methods to study human intestinal drug metabolism in vitro: precision-cut slices compared with ussing chamber preparations. *Drug Metab Dispos* **34:**1893-1902.

van de Waterbeemd H and Gifford E (2003) ADMET in silico modelling: towards prediction paradise? *Nat Rev Drug Discov* **2:**192-204.

Varma MV, Obach RS, Rotter C, Miller HR, Chang G, Steyn SJ, El-Kattan A and Troutman MD (2010) Physicochemical space for optimum oral bioavailability: contribution of human intestinal absorption and first-pass elimination. *J Med Chem* **53:**1098-1108.

von Richter O, Burk O, Fromm MF, Thon KP, Eichelbaum M and Kivisto KT (2004) Cytochrome P450 3A4 and P-glycoprotein expression in human small intestinal enterocytes and hepatocytes: a comparative analysis in paired tissue specimens. *Clin Pharmacol Ther* **75:**172-183.

von Richter O, Greiner B, Fromm MF, Fraser R, Omari T, Barclay ML, Dent J, Somogyi AA and Eichelbaum M (2001) Determination of in vivo absorption, metabolism, and transport of drugs by the human intestinal wall and liver with a novel perfusion technique. *Clin Pharmacol Ther* **70:**217-227.

Walker DK, Ackland MJ, James GC, Muirhead GJ, Rance DJ, Wastall P and Wright PA (1999) Pharmacokinetics and metabolism of sildenafil in mouse, rat, rabbit, dog and man. *Xenobiotica* **29:**297-310.

Walsky RL, Bauman JN, Bourcier K, Giddens G, Lapham K, Negahban A, Ryder TF, Obach RS, Hyland R and Goosen TC (2012) Optimized assays for human UDP-glucuronosyltransferase (UGT) activities: altered alamethicin concentration and utility to screen for UGT inhibitors. *Drug Metab Dispos* **40:**1051-1065.

Ward KW, Nagilla R and Jolivette LJ (2005) Comparative evaluation of oral systemic exposure of 56 xenobiotics in rat, dog, monkey and human. *Xenobiotica* **35:**191-210.

Ward KW and Smith BR (2004) A comprehensive quantitative and qualitative evaluation of extrapolation of intravenous pharmacokinetic parameters from rat, dog, and monkey to humans. I. Clearance. *Drug Metab Dispos* **32:**603-611.

Watanabe K, Furuno K, Eto K, Oishi R and Gomita Y (1994) First-pass metabolism of omeprazole in rats. *J Pharm Sci* **83:**1131-1134.

Watkins PB (1997) The barrier function of CYP3A4 and P-glycoprotein in the small bowel. *Adv Drug Deliv Rev* **27:**161-170.

Watkins PB, Wrighton SA, Schuetz EG, Molowa DT and Guzelian PS (1987) Identification of glucocorticoid-inducible cytochromes P-450 in the intestinal mucosa of rats and man. *J Clin Invest* **80:**1029-1036.

Weiser MM (1973) Intestinal epithelial cell surface membrane glycoprotein synthesis. I. An indicator of cellular differentiation. *J Biol Chem* **248:**2536-2541.

Wilkinson GR (1987) Clearance approaches in pharmacology. *Pharmacol Rev* **39:**1-47.

Wilson ZE, Rostami-Hodjegan A, Burn JL, Tooley A, Boyle J, Ellis SW and Tucker GT (2003) Inter-individual variability in levels of human microsomal protein and hepatocellularity per gram of liver. *Br J Clin Pharmacol* **56:**433-440.

Winiwarter S, Bonham NM, Ax F, Hallberg A, Lennernas H and Karlen A (1998) Correlation of human jejunal permeability (in vivo) of drugs with experimentally and theoretically derived parameters. A multivariate data analysis approach. *J Med Chem* **41:**4939-4949.

Wong H, Dockens RC, Pajor L, Yeola S, Grace JE, Jr., Stark AD, Taub RA, Yocca FD, Zaczek RC and Li YW (2007) 6-Hydroxybuspirone is a major active metabolite of buspirone: assessment of pharmacokinetics and 5-hydroxytryptamine1A receptor occupancy in rats. *Drug Metab Dispos* **35:**1387-1392.

Yakatan GJ, Maness DD, Scholler J, Johnston JT, Novick WJ, Jr. and Doluisio JT (1979) Plasma and tissue levels of furosemide in dogs and monkeys following single and multiple oral doses. *Res Commun Chem Pathol Pharmacol* **24:**465-482.

Yang J, Jamei M, Yeo KR, Tucker GT and Rostami-Hodjegan A (2007) Prediction of intestinal first-pass drug metabolism. *Curr Drug Metab* **8:**676-684.

Yang J, Tucker GT and Rostami-Hodjegan A (2004) Cytochrome P450 3A expression and activity in the human small intestine. *Clin Pharmacol Ther* **76:**391.

Yeh KC, Berger ET, Breault GO, Lei BW and McMahon FG (1982) Effect of sustained release on the pharmacokinetic profile of indomethacin in man. *Biopharm Drug Dispos* **3:**219-230.

Yoon IS, Choi MK, Kim JS, Shim CK, Chung SJ and Kim DD (2011) Pharmacokinetics and first-pass elimination of metoprolol in rats: contribution of intestinal first-pass extraction to low bioavailability of metoprolol. *Xenobiotica* **41:**243-251.

Yu LX and Amidon GL (1999) A compartmental absorption and transit model for estimating oral drug absorption. *Int J Pharm* **186:**119-125.

Zakeri-Milani P, Valizadeh H, Islambulchilar Z, Damani S and Mehtari M (2008) Investigation of the intestinal permeability of ciclosporin using the in situ technique in rats and the relevance of P-glycoprotein. *Arzneimittelforschung* **58:**188-192.

Zakeri-Milani P, Valizadeh H, Tajerzadeh H, Azarmi Y, Islambolchilar Z, Barzegar S and Barzegar-Jalali M (2007) Predicting human intestinal permeability using single-pass intestinal perfusion in rat. *J Pharm Pharm Sci* **10:**368-379.

Zeldin DC, Foley J, Goldsworthy SM, Cook ME, Boyle JE, Ma J, Moomaw CR, Tomer KB, Steenbergen C and Wu S (1997) CYP2J subfamily cytochrome P450s in the gastrointestinal tract: expression, localization, and potential functional significance. *Mol Pharmacol* **51:**931-943.

Zhang QY, Dunbar D and Kaminsky LS (2003) Characterization of mouse small intestinal cytochrome P450 expression. *Drug Metab Dispos* **31:**1346-1351.

Zhang QY, Dunbar D, Ostrowska A, Zeisloft S, Yang J and Kaminsky LS (1999) Characterization of human small intestinal cytochromes P-450. *Drug Metab Dispos* **27:**804-809.

Zhang QY, Wikoff J, Dunbar D and Kaminsky L (1996) Characterization of rat small intestinal cytochrome P450 composition and inducibility. *Drug Metab Dispos* **24:**322-328.

Zhao YH, Abraham MH, Le J, Hersey A, Luscombe CN, Beck G, Sherborne B and Cooper I (2003) Evaluation of rat intestinal absorption data and correlation with human intestinal absorption. *Eur J Med Chem* **38:**233-243.

Zimmermann C, Gutmann H, Hruz P, Gutzwiller JP, Beglinger C and Drewe J (2005) Mapping of multidrug resistance gene 1 and multidrug resistance-associated protein isoform 1 to 5 mRNA expression along the human intestinal tract. *Drug Metab Dispos* **33:**219-224.